# On the role of ribosomal proteins in stress resistance and fitness of *Listeria monocytogenes*

## *a laboratory evolution approach*

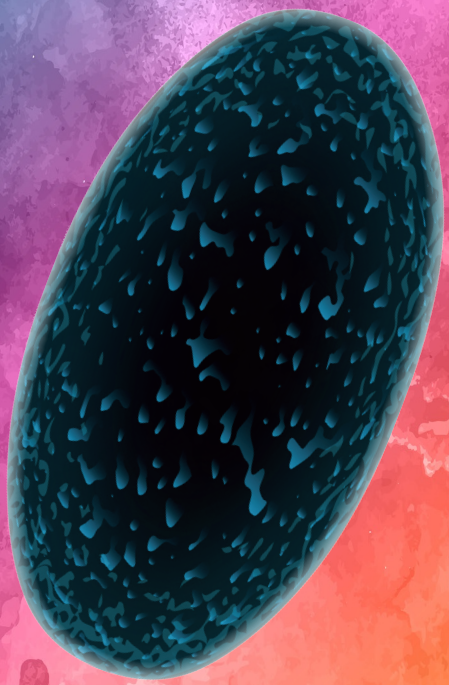

Jeroen Koomen

# Propositions

1. Switching between stress resistance and fitness in *Listeria monocytogenes* is possible through ribosomal mutations.
   (this thesis)

2. Lower fitness in stress resistant *rpsU* variants is not caused by SigB activation.
   (this thesis)

3. The finding that certain British birds adapt their beaks to birdfeeders (Bosse et al. (2017) SCIENCE Vol 358, pp. 365-368), indicates that fondness for birds can have unexpected side effects.

4. Trying to solve the antibiotic resistance crisis with new antibiotics is a dead-end road.

5. A programming language should be offered as a language in high school.

6. The use of gloves by operators in food stalls is a food safety risk.

Propositions belonging to the thesis, entitled

On the role of ribosomal proteins in stress resistance and fitness of *Listeria monocytogenes*: a laboratory evolution approach

Jeroen Koomen
Wageningen, 18 January 2022

# On the role of ribosomal proteins in stress resistance and fitness of *Listeria monocytogenes*

*a laboratory evolution approach*

Jeroen Koomen

**Thesis committee**

**Promotors**

Prof. Dr Tjakko Abee
Personal chair at the Laboratory of Food Microbiology
Wageningen University & Research

Dr Heidy M.W. den Besten
Associate professor, Laboratory of Food Microbiology
Wageningen University & Research

**Co-promotor**

Prof. Dr Marcel H. Zwietering
Professor of Food Microbiology
Wageningen University & Research

**Other members**

Prof. Dr M. Kleerebezem, Wageningen University & Research
Dr I.L. Bergval, National Institute for Public Health and the Environment, Bilthoven
Prof. Dr C. O'Byrne - National University of Ireland, Galway, Ireland
Dr M.N. Nierop Groot, Wageningen University & Research

This research was conducted under the auspices of the Graduate School VLAG (Advanced studies in Food Technology, Agrobiotechnology, Nutrition and Health Sciences).

# On the role of ribosomal proteins in stress resistance and fitness of *Listeria monocytogenes*

## *a laboratory evolution approach*

Jeroen Koomen

**Thesis**

submitted in fulfilment of the requirements for the degree of doctor
at Wageningen University
by the authority of the Rector Magnificus,
Prof. Dr A.P.J. Mol,
in the presence of the
Thesis Committee appointed by the Academic Board
to be defended in public
on Tuesday 18 January 2022
at 1:30 p.m. in the Aula

Jeroen Koomen

*On the role of ribosomal proteins in stress resistance and fitness of* Listeria monocytogenes *a laboratory evolution approach*

180 pages

PhD thesis, Wageningen University, Wageningen, the Netherlands (2022)

With references, with summary in English

ISBN 978-94-6447-029-1

DOI 10.18174/557306

# Table of contents

# 1

# General introduction and outline of the thesis

Parts of this introduction were previously published as: Impact of pathogen population heterogeneity and stress-resistant variants on food safety. Abee, T., Koomen, J., Metselaar, K.I., Zwietering, M.H., Den Besten, H.M.W., 2016. Annu. Rev. Food Sci. Technol. 7, 439–456. doi:10.1146/annurev-food-041715-033128

## General introduction and outline of the thesis

The production of healthy, nutritious, tasty, and safe foods requires efficient strategies to control foodborne pathogens along the food chain. Recent research developments include the implementation of genomics, transcriptomics, and proteomics, that may transform approaches to the detection, prevention, and treatment of foodborne pathogens (Bergholz et al., 2014). These omics-based techniques are already used as research tools to unravel the survival strategies of notorious foodborne pathogens such as *Listeria monocytogenes* (Arcari et al., 2020; Begley and Hill, 2015; Harrand et al., 2020; Radoshevich and Cossart, 2018). *L. monocytogenes* is a robust, ubiquitously present foodborne human pathogen and the causative agent of listeriosis (Toledo-Arana et al., 2009). It is well known that microbial variability ensures survival and persistence of pathogens in changing environments. *L. monocytogenes* is capable of growing and surviving in a wide range of adverse conditions such as low temperature, low pH, and low aw (NicAogáin and O'Byrne, 2016), and has served as a model in a large number of studies that addressed the impact of strain diversity and the role of population heterogeneity in adaptive stress response and survival capacity (Karatzas et al., 2005; Koomen et al., 2018; Metselaar et al., 2013; Van Boeijen et al., 2010; van der Veen and Abee, 2011a; Vanlint et al., 2012). The dynamic response of microorganisms to (changing) environmental conditions depends on the behaviour of individual cells within the population, and this can affect the efficiency of conventional control measures like heat inactivation procedures, and that of nonthermal processes such as high hydrostatic pressure (HHP) treatments. Enhanced survival of resistant subpopulations is reflected in a higher fraction of surviving cells. These resistant subpopulations include so-called persister cells that are more resistant than the majority of cells.

## Population heterogeneity and stress resistance

The term persistence is used in this thesis to describe the long-term survival of pathogens in specific environments, including processing plants (Carpentier and Cerf, 2011; Ferreira et al., 2014). Over the past 15 to 20 years, increasing evidence suggests that the persistence of foodborne pathogens such as *L. monocytogenes* in food processing plants for years or even decades is an important factor in the transmission of foodborne pathogens. In addition, *L. monocytogenes* persistence in other food-associated environments (e.g., farms and retail establishments) may also contribute to food contamination and transmission of the pathogen to humans (Ferreira et al., 2014).

Population heterogeneity is an important component of the survival strategy of a microbial population. The long-term success of the population depends on the robustness and fitness of the individual cells (Ryall et al., 2012). Obviously, optimization and validation of (novel) processing strategies is required, and detailed insight into inactivation kinetics is essential, requiring both information about strain heterogeneity (Van Boeijen et al., 2011; 2008; Zwietering et al., 2021), and strain-environment interaction (Chen et al., 2020; Harrand et al., 2019). When a population is uniform, the individual cells within the population have a similar probability per unit of time to be inactivated, and therefore the corresponding inactivation curve follows an exponential decline. When the inactivation curve is plotted on a logarithmic scale, this results in linear inactivation. Inactivation curves can deviate from linearity, and shoulders and tails in inactivation curvatures have been reported (Metselaar et al., 2013; Van Boeijen et al., 2008; Cerf, 1977). Various explanations have been proposed for observed shoulders in an inactivation curve. A shoulder curvature might be caused by organisms being present in clumps, and the length of the shoulder coincides with the time all but one cell in a clump have been killed (Cerf, 1977). Alternately, the shoulder period has been explained by the presence of a critical cellular component that needs to be destroyed before inactivation ensues (Geeraerd et al., 2000) (and references therein). Tailing has been observed for many pathogens upon exposure to different lethal stresses; here, the initial exponential inactivation is followed by a slower decrease. Tailing of inactivation curves has been attributed to heterogeneity in a microbial population with respect to variation in sensitivity of the single cells toward lethal stress. The reduced sensitivity can be attributed to both genotypic and phenotypic diversity, as the enhanced survival of persister cells can be a consequence of a transient phenotypic switch as well as of inheritable mutations (see, e.g., Avery, 2006; Balaban et al., 2004; Van Boeijen et al., 2010; Veening et al., 2008). Previous studies reported the isolation of stable stress-resistant variants derived from *L. monocytogenes* strains EGDe, LO28, and ScottA (see, e.g., Karatzas and Bennik, 2002; Metselaar et al., 2013; 2015; Rajkovic et al., 2009; Van Boeijen et al., 2011; 2008). The difference between transient and stable stress-resistant variants is summarized in Figure 1.1, together with the method used to isolate these variants.

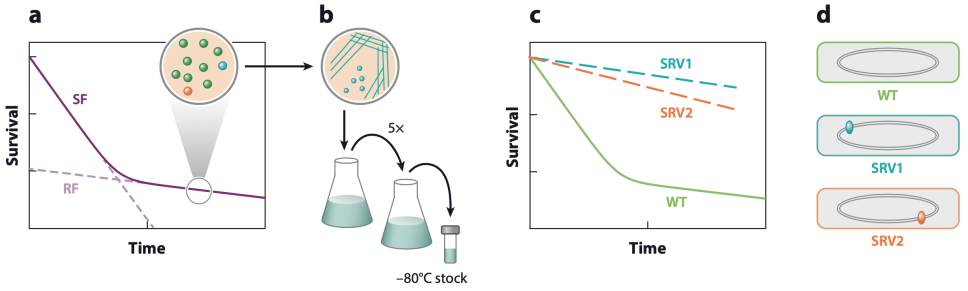


***Figure 1.1:*** *Schematic representation of the stress-resistant variant isolation strategy. (a) Upon exposure to stress, a sensitive wild-type (WT) fraction (SF) and a stress-resistant fraction (RF) can be identified, the latter composed of persister-type WT cells (green) and resistant variants (blue and orange). (b) Approximately 100 colonies are randomly selected from the tail and stored in the freezer. (c) Stress exposure of cultures derived from the approximately 100 stocks enable the identification and quantification of the number of stable stress-resistant variants (SRVs; represented by SRV1 and SRV2) that show enhanced survival compared to WT. (d) Subsequent comparative genome analysis allows for identification of mutations in the SRVs (adopted from Abee et al. 2016).*

## Mutations drive heterogeneity in bacterial populations

Mutational events are among the main drivers of heterogeneity in bacteria, and are the so-called fuel for adaptation. As such, mutations stand at the origin of the previously described *L. monocytogenes ctsR* and *rpsU* variants (e.g. Metselaar et al., 2013; Van Boeijen et al., 2008). Mutational events, including point mutations, insertions, and deletions, are caused by errors during copying of DNA, and occur spontaneously over time. In addition, mutations can also be generated by the stress-induced activation of repair systems such as the SOS-response that allows cells to read over specific types of DNA damage, at the expense of an increased risk of mutation (Schlacher and Goodman, 2007; van der Veen et al., 2010).

In a well-adapted system in a constant environment, where proteins are highly optimized to their function, most mutations will be deleterious (Elena and Lenski, 2003; Eyre-Walker and Keightley, 2007; Perfeito et al., 2007), and the rate at which mutations occur is expected to be kept low by population genetic forces (Drake et al., 1998). Especially in stressful environments, this mutation rate is of critical importance for the speed with which populations can adapt. Comparative studies using *L. monocytogenes* wild type(s) and targeted mutants have shown roles for the RecA controlled SOS response, and MutS/MutL

DNA damage repair proteins in maintaining a low mutation rate (Mérino et al., 2002; van der Veen and Abee, 2011b). Although so-called mutator strains with defects in DNA repair systems have been isolated from a number of foodborne pathogens including *Salmonella* spp. and *Staphylococcus aureus*, (Sheng et al., 2020; Wang et al., 2018; Wang et al., 2013) the isolation of mutator strains from *L. monocytogenes* from food or clinical samples has not been reported up to now.

## The mechanism of stress resistance

Despite the fact that the presence of stable stress-resistant subpopulations has been clearly demonstrated, the mechanisms behind the increased stress resistance are still not fully understood. Mutations in the class III heat shock repressor *ctsR* were shown to be responsible for the increased HHP and/or heat-resistant phenotype for a selection of *L. monocytogenes* ScottA, EGDe, and LO28 variants (Karatzas et al., 2003; Van Boeijen et al., 2011; 2010). Sequence comparison of wild type (WT) and variants allowed identification of a large number of mutations in *ctsR*, such as single nucleotide polymorphisms, inserts, and deletions. Mutations in *ctsR* can lead to a defect in the repression of a number of chaperone encoding genes like *clpC*, which results in transcription of these stress response genes, with concomitant activation of stress defense, providing increased stress resistance.

Next to HHP and heat treatment, acid stress treatment also resulted in selection of acid stress–resistant variants of *L. monocytogenes* (Metselaar et al., 2015; 2013). Phenotypic characterization of 23 stable acid-stress resistant variants demonstrated that the variants could be clustered in three clusters and four individual variants. The variants showed multiple-stress resistance, with both unique and overlapping features related to stress resistance, growth, motility, biofilm formation, and virulence indicators. Subsequent whole-genome sequencing (WGS) of the variants revealed mutations in *rpsU* that encodes ribosomal protein S21 in those variants that were grouped in the largest phenotypic cluster (11 isolates), whereas mutations in *ctsR* (see above) were not found in any of the acid- stress resistant variants. In *L. monocytogenes*, *rpsU* is located between *rsmE* (a putative 16S rRNA methyltransferase) and *yqeY* (GatB/YqeY domain-containing protein). There is not much known about the specific function of ribosomal protein S21 in *L. monocytogenes* or about its role in stress resistance in general. Some work has been done in *Bacillus subtilis*, and a *B. subtilis rpsU* mutant showed unusual ribosome profiles, a reduced growth rate, and reduced motility (Akanuma et al., 2012; Takada et al., 2014). Notably, a role in cold

adaptation and cold stress response has been suggested for specific ribosomal proteins (Durack et al., 2013; Ivy et al., 2012). In other microorganisms, expression of S21 was suggested to be temperature-regulated (O'Connell and Thomashow, 2000; Sato et al., 1997). The data of Metselaar et al. (2015) also suggested that in *L. monocytogenes* S21 plays a role in growth at lower temperatures, because all *rpsU* variants show a severely reduced growth rate in BHI at 7°C compared to the wild type. This growth defect is still visible at 30°C but restored at 37°C (Metselaar et al., 2013).

Understanding how the genotype–environment interactions between strain characteristics such as diversity and fitness, and environmental parameters affects stress response and subsequent microbial survival, is useful for designing effective intervention strategies.

## Stress response via SigB in *Listeria monocytogenes*

One of the primary stress-response systems in *L. monocytogenes* is Sigma factor B (SigB). SigB is the alternative transcription factor that controls the general stress response (GSR) (Liu et al., 2019; NicAogáin and O'Byrne, 2016). SigB activation by one type of stress is known to provide cross protection against other types of stress (Begley et al., 2002; Bergholz et al., 2012), providing an explanation for multiple stress resistance of cells in which SigB has been activated. Many SigB-dependent genes are differentially expressed under various growth conditions (Toledo-Arana et al., 2009), and environmental conditions play a major role in the activation of the SigB-mediated stress response (Shen et al., 2014). SigB activity is controlled both translationally and post translationally by the “stressosome” stress-signal sensing and integration hub. The structure of this hub has recently received attention from multiple research groups (Dessaux et al., 2020a; Guerreiro et al., 2020; Williams et al., 2019). Activation of SigB is controlled by the stressosome, a signal integration complex that relays a range of stress signals and activates the sigma B regulon (Dessaux et al., 2020b; Guldimann et al., 2016; NicAogáin and O'Byrne, 2016; Radoshevich and Cossart, 2018), see Figure 1.2. The exact mechanism by which the stressosome responds to signals is still under investigation, although recent work suggests that the adaptive stress response upon exposure to blue light involves the blue light sensor *rsbL* (Dorey et al., 2019).

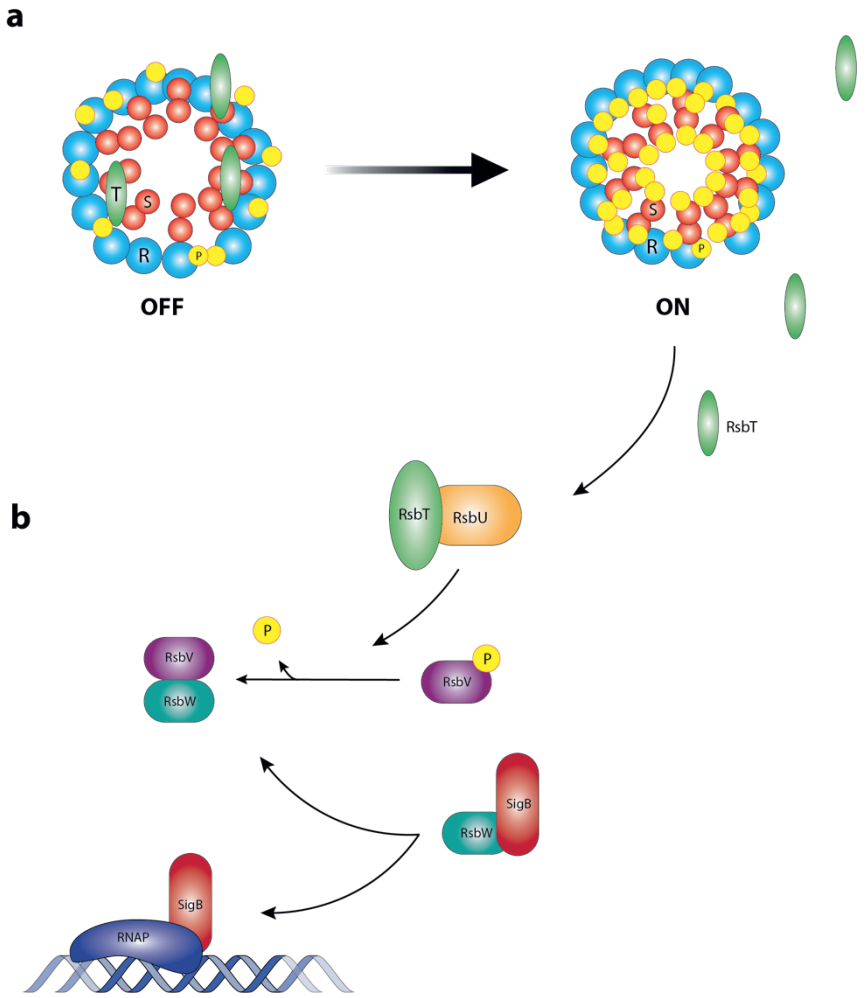


***Figure 1.2**: Schematic overview of the stressosome and SigB activation.*
*Following perception of a stress signal, RsbT dissociates from RsbR and RsbS (T, R and S in the stressosome), after activation of its kinase activity (a). RsbT is released from the stressosome and binds to RsbU. The phosphatase activity of RbsU is activated and removes a phosphate (P) group from RbsV. The anti-sigma factor RsbW has a higher affinity for the now dephosphorylated RsbV than for SigB, resulting in release of SigB allowing it to bind to RNA polymerase and initiate transcription of SigB regulon members (b) (adapted from Dessaux et al., 2020b and Cabeen et al., 2017).*

In the in vitro stressosome model proposed by Williams et al. (2019), phosphorylation of RsbR and RsbS (Figure 1.2a) triggers a signaling cascade of RsbU, RsbV and RsbW (Figure 1.2b), resulting in the activation of SigB. A revision of this stressosome model was proposed by Dessaux et al. in 2020, where they suggested an additional role for paralogues of RsbR in attenuating the generation of active stressosome complexes upon the sensing of stress, possibly giving rise to environmental modulation of stressosome related activation of SigB.

Further work is required to elucidate the details of the underlying mechanisms of this SigB-involved signalling cascade and the ribosome-induced modulation of *L. monocytogenes* fitness and stress resistance.

## Outline of this thesis

Population heterogeneity appears to be an important aspect of *L. monocytogenes* survival and transmission, and mutations drive this heterogeneity in bacterial populations. To date, isolation of *L. monocytogenes* mutators strains from food has not been described. Therefore, in **chapter 2** we investigated the rate at which mutations occur for a set of 20 *Listeria monocytogenes* strains, and focus on a foodborne isolate that showed to be a mutator strain. We combined a whole genome sequencing approach with targeted mutations to assess the role of *mutS* in this mutator phenotype.

Two of the previously isolated multiple-stress resistant *rpsU* variants are described in more detail in **chapter 3**, where we investigated the phenotypic effects of a deletion, and a point mutation in *rpsU* in variants 14 and 15, respectively. We focus on the differences and overlap in the stress response of these two variants that harbour a different mutation, but share a largely overlapping phenotype.

From recent work on comparative whole genome sequencing analysis of *Listeria monocytogenes* food and clinical isolates, of which some isolates were isolated decades apart, we know that strains can persist in the food processing environment for many years, where strains are exposed to continuous selection pressures. The possibility of the presence of (stress resistant) *L. monocytogenes* cells in food processing environments for a prolonged period of time, in combination with selection on increased growth rate, raises the question of how the low-fitness, stress-resistant variants 14 and 15 will evolve over time. In **chapters 4 and 5** we explore this concept by using an experimental evolution protocol where we selected for increased fitness, defined as a higher maximum specific growth rate ($\mu_{max}$)

compared to the ancestor variant 15 or 14, respectively, while monitoring both fitness and stress-resistance of the evolved strains. Finally, in **chapter 6** the results of the work in this thesis are combined, the relevance and impact are discussed and recommendations for future research are presented. For an overview of all chapters, see Figure 1.3. Overall, the work presented in this thesis provides more insight into the adaptive stress behaviour of *L. monocytogenes* and increases our understanding how this notorious pathogen is able to grow and survive in changing environments.

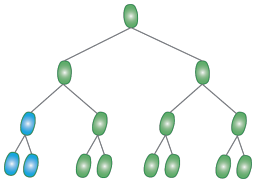

**Chapter 2**: Determination of spontaneous mutation rates in *Listeria monocytogenes* food isolates identified a hypermutator strain with an insertion in DNA mismatch repair protein MutS.

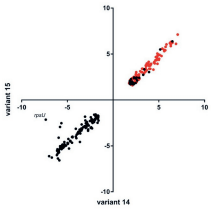


**Chapter 3**: Gene profiling-based phenotyping for identification of cellular parameters that contribute to fitness, stress-tolerance and virulence of *Listeria monocytogenes* variants.

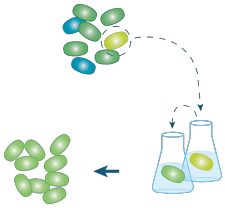

**Chapter 4**: Amino acid substitutions in ribosomal protein RpsU enable switching between high fitness and multiple-stress resistance in *Listeria monocytogenes*.

**Chapter 5**: Low fitness and high stress resistance in a *Listeria monocytogenes* RpsU deletion mutant is reversed by single amino acid substitutions in ribosomal protein RpsB.

***Figure 1.3**: Schematic overview of the research presented in this thesis.*

## References

**Abee, T., Koomen, J., Metselaar, K.I., Zwietering, M.H., Den Besten, H.M.W.**, 2016. Impact of pathogen population heterogeneity and stress-resistant variants on food safety. Annu. Rev. Food Sci. Technol. 7, 439–456. doi:10.1146/annurev-food-041715-033128

**Akanuma, G., Nanamiya, H., Natori, Y., Yano, K., Suzuki, S., Omata, S., Ishizuka, M., Sekine, Y., Kawamura, F.**, 2012. Inactivation of ribosomal protein genes in *Bacillus subtilis* reveals importance of each ribosomal protein for cell proliferation and cell differentiation. J. Bacteriol. 194, 6282–6291. doi:10.1128/JB.01544-12

**Arcari, T., Feger, M.-L., Guerreiro, D.N., Wu, J., O'Byrne, C.P.**, 2020. Comparative review of the responses of *Listeria monocytogenes* and *Escherichia coli* to low pH stress. Genes. 11, 1330. doi:10.3390/genes11111330

**Avery, S.V.**, 2006. Microbial cell individuality and the underlying sources of heterogeneity. Nat. Rev. Micro. 4, 577–587. doi:10.1038/nrmicro1460

**Balaban, N.Q., Merrin, J., Chait, R., Kowalik, L., Leibler, S.**, 2004. Bacterial persistence as a phenotypic switch. Science 305, 1622–1625. doi:10.1126/science.1099390

**Begley, M., Gahan, C.G.M., Hill, C.**, 2002. Bile stress response in *Listeria monocytogenes* LO28: adaptation, cross-protection, and identification of genetic loci involved in bile resistance. Appl. Environ. Microbiol. 68, 6005–6012. doi:10.1128/aem.68.12.6005-6012.2002

**Begley, M., Hill, C.**, 2015. Stress adaptation in foodborne pathogens. Annu. Rev. Food. Sci. Technol. 6, 191-210. http://dx.doi.org/10.1146/annurev-food-030713-092350.

**Ryall B., Eydallin, G., Ferenci, T.,** 2012. Culture history and population heterogeneity as determinants of bacterial adaptation: the adaptomics of a single environmental transition. Microbiol. Mol. Biol. Rev. 76, 597–625. doi:10.1128/MMBR.05028-11

**Bergholz, T.M., Bowen, B., Wiedmann, M., Boor, K.J.,** 2012. *Listeria monocytogenes* shows temperature-dependent and -independent responses to salt stress, including responses that induce cross-protection against other stresses. Appl. Environ. Microbiol. 78, 2602–2612. doi:10.1128/AEM.07658-11

**Bergholz, T.M., Switt, A.I.M., Wiedmann, M.,** 2014. Omics approaches in food safety: fulfilling the promise? Trends Microbiol. 22, 275–281. doi:10.1016/j.tim.2014.01.006

**Cabeen, M.T., Russell, J.R., Paulsson, J., Losick, R.,** 2017. Use of a microfluidic platform to uncover basic features of energy and environmental stress responses in individual cells of *Bacillus subtilis*. PLOS Genet. 13, e1006901. doi:10.1371/journal.pgen.1006901

**Carpentier, B., Cerf, O.,** 2011. Review--Persistence of *Listeria monocytogenes* in food industry equipment and premises. Int. J. Food Microbiol. 145, 1–8. doi:10.1016/j.ijfoodmicro.2011.01.005

**Cerf, O.,** 1977. Tailing of survival curves of bacterial spores. J. Appl. Bacteriol. 42, 1–19. doi:10.1111/j.1365-2672.1977.tb00665.x

**Chen, R., Skeens, J., Orsi, R.H., Wiedmann, M., Guariglia-Oropeza, V.,** 2020. Pre-growth conditions and strain diversity affect nisin treatment efficacy against *Listeria monocytogenes* on cold-smoked salmon. Int. J. Food Microbiol. 333, 108793. doi:10.1016/j.ijfoodmicro.2020.108793

**Dessaux, C., Guerreiro, D.N., Pucciarelli, M.G., O'Byrne, C.P., García-Del Portillo, F.,** 2020a. Impact of osmotic stress on the phosphorylation and subcellular location of *Listeria monocytogenes* stressosome proteins. Sci Rep 10, 20837–15. doi:10.1038/s41598-020-77738-z

**Dessaux, C., Guerreiro, D.N., Pucciarelli, M.G., O'Byrne, C.P., Portillo, F.G.-D., 2020b**. Impact of osmotic stress on the phosphorylation and subcellular location of *Listeria monocytogenes* stressosome proteins. Sci Rep 1–15. doi:10.1038/s41598-020-77738-z

**Dorey, A.L., Lee, B.-H., Rotter, B., O'Byrne, C.P.,** 2019. Blue light Sensing in *Listeria monocytogenes* is temperature-dependent and the transcriptional response to it is predominantly SigB-dependent. Front. Microbiol. 10, 2497. doi:10.3389/fmicb.2019.02497

**Drake, J.W., Charlesworth, B., Charlesworth, D., Crow, J.F.,** 1998. Rates of spontaneous mutation. Genetics 148, 1667–1686. doi:10.2307/2410123

**Durack, J., Ross, T., Bowman, J.P.,** 2013. Characterisation of the transcriptomes of genetically diverse *Listeria monocytogenes* exposed to hyperosmotic and low temperature conditions reveal global stress-adaptation mechanisms. PLoS One 8, e73603. doi:10.1371/journal.pone.0073603

**Elena, S.F., Lenski, R.E.,** 2003. Evolution experiments with microorganisms: the dynamics and genetic bases of adaptation. Nat. Rev. Genet. 4, 457–469. doi:10.1038/nrg1088

**Eyre-Walker, A., Keightley, P.D.,** 2007. The distribution of fitness effects of new mutations. Nat. Rev. Genet. 8, 610–618. doi:10.1038/nrg2146

**Ferreira, V., Wiedmann, M., Teixeira, P., Stasiewicz, M.J.,** 2014. *Listeria monocytogenes* persistence in food-associated environments: epidemiology, strain characteristics, and implications for public health. J Food Prot. 77, 150–170. doi:10.4315/0362-028X.JFP-13-150

**Geeraerd, A.H., Herremans, C.H., Van Impe, J.F.,** 2000. Structural model requirements to describe microbial inactivation during a mild heat treatment. Int. J. Food Microbiol. 59, 185–209. doi:10.1016/s0168-1605(00)00362-7

**Guerreiro, D.N., Arcari, T., O'Byrne, C.P.,** 2020. The σB-mediated general stress response of *Listeria monocytogenes*: life and death decision making in a pathogen. Front. Microbiol. 11, 1505. doi:10.3389/fmicb.2020.01505

**Guldimann, C., Boor, K.J., Wiedmann, M., Guariglia-Oropeza, V.,** 2016. Resilience in the face of uncertainty: Sigma factor b fine-tunes gene expression to support homeostasis in Gram-positive bacteria. Appl. Environ. Microbiol. 82, 4456–4469. doi:10.1128/AEM.00714-16

**Harrand, A.S., Jagadeesan, B., Baert, L., Wiedmann, M., Orsi, R.H., Dudley, E.G.,** 2020. Evolution of *Listeria monocytogenes* in a food processing plant involves limited

single-nucleotide substitutions but considerable diversification by gain and loss of prophages. Appl. Environ. Microbiol. 86, 38. doi:10.1128/AEM.02493-19

**Harrand, A.S., Kovac, J., Carroll, L.M., Guariglia-Oropeza, V., Kent, D.J., Wiedmann, M.,** 2019. Assembly and characterization of a pathogen strain collection for produce safety applications: pre-growth conditions have a larger effect on peroxyacetic acid tolerance than strain diversity. Front. Microbiol. 10. doi:10.3389/fmicb.2019.01223

**Ivy, R.A., Wiedmann, M., Boor, K.J**., 2012. *Listeria monocytogenes* grown at 7°C shows reduced acid survival and an altered transcriptional response to acid shock compared to *L. monocytogenes* grown at 37°C. Appl. Environ. Microbiol. 78, 3824–3836. doi:10.1128/AEM.00051-12

**Karatzas, K.A.G., Bennik, M.H.J.,** 2002. Characterization of a *Listeria monocytogenes* Scott A isolate with high tolerance towards high hydrostatic pressure. Appl. Environ. Microbiol. 68, 3183–3189. doi:10.1128/AEM.68.7.3183-3189.2002

**Karatzas, K.A.G., Valdramidis, V.P., Wells-Bennik, M.H.J.,** 2005. Contingency locus in *ctsR* of *Listeria monocytogenes* Scott A: a strategy for occurrence of abundant piezotolerant isolates within clonal populations. Appl. Environ. Microbiol. 71, 8390–8396. doi:10.1128/AEM.71.12.8390-8396.2005

**Karatzas, K.A.G., Wouters, J.A., Gahan, C.G.M., Hill, C., Abee, T., Bennik, M.H.J.,** 2003. The CtsR regulator of *Listeria monocytogenes* contains a variant glycine repeat region that affects piezotolerance, stress resistance, motility and virulence. Mol. Microbiol. 49, 1227–1238. doi:10.1046/j.1365-2958.2003.03636.x

**Koomen, J., Den Besten, H.M.W., Metselaar, K.I., Tempelaars, M.H., Wijnands, L.M., Zwietering, M.H., Abee, T.,** 2018. Gene profiling-based phenotyping for identification of cellular parameters that contribute to fitness, stress-tolerance and virulence of *Listeria monocytogenes* variants. Int. J. Food Microbiol. 283, 14–21. doi:10.1016/j.ijfoodmicro.2018.06.003

**Liu, Y., Orsi, R.H., Gaballa, A., Wiedmann, M., Boor, K.J., Guariglia-Oropeza, V.,** 2019. Systematic review of the *Listeria monocytogenes* σB regulon supports a role in stress response, virulence and metabolism. Future Microbiol. 14, 801–828. doi:10.2217/fmb-2019-0072

**Metselaar, K.I., Den Besten, H.M.W., Abee, T., Moezelaar, R., Zwietering, M.H.,** 2013. Isolation and quantification of highly acid resistant variants of *Listeria monocytogenes.* Int. J. Food Microbiol. 166, 508–514. doi:10.1016/j.ijfoodmicro.2013.08.011

**Metselaar, K.I., Den Besten, H.M.W., Boekhorst, J., van Hijum, S.A.F.T., Zwietering, M.H., Abee, T.,** 2015. Diversity of acid stress resistant variants of *Listeria monocytogenes* and the potential role of ribosomal protein S21 encoded by r*psU*. Front. Microbiol. 6, 422. doi:10.3389/fmicb.2015.00422

**Mérino, D., Poupet, H.R., Berche, P., Charbit, A.,** 2002. A hypermutator phenotype attenuates the virulence of *Listeria monocytogenes* in a mouse model. Mol. Microbiol. 44, 877–887. doi:10.1046/j.1365-2958.2002.02929.x

**NicAogáin, K., O'Byrne, C.P.,** 2016. The role of stress and stress adaptations in determining the fate of the bacterial pathogen *Listeria monocytogenes* in the food chain. Front. Microbiol. 7, 1962–16. doi:10.3389/fmicb.2016.01865

**O'Connell, K.P., Thomashow, M.F.,** 2000. Transcriptional organization and regulation of a polycistronic cold shock operon in *Sinorhizobium meliloti* RM1021 encoding homologs of the *Escherichia coli* major cold shock gene *cspA* and ribosomal protein gene *rpsU*. Appl. Environ. Microbiol. 66, 392–400. doi:10.1128/aem.66.1.392-400.2000

**Perfeito, L., Fernandes, L., Mota, C., Gordo, I.,** 2007. Adaptive mutations in bacteria: high rate and small effects. Science 317, 813–815. doi:10.1126/science.1142284

**Radoshevich, L., Cossart, P.,** 2018. *Listeria monocytogenes*: towards a complete picture of its physiology and pathogenesis. Nat. Rev. Microbiol. 16, 32–46. doi:10.1038/nrmicro.2017.126

**Rajkovic, A., Smigic, N., Uyttendaele, M., Medic, H., de Zutter, L., Devlieghere, F.,** 2009. Resistance of *Listeria monocytogenes*, *Escherichia coli* O157:H7 and *Campylobacter jejuni* after exposure to repetitive cycles of mild bactericidal treatments. Food Microbiol. 26, 889–895. doi:10.1016/j.fm.2009.06.006

**Sato, N., Tachikawa, T., Wada, A., Tanaka, A.,** 1997. Temperature-dependent regulation of the ribosomal small-subunit protein S21 in the cyanobacterium *Anabaena variabilis* M3. J. Bacteriol. 179, 7063–7071. doi:10.1128/jb.179.22.7063-7071.1997

**Schlacher, K., Goodman, M.F.,** 2007. Lessons from 50 years of SOS DNA-damage-induced mutagenesis. Nat. Rev. Mol. Cell Biol. 8, 587–594. doi:10.1038/nrm2198

**Shen, Q., Soni, K.A., Nannapaneni, R.,** 2014. Influence of temperature on acid-stress adaptation in *Listeria monocytogenes*. Foodborne Pathog. Dis. 11, 43–49. doi:10.1089/fpd.2013.1611

**Sheng, H., Huang, J., Han, Z., Liu, M., Lü, Z., Zhang, Q., Zhang, J., Yang, J., Cui, S., Yang, B.,** 2020. Genes and Proteomes associated with increased mutation frequency and multidrug resistance of naturally occurring mismatch repair-deficient *Salmonella* hypermutators. Front. Microbiol. 11, 770. doi:10.3389/fmicb.2020.00770

**Takada, H., Morita, M., Shiwa, Y., Sugimoto, R., Suzuki, S., Kawamura, F., Yoshikawa, H.,** 2014. Cell motility and biofilm formation in *Bacillus subtilis* are affected by the ribosomal proteins, S11 and S21. Biosci. Biotechnol. Biochem. 78, 898–907. doi:10.1080/09168451.2014.915729

**Toledo-Arana, A., Dussurget, O., Nikitas, G., Sesto, N., Guet-Revillet, H., Balestrino, D., Loh, E., Gripenland, J., Tiensuu, T., Vaitkevicius, K., Barthelemy, M., Vergassola, M., Nahori, M.-A., Soubigou, G., Régnault, B., Coppée, J.-Y., Lecuit, M., Johansson, J., Cossart, P.,** 2009. The *Listeria* transcriptional landscape from saprophytism to virulence. Nature 459, 950–956. doi:10.1038/nature08080

**Van Boeijen, I.K.H., Chavaroche, A.A.E., Valderrama, W.B., Moezelaar, R., Zwietering, M.H., Abee, T.,** 2010. Population diversity of *Listeria monocytogenes* LO28: phenotypic and genotypic characterization of variants resistant to high hydrostatic pressure. Appl. Environ. Microbiol. 76, 2225–2233. doi:10.1128/AEM.02434-09

**Van Boeijen, I.K.H., Francke, C., Moezelaar, R., Abee, T., Zwietering, M.H.,** 2011. Isolation of highly heat-resistant *Listeria monocytogenes* variants by use of a kinetic

modeling-based sampling scheme. Appl. Environ. Microbiol. 77, 2617–2624. doi:10.1128/AEM.02617-10

**Van Boeijen, I.K.H., Moezelaar, R., Abee, T., Zwietering, M.H.,** 2008. Inactivation kinetics of three *Listeria monocytogenes* strains under high hydrostatic pressure. J. Food Prot. 71, 2007–2013. doi:10.4315/0362-028x-71.10.2007

**van der Veen, S., Abee, T.,** 2011a. Contribution of *Listeria monocytogenes* RecA to acid and bile survival and invasion of human intestinal Caco-2 cells. Int. J. Med. Microbiol. 301, 334–340. doi:10.1016/j.ijmm.2010.11.006

**van der Veen, S., Abee, T.,** 2011b. Generation of variants in *Listeria monocytogenes* continuous-flow biofilms is dependent on radical-induced DNA damage and RecA-mediated repair. PLoS One 6, e28590–8. doi:10.1371/journal.pone.002859

**van der Veen, S., van Schalkwijk, S., Molenaar, D., de Vos, W.M., Abee, T., Wells-Bennik, M.H.J.,** 2010. The SOS response of *Listeria monocytogenes* is involved in stress resistance and mutagenesis. Microbiology 156, 374–384. doi:10.1099/mic.0.035196-0

**Vanlint, D., Rutten, N., Michiels, C.W., Aertsen, A.,** 2012. Emergence and stability of high-pressure resistance in different food-borne pathogens. Appl. Environ. Microbiol. 78, 3234–3241. doi:10.1128/AEM.00030-12

**Veening, J.-W., Smits, W.K., Kuipers, O.P.,** 2008. Bistability, epigenetics, and bet-hedging in bacteria. Annu. Rev. Microbiol. 62, 193–210. doi:10.1146/annurev.micro.62.081307.163002

**Wang, H., Xing, X., Wang, J., Pang, B., Liu, M., Larios-Valencia, J., Liu, T., Liu, G., Xie, S., Hao, G., Liu, Z., Kan, B., Zhu, J.,** 2018. Hypermutation-induced in vivo oxidative stress resistance enhances *Vibrio cholerae* host adaptation. PLoS Pathog. 14, e1007413. doi:10.1371/journal.ppat.1007413

**Wang, S., Wu, C., Shen, J., Wu, Y., Wang, Y.,** 2013. Hypermutable *Staphylococcus aureus* strains present at high frequency in subclinical bovine mastitis isolates are associated with the development of antibiotic resistance. Vet. Microbiol. 165, 410–415. doi:10.1016/j.vetmic.2013.04.009

**Williams, A.H., Redzej, A., Rolhion, N., Costa, T.R.D., Rifflet, A., Waksman, G., Cossart, P.,** 2019. The cryo-electron microscopy supramolecular structure of the bacterial stressosome unveils its mechanism of activation. Nat. Commun. 10, 3005–3010. doi:10.1038/s41467-019-10782-0

**Zwietering, M.H., Garre, A., Den Besten, H.M.W.,** 2021. Incorporating strain variability in the design of heat treatments: A stochastic approach and a kinetic approach. Food Res. Int. 139, 109973. doi:10.1016/j.foodres.2020.109973

# 2

# Determination of spontaneous mutation rates in *Listeria monocytogenes* food isolates identified a hypermutator strain with an insertion in DNA mismatch repair protein MutS

Jeroen Koomen, Peter Schubert, Marcel H. Tempelaars, Tjakko Abee.

## Abstract

Population heterogeneity is an important element of the survival strategy of the food pathogen *Listeria monocytogenes* to cope with environmental stresses and to survive during transmission to the human host. Most research in this field has focussed on the description of standing genetic variation i.e., the heterogeneity that is already present in a population, without investigating the rate at which populations can acquire new mutations. Here, we used a high-throughput version of the classical Luria-Delbrück fluctuation assay, to investigate the rate of spontaneous mutation in a set of 20 whole genome sequenced (WGS) *L. monocytogenes* food isolates. All strains, except one, had a mutation rate of between $4.6 \cdot 10^{-10}$ and $3.5 \cdot 10^{-9}$, while the strain FBR16 showed an approximately 100-fold to 1000-fold higher mutation rate of $2.9 \cdot 10^{-7}$ mutations per gene per generation. Subsequent WGS analysis of previously sequenced genomes revealed a 179 bp insertion in the DNA mismatch repair gene *mutS* gene of FBR16 as the cause of the mutator phenotype. The mutator phenotype was lost upon restoration of the *mutS* gene, confirming the insertion-induced reduction of MutS activity.

## Introduction

*Listeria monocytogenes* is a ubiquitous food pathogen, that can cause listeriosis, a rare disease with high mortality rate (Toledo-Arana et al., 2009). It is a model species to describe transmission from the environment to the human host that relies on population heterogeneity, strain variability, and adaptive behaviour to cope with environmental stresses during this transmission (Abee et al., 2016). When a population of cells is exposed to stress, the inherent heterogeneity in a population can lead to the differential survival of a subset of cells, resulting in a tailing of the inactivation curve (Cerf, 1977). The role of population heterogeneity in the stress survival capacity of *L. monocytogenes* has been under intense study. Part of this heterogeneity is heritable, and stable multiple-stress resistant variants have been isolated from diverse strains such as EGDe, LO28, and ScottA after a single exposure to stress (Karatzas and Bennik, 2002; Metselaar et al., 2013; 2015; Rajkovic et al., 2009; Van Boeijen et al., 2011; 2008). However, most work on the diversity and heterogeneity of *L. monocytogenes* is done on standing genetic variation. Most authors have investigated the diversity and heterogeneity that is already present in populations of *L. monocytogenes*, giving very little attention to the fundamental process of mutagenesis that is underlying this variation, and the speed at which new mutations occur.

Mutations in bacteria are produced stochastically during replication of DNA, or after environmental insults that lead to DNA damage, requiring repair by genes involved in the SOS response (van der Veen et al., 2010). The SOS response includes the activation of a translesion polymerase that allows cells to read over damaged parts of the DNA, reviving stalled replication forks at the cost of an increase in mutation rate (van der Veen et al., 2010), see Maslowska et al. (2019) for a review. The generation of mutations is considered to be neutral with respect to their effect on fitness (Luria and Delbrück, 1943), i.e., cells produce both beneficial, neutral, and deleterious mutations. However, most cells are well adapted to their environment, and in stable environmental conditions, random mutations are more likely to be deleterious than beneficial (Elena and Lenski, 2003; Eyre-Walker and Keightley, 2007; Kimura, 1967; Perfeito et al., 2007). Therefore, there is a trade-off between mutations (which increase adaptability to novel environments), and an increase in genetic load (the negative effects of deleterious mutations). This trade-off is believed to be the cause of the low mutation rates in populations that are typically observed. The energy requirements needed for higher fidelity, and thus a lower mutation rate, are often seen as a barrier that prevent an even lower mutation rate. In addition, population genetic forces

such as drift will limit selection on even lower mutation rates (Lynch et al., 2016). However, mutator strains, with mutation frequencies that are at least an order of magnitude above the species baseline, have been isolated and characterized for a range of bacterial species including foodborne pathogens (Prunier and Leclercq, 2005; Sniegowski et al., 1997). These mutator strains typically have mutations in DNA mismatch repair genes such as *mutS* (lmo1403) and *mutL* (lmo1404). In *L. monocytogenes, mutS* (lmo1403) and *mutL* are co-transcribed in an operon together with lmo1405 (glycerol uptake operon antiterminator regulatory protein), and deletion of *mutSL* results in a strong increase in mutations, including those leading to rifampicin resistance (Mérino et al., 2002).

Currently, studies on mutation rate in *L. monocytogenes* have used whole genome sequencing data of long-term studies in food processing facilities to infer mutation rate (Harrand et al., 2020) However, that method is impractical in situations where long term histories of strains are not available. Here, we use a high-throughput method based on the Luria-Delbrück fluctuation assay (Luria and Delbrück, 1943) to investigate the spontaneous mutation rate in 20 selected strains of *L. monocytogenes*, and we applied a whole genome approach to assess to role of *mutS* in a hypermutator foodborne isolate.

## Materials and methods

### Strains and growth conditions

A set of 20 strains of whole genome sequenced *L. monocytogenes* with different origins, and various histories of laboratory usage (Aryani et al., 2015) was used. Cells from -80°C stocks were grown at 30°C for 48 hours on brain heart infusion (BHI, Oxoid, Hampshire) agar (1.5 % [w/w], bacteriological agar no. 1 Oxoid, Hampshire) plates. A single colony was used to inoculate 10 ml of BHI broth in a 12 ml tube (Greiner) and incubated overnight (ON, 18 to 22 hours) at 30°C under continuous shaking at 160 rpm.

### Selective medium

Rifampicin (Rif, Sigma-Aldrich GmbH, St. Luis MO, USA) was stored as stock solutions of 2 mg/ml or 64 mg/ml in DMSO and kept at 4°C. Stocks were used within 6 months as advised by stability studies by (Yu et al. 2011) and (Karlson and Ulrich, 1969). Rif-supplemented media were prepared by adding appropriate volumes of stock solution to the medium after cooling down to 55°C. Rif-supplemented broth was prepared on the day of use, and rif-supplemented agar plates were kept at 4°C for a maximum of 2 days. Agar plates for spotting (see below) were dried for up to an hour in a laminar-flow cabinet before use.

### Fluctuation analysis

Fluctuation analysis was performed as described by (Pope et al., 2008; Rosche and Foster, 2000), also see Appendix 1. This version of the Luria-Delbrück fluctuation assay estimates the mutation rate using the number of mutants that have gained resistance to rifampicin. By determining the number of rifampicin resistant mutants in up to 48 parallel cultures per strain, we were able to estimate the number of mutational events that have led to the observed distribution of mutants (see Appendix 1).

Briefly, ON-cultures were serially diluted in BHI to approximately $5 \cdot 10^4$ cfu/ml, of which 200 µl was transferred into 96-microwell plates resulting in approximately $1 \cdot 10^4$ cfu per well, and plates were incubated at 30°C for 17±2 hours.

The total viable counts (TVCs) of the parallel cultures just after inoculation of the wells (i.e. $N_0$) was estimated by spotting 4 aliquots of 20 µl of appropriate dilutions onto BHI agar plates, and incubating at 30°C for 24 hours. To estimate the mean final cell density of the parallel cultures (i.e., $N_{max}$) TVC was determined by spot plating as described above. To quantify the number of rif-resistant (rifR) mutants in these cultures, an aliquot of 30 µl of

all the parallel cultures was spotted on square Rif-BHI-agar plates using a multichannel pipet. The concentration of Rif was set at 2 µg/ml, approximately four times the highest minimal inhibitory concentration (MIC) of WT strains, as suggested by Rosche and Foster, 2000. Plates were incubated at 30°C for 96 hours before enumeration of colonies. Jackpot cultures, containing an uncountably high number of mutants, were truncated, scored at 120 mutant colonies/spot, and used as the "Winsorization" parameter during later analysis in FLAN. Mutant colonies and the mean final number of the cells of the parallel cultures were used to calculate the mutation rate in the statistical programming language R, using the FLAN package version 0.8 (Mazoyer and Drouilhet, 2017), using mutestim() with parameters: model= "LD", method= "ML", plateff= 0.3, winsor=120.

The FBR16_mutS_repaired mutant (see below Construction of the FBR16_mutS_repaired mutant) was tested together with FBR16 WT, in 24 parallel wells filled with cultures of 100 µl, and subsequent plating of the whole well content was done on a 9-cm diameter petri dish. This higher plating volume allows for higher resolution in the number of rifR colonies, and supported the more accurate estimation of mutation rates for these two strains.

### Construction of the FBR16_mutS_repaired mutant

Mutant strain FBR16_mutS_repaired was constructed using the temperature sensitive suicide plasmid pAULA (Chakraborty et al., 1992). As the *mutS* gene from strain FBR12 was identical to that of FBR16, but without the insertion, we amplified *mutS* from genomic DNA of FBR12 using a KAPA HiFi Hotstart ReadyMix polymerase (KAPA Biosystems, USA), and primers MutSrepair_F: 5'-TGAAGAATTCGTAAGGGATGATGAGATAATGACAGA-3' and MutSrepair_R: 5'-ATGAGTCGACATCCCGCTTCTTCCACTAAAATA-3'. The resulting fragment was ligated in frame to the pAULA multiple cloning site via the EcoR1 and Sal1 restriction sites that were introduced to the fragments by the respective primers. The resulting plasmid was electroporated (2.5 kV, 25 µF, 200 Ω), in a 0.2 cm cuvette using a BIO-RAD GenePulser, to cells of FBR16, and plated on BHI agar at 30°C with 5 µg/ml erythromycin to select for transformants.

Two erythromycin resistant colonies were inoculated in separate tubes in BHI broth supplemented with 5 µg/ml erythromycin and grown overnight at 42°C to select for plasmid integration. Selected strains resulting from a single cross-over integration event were grown overnight in BHI at 30°C to induce double crossover events and were subsequently plated at 30°C. Resulting colonies were plated on BHI with and without 5 µg/ml erythromycin and incubated at 30°C. Colonies sensitive to erythromycin were selected. PCR with primers

MutS_F 5'-CGTCCGTTAATAGACCGAAAAA-3' and MutS_R 5'-AGCGGCCTTCTGGGAGCA-3' was used to confirm the ~200 bp difference between the mutS of FBR16 and FBR16_mutS_repaired. Subsequently, PCR and amplicon sequencing using the primers: MutS_seqCheck_F: 5'-CTGTGCACGAAGAAGATACGATT-3', and MutS_seqCheck_R: 5'-CAGCGGGAACAAAACAACC-3' confirmed the correct insertion of the FBR 12 *mutS* gene and deletion of the original FBR16 *mutS* gene that harboured the insertion.

### In silico analysis of insertions in *mutS*

The *mutS* genes of the 20 strains were aligned locally by MAFFT (v7.419) (Rozewicki et al., 2019), and the alignment was visualized with the MSA viewer as implemented at www.ncbi.nlm.nih.gov/. To investigate the number of *mutS* sequences with insertions in WGS sequences deposited to online databases, we performed a blast search on www.ncbi.nlm.nih.gov/. Using *mutS* of *L. monocytogenes* EGDe as reference we queried the RefSeq Genome Database, limited to *Listeria monocytogenes* (taxid:1639). The output was downloaded as .txt and aligned locally with MAFFT. Sequences were manually compared in Mesquite 3.61 (Maddison and Maddison, 2019).

## Results and discussion

### Spontaneous mutation rate in 20 strains

We have used a high-throughput version of the Luria-Delbrück fluctuation assay on a set of 20 strains, that includes laboratory reference strains (e.g., EGDe, ScottA, and LO28), as well as food isolates, to determine the spontaneous mutation rate. Nineteen of the twenty strains showed mutation rates between $4.6 \cdot 10^{-10}$ and $3.5 \cdot 10^{-9}$ mutations per gene per generation. However, strain FBR16 showed a much higher mutation rate (Figure 2.1), pointing to a mutator strain phenotype. This strain was selected for more detailed genetic analysis and quantification of its mutation rate.

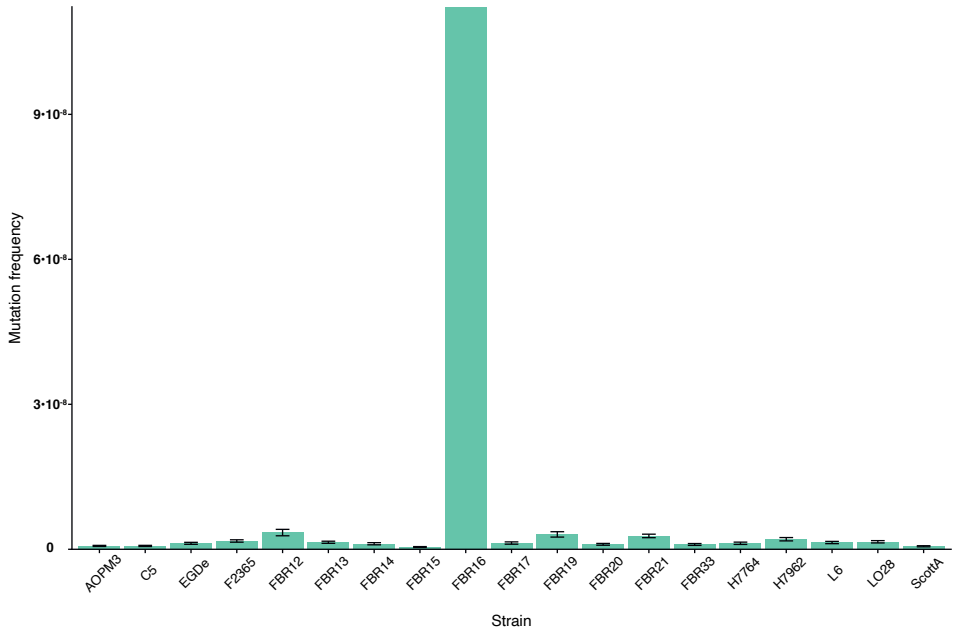


***Figure 2.1**: Mutation frequency of selected strains of* Listeria monocytogenes *as determined by the LD fluctuation assay. The value for FBR16 is an estimation, as the winsoriszation cutoff was reached in all tested parallel lines.*

### Insertion in *mutS* of FBR16

Alterations in conserved DNA mismatch repair genes such as *mutS* (lmo1403) and *mutL* (lmo1404) are known to increase mutation rates in several species, including *L. monocytogenes* (Mérino et al., 2002). Comparison of previously obtained whole genome sequences of the 20 strains revealed a 179 bp insertion in the *mutS* DNA repair gene of FBR16 (Figure 2.2a and 2.2b). Moreover, this insertion resulted in a premature stopcodon (TGA), 12 nucleotides from the start of the insertion (see Figure 2.2b), suggesting that the MutS protein in FBR16 will be truncated. In *L. monocytogenes*, *mutS* and *mutL* are transcribed in an operon together with the glycerol uptake operon antiterminator regulatory protein lmo1405 (Mérino et al., 2002), and truncation of *mutS* will have conceivable effects on both the functionality of MutS, and of MutL. Mérino et al. have determined the effect of a deletion of both *mutS* and *MutL* on the mutant fraction in *L. monocytogenes* EGD, and found a 100- to 1000-fold increase in mutant fraction, as well as a 15-fold increase in homologous recombination in a Δ*mutSL* mutant. A large insertion in

*mutS* such as the one found in FBR16, appears to be rare, as we did not identify similar insertions in the 3553 whole genome sequences from RefSeq that were screened. Insertions such as the 179 bp insertion in *mutS* of FBR16 can only be restored by homologous recombination. Interestingly, the increased homologous recombination rate associated with non-functioning *mutSL* system (Mérino et al., 2002) might provide the possibility of a transient mutator phenotype.

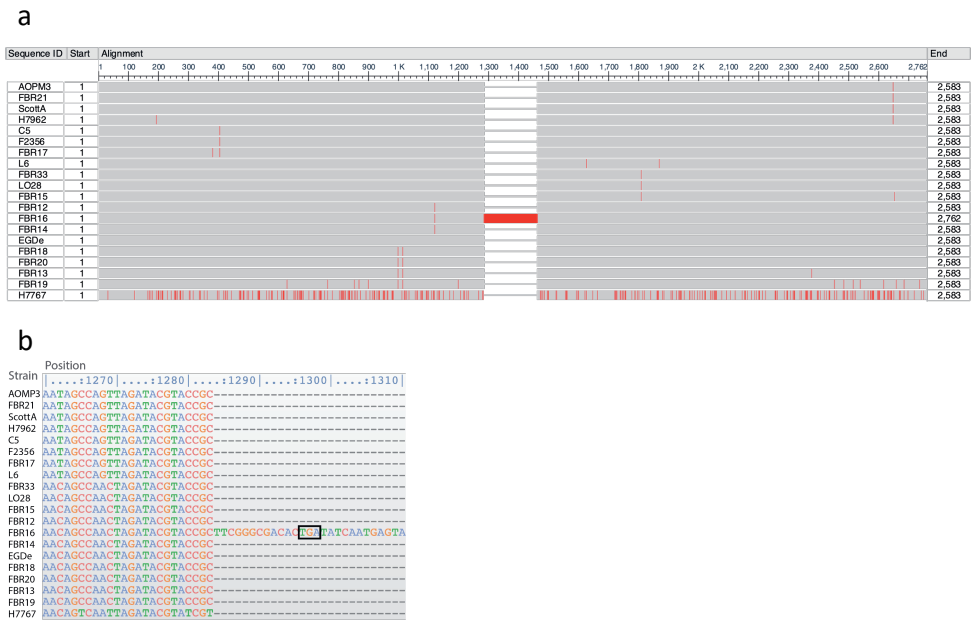


***Figure 2.2:*** *Alignment of the mutS gene in 20* L. monocytogenes *strains. (a) Alignment of DNA sequences of the* mutS *gene for the 20 strains of* L. monocytogenes*. Differences to the top sequence (AOPM3) are shown in red. The 179 bp insertion in FBR16 ranging from position 1284 to 1463 is shown as a red bar. (b) Partial alignment of the DNA sequence of* mutS *for the 20 strains* of L. monocytogenes*. Position is shown as base pairs from the start of the* mutS *gene. Only the first 27 bases of the 197 bp insertion of FBR16 are shown. The premature stopcodon (TGA) is shown in the black box.*

Experiments by Mérino et al. in 2002 have shown that the combined deletion of *mutS* and *mutL* from *L. monocytogenes* EGD did not result in differences in fitness. However, virulence in a mouse model was attenuated for a Δ*mutSL* mutant, when compared to the EGD WT. On possible explanation for the decreased virulence may be the increased mutational load. The intracellular environment is stressful, which may lead to an increased mutation rate, which would be more deleterious for the mutator strain than for the WT. Whether fitness and virulence are affected by the *mutS* insertion in FBR16 remains to be elucidated by comparing FBR16 Δ*mutSL* and FBR16 in mutant studies.

In a well-adapted system, as most mutations will be deleterious (Elena and Lenski, 2003; Eyre-Walker and Keightley, 2007; Kimura, 1967; Perfeito et al., 2007), mutator strains are expected to be selected only in specific circumstances. For instance, after a recent environmental change, mutator strains may have an early advantage by generating mutations faster, leading to their establishment based on their increased adaptability (Desai and Fisher, 2011; Sniegowski et al., 2000). A second conceivable scenario in which a high mutation rate can be selected is when a mutator allele generates a beneficial mutation by chance. Then, positive selection for this adaptive property, and the linked mutator allele, allow the mutator allele to spread through the population as a consequence, a process that is known as second order selection (Gentile et al., 2011; Giraud et al., 2001; Woods et al., 2011). Although the *mutSL* operon has been studied in *L. monocytogenes* (Mérino et al., 2002), and has been found to influence salt sensitivity in transposon experiments (Gardan et al., 2003), to our knowledge, this is the first description of a mutator strain, generated by an insertion in *mutS* in a *L. monocytogenes* foodborne isolate.

In addition, over the 2583 bp length of the *mutS* gene, we found 331 SNPs in strain H7767 when compared to the EGDe reference genome (Figure 2.2a). The mutation rate of strain H7767 was in the order of magnitude of the other 18 strains, suggesting that the functionality of *mutS* in this strain is unchanged. This amount of sequence divergence is rare for a functional gene, and additional investigation into the distribution of SNPs in *mutS* in *L. monocytogenes* is warranted.

### Mutation rate of the FBR16_MutS_repaired strain

As the 179 bp insertion in *mutS* of FBR16 was expected to disrupt protein function and increase the mutation rate, we replaced the *mutS* gene of FBR16 with the *mutS* gene of FBR12, which is identical to that of FBR16, except for the insertion, yielding the mutant

strain FBR16_mutS_repaired. PCR analysis confirmed the approximately 200 bp size difference between *mutS* of FBR16 and FBR16_mutS_repaired (data not shown). FBR16_mutS_repaired was tested in a fluctuation assay together with the original FBR16 as reference. Using an adapted protocol that included plating of higher volumes (see methods section), the mutation rate of FBR16 was estimated to be at $2.9 \cdot 10^{-7}$ per gene per generation (Figure 2.3), while the mutation rate of FBR16_mutS_repaired was estimated at $4.7 \cdot 10^{-9}$, and this was in the same range as the mutation rate of the other 19 strains (Figure 2.1), indicating that the insertion in *mutS* was responsible for the increased mutation rate in FBR16.

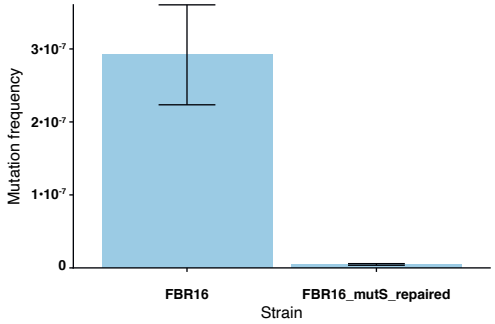


***Figure 2.3:*** *Mutation rate of* Listeria monocytogenes *FBR16 and FBR16_mutS_repaired. The mutation rate of FBR16, with its disrupted* mutS*, is $2.9 \cdot 10^{-7}$ per gene per generation, and that of FBR16_mutS_repaired is $4.7 \cdot 10^{-9}$ per gene per generation.*

In conclusion, we have designed a high throughput protocol for the estimation of mutation rates in *L. monocytogenes*. Using this protocol, we demonstrated that the food isolate FBR16 is a mutator strain, and showed that the 179 bp insertion in the *mutS* gene was responsible for this increased mutation rate. Moreover, we show that large mutations in *mutS* are very rare, as we did not identify similar insertions among 3553 strains evaluated in an *in-silico* approach.

## Appendix 1, fluctuation analysis

Spontaneous mutations can arise stochastically during cell replication, or after environmental insults that lead to DNA damage requiring repair by genes involved in the SOS response (van der Veen et al., 2010). Mutations occur at a certain rate that can be measured using the Luria-Delbrück fluctuation analysis (Luria and Delbruck 1964). It is however important to acknowledge that mutation rates are not simply the number of mutant cells in a population. The mutation rate represents the probability that a mutation in the rifampicin occurs during the lifetime of a cell (Rosche and Foster, 2000). After a mutational event, the mutant cells will propagate and grow to a certain fraction of the total population, represented by its frequency within that final population. One mutational event can therefore lead to very different mutation frequencies, while both cultures have the same mutation rate, see Figure A2.1a.

Therefore, the mutation rate is a far more reliable unit when investigating the occurrence of mutations than the frequency of mutants in a population (Rosche and Foster, 2000). To estimate a mutation rate, we grow several small liquid cultures (typically between 20-50 parallel cultures) from a diluted inoculum that is assumed not to contain any mutants. Then, after incubation we plate (a portion of) the parallel cultures on solid medium containing an antibiotic. The resistance against the antibiotic rifampicin as conferred by mutations in the *rpoB* gene is a selectable marker for mutant cells, as resistant mutants will be able to form colonies. The numbers of mutant colonies on the rifampicin-agar plates can be used together with the mean final number of cells in the parallel cultures to estimate the mutation rate that gave rise to this distribution of mutant cells over the cultures (Figure A2.1b). To estimate the mean final number of cells per strain, we plated three parallel cultures per strain on BHI-agar to estimate the total viable count. The number of mutant cells per parallel line, and the mean final number of cells were used to calculate the mutation rate with the R package FLAN (Mazoyer and Drouilhet, 2017).

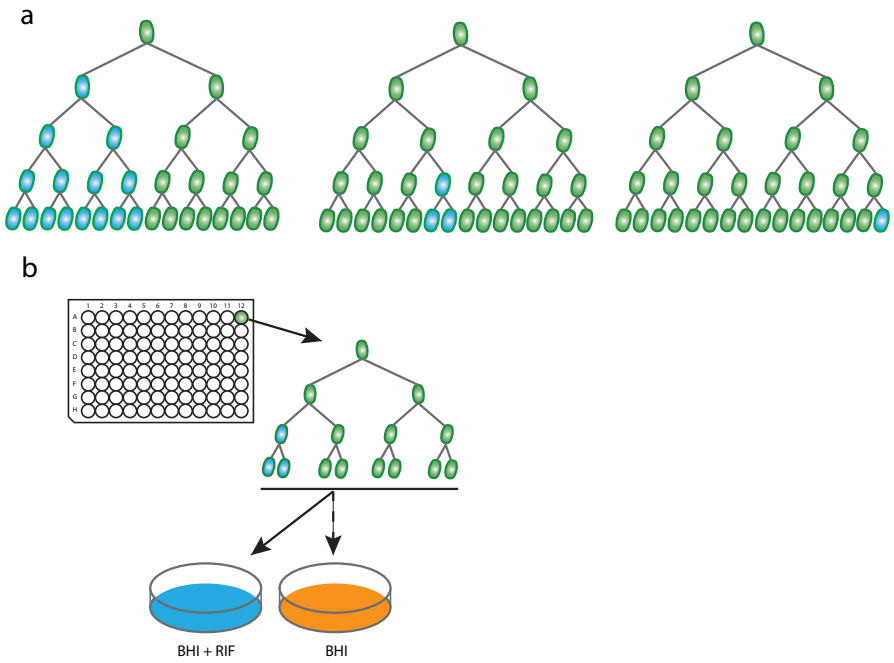


Figure A2.1: Fluctuation analysis. (a) The same mutation rate can lead to a significant difference in mutant cells. (b) Multiple parallel cultures can be grown in a multiwell plate, and tested for mutant cells.

## References

**Abee, T., Koomen, J., Metselaar, K.I., Zwietering, M.H., Den Besten, H.M.W.,** 2016. Impact of pathogen population heterogeneity and stress-resistant variants on food safety. Annu. Rev. Food Sci. Technol. 7, 439–456. doi:10.1146/annurev-food-041715-033128

**Aryani, D.C., Den Besten, H.M.W., Hazeleger, W.C., Zwietering, M.H.,** 2015. Quantifying variability on thermal resistance of *Listeria monocytogenes*. Int. J. Food Microbiol. 193, 130–138. doi:10.1016/j.ijfoodmicro.2014.10.021

**Cerf, O.,** 1977. Tailing of survival curves of bacterial spores. J. Appl. Bacteriol. 42, 1–19. doi:10.1111/j.1365-2672.1977.tb00665.x

**Chakraborty, T., Leimeister-Wächter, M., Domann, E., Hartl, M., Goebel, W., Nichterlein, T., Notermans, S.,** 1992. Coordinate regulation of virulence genes in *Listeria monocytogenes* requires the product of the *prfA* gene. J. Bacteriol. 174, 568–574. doi:10.1128/jb.174.2.568-574.1992

**Desai, M.M., Fisher, D.S.,** 2011. The balance between mutators and nonmutators in asexual populations. Genetics 188, 997–1014. doi:10.1534/genetics.111.128116

**Elena, S.F., Lenski, R.E.,** 2003. Evolution experiments with microorganisms: the dynamics and genetic bases of adaptation. Nat. Rev. Genet. 4, 457–469. doi:10.1038/nrg1088

**Eyre-Walker, A., Keightley, P.D.,** 2007. The distribution of fitness effects of new mutations. Nat. Rev. Genet. 8, 610–618. doi:10.1038/nrg2146

**Gardan, R., Cossart, P., Labadie, J., European Listeria Genome Consortium,** 2003. Identification of *Listeria monocytogenes* genes involved in salt and alkaline-pH tolerance. Appl. Environ. Microbiol. 69, 3137–3143. doi:10.1128/aem.69.6.3137-3143.2003

**Gentile, C.F., Yu, S.-C., Serrano, S.A., Gerrish, P.J., Sniegowski, P.D.,** 2011. Competition between high- and higher-mutating strains of *Escherichia coli*. Biol. Lett. 7, 422–424. doi:10.1098/rsbl.2010.1036

**Giraud, A., Matic, I., Tenaillon, O., Clara, A., Radman, M., Fons, M., Taddei, F.,** 2001. Costs and benefits of high mutation rates: adaptive evolution of bacteria in the mouse gut. Science 291, 2606–2608. doi:10.1126/science.1056421

**Harrand, A.S., Jagadeesan, B., Baert, L., Wiedmann, M., Orsi, R.H., Dudley, E.G.,** 2020. Evolution of *Listeria monocytogenes* in a food processing plant involves limited single-nucleotide substitutions but considerable diversification by gain and loss of prophages. Appl. Environ. Microbiol. 86, 38. doi:10.1128/AEM.02493-19

**Karatzas, K.A.G., Bennik, M.H.J.,** 2002. Characterization of a *Listeria monocytogenes* Scott A isolate with high tolerance towards high hydrostatic pressure. Appl. Environ. Microbiol. 68, 3183–3189. doi:10.1128/AEM.68.7.3183-3189.2002

**Karlson, A.G., Ulrich, J.A.,** 1969. Stability of rifampin in dimethylsulfoxide. Appl Microbiol 18, 692–693.

**Kimura, M.,** 1967. On the evolutionary adjustment of spontaneous mutation rates. Genet. Res. 9, 23–34. doi:10.1017/S0016672300010284

**Luria, S.E., Delbrück, M.,** 1943. Mutations of bacteria from virus sensitivity to virus resistance. Genetics 28, 491–511.

**Lynch, M., Ackerman, M.S., Gout, J.-F., Long, H., Sung, W., Thomas, W.K., Foster, P.L.,** 2016. Genetic drift, selection and the evolution of the mutation rate. Nat. Rev. Genet. 17, 704–714. doi:10.1038/nrg.2016.104

**Maddison, W. P., D.R. Maddison.,** 2019. Mesquite: a modular system for evolutionary analysis. Version 3.61 http://www.mesquiteproject.org.

**Maslowska, K.H., Dzbenska, K.M., Fijalkowska, I.J.,** 2019. The SOS system: A complex and tightly regulated response to DNA damage. Environmental and Molecular Mutagenesis 60, 368–384. doi:10.1002/em.22267

**Mazoyer, A., Drouilhet, R., R, S.D.T.,** 2017, flan: An R package for inference on mutation models. hal.archives-ouvertes.fr. doi:10.32614/RJ-2017-029

**Metselaar, K.I., Den Besten, H.M.W., Abee, T., Moezelaar, R., Zwietering, M.H.,** 2013. Isolation and quantification of highly acid resistant variants of *Listeria monocytogenes.* Int. J. Food Microbiol. 166, 508–514. doi:10.1016/j.ijfoodmicro.2013.08.011

**Metselaar, K.I., Den Besten, H.M.W., Boekhorst, J., van Hijum, S.A.F.T., Zwietering, M.H., Abee, T.,** 2015. Diversity of acid stress resistant variants of *Listeria monocytogenes* and the potential role of ribosomal protein S21 encoded by *rpsU*. Front. Microbiol. 6, 422. doi:10.3389/fmicb.2015.00422

**Mérino, D., Poupet, H.R., Berche, P., Charbit, A.,** 2002. A hypermutator phenotype attenuates the virulence of *Listeria monocytogenes* in a mouse model. Mol. Microbiol. 44, 877–887. doi:10.1046/j.1365-2958.2002.02929.x

**Perfeito, L., Fernandes, L., Mota, C., Gordo, I.,** 2007. Adaptive mutations in bacteria: high rate and small effects. Science 317, 813–815. doi:10.1126/science.1142284

**Pope, C.F., O'Sullivan, D.M., McHugh, T.D., Gillespie, S.H.,** 2008. A practical guide to measuring mutation rates in antibiotic resistance. Antimicrob. Agents Chemother. 52, 1209–1214. doi:10.1128/AAC.01152-07

**Prunier, A.L., Leclercq, R.,** 2005. Role of *mutS* and *mutL* genes in hypermutability and recombination in *Staphylococcus aureus*. J. Bacteriol. 187, 3455–3464. doi:10.1128/JB.187.10.3455-3464.2005

**Rajkovic, A., Smigic, N., Uyttendaele, M., Medic, H., de Zutter, L., Devlieghere, F.,** 2009. Resistance of *Listeria monocytogenes*, *Escherichia coli* O157:H7 and *Campylobacter jejuni* after exposure to repetitive cycles of mild bactericidal treatments. Food Microbiol. 26, 889–895. doi:10.1016/j.fm.2009.06.006

**Rosche, W.A., Foster, P.L.,** 2000. Determining mutation rates in bacterial populations. Methods. 20, 4–17. doi:10.1006/meth.1999.0901

**Rozewicki, J., Li, S., Amada, K.M., Standley, D.M., Katoh, K.,** 2019. MAFFT-DASH: integrated protein sequence and structural alignment. Nucleic Acids Res. 14, 249. doi:10.1093/nar/gkz342

**Sniegowski, P.D., Gerrish, P.J., Johnson, T., Shaver, A.,** 2000. The evolution of mutation rates: separating causes from consequences. BioEssays 22, 1057–1066. doi:10.1002/1521-1878(200012)22:12<1057::AID-BIES3>3.0.CO;2-W

**Sniegowski, P.D., Gerrish, P.J., Lenski, R.E.,** 1997. Evolution of high mutation rates in experimental populations of *E. coli.* Nature 387, 703–705. doi:10.1038/42701

**Toledo-Arana, A., Dussurget, O., Nikitas, G., Sesto, N., Guet-Revillet, H., Balestrino, D., Loh, E., Gripenland, J., Tiensuu, T., Vaitkevicius, K., Barthelemy, M., Vergassola, M., Nahori, M.-A., Soubigou, G., Régnault, B., Coppée, J.-Y., Lecuit, M., Johansson, J., Cossart, P.,** 2009. The *Listeria* transcriptional landscape from saprophytism to virulence. Nature 459, 950–956. doi:10.1038/nature08080

**Van Boeijen, I.K.H., Francke, C., Moezelaar, R., Abee, T., Zwietering, M.H.,** 2011. Isolation of highly heat-resistant *Listeria monocytogenes* variants by use of a kinetic modeling-based sampling scheme. Appl. Environ. Microbiol. 77, 2617–2624. doi:10.1128/AEM.02617-10

**Van Boeijen, I.K.H., Moezelaar, R., Abee, T., Zwietering, M.H.,** 2008. Inactivation kinetics of three *Listeria monocytogenes* strains under high hydrostatic pressure. J. Food Prot. 71, 2007–2013. doi:10.4315/0362-028x-71.10.2007

**van der Veen, S., van Schalkwijk, S., Molenaar, D., de Vos, W.M., Abee, T., Wells-Bennik, M.H.J.,** 2010. The SOS response of *Listeria monocytogenes* is involved in stress resistance and mutagenesis. Microbiology 156, 374–384. doi:10.1099/mic.0.035196-0

**Woods, R.J., Barrick, J.E., Cooper, T.F., Shrestha, U., Kauth, M.R., Lenski, R.E.**, 2011. Second-order selection for evolvability in a large *Escherichia coli* population. Science 331, 1433–1436. doi:10.1126/science.1198914

# 3

# Gene profiling-based phenotyping for identification of cellular parameters that contribute to fitness, stress-tolerance and virulence of *Listeria monocytogenes* variants

Jeroen Koomen, Heidy M.W. den Besten, Karin I. Metselaar, Marcel H. Tempelaars, Lucas M. Wijnands, Marcel H. Zwietering, and Tjakko Abee.

**Published in:**

International Journal of Food Microbiology (2018) 283: p. 14–21.

## Abstract

Microbial population heterogeneity allows for a differential microbial response to environmental stresses and can lead to the selection of stress resistant variants. In this study, we have used two different stress resistant variants of *Listeria monocytogenes* LO28 with mutations in the *rpsU* gene encoding ribosomal protein S21, to elucidate features that can contribute to fitness, stress-tolerance and host interaction using a comparative gene profiling and phenotyping approach. Transcriptome analysis showed that 116 genes were upregulated and 114 genes were downregulated in both *rpsU* variants. Upregulated genes included a major contribution of SigB-controlled genes such as intracellular acid resistance-associated glutamate decarboxylase (GAD) (*gad*3), genes involved in compatible solute uptake (*opuC*), glycerol metabolism (*glpF*, *glpK*, *glpD*), and virulence (*inlA*, *inlB*). Downregulated genes in the two variants involved mainly genes involved in flagella synthesis and motility. Phenotyping results of the two *rpsU* variants matched the gene profiling data including enhanced freezing resistance conceivably linked to compatible solute accumulation, higher glycerol utilisation rates, and better adhesion to Caco 2 cells presumably linked to higher expression of internalins. Also, bright field and electron microscopy analysis confirmed reduced flagellation of the variants. The activation of SigB-mediated stress defence offers an explanation for the multiple-stress resistant phenotype in *rpsU* variants.

## Introduction

*Listeria monocytogenes* is a ubiquitous Gram-positive foodborne pathogen that can cause the rare but severe disease listeriosis (Toledo-Arana et al., 2009). Due to its ubiquitous nature, *L. monocytogenes* needs to be able to adapt to environmental stresses in its transition from the environment to the human gastro-intestinal tract. Population heterogeneity is an inherent feature of microorganisms and heterogeneity in stress response between individual cells of a population can result in survival of a small fraction of the population when subjected to (food-relevant) lethal stresses such as heat or low pH. This type of non-uniform killing leads to non-linear inactivation kinetics and tailing of the inactivation curve (Avery, 2006). Tailing leads to higher-than-expected number of cells surviving an inactivation treatment, which can be problematic for the accurate modelling of inactivation procedures. Moreover, non-homogeneous killing can lead to the selection of stress resistant variants from a population. The fraction of stress resistant cells in a population has been shown to be comprised of both cells that show a transient phenotypic resistance, and cells that show a stable genotypic resistance (Metselaar et al., 2013; Van Boeijen et al., 2011; Van Boeijen et al., 2008). Indeed, from the tail of the inactivation curve, stable stress resistant variants have been isolated for *L. monocytogenes* EGDe, LO28, and ScottA when exposed to either heat, low pH or high hydrostatic pressure (HHP) (Karatzas and Bennik, 2002; Metselaar et al., 2013; Metselaar et al., 2015; Van Boeijen et al., 2011; Van Boeijen et al., 2008). However, the specific mechanism of resistance in these stable stress resistant variants is still poorly understood. For variants selected by HHP treatment, a mutation in the class III heat shock repressor *ctsR* was shown to be responsible for the increased stress resistance in some of the variants (Van Boeijen et al., 2010). Interestingly, these HHP selected variants showed cross resistance to other stresses including heat and acid stress. In 2013, Metselaar et al. could isolate 23 stable stress resistant variants upon acid treatment. Although phenotypic characteristics such as heat and acid resistance and impaired growth rate were observed in both the HHP selected and the acid stress selected variants, a whole genome sequencing and Structural Variation (SV) analysis on the acid stress selected variants of *L. monocytogenes* LO28 revealed no mutations in the *ctsR* region in any of the 23 variants. The SV analysis revealed that 11 of the 23 acid stress selected variants that shared similar phenotypes all had a mutation in the *rpsU* gene locus. Our current study focuses on two of these *rpsU* variants, namely, variant 14, which has a deletion encompassing *rpsU, yqeY and* half of *phoH*, and variant 15 that carries a single

point mutation resulting in an amino acid substitution, changing an arginine into a proline. In previous work (Metselaar et al., 2015) RT-PCR analysis revealed significantly lower expression of the *rpsU* gene in variant 15, and as expected, no transcript in variant 14. For these variants, protection from lethal acid stress seems to be correlated (Metselaar et al., 2015) with increased activity of the glutamate decarboxylase (GAD) system (Cotter et al., 2001; Feehily and Karatzas, 2013; Karatzas et al., 2012), but complementary mechanisms contributing to the observed multiple stress-resistant phenotype of the variants are unknown. Therefore, in the current study we investigated the differential transcriptomic and phenotypic responses of *L. monocytogenes* LO28 variants 14 and 15 in comparison to the wild type to further characterize the variants and to elucidate features that can contribute to fitness, stress-tolerance, and virulence.

## Materials and methods

### Bacterial strains and culture conditions

*Listeria monocytogenes* LO28 wild type (WT) strain (Wageningen Food & Biobased Research, The Netherlands) and stress resistant variants 14 and 15 (Metselaar et al., 2013) were used in this study. All bacterial cultures were cultured as described elsewhere (Metselaar et al., 2013). Briefly, cells from -80°C stock were grown at 30°C for 48 hours on brain heart infusion (BHI, Oxoid, Hampshire) agar (1.5 % [w/w], bacteriological agar no. 1 Oxoid, Hampshire) plates. A single colony was then used to inoculate 20 ml of BHI broth in a 100 ml Erlenmeyer flask (Fisher, USA). After overnight (ON) culturing at 30°C under shaking at 160 rpm, (Innova 42; New Brunswick Scientific, Edison, NJ) 0.5% (v/v) inoculum was added to fresh BHI broth. Cells were grown under shaking at 160 rpm in BHI at 30°C until the late-exponential growth phase ($OD_{600}$ = 0.4-0.5).

### RNA isolation, cDNA synthesis and labelling

RNA was isolated from late-exponentially growing cultures of the WT and variants 14 and 15. Cultures (20 ml) were centrifuged in 50 ml Falcon tubes for 1 min at room temperature (11.000 x *g*). Immediately after centrifugation the pellet was resuspended in 1 ml TRI reagent (Ambion) by vortexing, snap frozen in liquid nitrogen and stored at -80°C until use. RNA was extracted according to the RNAwiz (Ambion) protocol. Residual DNA was enzymatically removed using the TURBO DNA-free kit (Ambion) according to manufacturer's instructions. The quality of the extracted RNA was checked by using the Bioanalyzer (Agilent) with the Agilent RNA 6000 Nano kit, according to manufacturer's

instructions. RIN scores were between 8.5 and 10. Complementary DNA (cDNA) with amino-allyl-labelled dUTP (Ambion) was synthesized from RNA by using Superscript III reverse transcriptase (Invitrogen). Labelling and hybridization were performed as described elsewhere (Mols et al., 2013).

### Microarray design and data analysis

A custom-made array design for *L. monocytogenes* LO28 was based on the 8 x 15K platform of Agilent Technologies (GEO accession number: GSE114672, on the GPL25009 platform) and the genome sequence of *L. monocytogenes* EGDe (NCBI accession number NC_003210.1). Two biological replicates of variant 14, and three biological replicates of variant 15 were used. Microarrays were scanned with an Agilent G2505C scanner. Image analysis and processing were performed with the Agilent Feature Extraction software (version 10.7.3.1). Transcriptome profiles were normalized using LOWESS normalization (Yang et al., 2002) as implemented in MicroPreP (van Hijum et al., 2003). The data were corrected for inter-slide differences based on total signal intensity per slide using Postprep (Yang et al., 2002) and median intensity of the different probes per gene was selected as the gene expression intensity. CyberT software was used to compare the different transcriptomes (Baldi and Long, 2001) resulting in gene expression ratios and false discovery rates (FDR) for each gene. The gene was considered significantly differentially expressed when FDR-adjusted P value was <0.05 and expression fold change was higher than 3 ($\log_2$ ratio > 1.58 for upregulation, and < -1.58 for downregulation) (Hayrapetyan et al., 2015). FunRich version 2.1.2 (Pathan et al., 2015) was used for functional enrichment analysis.

### Freeze-thaw resistance

100 µl of late exponential phase cultures of the WT strain and variants 14 and 15 were each transferred into 10 ml of fresh BHI and BHI supplemented with 100 µg/ml chloramphenicol as an inhibitor of protein synthesis. For each culture, 1.5 ml of inoculated BHI was transferred into a 2.0 ml Eppendorf tube, after which the Eppendorf tubes were collected in a water bath floater and placed in a tray containing a coolant mixture of 50% (v/v) glycerol (Fluca, Buchs) and deionized water pre-cooled to -20°C to ensure an even rate of freezing of the three cultures. After freezing for 2 h, all samples were thawed for 15 min in a water bath (Julabo JW II, Germany) set to 25°C. Appropriate dilutions of the first sample were prepared in Peptone Physiological Salt (PPS) solution, 0.1% w/v peptone, and 0.9% w/v NaCl (Tritium Microbiologie, The Netherlands) and spiral plated on BHI agar plates (Eddy Jet, IUL

Instruments) in duplicate. Samples for the second and third round of freezing and thawing were frozen again, after which the samples of the second round were thawed and plated. This process was repeated for the third round. Plates were counted after 3-4 days to allow recovery of the cells. Experiments were done with independent biological triplicates.

### Glycerol consumption

100 ml cultures of the WT strain and variants 14 and 15 were grown in BHI medium in 500 ml Erlenmeyer flasks. Late-exponential phase cells were harvested by centrifuging 2 x 50 ml of cell suspension for 5 min at 2880 x *g*. Pellets were resuspended in phosphate buffered saline, pH 7.4 (PBS, $KH_2PO_4$ 1.06 mM; NaCl 155.17 mM; $Na_2HPO_4$-$7H_2O$ 2.97 mM) (Gibco, Life Technologies, Scotland), and centrifuged again for 5 min at 2880 x *g* to remove all traces of BHI medium. The pellet was resuspended in 20 ml of nutrient broth (NB) (Oxoid, Hampshire) supplemented with 25 mM glycerol, 100 µg of chloramphenicol as an inhibitor of protein synthesis per ml and incubated in a 100 ml Erlenmeyer flask (Fisher, USA) at 30°C. A 1 ml sample was taken directly after resuspension in NB as time point zero, followed by sampling after 60, 120 and 180 minutes of incubation. Samples were centrifuged for 5 min at 17.000 x *g* to remove cells. The supernatant was filter sterilized using a 0.2 µm syringe filter (Minisart NML, Sartorius Stedim Biotech GmbH, Germany). 0.5 ml of supernatant was deproteinized by the Carrez AB method. Briefly, 0.25 ml of cold Carrez A (42.20 g/l $K_4FE(CN)_6.3H_2O$) was added to 0.5 ml of sample. After thorough mixing with a MS 2 minishaker (IKA, Staufen, Germany) 0.25 ml of Carrez B (57.50 g/l $ZnSO_4.7H_2O$) was added, and the sample was centrifuged at 17.000 x *g* for 5 min. 10 µl of supernatant was analysed using an Ultimate 3000 HPLC (Dionex, USA) equipped with a 300 x 7.8 mm Aminex HPX 87-H ion exclusion column (Biorad, USA), kept at 40°C with 0.05 M $H_2SO_4$ as eluent at a flow of 0.6 ml/min. Glycerol was detected by a Shodex R-101 refractive index detector (Shodex, USA). A standard curve was constructed by serial dilutions of glycerol in Milli-Q water (Millipore, USA). Peaks were annotated and integrated using Chromelion version 7.2 SR4 analysis software.

Differences in glycerol consumption between the WT and variants were evaluated by a Student t-test using Microsoft Excel. Differences were considered significantly different when $p < 0.05$.

### Flagella imaging

Late-exponential phase cells of the WT strain and variants 14 and 15, grown at 30°C were

visualized using either the Ryu protocol (Kodaka et al., 1982; Ryu, 1937) or transmission electron microscopy (TEM). In the Ryu protocol, a wet mount of a cell suspension was made using a glass microscope slide with a coverslip. Then, a solution of one-part dye (saturated crystal violet in ethanol absolute) was added to 10 parts of mordant solution (aluminum potassium sulfate ($AlKO_8S_2 \cdot 12\ H_2O$) 57 g/l; Phenol ($C_6H_5OH$) 25 g/l; Tannic Acid ($C_{76}H_{52}O_{46}$) 20 g/l). A drop of this dye-mordant solution was placed on the side of the coverslip, allowing the dye-mordant solution to enter the wet mount via capillary action. Images were taken at phase contrast settings using an Olympus BX 41 microscope with an Olympus UIS-2 PLAN-C 100x PH3 oil immersion lens coupled to an Olympus XC 30 digital camera via a 0.63x magnifier tube. Olympus CellB version 3.5 software running under Windows 7 (Microsoft, USA) was used for image acquisition. Contrast was enhanced over the entire image using ImageJ (version 1.5f National Institutes of Health, Maryland, USA). For TEM, cells were pelleted at 2880 x *g* and washed with phosphate buffered saline to remove traces of BHI and applied to copper TEM grids and stained with 2% uranyl acetate for 30s. The samples were visualized using a JEOL 1100, (Wageningen Electron Microscopy Centre, Wageningen University & Research, The Netherlands) operated at 100kV. Experiments were performed with independent biological triplicates.

### Caco-2 adhesion and invasion assay

Caco-2 human intestine epithelial cells were obtained from the American Type Culture Collection (Caco-2, ATCC HTB-37) and cells at passage (41) were used for all experiments. Cells were routinely cultured in Tissue culture medium (TCM), containing Dulbecco's Modified Eagle's Medium (DMEM, Scotland) supplemented with 10% heat-inactivated fetal bovine serum (FBS, Integro, The Netherlands), 1% (200 mM) glutamine (Gibco), Non-Essential Amino Acids (10 mM/amino acid, Gibco) and 0.1% w/v gentamycin (50.0 mg/ml, Gibco) in 75 $cm^2$ flasks (Corning Incorporated, NY, USA).

The cells were grown to confluence in 12-well tissue culture plates (Corning Incorporated, NY, USA) following the procedure described previously (Oliveira et al., 2011) at 37°C in a humidified atmosphere of 95% air and 5% $CO_2$. 12-well plates were seeded in each well with $1.6 \cdot 10^5$ cells/ml. Medium was replaced every 2-3 days. Inoculated 12-well plates were incubated for 12-14 days at 37°C in a humidified atmosphere of 95% air and 5% $CO_2$ for full cell differentiation. Prior to all experiments, Caco-2 cells were washed three times with TCM without gentamycin and FBS pre-warmed to 37°C. An final inoculum concentration of 6.7 log cfu/ml was obtained by adding 40 µl of late exponential phase cells of *L. monocytogenes*

WT and variants 14 and 15 to the monolayers. After inoculation, the 12 well plates were centrifuged (Hettich Rotina 420R, with 4784A swing-out rotor, Hettich Benelux, The Netherlands) for 1 min at 175 x *g* to create a proximity between the Caco-2 and *L. monocytogenes* cells. The bacteria suspension was removed after one hour of incubation at 37°C in a humidified atmosphere of 95% air and 5% $CO_2$. Then, the Caco-2 monolayers were washed 3 times with 1 ml of pre-warmed PPS. To quantify the number of cells adhered and/or invaded to the Caco-2 cells, the Caco-2 cells were lysed with 1 ml of 1% v/v Triton-X100 (Sigma–Aldrich, Steinheim, Germany) in PPS and serially diluted in PPS. Appropriate dilutions were plated on BHI agar in duplicate, and colonies were enumerated after 2 days of incubation at 37°C. The ratio of percentage recovery (defined as number of cells (cfu/ml) attached and/or invaded divided by number of cells (cfu/ml) inoculated) in the variants over percentage recovery in the WT was reported. Two technical replicates were used with three wells per replicate.

## Results

### General transcriptome response of variants 14 and 15

Microarray analysis showed that gene expression was different between the WT and variants 14 and 15. The number of differentially expressed genes in variants 14 and 15 is shown in Figure 3.1. There was a clear overlap in the expression profiles of both variants, as 116 and 114 genes were upregulated and downregulated in both variants, respectively. To provide a more detailed insight into the transcriptomic responses of variants 14 and 15, the COG classes of the overlapping set of genes are shown in Figure 3.1c (for a complete list of genes in the overlapping set and their corresponding COG classes, see supplementary table S3.1 and S3.2). Notable shifts in expression in the variants were seen in COG classes related to metabolism and energy conversion (G: carbohydrate transport and metabolism, E: Amino acid transport and metabolism, C: Energy production and conversion), cell motility (N), signal transduction mechanisms (T), and transcription (K). Based on the previously described multiple-stress resistant phenotype of the *rpsU* variants, we first focused on parameters involved in stress response.

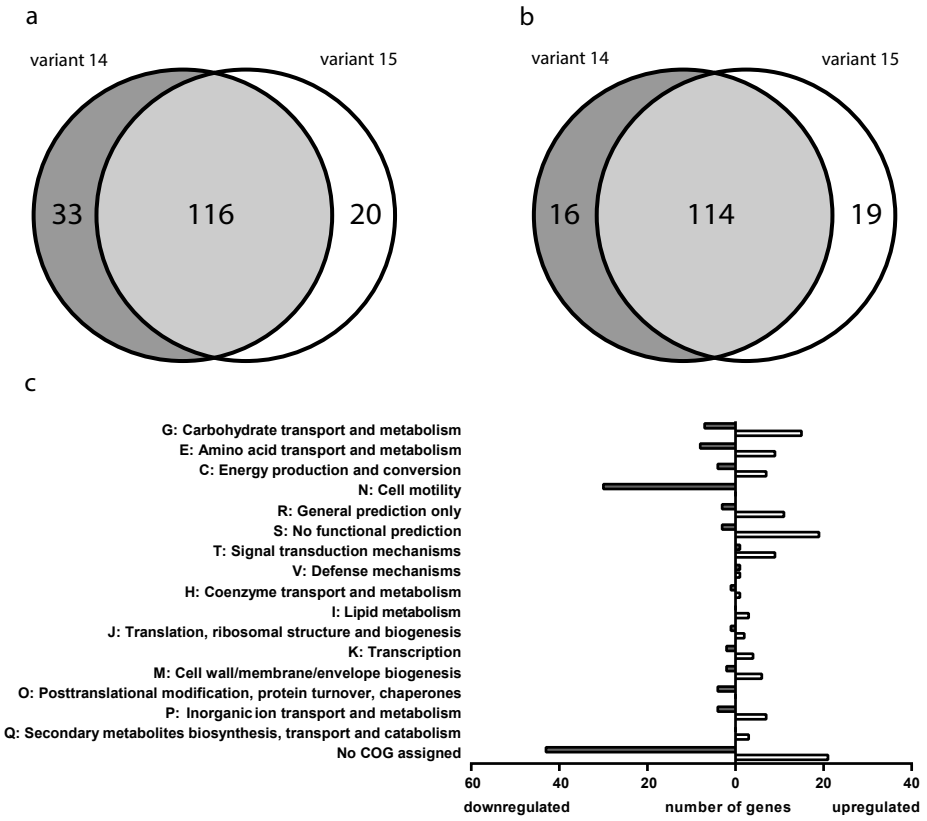


***Figure 3.1:*** *Differentially expressed genes* in L. monocytogenes *LO28 variants 14 and 15 compared to the wild type. Panel (a) represents genes that were upregulated in the variants compared to the wild type, panel (b) represents genes that were downregulated in the variants compared to the wild type. The dark grey shaded circle part represents genes only up- or downregulated in variant 14, the white circle part represents genes only up- or downregulated in variant 15. The light grey circle part represents the overlap in expression between the variants, with 116 and 114 genes up- and downregulated, respectively. (c) COG assignment of the number of upregulated (open bars) and downregulated genes (shaded bars) in both variants 14 and 15 compared to the wild type. Expression of individual genes is listed in tables S3.1 to S3.6.*

### General stress response

The alternative transcription factor SigB and its regulon are known to play a key role in general stress adaptation in *L. monocytogenes* (Guldimann et al., 2016, NicAogain and O'Byrne, 2016). The SigB regulon has been investigated in several studies using different methods, including DNA microarrays and RNAseq (Mujahid et al., 2013; Oliver et al., 2010; Ollinger et al., 2009; Raengpradub et al., 2008), see Guldimann et al., (2016) for a recent overview of SigB in relation to resilience. Here we used the SigB regulon described by Mujahid et al. in 2013 based on a gene expression dataset obtained by DNA microarrays and RNAseq, and compared the differential expression of these SigB-regulated genes in variants 14 and 15.

The transcriptome analysis of the variants showed that the majority (ca. 70%) of the SigB regulon, consisting in total of around 145 genes was upregulated. Additionally, the SigB-controlled *ctc* gene encoding ribosomal protein L25 (previously referred to as general stress protein Ctc) (Gardan et al., 2003), was found to be higher expressed in the *rpsU* variants (Figure 3.2a/b, supplementary table S3.15). This pointed to an important role of the SigB regulon in acquired stress resistance of the variants, although the differential expression of the gene coding for the alternative transcription factor *sigB* (Sigma B, lmo0895) was significant (1.47 and 1.08 $\log_2$ fold change respectively for variant 14 and 15 with FDR <0.005), but just below the stringent cut-off that was used (i.e. 1.58 $\log_2$ fold change). A selection of the SigB-regulated genes with known impact on *L. monocytogenes* stress-tolerance and host interaction is presented in Figure 3.2c. The SigB-regulated *gad-D3* gene (lmo2434) (Kazmierczak et al., 2003) is responsible for intracellular conversion of glutamate into GABA (Feehily and Karatzas, 2013) and was upregulated in both variants (Figure 3.2c). Additionally, genes involved in the SigB and PrfA controlled arginine deiminase (ADI) system (Ryan et al., 2009) were upregulated (see supplementary table S3.8). Upregulation of these genes aligns with the previously reported increased acid resistance of these variants (Metselaar et al., 2015). In the genome of *L. monocytogenes* various SigB-controlled genes encoding compatible solute transporters have been identified (Sleator and Hill, 2010; Sleator et al., 2001), and genes encoding for the compatible solute transporter OpuC (encoded by the *opuC* operon) were among the highest upregulated genes in the variants (Figure 3.2c). Also, SigB-regulated genes involved in glycerol metabolism (represented by *glpF/K/D, dhaK/L*) were upregulated, pointing to a shift in metabolism compared to the WT, as well as SigB-regulated genes known to be involved in initial attachment to epithelium cells (represented by *inlA* in Figure 3.2c). Based on these observations a range of

experiments was designed to determine corresponding relevant phenotypes of the two variants.

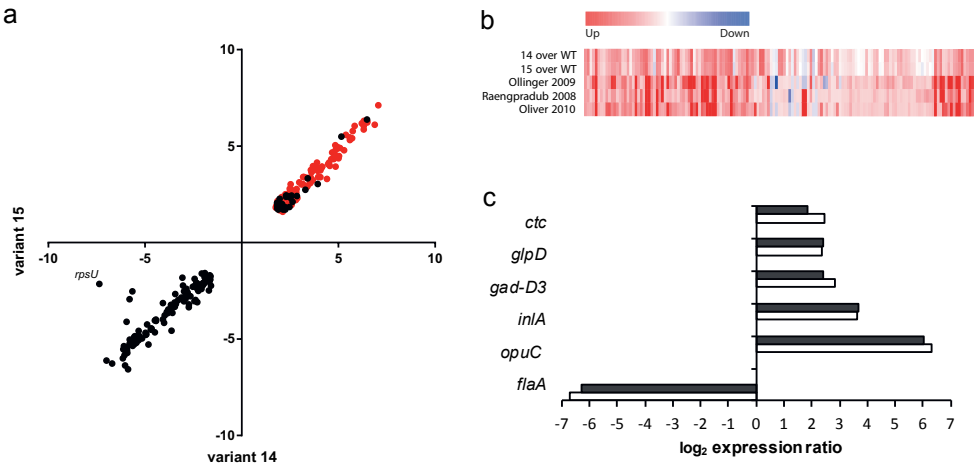


**Figure 3.2:** *Expression of representative SigB-regulated genes in* L. monocytogenes *variants compared to the wild type. (a) Regression of all genes that were significantly up- or downregulated in both variants 14 and 15. Genes shown in red are part of the SigB operon as described by Mujahid et al., 2013 (b) The heatmap displays relative expression of SigB-related genes in variants 14 and 15 compared to the wild type, and relative expression of these SigB-regulated genes as reported by Ollinger et al. 2009, Raengpradub et al. 2008 and Oliver et al. 2010. (c) Relative expression of selected SigB-regulated genes. The filled bars represent expression of genes in variant 15, the open bars represent expression of genes in variant 14. Expression of individual genes is listed in table S3.1 and S3.2*

### Freeze-thaw resistance

*Listeria monocytogenes* may be exposed to freezing-thawing stress in natural environments, as well as during storage and transport of foods. Compatible solutes are known to have a role in resistance to freezing-thawing stress (Sleator and Hill, 2010; Wemekamp-Kamphuis, Sleator, et al., 2004), and the observed upregulation of the SigB-regulated *opuC* operon in variants 14 and 15 conceivably results in higher intracellular concentrations of compatible solutes such as carnitine present in BHI leading to improved freezing-thawing resistance. Therefore, *L. monocytogenes* LO28 WT and variants 14 and 15 were exposed to consecutive cycles of freezing and thawing. Indeed, while the WT decreases up to 3 to 4 log cfu/ml after three rounds of freezing and thawing, the cell counts of both variants did not decline, indicating enhanced stress-tolerance (Figure 3.3). Experiments with chloramphenicol as inhibitor of protein synthesis showed a similar trend with slightly higher variation between the data points (data not shown) indicating that *de novo* protein synthesis was not required to sustain enhanced stress-tolerance of the variants. In addition to protection against freezing and thawing stress, compatible solutes are involved in osmoprotection. Therefore, *L. monocytogenes* LO28 WT and variants 14 and 15 were also exposed to a 24% w/v solution of NaCl in PPS for 16 hours, but no killing was observed for WT or variants 14 and 15 (data not shown).

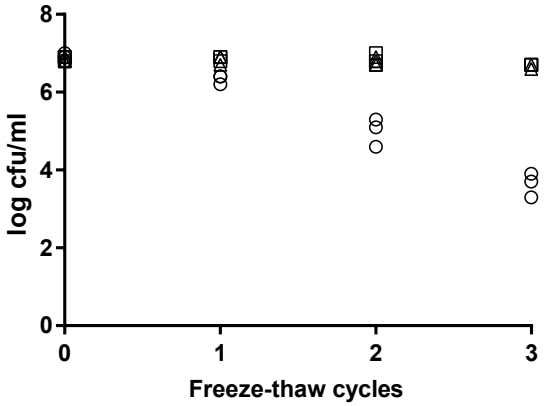


**Figure 3.3:** *Survival of* L. monocytogenes *LO28 wild type and variants after, 0 (equals the initial concentration), 1, 2, and 3 cycles of freezing and thawing. The wild type is represented by circles, variant 14 by squares, and variant 15 by triangles.*

## Glycerol metabolism

Increased expression of glycerol metabolism associated genes (Figure 3.4a and supplementary table S3.10) indicates an increased production of glycerol metabolic enzymes in the variants. Glycerol catabolism in *L. monocytogenes* is strongly linked to the expression of *sigB* (Abram et al., 2008), while simultaneous upregulation of *prfA* has been reported in glycerol grown cultures (Joseph et al., 2008). The transcriptome analysis showed that indeed *prfA* was upregulated in both variants as well as the SigB-regulated gene encoding the putative glycerol uptake facilitator protein $GlpF_1$ (lmo1539), while the second non SigB-regulated gene encoding the putative glycerol uptake facilitator protein $GlpF_2$ (lmo1167) was not differentially expressed. After facilitated diffusion of glycerol into the cell via $GlpF_1$, glycerol can be metabolized into dihydroxyacetone phosphate (DHA-P) via glycerol-3-phosphate (Figure 3.4a). The glycerol kinase gene (*glpK,* lmo1538) was upregulated in both variants and is suspected to catalyse the ATP-dependent phosphorylation of glycerol to yield glycerol-3-phosphate (Joseph et al., 2008). The *glpD* (lmo1293) gene coding for GlpD, which catalyzes the conversion of glycerol-3-phosphate into DHA-P was also upregulated in variants 14 and 15. Previous work on glycerol metabolism in *Listeria innocua* (Monniot et al., 2012) described the *golD* operon in *L. innocua* (lin0359-lin0369), and a homologous operon (*golD*) is present in *L. monocytogenes* (lmo0341-lmo0351). This *gol* operon is part of the second glycerol utilization pathway that depends on GolD for the conversion of glycerol into dihydroxyacetone (DHA). While the *golD* gene (lmo0344) was not upregulated in variants 14 and 15, the genes needed to perform the subsequent utilisation steps in this pathway (*dhaK/L*) were upregulated. Consequently, glycerol consumption was assessed in exponentially growing cells of *L. monocytogenes* LO28 WT and variants 14 and 15. Indeed, glycerol utilisation was increased in the variants compared to the WT after three hours of incubation in glycerol supplemented medium (Figure 3.4b). This pattern was observed while the cells were incubated with chloramphenicol, indicating that *de novo* protein synthesis did not contribute to this phenotype. Notably, the genes lmo0722 and lmo1381 encoding pyruvate oxidase and acylphosphatase, respectively, were also higher expressed (supplementary table S3.11). This points to downstream utilization of pyruvate generated from glycerol via acetyl phosphate leading to the production of acetate. HPLC analysis of samples obtained after 3 h incubation demonstrated that glycerol was indeed preferentially converted into acetate in the variants (data not shown).

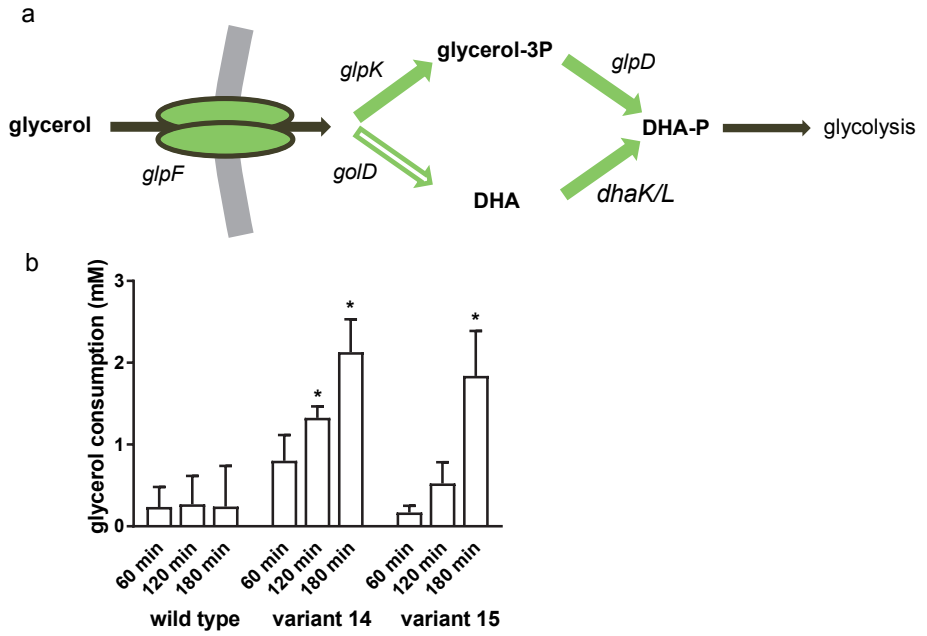


***Figure 3.4:*** *Glycerol uptake and consumption in* L. monocytogenes *LO28 wild type and variants. (a) Glycerol is imported in the cell via GlpF and can be converted to glycerol-3 phosphate by GlpK or to dihydroxyacetone (DHA) by GolD, before entering glycolysis as dihydroxyacetone phosphate (DHA-P). Closed arrows represent upregulated genes in both variants 14 and 15 relative to the wild type, open arrows represent no differential expression in both variants. glpK is upregulated in variant 14, however expression in variant 15 falls just below the stringent cut-off used here (see table S10). (b) Glycerol usage by* Listeria monocytogenes *LO28 WT and variants. Late exponential cells were concentrated and incubated in nutrient broth supplemented with glycerol for 60, 120 and 180 minutes. Error bars indicate standard errors. * indicates significant difference over the same time point in the WT.*

## Motility

In our study, both flagella cluster 1 and putative flagella cluster 2 were downregulated in variants 14 and 15 (supplementary Figure S3.1 and supplementary Table S3.11), and therefore flagella staining was used to analyse the presence or absence of flagella in WT

and variants 14 and 15. Figure 3.5 shows the reduced presence of flagella (no flagella for 30 observed cells) in both variants, while flagella were clearly observed for approximately 50% of the cells in the WT strain.

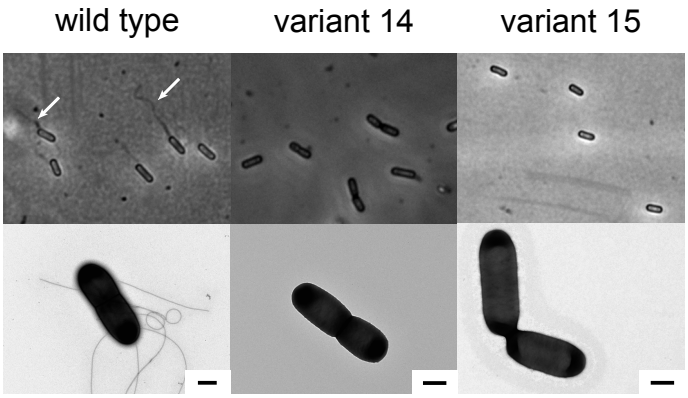


***Figure 3.5:*** *Flagella imaging of* L. monocytogenes *LO28 WT and variants. Top row, L. monocytogenes flagella staining with crystal violet as described in Ryu et al. (1937). White arrows indicate flagella in WT. Bottom row, TEM image of* L. monocytogenes *cells. Scale bar indicates 500 nm.*

### Caco-2 attachment and invasion

After stomach passage and crossing of the intestinal barrier, *L. monocytogenes* induces internalisation by non-phagocytal host cells using the cell surface proteins internalin A (*inlA*) and B (*inlB*). The InlA protein mediates the infection of human enterocyte like cells lines such as Caco-2 via the human E-cadherin receptor (Bonazzi et al., 2009) while InlB is specific for the hepatocyte growth factor (HGF) receptor Met (Pizarro-Cerda et al., 2012). In vitro, expression of either *inlA* or *inlB* is sufficient for attachment to and internalization in non-phagocytic cells (Pizarro-Cerda et al., 2012). In variants 14 and 15, both *inlA* and *inlB* were upregulated (see Figure 3.2 and supplementary Table S3.14). Therefore, the attachment and invasion of *L. monocytogenes* LO28 WT strain and variants 14 and 15 during incubation with Caco-2 cells was determined. The recovery ratio in Caco-2 cells of both variants 14 and 15 was eight-fold higher in comparison to the WT (Figure 3.6), indicating that the variants performed better in attachment and/or invasion than the WT strain.

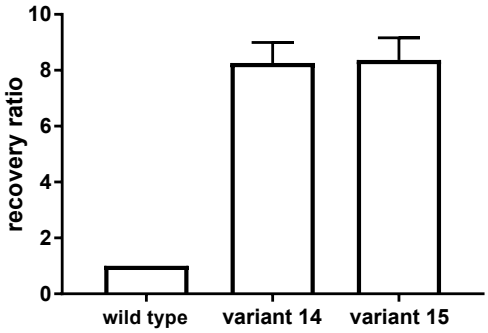


***Figure 3.6:*** *Recovery ratio of* Listeria monocytogenes *LO28 wild type compared to variants 14 and 15 from Caco-2 cells. Recovery ratio is defined as N recovered (attached and invaded) over N inoculated. Wild type recovery ratio is set at 1. Error bars represent standard error of three technical replicates.*

## Discussion

Genotypic heterogeneity within a bacterial population may allow for elevated survival when a population of bacteria is subjected to food relevant stresses. In this study we focused on the transcriptomic behaviour of two multiple-stress resistant *rpsU* variants of *L. monocytogenes* LO28 that were previously isolated from a heterogeneous population. Notably, the transcriptomic response of variant 14, harbouring a large deletion that spans the ribosomal *rpsU* gene, as well as *yqeY* and half of *phoH*, was highly similar to the transcriptomic response of variant 15, harbouring a single point mutation in *rpsU,* that resulted in an amino acid change from arginine to proline. Despite the mutation in *rpsU*, and the strikingly lower expression of *rpsU* in variant 15 both variants apparently possessed functional ribosomes, and were highly stress resistant. Using a comparative gene-profiling and phenotyping approach, we now provided evidence that the multiple stress resistant phenotype could be explained by the activation of the SigB regulon. Both variants show an upregulation of about 70% of the 145 genes of the SigB regulon included in the analysis, although no mutations in *sigB* or its regulatory sequences were found (Metselaar et al., 2015). Whether additional factors are contributing to the observed multiple stress resistance phenotype of the variants remains to be elucidated.

One of the primary systems to overcome acid stress in *L. monocytogenes* is the partially SigB-regulated GAD system. This system exchanges extracellular glutamate for

intracellularly produced gamma-aminobutyrate ($GABA_i$) under acidic conditions using the gadT1 and gadT2 antiporters. Intracellular glutamate is decarboxylated into $GABA_i$ by gadD1, gadD2, or gadD3 while consuming a proton, thereby increasing the pH of the cytoplasm (Karatzas et al., 2010). As in previous work, (Metselaar et al., 2015), we did not find an elevated transcription of antiporter/decarboxylase pair *gadT1D1* or gad*T2D2* of the external GAD system. However, the SigB-regulated *gadD3* of the internal GAD system, operating without a glutamate/GABA antiporter was upregulated. GadD3 is hypothesised to play an important role in acid resistance by mediating the conversion of glutamate into $GABA_i$ with concomitant consumption (removal) of protons in the cytoplasm (Karatzas et al., 2010; Wemekamp-Kamphuis, Wouters, et al., 2004), and indeed elevated accumulation of $GABA_i$ has been previously found in variants 14 and 15 in response to acid stress (Metselaar et al., 2015).

In *L. monocytogenes*, transcription of genes involved in glycerol catabolism was shown to be SigB dependent (Abram et al., 2008). In variants 14 and 15, increased transcription of the SigB-regulated $GlpF_1$ (lmo1539) gene pointed to increased glycerol catabolism in variants 14 and 15. Indeed, during exponential growth in BHI we found upregulation of a specific set of genes in the variants involved in glycerol uptake: $glpF_1$ (lmo1539), $glpK_1$ (lm1538) and *glpD* (lmo1293) but not of $glpF_2$ (lmo1167) and $glpK_2$ (lmo1034). During growth, *L. monocytogenes* preferentially uses sugars that are taken up by the phosphoenol-pyruvate (PEP): phosphotransferase systems (PTS) such as glucose (Joseph et al., 2008). The main carbon source in BHI is glucose, and the presence of PTS sugars in the medium normally inhibits the catabolism of non-PTS carbon sources such as glycerol via carbon catabolite repression (CCR) (Gilbreth et al., 2004; Joseph et al., 2008; Milenbachs et al., 1997; Park and Kroll, 1993). However, our variants 14 and 15, when grown in BHI display a pattern of gene expression like WT cells of *L. monocytogenes* EGDe grown to $OD_{600}$ 0.5 in defined minimal medium with glycerol (Joseph et al., 2008) suggesting mitigation of catabolite repression.

Another study reported that cells grown in the presence of a non-PTS carbon source such as glycerol, show a high activity of *prfA* (Joseph and Goebel, 2007; Mertins et al., 2007) and experiments with Δ*glpk* and Δ*glpD* mutants indicated that components related to glycerol metabolism may modulate the transcription of *prfA*. Notably, glycerol has been reported as one of the main carbon sources for *L. monocytogenes* during cytosolic growth (Bruno and Freitag, 2010; Fuchs et al., 2012). Therefore, the observation that both *prfA* and the genes

for glycerol metabolism are constitutively expressed in the variants suggests that variants 14 and 15 are metabolically primed for replication in eukaryotic cells (Bruno and Freitag, 2010), conceivably affecting their virulence potential. Indeed, in variants 14 and 15, with upregulated *glpK* and *glpD*, we see upregulation of the PrfA/SigB-regulated *inlA* and *inlB*. InlA is essential for attachment and invasion of enterocytes and enterocyte cell lines such as Caco-2, while InlB mediates the attachment of *L. monocytogenes* to fibroblasts and hepatocytes. Although *L. monocytogenes* LO28 carries a premature stopcodon in *inlA*, truncating the InlA protein at 63 kDa as opposed to the 80 kDa InlA of epidemic strains, infection studies show that *L. monocytogenes* LO28 is still able to adhere to and invade Caco-2 cells (Olier et al., 2003). In variants 14 and 15, we observed an eight-fold increase over the WT in attachment and invasion to a Caco-2 cell line, indicating a higher potential for adhesion and invasion in the variants.

Both variants 14 and 15 showed a clear reduction in expression of motility associated genes, including flagellar biosynthesis genes (*fliN, fliP, fliQ, fliR, flhB, flhA, flhF*, and *flgG*) and motor control genes (*motA, motB*). In variants 14 and 15, there was no significant difference in expression of the motility gene repressor *mogR* over the wild type (see table S13). In line with the downregulation of the flagellar biosynthesis genes, the *gmrA* gene encoding the MogR-anti-repressor GmrA, was strongly downregulated in both variants (see table S13), conceivably allowing the MogR protein to repress expression of the flagella operon (Lebreton and Cossart, 2016). Whether the previously described SigB-activated long antisense RNA Anti0677 (Lebreton and Cossart, 2016; Schultze et al., 2014; Toledo-Arana et al., 2009) plays an additional role in the observed downregulation of motility genes in the flagella operon in the two *L. monocytogenes* variants remains to be elucidated.

Activation of a systemic stress defence response via SigB is energetically costly, and shutdown of the energy consuming flagella synthesis apparatus can reduce some of the energetic costs of SigB activation. Indeed, *rpsU* variants have been described to have reduced fitness relative to the WT, showing reduced growth rates at 7°C and 30°C (Metselaar et al., 2015). Notably, Metselaar et al. (2013) described growth rate differences that were a function of media pH for *rpsU* variants, suggesting that stress resistance and growth rate are growth condition dependent and mechanically linked. This could provide a clue to elucidate the correlation between the *rpsU* mutations and activation of the SigB regulon reported in the current paper. SigB activity is controlled both translationally and

posttranslationally in *Listeria*, allowing the bacterial cells to rapidly respond to changes in environmental conditions. The posttranslational control of SigB activity involves a phosphorylation cascade that is highly conserved in species containing *sigB*, including *L. monocytogenes* (Ferreira et al., 2004) and is governed by the "stressosome", a signal relay hub that integrates multiple environmental (stress) signals to regulate SigB activity. A published overview of network motifs in *L. monocytogenes* (Guariglia-Oropeza et al., 2014) underlines the role of *sigB* as a central hub in the stress response of *L. monocytogenes*. In variants 14 and 15, we found strong upregulation of genes that were under the direct control of SigB (eg. *uspL*1-3, *inlAB, bsh*) in these regulatory networks, but not of genes that were co-regulated by other regulators. However, additional network effects remain to be elucidated.

In conclusion, the activation of SigB-mediated stress defence offers an explanation for the multiple-stress resistant phenotype observed in *rpsU* variants. Strikingly, our DNA microarray analysis showed that expression of upregulated or downregulated genes largely overlaps between variants 14 and 15, while variant 14 carries a deletion of the *rpsU* and *yqeY* gene, and a partial deletion of *phoH*, whereas variant 15 carries only an amino acid substitution in the *rpsU* gene which may affect functionality of the RpsU protein. The exact mechanism of SigB induction via *rpsU* and stressosome associated genes remains to be elucidated. Moreover, a better mechanistic understanding of *rpsU* associated multi-stress resistance will provide valuable insights into the generation of genotypic heterogeneity within bacterial populations.

## Acknowledgments

The authors would like to thank Jos Boekhorst for assistance in normalization of the microarray data, Natalia Crespo for Figure 3.3a, and Maren Lanzl for assistance in Caco-2 experiments. We would also like to thank the Wageningen Electron Microscopy Centre for providing training on the JEOL 1100 TEM.

## References

**Abram, F., Su, W.L., Wiedmann, M., Boor, K.J., Coote, P., Botting, C., Karatzas, K.A., O'Byrne, C.P.,** 2008. Proteomic analyses of a *Listeria monocytogenes* mutant lacking σB identify new components of the σB regulon and highlight a role for σB in the utilization of glycerol. Appl. Environ. Microbiol. 74, 594-604.

**Avery, S.V.,** 2006. Microbial cell individuality and the underlying sources of heterogeneity. Nat. Rev. Microbiol. 4, 577-587.

**Baldi, P., Long, A.D.,** 2001. A Bayesian framework for the analysis of microarray expression data: regularized t-test and statistical inferences of gene changes. Bioinformatics 17, 509-519.

**Bonazzi, M., Lecuit, M., Cossart, P.,** 2009. *Listeria monocytogenes* internalin and E-cadherin: from bench to bedside. Cold Spring Harbor Perspect. Biol. 1, a003087.

**Bruno, J.C., Jr., Freitag, N.E.,** 2010. Constitutive activation of PrfA tilts the balance of *Listeria monocytogenes* fitness towards life within the host versus environmental survival. PloS One 5, e15138.

**Cotter, P.D., Gahan, C.G., Hill, C.,** 2001. A glutamate decarboxylase system protects *Listeria monocytogenes* in gastric fluid. Mol. Microbiol. 40, 465-475.

**Feehily, C., Karatzas, K.A.,** 2013. Role of glutamate metabolism in bacterial responses towards acid and other stresses. J. Appl. Microbiol. 114, 11-24.

**Ferreira, A., Gray, M., Wiedmann, M., Boor, K.J.,** 2004. Comparative genomic analysis of the sigB operon in *Listeria monocytogenes* and in other Gram-positive bacteria. Curr. Microbiol. 48, 39-46.

**Fuchs, T.M., Eisenreich, W., Kern, T., Dandekar, T.,** 2012. Toward a systemic understanding of *Listeria monocytogenes* metabolism during infection. Front. Microbiol. 3, 23.

**Gardan, R., Duche, O., Leroy-Setrin, S., Labadie, J.,** 2003. Role of *ctc* from *Listeria monocytogenes* in osmotolerance. Appl. Environ. Microbiol. 69, 154-161.

**Gilbreth, S.E., Benson, A.K., Hutkins, R.W.,** 2004. Catabolite repression and virulence gene expression in *Listeria monocytogenes*. Curr. Microbiol. 49, 95-98.

**Guariglia-Oropeza, V., Orsi, R.H., Yu, H., Boor, K.J., Wiedmann, M., Guldimann, C.,** 2014. Regulatory network features in *Listeria monocytogenes*-changing the way we talk. Front. Cell. Infect. Microbiol. 4, 14.

**Guldimann, C., Boor, K.J., Wiedmann, M., Guariglia-Oropeza, V.,** 2016. Resilience in the face of uncertainty: sigma factor B fine-tunes gene expression to support homeostasis in Gram-positive bacteria. Appl. Environ. Microbiol. 82, 4456-4469.

**Hayrapetyan, H., Tempelaars, M., Nierop Groot, M., Abee, T.,** 2015. *Bacillus cereus* ATCC 14579 RpoN (Sigma 54) is a pleiotropic regulator of growth, carbohydrate metabolism, motility, biofilm formation and toxin production. PloS One 10, e0134872.

**Joseph, B., Goebel, W.,** 2007. Life of *Listeria monocytogenes* in the host cells' cytosol. Microbes Infect. 9, 1188-1195.

**Joseph, B., Mertins, S., Stoll, R., Schar, J., Umesha, K.R., Luo, Q., Muller-Altrock, S., Goebel, W.,** 2008. Glycerol metabolism and PrfA activity in *Listeria monocytogenes.* J. Bacteriol. 190, 5412-5430.

**Karatzas, K.A., Brennan, O., Heavin, S., Morrissey, J., O'Byrne, C.P.,** 2010. Intracellular accumulation of high levels of γ-aminobutyrate by *Listeria monocytogenes* 10403S in response to low pH: uncoupling of γ-aminobutyrate synthesis from efflux in a chemically defined medium. Appl. Environ. Microbiol. 76, 3529-3537.

**Karatzas, K.A.G., Suur, L., O'Byrne, C.P.,** 2012. Characterization of the intracellular glutamate decarboxylase system: analysis of its function, transcription, and role in the acid resistance of various strains of *Listeria monocytogenes*. Appl. Environ. Microbiol. 78, 3571-3579.

**Karatzas, K.A.G., Bennik, M.H.J.,** 2002. Characterization of a *Listeria monocytogenes* Scott A isolate with high tolerance towards high hydrostatic pressure. Appl. Environ. Microbiol. 68, 3183-3189.

**Kazmierczak, M.J., Mithoe, S.C., Boor, K.J., Wiedmann, M.,** 2003. *Listeria monocytogenes* σB regulates stress response and virulence functions. J. Bacteriol. 185, 5722-5734.

**Kodaka, H., Armfield, A.Y., Lombard, G.L., Dowell, V.R., Jr.,** 1982. Practical procedure for demonstrating bacterial flagella. J. Clin. Microbiol. 16, 948-952.

**Lebreton, A., Cossart, P.,** 2016. RNA- and protein-mediated control of *Listeria monocytogenes* virulence gene expression. RNA Biol. 14, 460-470.

**Mertins, S., Joseph, B., Goetz, M., Ecke, R., Seidel, G., Sprehe, M., Hillen, W., Goebel, W., Muller-Altrock, S.,** 2007. Interference of components of the phosphoenolpyruvate phosphotransferase system with the central virulence gene regulator PrfA of *Listeria monocytogenes*. J. Bacteriol. 189, 473-490.

**Metselaar, K.I., Den Besten, H.M.W., Abee, T., Moezelaar, R., Zwietering, M.H.,** 2013. Isolation and quantification of highly acid resistant variants of *Listeria monocytogenes.* Int. J. Food Microbiol. 166, 508-514.

**Metselaar, K.I., Den Besten, H.M.W., Boekhorst, J., van Hijum, S.A., Zwietering, M.H., Abee, T.,** 2015. Diversity of acid stress resistant variants of *Listeria monocytogenes* and the potential role of ribosomal protein S21 encoded by *rpsU*. Front. Microbiol. 6, 422.

**Milenbachs, A.A., Brown, D.P., Moors, M., Youngman, P.,** 1997. Carbon-source regulation of virulence gene expression in *Listeria monocytogenes*. Mol. Microbiol. 23, 1075-1085.

**Mols, M., Mastwijk, H., Nierop Groot, M., Abee, T.,** 2013. Physiological and transcriptional response of *Bacillus cereus* treated with low-temperature nitrogen gas plasma. J. Appl. Microbiol. 115, 689-702.

**Monniot, C., Zebre, A.C., Ake, F.M., Deutscher, J., Milohanic, E.,** 2012. Novel listerial glycerol dehydrogenase- and phosphoenolpyruvate-dependent dihydroxyacetone kinase system connected to the pentose phosphate pathway. J. Bacteriol. 194, 4972-4982.

**Mujahid, S., Orsi, R.H., Vangay, P., Boor, K.J., Wiedmann, M.,** 2013. Refinement of the *Listeria monocytogenes* σB regulon through quantitative proteomic analysis. Microbiol. 159, 1109-1119.

**NicAogain, K., O'Byrne, C.P.,** 2016. The role of stress and stress adaptations in determining the fate of the bacterial pathogen *Listeria monocytogenes* in the food chain. Front. Microbiol. 7, 1865.

**Olier, M., Pierre, F., Rousseaux, S., Lemaitre, J.P., Rousset, A., Piveteau, P., Guzzo, J.,** 2003. Expression of truncated internalin A is involved in impaired internalization of some *Listeria monocytogenes* isolates carried asymptomatically by humans. Infect. Immun. 71, 1217-1224.

**Oliveira, M., Wijnands, L., Abadias, M., Aarts, H., Franz, E.,** 2011. Pathogenic potential of *Salmonella* Typhimurium DT104 following sequential passage through soil, packaged fresh-cut lettuce and a model gastrointestinal tract. Int. J. Food Microbiol. 148, 149-155.

**Oliver, H.F., Orsi, R.H., Wiedmann, M., Boor, K.J.,** 2010. *Listeria monocytogenes* σB has a small core regulon and a conserved role in virulence but makes differential contributions to stress tolerance across a diverse collection of strains. Appl. Environ. Microbiol. 76, 4216-4232.

**Ollinger, J., Bowen, B., Wiedmann, M., Boor, K.J., Bergholz, T.M.,** 2009. *Listeria monocytogenes* σB modulates PrfA-mediated virulence factor expression. Infect. Immun. 77, 2113-2124.

**Park, S.F., Kroll, R.G.,** 1993. Expression of listeriolysin and phosphatidylinositol-specific phospholipase C is repressed by the plant-derived molecule cellobiose in *Listeria monocytogenes.* Mol. Microbiol. 8, 653-661.

**Pathan, M., Keerthikumar, S., Ang, C.S., Gangoda, L., Quek, C.Y., Williamson, N.A., Mouradov, D., Sieber, O.M., Simpson, R.J., Salim, A., Bacic, A., Hill, A.F., Stroud, D.A., Ryan, M.T., Agbinya, J.I., Mariadason, J.M., Burgess, A.W., Mathivanan, S.,** 2015. FunRich: An open access standalone functional enrichment and interaction network analysis tool. Proteomics 15, 2597-2601.

**Pizarro-Cerda, J., Kuhbacher, A., Cossart, P.,** 2012. Entry of *Listeria monocytogenes* in mammalian epithelial cells: an updated view. Cold Spring Harb. Perspect. Med. 2, a010009.

**Raengpradub, S., Wiedmann, M., Boor, K.J.,** 2008. Comparative analysis of the σB-dependent stress responses in *Listeria monocytogenes* and *Listeria innocua* strains exposed to selected stress conditions. Appl. Environ. Microbiol. 74, 158-171.

**Ryan, S., Begley, M., Gahan, C.G., Hill, C.,** 2009. Molecular characterization of the arginine deiminase system in *Listeria monocytogenes*: regulation and role in acid tolerance. Environ. Microbiol. 11, 432-445.

**Ryu, E.,** 1937. A simple method of staining bacterial flagella. Kitasato Arch Exp Med. 14, 218-219.

**Schultze, T., Izar, B., Qing, X., Mannala, G.K., Hain, T.,** 2014. Current status of antisense RNA-mediated gene regulation in *Listeria monocytogenes*. Front. Cell. Infect. Microbiol. 4, 135.

**Sleator, R.D., Hill, C.,** 2010. Compatible solutes: the key to *Listeria's* success as a versatile gastrointestinal pathogen? Gut Pathogens 2, 20.

**Sleator, R.D., Wouters, J., Gahan, C.G., Abee, T., Hill, C.,** 2001. Analysis of the role of OpuC, an osmolyte transport system, in salt tolerance and virulence potential of *Listeria monocytogenes*. Appl. Environ. Microbiol. 67, 2692-2698.

**Toledo-Arana, A., Dussurget, O., Nikitas, G., Sesto, N., Guet-Revillet, H., Balestrino, D., Loh, E., Gripenland, J., Tiensuu, T., Vaitkevicius, K., Barthelemy, M., Vergassola, M., Nahori, M.A., Soubigou, G., Regnault, B., Coppee, J.Y., Lecuit, M., Johansson, J., Cossart, P.,** 2009. The *Listeria* transcriptional landscape from saprophytism to virulence. Nature 459, 950-956.

**Van Boeijen, I.K., Chavaroche, A.A., Valderrama, W.B., Moezelaar, R., Zwietering, M.H., Abee, T.,** 2010. Population diversity of *Listeria monocytogenes* LO28: phenotypic and genotypic characterization of variants resistant to high hydrostatic pressure. Appl. Environ. Microbiol. 76, 2225-2233.

**Van Boeijen, I.K., Francke, C., Moezelaar, R., Abee, T., Zwietering, M.H.,** 2011. Isolation of highly heat-resistant *Listeria monocytogenes* variants by use of a kinetic modeling-based sampling scheme. Appl. Environ. Microbiol. 77, 2617-2624.

**Van Boeijen, I.K., Moezelaar, R., Abee, T., Zwietering, M.H.,** 2008. Inactivation kinetics of three *Listeria monocytogenes* strains under high hydrostatic pressure. J. Food Prot. 71, 2007-2013.

**van Hijum, S.A., Garcia de la Nava, J., Trelles, O., Kok, J., Kuipers, O.P.,** 2003. MicroPreP: a cDNA microarray data pre-processing framework. Appl. Bioinformatics 2, 241-244.

**Wemekamp-Kamphuis, H.H., Sleator, R.D., Wouters, J.A., Hill, C., Abee, T.,** 2004. Molecular and physiological analysis of the role of osmolyte transporters BetL, Gbu, and OpuC in growth of *Listeria monocytogenes* at low temperatures. Appl. Environ. Microbiol. 70, 2912-2918.

**Wemekamp-Kamphuis, H.H., Wouters, J.A., de Leeuw, P.P., Hain, T., Chakraborty, T., Abee, T.,** 2004. Identification of sigma factor σB-controlled genes and their impact on acid stress, high hydrostatic pressure, and freeze survival in *Listeria monocytogenes* EGD-e. Appl. Environ. Microbiol. 70, 3457-3466.

**Yang, Y.H., Dudoit, S., Luu, P., Lin, D.M., Peng, V., Ngai, J., Speed, T.P.,** 2002. Normalization for cDNA microarray data: a robust composite method addressing single and multiple slide systematic variation. Nucleic Acids Res. 30, e15.

Supplementary material

Table S3.1 (1 of 3): Expression of genes upregulated in both *L. monocytogenes* LO28 variant 14 and variant 15 compared to the wild type. Values in bold are considered significant

| LO28 | lmo | Gene | COG class | COG description | Product | variant 14 | | variant 15 | |
|---|---|---|---|---|---|---|---|---|---|
| | | | | | | $log_2$ fold change | FDR | $log_2$ fold change | FDR |
| LO28_2671 | lmo1988 | *leuB* | C | Energy production and conversion | 3-isopropylmalate dehydrogenase | **2.63** | 0.0007 | **2.12** | 0.0018 |
| LO28_0878 | lmo1651 | | V | Defense mechanisms | ABC transporter | **2.04** | 0.0000 | **1.85** | 0.0000 |
| LO28_0923 | lmo2603 | | C | Energy production and conversion | Acetamidase/formamidase family protein | **2.64** | 0.0015 | **2.55** | 0.0003 |
| LO28_2350 | lmo0265 | | E | Amino acid transport and metabolism | Acetylornithine deacetylase | **3.17** | 0.0037 | **3.03** | 0.0009 |
| LO28_1323 | lmo0134 | | R | General prediction only | Acetyltransferase, GNAT family | **4.10** | 0.0000 | **3.84** | 0.0000 |
| LO28_2005 | lmo0602 | | K | Transcription | Acetyltransferase, GNAT family | **5.58** | 0.0000 | **5.45** | 0.0000 |
| LO28_0517 | lmo1293 | *glpD* | C | Energy production and conversion | Aerobic glycerol-3-phosphate dehydrogenase | **2.38** | 0.0000 | **2.39** | 0.0000 |
| LO28_2843 | lmo2157 | *sepA* | Q | Secondary metabolites biosynthesis, transport and catabolism | Alkyl sulfatase | **3.52** | 0.0000 | **3.06** | 0.0000 |
| LO28_1232 | lmo0043 | | E | Amino acid transport and metabolism | Arginine deiminase | **4.15** | 0.0000 | **3.93** | 0.0000 |
| LO28_2917 | lmo2230 | | T | Signal transduction mechanisms | Arsenate reductase | **5.84** | 0.0000 | **6.04** | 0.0000 |
| LO28_2028 | lmo0579 | | S | No functional prediction | Bacterial seryl-tRNA synthetase related | **2.24** | 0.0000 | **2.31** | 0.0000 |
| LO28_1554 | lmo2573 | | C | Energy production and conversion | Bifunctional protein: zinc-containing alcohol dehydrogenase | **3.99** | 0.0000 | **3.84** | 0.0000 |
| LO28_2468 | lmo1694 | | R | General prediction only | Cell division inhibitor Slr1223 (YfcH in EC) | **5.08** | 0.0000 | **4.90** | 0.0000 |
| LO28_1501 | lmo2522 | | S | No functional prediction | Cell wall-binding protein | **1.83** | 0.0000 | **2.06** | 0.0000 |
| LO28_2750 | lmo2067 | | M | Cell wall/membrane/envelope biogenesis | Choloylglycine hydrolase | **4.47** | 0.0000 | **4.07** | 0.0000 |
| LO28_2918 | lmo2231 | | P | Inorganic ion transport and metabolism | Cobalt-zinc-cadmium resistance protein | **5.59** | 0.0000 | **5.31** | 0.0000 |
| LO28_2017 | lmo0590 | | R | General prediction only | DAK2 domain protein | **3.38** | 0.0000 | **2.89** | 0.0000 |
| LO28_1553 | lmo2572 | | H | Coenzyme transport and metabolism | Dihydrofolate reductase | **4.52** | 0.0000 | **4.15** | 0.0000 |
| LO28_0827 | lmo1601 | | R | General prediction only | General stress protein | **2.48** | 0.0000 | **2.79** | 0.0000 |
| LO28_0828 | lmo1602 | | R | General prediction only | General stress protein | **2.53** | 0.0000 | **3.02** | 0.0000 |
| LO28_1079 | lmo2748 | | R | General prediction only | General stress protein | **5.39** | 0.0000 | **5.58** | 0.0000 |
| LO28_2860 | lmo2174 | | T | Signal transduction mechanisms | GGDEF domain protein | **2.23** | 0.0000 | **1.84** | 0.0001 |
| LO28_1584 | lmo0169 | | G | Carbohydrate transport and metabolism | Glucose uptake protein | **4.63** | 0.0000 | **4.32** | 0.0000 |
| LO28_1411 | lmo2434 | | E | Amino acid transport and metabolism | Glutamate decarboxylase | **2.85** | 0.0000 | **2.41** | 0.0000 |
| LO28_0656 | lmo1433 | | C | Energy production and conversion | Glutathione reductase | **4.68** | 0.0000 | **4.67** | 0.0000 |
| LO28_0765 | lmo1539 | | G | Carbohydrate transport and metabolism | Glycerol uptake facilitator protein | **2.57** | 0.0001 | **1.95** | 0.0012 |
| LO28_0645 | lmo1422 | | M | Cell wall/membrane/envelope biogenesis | Glycine betaine ABC transport system | **3.60** | 0.0000 | **3.64** | 0.0000 |
| LO28_0644 | lmo1421 | | E | Amino acid transport and metabolism | Glycine betaine ABC transport system | **3.68** | 0.0000 | **3.96** | 0.0000 |
| LO28_2016 | lmo0591 | | S | No functional prediction | Hypothetical protein | **3.29** | 0.0000 | **2.74** | 0.0000 |
| LO28_2011 | lmo0596 | | No COG | | Hypothetical protein | **6.31** | 0.0000 | **5.86** | 0.0000 |
| LO28_1208 | lmo0019 | | S | No functional prediction | Hypothetical protein | **5.29** | 0.0004 | **4.79** | 0.0001 |
| LO28_0173 | lmo0994 | | No COG | | Hypothetical protein | **6.88** | 0.0000 | **6.11** | 0.0000 |
| LO28_2818 | lmo2132 | | T | Signal transduction mechanisms | Hypothetical protein | **2.34** | 0.0262 | **1.94** | 0.0200 |
| LO28_1979 | lmo0628 | | No COG | | Hypothetical protein | **4.16** | 0.0001 | **3.93** | 0.0000 |
| LO28_1610 | lmo2387 | | No COG | | Hypothetical protein | **3.56** | 0.0000 | **3.39** | 0.0000 |
| LO28_1936 | | | No COG | | Hypothetical protein | **5.15** | 0.0000 | **5.49** | 0.0000 |
| LO28_0655 | lmo1432 | | No COG | | Hypothetical protein | **2.60** | 0.0000 | **2.43** | 0.0000 |
| LO28_2018 | lmo0589 | | S | No functional prediction | Hypothetical protein | **3.93** | 0.0000 | **3.03** | 0.0000 |
| LO28_1440 | lmo2463 | | R | General prediction only | Hypothetical protein | **3.96** | 0.0000 | **3.40** | 0.0000 |
| LO28_1959 | lmo0647 | | No COG | | Hypothetical protein | **3.42** | 0.0000 | **3.33** | 0.0000 |
| LO28_1934 | lmo0670 | | S | No functional prediction | Hypothetical protein | **4.96** | 0.0000 | **4.95** | 0.0000 |
| LO28_0992 | lmo2671 | | No COG | | Hypothetical protein | **1.96** | 0.0000 | **1.67** | 0.0000 |
| LO28_0301 | lmo1140 | | S | No functional prediction | Hypothetical protein | **3.68** | 0.0012 | **3.23** | 0.0004 |
| LO28_1414 | lmo2437 | | R | General prediction only | Hypothetical protein | **2.57** | 0.0001 | **2.44** | 0.0000 |
| LO28_0752 | lmo1526 | | S | No functional prediction | Hypothetical protein | **2.97** | 0.0000 | **3.12** | 0.0000 |
| LO28_1322 | lmo0133 | | S | No functional prediction | Hypothetical protein | **2.41** | 0.0003 | **2.25** | 0.0001 |
| LO28_2341 | lmo0274 | | T | Signal transduction mechanisms | Hypothetical protein | **2.07** | 0.0000 | **2.36** | 0.0000 |
| LO28_1551 | lmo2570 | | S | No functional prediction | Hypothetical protein | **4.41** | 0.0000 | **3.30** | 0.0000 |
| LO28_2167 | lmo0445 | | No COG | | Hypothetical protein | **3.84** | 0.0000 | **3.88** | 0.0000 |
| LO28_0114 | lmo0937 | | No COG | | Hypothetical protein | **2.56** | 0.0001 | **2.75** | 0.0000 |
| LO28_1932 | | | No COG | | Hypothetical protein | **2.52** | 0.0066 | **2.32** | 0.0041 |
| LO28_1952 | lmo0654 | | No COG | | Hypothetical protein | **2.26** | 0.0001 | **2.50** | 0.0000 |
| LO28_2956 | lmo2269 | | No COG | | Hypothetical protein | **4.76** | 0.0000 | **4.33** | 0.0000 |

Table S3.1 continued (2 of 3): Expression of genes upregulated in both *L. monocytogenes* LO28 variant 14 and variant 15 compared to the wild type. Values in bold are considered significant

| LO28 | lmo | Gene | COG class | COG description | Product | variant 14 | | variant 15 | |
|---|---|---|---|---|---|---|---|---|---|
| | | | | | | log$_2$ fold change | FDR | log$_2$ fold change | FDR |
| LO28_2179 | lmo0433 | *inlA* | No COG | | Internalin A (LPXTG motif) | **3.64** | 0.0000 | **3.70** | 0.0000 |
| LO28_2178 | lmo0434 | *inlB* | S | No functional prediction | Internalin B (GW modules) | **1.85** | 0.0029 | **2.15** | 0.0001 |
| LO28_2352 | lmo0263 | *inlH* | S | No functional prediction | Internalin H (LPXTG motif) | **6.21** | 0.0000 | **6.18** | 0.0000 |
| LO28_1997 | lmo0610 | | No COG | | Internalin-like protein (LPXTG motif) Lmo0610homolog | **4.84** | 0.0000 | **5.05** | 0.0000 |
| LO28_1978 | lmo0629 | | Q | Secondary metabolites biosynthesis, transport and catabolism | Isochorismatase | **4.73** | 0.0001 | **4.65** | 0.0000 |
| LO28_1737 | lmo0211 | *ctc* | J | Translation, ribosomal structure and biogenesis | LSU ribosomal protein L25p | **2.47** | 0.0000 | **1.84** | 0.0000 |
| LO28_1958 | lmo0648 | | P | Inorganic ion transport and metabolism | Magnesium and cobalt transport protein CorA | **2.82** | 0.0000 | **2.60** | 0.0000 |
| LO28_0174 | lmo0995 | | G | Carbohydrate transport and metabolism | Membrane protein | **2.80** | 0.0005 | **2.21** | 0.0004 |
| LO28_0486 | lmo1261 | | No COG | | Membrane protein | **2.88** | 0.0000 | **2.31** | 0.0000 |
| LO28_1462 | lmo2484 | | S | No functional prediction | Membrane protein | **2.12** | 0.0016 | **1.60** | 0.0009 |
| LO28_2294 | lmo0321 | | No COG | | Membrane protein | **4.07** | 0.0000 | **3.39** | 0.0000 |
| LO28_0922 | lmo2602 | | S | No functional prediction | Mg(2+) transport ATPase protein C | **3.39** | 0.0000 | **2.94** | 0.0000 |
| LO28_0133 | lmo0956 | | G | Carbohydrate transport and metabolism | N-acetylglucosamine-6-phosphate deacetylase | **1.78** | 0.0000 | **1.89** | 0.0000 |
| LO28_2054 | lmo0554 | | C | Energy production and conversion | NADH-dependent butanol dehydrogenase A | **3.56** | 0.0000 | **3.10** | 0.0000 |
| LO28_1552 | lmo2571 | | Q | Secondary metabolites biosynthesis, transport and catabolism | Nicotinamidase | **4.15** | 0.0000 | **3.92** | 0.0000 |
| LO28_0120 | lmo0943 | *fri* | P | Inorganic ion transport and metabolism | Non-specific DNA-binding protein Dps /Iron-binding ferritin-like antioxidant protein | **1.96** | 0.0000 | **2.26** | 0.0000 |
| LO28_0651 | lmo1428 | *opuCA* | E | Amino acid transport and metabolism | Osmotically activated L-carnitine/choline ABCtransporter, ATP-binding protein OpuCA | **6.31** | 0.0000 | **6.04** | 0.0000 |
| LO28_0650 | lmo1427 | *opuCB* | E | Amino acid transport and metabolism | Osmotically activated L-carnitine/choline ABCtransporter, permease protein OpuCB | **6.48** | 0.0000 | **6.37** | 0.0000 |
| LO28_0648 | lmo1425 | *opuCD* | E | Amino acid transport and metabolism | Osmotically activated L-carnitine/choline ABCtransporter, permease protein OpuCD | **6.49** | 0.0000 | **6.22** | 0.0000 |
| LO28_0649 | lmo1426 | *opuCC* | M | Cell wall/membrane/envelope biogenesis | Osmotically activated L-carnitine/choline ABCtransporter, substrate-binding protein OpuCC | **6.50** | 0.0000 | **6.28** | 0.0000 |
| LO28_1614 | lmo2391 | | M | Cell wall/membrane/envelope biogenesis | Oxidoreductase ylbE | **3.36** | 0.0000 | **3.36** | 0.0000 |
| LO28_1935 | lmo0669 | | I | Lipid metabolism | Oxidoreductase, short-chain dehydrogenase/reductase family | **5.74** | 0.0000 | **5.78** | 0.0000 |
| LO28_0598 | lmo1375 | | E | Amino acid transport and metabolism | Peptidase T | **2.08** | 0.0000 | **2.14** | 0.0000 |
| LO28_1956 | lmo0650 | | S | No functional prediction | Phage infection protein | **1.89** | 0.0000 | **1.71** | 0.0000 |
| LO28_1474 | lmo2496 | | P | Inorganic ion transport and metabolism | Phosphate transport ATP-binding protein PstB | **2.25** | 0.0337 | **1.71** | 0.0484 |
| LO28_1472 | lmo2494 | | P | Inorganic ion transport and metabolism | Phosphate transport system regulatory protein PhoU | **3.89** | 0.0001 | **4.15** | 0.0000 |
| LO28_1028 | lmo2696 | | G | Carbohydrate transport and metabolism | Phosphoenolpyruvate-dihydroxyacetonephosphotransferase, ADP-binding subunit DhaL | **4.86** | 0.0000 | **4.81** | 0.0000 |
| LO28_1027 | lmo2695 | | G | Carbohydrate transport and metabolism | Phosphoenolpyruvate-dihydroxyacetonephosphotransferase, subunit DhaK | **4.80** | 0.0000 | **4.58** | 0.0000 |
| LO28_1029 | lmo2697 | | S | No functional prediction | Phosphoenolpyruvate-dihydroxyacetonephosphotransferase, subunit DhaM | **3.52** | 0.0001 | **3.21** | 0.0000 |
| LO28_2892 | lmo2205 | | G | Carbohydrate transport and metabolism | Phosphoglycerate mutase | **2.12** | 0.0000 | **2.34** | 0.0000 |
| LO28_2027 | lmo0580 | | R | General prediction only | Phospholipase/carboxylesterase family protein | **1.94** | 0.0000 | **2.02** | 0.0000 |
| LO28_1370 | lmo1798 | | No COG | | Poly (glycerol-phosphate)alpha-glucosyltransferase | **2.08** | 0.0324 | **2.00** | 0.0146 |
| LO28_2207 | lmo0405 | | P | Inorganic ion transport and metabolism | Probable low-affinity inorganic phosphatetransporter | **2.38** | 0.0000 | **2.01** | 0.0000 |
| LO28_1818 | lmo0784 | | G | Carbohydrate transport and metabolism | PTS system, mannose-specific IIA component / PTS system, mannose-specific IIB component | **4.94** | 0.0000 | **4.43** | 0.0000 |
| LO28_1819 | lmo0783 | | G | Carbohydrate transport and metabolism | PTS system, mannose-specific IIB component | **5.01** | 0.0000 | **4.37** | 0.0000 |
| LO28_1820 | lmo0782 | | G | Carbohydrate transport and metabolism | PTS system, mannose-specific IIC component | **4.85** | 0.0000 | **3.94** | 0.0000 |
| LO28_1821 | lmo0781 | | G | Carbohydrate transport and metabolism | PTS system, mannose-specific IID component | **4.55** | 0.0000 | **3.97** | 0.0000 |
| LO28_0464 | lmo1241 | | S | No functional prediction | Putative exported protein | **2.63** | 0.0049 | **2.25** | 0.0029 |
| LO28_1585 | lmo0170 | | S | No functional prediction | Putative exported protein | **3.94** | 0.0000 | **3.71** | 0.0000 |
| LO28_0056 | lmo0880 | | M | Cell wall/membrane/envelope biogenesis | Putative peptidoglycan bound protein (LPXTGmotif) Lmo0880 homolog | **3.17** | 0.0024 | **3.40** | 0.0002 |
| LO28_0893 | lmo1666 | | No COG | | Putative peptidoglycan bound protein (LPXTGmotif) Lmo1666 homolog | **2.49** | 0.0000 | **2.64** | 0.0000 |
| LO28_2770 | lmo2085 | | M | Cell wall/membrane/envelope biogenesis | Putative peptidoglycan bound protein (LPXTGmotif) Lmo2085 homolog | **5.03** | 0.0000 | **4.48** | 0.0000 |
| LO28_1066 | lmo2735 | | G | Carbohydrate transport and metabolism | Putative sucrose phosphorylase | **2.14** | 0.0366 | **1.72** | 0.0355 |
| LO28_1881 | lmo0722 | | E | Amino acid transport and metabolism | Pyruvate oxidase [ubiquinone, cytochrome] | **6.32** | 0.0000 | **6.31** | 0.0000 |
| LO28_0995 | lmo2674 | | G | Carbohydrate transport and metabolism | Ribose 5-phosphate isomerase B | **2.79** | 0.0000 | **2.46** | 0.0000 |
| LO28_1489 | lmo2511 | | J | Translation, ribosomal structure and biogenesis | Ribosomal subunit interface protein | **1.84** | 0.0000 | **1.88** | 0.0000 |
| LO28_2176 | lmo0436 | | K | Transcription | Rrf2 family transcriptional regulator, group III | **1.84** | 0.0019 | **2.03** | 0.0003 |
| LO28_1808 | lmo0794 | | R | General prediction only | Rrf2-linked NADH-flavin reductase | **3.58** | 0.0000 | **3.76** | 0.0000 |
| LO28_1951 | lmo0655 | | T | Signal transduction mechanisms | Serine/threonine protein phosphatase | **2.84** | 0.0001 | **2.77** | 0.0000 |
| LO28_2512 | lmo1830 | | I | Lipid metabolism | Short chain dehydrogenase | **1.76** | 0.0033 | **1.81** | 0.0007 |
| LO28_2173 | lmo0439 | | R | General prediction only | Siderophore/Surfactin synthetase relatedprotein | **5.71** | 0.0000 | **5.41** | 0.0000 |
| LO28_0090 | lmo0913 | | C | Energy production and conversion | Succinate-semialdehyde dehydrogenase [NAD(P)+] | **2.02** | 0.0242 | **1.86** | 0.0092 |
| LO28_2084 | lmo0524 | | P | Inorganic ion transport and metabolism | Sulfate permease | **1.84** | 0.0000 | **1.95** | 0.0000 |

Table S3.1 continued (3 of 3): Expression of genes upregulated in both *L. monocytogenes* LO28 variant 14 and variant 15 compared to the wild type. Values in bold are considered significant

| LO28 | lmo | Gene | COG class | COG description | Product | variant 14 | | variant 15 | |
|---|---|---|---|---|---|---|---|---|---|
| | | | | | | $log_2$ fold change | FDR | $log_2$ fold change | FDR |
| LO28_2069 | lmo0539 | | G | Carbohydrate transport and metabolism | Tagatose 1,6-diphosphate aldolase | **4.07** | 0.0000 | **3.75** | 0.0000 |
| LO28_0993 | lmo2672 | | No COG | | Transcriptional regulator, AraC family | **2.74** | 0.0000 | **2.48** | 0.0000 |
| LO28_1957 | lmo0649 | | K | Transcription | Transcriptional regulator, GntR family | **2.29** | 0.0000 | **2.38** | 0.0000 |
| LO28_1360 | lmo1788 | | K | Transcription | Transcriptional regulator, MerR family | **1.83** | 0.0001 | **1.77** | 0.0001 |
| LO28_2900 | lmo2213 | | No COG | | Uncharacterized protein, homolog of *B.subtilis yhgC* | **4.92** | 0.0000 | **4.87** | 0.0000 |
| LO28_0806 | lmo1580 | | T | Signal transduction mechanisms | Universal stress protein family | **2.22** | 0.0000 | **2.33** | 0.0000 |
| LO28_0994 | lmo2673 | | T | Signal transduction mechanisms | Universal stress protein family | **7.06** | 0.0002 | **7.11** | 0.0000 |
| LO28_2093 | lmo0515 | | T | Signal transduction mechanisms | Universal stress protein family | **3.10** | 0.0040 | **3.01** | 0.0009 |
| LO28_1748 | lmo0200 | *prfA* | T | Signal transduction mechanisms | Virulence regulatory factor PrfA/Transcriptional regulator, CrP/Fnr family | **2.30** | 0.0000 | **2.45** | 0.0000 |
| LO28_1806 | lmo0796 | | S | No functional prediction | Ycel like family protein | **3.22** | 0.0000 | **3.40** | 0.0000 |

Table S3.2 (1 of 3): Expression of downregulated genes in both *L. monocytogenes* LO28 variant 14 and variant 15 compared to the wild type. Values in bold are considered significant

| LO28 | lmo | Gene | COG class | COG description | Product | variant 14 | | variant 15 | |
|---|---|---|---|---|---|---|---|---|---|
| | | | | | | $log_2$ fold change | FDR | $log_2$ fold change | FDR |
| LO28_2938 | lmo2250 | *arpJ* | E | Amino acid transport and metabolism | Amino acid ABC transporter, aminoacid-binding/permease protein | **-4.01** | 0.0001 | **-4.16** | 0.0000 |
| LO28_2939 | lmo2251 | | E | Amino acid transport and metabolism | Amino acid ABC transporter, ATP-bindingprotein | **-3.87** | 0.0001 | **-3.60** | 0.0000 |
| LO28_1446 | lmo2469 | | E | Amino acid transport and metabolism | Amino acid permease family protein | **-1.68** | 0.0000 | **-2.04** | 0.0000 |
| LO28_0829 | lmo1603 | | E | Amino acid transport and metabolism | Aminopeptidase | **-1.75** | 0.0000 | **-1.89** | 0.0000 |
| LO28_2776 | lmo2091 | *argH* | E | Amino acid transport and metabolism | Argininosuccinate lyase | **-5.88** | 0.0047 | **-6.57** | 0.0007 |
| LO28_2775 | lmo2090 | *argG* | E | Amino acid transport and metabolism | Argininosuccinate synthase | **-4.83** | 0.0012 | **-5.29** | 0.0001 |
| LO28_2940 | lmo2252 | | E | Amino acid transport and metabolism | Aspartate aminotransferase | **-2.83** | 0.0003 | **-2.69** | 0.0001 |
| LO28_0446 | | | No COG | | Bacteriophage | **-3.58** | 0.0000 | **-3.65** | 0.0000 |
| LO28_1914 | lmo0689 | | N | Cell motility | Chemotaxis protein CheV | **-5.55** | 0.0000 | **-5.26** | 0.0000 |
| LO28_1920 | lmo0683 | | N | Cell motility | Chemotaxis protein methyltransferase CheR | **-5.16** | 0.0000 | **-4.97** | 0.0000 |
| LO28_1912 | lmo0691 | *cheY* | T | Signal transduction mechanisms | Chemotaxis regulator transmits chemoreceptorsignals to flagelllar motor components CheY | **-6.12** | 0.0000 | **-5.53** | 0.0000 |
| LO28_1915 | lmo0688 | | M | Cell wall/membrane/envelope biogenesis | Dolichol-phosphate mannosyltransferase in lipid-linked oligosaccharide synthesis cluster | **-4.89** | 0.0000 | **-4.24** | 0.0000 |
| LO28_2790 | lmo2105 | | P | Inorganic ion transport and metabolism | Ferrous iron transport protein B | **-2.30** | 0.0000 | **-3.09** | 0.0000 |
| LO28_1885 | lmo0718 | | No COG | | Hypothetical protein | **-3.44** | 0.0000 | **-2.67** | 0.0000 |
| LO28_2791 | | | No COG | | Hypothetical protein | **-2.73** | 0.0000 | **-3.20** | 0.0000 |
| LO28_1548 | lmo2567 | | No COG | | Hypothetical protein | **-2.98** | 0.0064 | **-2.53** | 0.0175 |
| LO28_1879 | lmo0724 | | S | No functional prediction | Hypothetical protein | **-2.25** | 0.0000 | **-2.51** | 0.0000 |
| LO28_1916 | lmo0687 | | No COG | | Hypothetical protein | **-4.93** | 0.0000 | **-4.75** | 0.0000 |
| LO28_1901 | lmo0702 | | No COG | | Hypothetical protein | **-5.43** | 0.0000 | **-5.02** | 0.0000 |
| LO28_1919 | lmo0684 | | No COG | | Hypothetical protein | **-6.06** | 0.0000 | **-5.84** | 0.0000 |
| LO28_1902 | lmo0701 | | No COG | | Hypothetical protein | **-6.00** | 0.0000 | **-5.64** | 0.0000 |
| LO28_0452 | | | No COG | | Hypothetical protein | **-2.34** | 0.0004 | **-2.08** | 0.0001 |
| LO28_1899 | lmo0704 | | No COG | | Hypothetical protein | **-6.10** | 0.0000 | **-5.37** | 0.0000 |
| LO28_1909 | lmo0694 | | No COG | | Hypothetical protein | **-4.49** | 0.0000 | **-4.04** | 0.0000 |
| LO28_0008 | lmo0834 | | No COG | | Hypothetical protein | **-2.07** | 0.0001 | **-1.60** | 0.0003 |
| LO28_1894 | lmo0708 | | No COG | | Hypothetical protein | **-5.79** | 0.0000 | **-5.03** | 0.0000 |
| LO28_2462 | lmo1700 | | No COG | | Hypothetical protein | **-7.00** | 0.0000 | **-6.12** | 0.0000 |
| LO28_0414 | | | No COG | | Hypothetical protein | **-1.90** | 0.0005 | **-1.58** | 0.0003 |
| LO28_0449 | | | No COG | | Hypothetical protein | **-3.66** | 0.0000 | **-3.23** | 0.0000 |
| LO28_0408 | | | No COG | | Hypothetical protein | **-3.06** | 0.0000 | **-1.82** | 0.0012 |
| LO28_0421 | lmo2309 | | No COG | | Hypothetical protein | **-2.40** | 0.0024 | **-2.22** | 0.0028 |
| LO28_0448 | | | No COG | | Hypothetical protein | **-3.80** | 0.0000 | **-3.47** | 0.0000 |
| LO28_0445 | | | No COG | | Hypothetical protein | **-2.91** | 0.0000 | **-2.76** | 0.0000 |
| LO28_0454 | | | No COG | | Hypothetical protein | **-2.80** | 0.0000 | **-2.59** | 0.0000 |
| LO28_2289 | lmo0326 | | K | Transcription | Transcriptional activator of Lmo0327 homolog | **-1.81** | 0.0386 | **-1.75** | 0.0119 |
| LO28_1888 | lmo0715 | *fliH* | No COG | | Flagellar assembly protein FliH | **-4.66** | 0.0000 | **-4.46** | 0.0000 |
| LO28_1907 | lmo0696 | *flgD* | N | Cell motility | Flagellar basal-body rod modification protein FlgD | **-4.70** | 0.0000 | **-4.52** | 0.0000 |
| LO28_1893 | lmo0710 | *flgB* | N | Cell motility | Flagellar basal-body rod protein FlgB | **-4.96** | 0.0000 | **-4.78** | 0.0000 |
| LO28_1892 | lmo0711 | *flgC* | N | Cell motility | Flagellar basal-body rod protein FlgC | **-4.43** | 0.0000 | **-4.06** | 0.0000 |

Table S3.2 continued (2 of 3): Expression of downregulated genes in both *L. monocytogenes* LO28 variant 14 and variant 15 compared to the wild type. Values in bold are considered significant

| | | | | | | variant 14 | | variant 15 | |
|---|---|---|---|---|---|---|---|---|---|
| LO28 | lmo | Gene | COG class | COG description | Product | $log_2$ fold change | FDR | $log_2$ fold change | FDR |
| LO28_1921 | lmo0682 | *flgG* | N | Cell motility | Flagellar basal-body rod protein FlgG | **-6.03** | 0.0000 | **-6.37** | 0.0000 |
| LO28_1923 | lmo0680 | *flhA* | N | Cell motility | Flagellar biosynthesis protein FlhA | **-5.31** | 0.0000 | **-4.83** | 0.0000 |
| LO28_1924 | lmo0679 | *flhB* | N | Cell motility | Flagellar biosynthesis protein FlhB | **-4.49** | 0.0000 | **-4.65** | 0.0000 |
| LO28_1922 | lmo0681 | | N | Cell motility | Flagellar biosynthesis protein FlhF | **-5.57** | 0.0000 | **-4.91** | 0.0000 |
| LO28_1927 | lmo0676 | *fliP* | N | Cell motility | Flagellar biosynthesis protein FliP | **-2.91** | 0.0000 | **-2.93** | 0.0000 |
| LO28_1926 | lmo0677 | *fliQ* | N | Cell motility | Flagellar biosynthesis protein FliQ | **-2.99** | 0.0000 | **-3.04** | 0.0000 |
| LO28_1925 | lmo0678 | *fliR* | N | Cell motility | Flagellar biosynthesis protein FliR | **-3.12** | 0.0000 | **-2.85** | 0.0000 |
| LO28_1895 | lmo0708 | | No COG | | Flagellar biosynthesis protein FliS | **-5.38** | 0.0000 | **-4.86** | 0.0000 |
| LO28_1906 | lmo0697 | *flgE* | N | Cell motility | Flagellar hook protein FlgE | **-5.44** | 0.0000 | **-5.20** | 0.0000 |
| LO28_1898 | lmo0705 | *flgK* | N | Cell motility | Flagellar hook-associated protein FlgK | **-5.59** | 0.0000 | **-5.16** | 0.0000 |
| LO28_1897 | lmo0706 | *flgL* | N | Cell motility | Flagellar hook-associated protein FlgL | **-5.53** | 0.0000 | **-4.85** | 0.0000 |
| LO28_1896 | lmo0707 | *fliD* | N | Cell motility | Flagellar hook-associated protein FliD | **-5.33** | 0.0000 | **-4.57** | 0.0000 |
| LO28_1891 | lmo0712 | *fliE* | N | Cell motility | Flagellar hook-basal body complex protein FliE | **-5.37** | 0.0000 | **-4.89** | 0.0000 |
| LO28_1918 | lmo0685 | *motA* | N | Cell motility | Flagellar motor rotation protein MotA | **-5.92** | 0.0000 | **-5.71** | 0.0000 |
| LO28_1917 | | *motB* | N | Cell motility | Flagellar motor rotation protein MotB | **-5.33** | 0.0000 | **-5.06** | 0.0000 |
| LO28_1889 | lmo0714 | *fliG* | N | Cell motility | Flagellar motor switch protein FliG | **-4.69** | 0.0000 | **-4.45** | 0.0000 |
| LO28_1904 | lmo0699 | *fliM* | N | Cell motility | Flagellar motor switch protein FliM | **-5.93** | 0.0000 | **-5.58** | 0.0000 |
| LO28_1903 | lmo0700 | | N | Cell motility | Flagellar motor switch protein FliN | **-5.66** | 0.0000 | **-5.29** | 0.0000 |
| LO28_1905 | lmo0698 | | N | Cell motility | Flagellar motor switch protein FliN | **-5.64** | 0.0000 | **-5.35** | 0.0000 |
| LO28_1910 | lmo0693 | | N | Cell motility | Flagellar motor switch protein FliN | **-5.91** | 0.0000 | **-5.40** | 0.0000 |
| LO28_1928 | lmo0675 | | N | | Flagellar motor switch protein FliN | **-2.53** | 0.0000 | **-2.29** | 0.0000 |
| LO28_1890 | lmo0713 | *fliF* | N | Cell motility | Flagellar M-ring protein FliF | **-4.98** | 0.0000 | **-4.67** | 0.0000 |
| LO28_1913 | lmo0690 | *flaA* | N | Cell motility | Flagellin protein FlaA | **-6.70** | 0.0000 | **-6.27** | 0.0000 |
| LO28_1887 | lmo0716 | *fliI* | N | Cell motility | Flagellum-specific ATP synthase FliI | **-4.44** | 0.0000 | **-3.99** | 0.0000 |
| LO28_2260 | lmo0355 | | C | Energy production and conversion | Fumarate reductase flavoprotein subunit | **-2.02** | 0.0005 | **-2.23** | 0.0000 |
| LO28_0410 | | | No COG | | Gp31 protein | **-5.80** | 0.0000 | **-2.93** | 0.0000 |
| LO28_0412 | | | No COG | | Hypothetical protein | **-3.04** | 0.0001 | **-2.97** | 0.0000 |
| LO28_0413 | | | No COG | | Hypothetical protein | **-2.29** | 0.0000 | **-2.41** | 0.0028 |
| LO28_0416 | | | No COG | | Hypothetical protein | **-2.31** | 0.0006 | **-2.34** | 0.0001 |
| LO28_0418 | lmo2312 | | S | No functional prediction | Hypothetical protein | **-2.29** | 0.0001 | **-2.13** | 0.0000 |
| LO28_0419 | | | No COG | | Hypothetical protein | **-1.76** | 0.0012 | **-1.94** | 0.0002 |
| LO28_0424 | | | No COG | | Hypothetical protein | **-2.41** | 0.0071 | **-2.24** | 0.0080 |
| LO28_0451 | | | No COG | | Hypothetical protein | **-5.96** | 0.0000 | **-4.10** | 0.0000 |
| LO28_1908 | lmo0695 | | No COG | | Hypothetical protein | **-4.08** | 0.0000 | **-3.98** | 0.0000 |
| LO28_2034 | lmo0573 | | R | General prediction only | Hypoxanthine/guanine permease PbuG | **-2.39** | 0.0070 | **-2.98** | 0.0004 |
| LO28_0438 | | | No COG | | Lin2582 protein | **-3.46** | 0.0000 | **-3.11** | 0.0000 |
| LO28_0426 | | | No COG | | Lin2592 protein | **-2.44** | 0.0001 | **-1.88** | 0.0003 |
| LO28_2810 | lmo2124 | | G | Carbohydrate transport and metabolism | Maltose/maltodextrin ABC transporter, permeaseprotein MalF | **-2.74** | 0.0008 | **-3.35** | 0.0000 |
| LO28_2809 | lmo2123 | | G | Carbohydrate transport and metabolism | Maltose/maltodextrin ABC transporter, permeaseprotein MalG | **-2.66** | 0.0007 | **-2.78** | 0.0001 |
| LO28_2811 | lmo2125 | | G | Carbohydrate transport and metabolism | Maltose/maltodextrin ABC transporter, substratebinding periplasmic protein MalE | **-2.73** | 0.0068 | **-2.75** | 0.0011 |
| LO28_2530 | lmo1848 | | P | Inorganic ion transport and metabolism | Manganese ABC transporter, inner membranepermease protein SitD | **-1.59** | 0.0000 | **-2.24** | 0.0000 |
| LO28_2529 | lmo1847 | | P | Inorganic ion transport and metabolism | Manganese ABC transporter, periplasmic-bindingprotein SitA | **-2.21** | 0.0000 | **-2.33** | 0.0000 |
| LO28_1880 | lmo0723 | | N | Cell motility | Methyl-accepting chemotaxis protein | **-1.96** | 0.0000 | **-2.07** | 0.0000 |
| LO28_2463 | lmo1699 | | N | Cell motility | Methyl-accepting chemotaxis protein | **-6.15** | 0.0000 | **-6.00** | 0.0000 |
| LO28_2528 | lmo1846 | | V | Defense mechanisms | Multi antimicrobial extrusion protein(Na(+)/drug antiporter), MATE family of efflux pumps | **-1.70** | 0.0008 | **-2.48** | 0.0000 |
| LO28_0817 | lmo1591 | *argC* | E | Amino acid transport and metabolism | N-acetyl-gamma-glutamyl-phosphate reductase | **-3.63** | 0.0008 | **-4.57** | 0.0000 |
| LO28_0959 | lmo2638 | | C | Energy production and conversion | NADH dehydrogenase in clusterwith putative pheromone precursor | **-1.64** | 0.0001 | **-1.92** | 0.0000 |
| LO28_0138 | lmo0961 | | O | Posttranslational modification, protein turnover, chaperones | Peptidase, U32 family large subunit [C1] | **-2.08** | 0.0000 | **-2.41** | 0.0000 |
| LO28_0137 | lmo0960 | | O | Posttranslational modification, protein turnover, chaperones | Peptidase, U32 family small subunit [C1] | **-1.80** | 0.0000 | **-1.88** | 0.0000 |
| LO28_0444 | | | No COG | | Phage major capsid protein | **-3.46** | 0.0000 | **-3.33** | 0.0000 |
| LO28_0450 | | | No COG | | Phage major tail protein | **-3.41** | 0.0000 | **-3.19** | 0.0000 |
| LO28_0455 | | | No COG | | Phage minor structural protein, N-terminalregion domain protein | **-3.83** | 0.0000 | **-3.66** | 0.0000 |
| LO28_0442 | | | No COG | | Phage portal (connector) protein | **-3.04** | 0.0000 | **-2.23** | 0.0000 |

Table S3.2 continued (3 of 3): Expression of downregulated genes in both *L. monocytogenes* LO28 variant 14 and variant 15 compared to the wild type. Values in bold are considered significant

| LO28 | lmo | Gene | COG class | COG description | Product | variant 14 | | variant 15 | |
|---|---|---|---|---|---|---|---|---|---|
| | | | | | | $log_2$ fold change | FDR | $log_2$ fold change | FDR |
| LO28_0425 | | | No COG | | Phage protein | **-1.71** | 0.0030 | **-1.82** | 0.0006 |
| LO28_0447 | | | No COG | | Phage protein | **-3.59** | 0.0000 | **-3.39** | 0.0000 |
| LO28_0437 | | | No COG | | Phage regulatory protein | **-1.65** | 0.0199 | **-1.70** | 0.0067 |
| LO28_0453 | | | R | General prediction only | Phage tail length tape-measure protein | **-2.86** | 0.0000 | **-2.39** | 0.0000 |
| LO28_0443 | | | O | Posttranslational modification, protein turnover, chaperones | Prophage Clp protease-like protein | **-3.40** | 0.0000 | **-3.14** | 0.0000 |
| LO28_0456 | | | No COG | | Protein gp23 [Bacteriophage A118] | **-4.07** | 0.0000 | **-3.13** | 0.0000 |
| LO28_1015 | lmo2683 | | G | Carbohydrate transport and metabolism | PTS system, cellobiose-specific IIB component | **-1.91** | 0.0004 | **-2.02** | 0.0000 |
| LO28_1016 | lmo2684 | | G | Carbohydrate transport and metabolism | PTS system, cellobiose-specific IIC component | **-1.78** | 0.0001 | **-1.84** | 0.0000 |
| LO28_2684 | lmo2001 | | G | Carbohydrate transport and metabolism | PTS system, mannose-specific IIC component | **-3.28** | 0.0127 | **-2.98** | 0.0000 |
| LO28_0480 | lmo1255 | | G | Carbohydrate transport and metabolism | PTS system, trehalose-specific IIB component/ PTS system, trehalose-specific IIC component | **-1.71** | 0.0000 | **-1.99** | 0.0000 |
| LO28_2787 | lmo2102 | | H | Coenzyme transport and metabolism | Pyridoxine biosynthesis glutamineamidotransferase, glutaminase subunit | **-1.95** | 0.0000 | **-2.13** | 0.0000 |
| LO28_0629 | lmo1406 | *pflB* | C | Energy production and conversion | Pyruvate formate-lyase | **-1.64** | 0.0000 | **-1.92** | 0.0000 |
| LO28_2598 | lmo1917 | *pflA* | C | Energy production and conversion | Pyruvate formate-lyase | **-1.92** | 0.0064 | **-1.80** | 0.0026 |
| LO28_0630 | lmo1407 | *pflC* | O | Posttranslational modification, protein turnover, chaperones | Pyruvate formate-lyase activating enzyme | **-2.44** | 0.0000 | **-3.04** | 0.0000 |
| LO28_0963 | lmo2642 | | R | General prediction only | Serine/threonine protein phosphatase familyprotein | **-1.61** | 0.0000 | **-1.75** | 0.0000 |
| LO28_1911 | lmo0692 | *cheA* | N | Cell motility | Signal transduction histidine kinase CheA | **-5.79** | 0.0000 | **-5.23** | 0.0000 |
| LO28_1886 | lmo0717 | | M | Cell wall/membrane/envelope biogenesis | Soluble lytic murein transglycosylase precursor | **-3.99** | 0.0000 | **-3.78** | 0.0000 |
| LO28_0693 | | *rpsU* | J | Translation, ribosomal structure and biogenesis | SSU ribosomal protein S21p | **-7.37** | 0.0000 | **-2.15** | 0.0000 |
| LO28_0073 | lmo0897 | | P | Inorganic ion transport and metabolism | Sulfate permease | **-1.79** | 0.0000 | **-1.94** | 0.0000 |
| LO28_0692 | lmo1468 | | S | No functional prediction | Transamidase GatB domain protein | **-5.65** | 0.0000 | **-2.53** | 0.0000 |
| LO28_2318 | lmo0297 | | K | Transcription | Transcriptional antiterminator of lichenanoperon, BglG family | **-2.01** | 0.0037 | **-2.10** | 0.0000 |
| LO28_1900 | lmo0703 | | No COG | | UDP-N-acetylenolpyruvoylglucosamine reductase | **-5.66** | 0.0000 | **-5.23** | 0.0000 |

Table S3.3: Expression of genes that were only upregulated in *L. monocytogenes* LO28 variant 14 compared to the wild type. Values in bold are considered significant

| LO28 | lmo | Gene | Product | variant 14 | |
|---|---|---|---|---|---|
| | | | | $log_2$ fold change | FDR |
| LO28_0088 | lmo0911 | | Hypothetical protein | **1.62** | 0.0000 |
| LO28_0338 | lmo1177 | | Ethanolamine utilization polyhedral-body-like protein EutL | **2.09** | 0.0219 |
| LO28_0764 | lmo1538 | *glpK* | Glycerol kinase | **2.06** | 0.0003 |
| LO28_0877 | lmo1650 | | CcdC protein | **1.68** | 0.0001 |
| LO28_1225 | lmo0036 | | Putrescine carbamoyltransferase | **1.75** | 0.0037 |
| LO28_1226 | lmo0037 | | Agmatine/putrescine antiporter, associated with agmatine catabolism | **1.59** | 0.0060 |
| LO28_1228 | lmo0039 | | Carbamate kinase | **1.92** | 0.0022 |
| LO28_1335 | lmo0146 | | Hypothetical protein | **1.69** | 0.0253 |
| LO28_1361 | lmo1789 | | Flavodoxin-like fold domain protein | **1.64** | 0.0000 |
| LO28_1362 | lmo1790 | | Metallo-beta-lactamase family protein | **1.65** | 0.0003 |
| LO28_1463 | lmo2485 | | PspC domain protein, truncated | **1.82** | 0.0015 |
| LO28_1569 | lmo2587 | | Hypothetical protein | **1.73** | 0.0001 |
| LO28_1783 | lmo0819 | | Hypothetical protein | **1.85** | 0.0001 |
| LO28_1841 | lmo0761 | | Nitrilotriacetate monooxygenase component B | **2.14** | 0.0052 |
| LO28_1842 | lmo0760 | | Carboxylesterase | **1.68** | 0.0000 |
| LO28_1870 | lmo0732 | | Internalin-like protein (LPXTG motif) Lmo0732 homolog | **2.07** | 0.0072 |
| LO28_1946 | lmo0660 | | Mobile element protein | **2.27** | 0.0001 |
| LO28_2015 | lmo0592 | | Hypothetical protein | **1.81** | 0.0000 |
| LO28_2041 | lmo0566 | *hisB* | Imidazoleglycerol-phosphate dehydratase | **1.69** | 0.0048 |
| LO28_2044 | lmo0563 | *hisF* | Imidazole glycerol phosphate synthase cyclasesubunit | **1.63** | 0.0007 |
| LO28_2045 | lmo0562 | *hisI* | Phosphoribosyl-AMP cyclohydrolase | **1.81** | 0.0057 |
| LO28_2053 | lmo0555 | | Di/tripeptide permease DtpT | **2.03** | 0.0000 |
| LO28_2390 | lmo1772 | *purC* | Phosphoribosylaminoimidazole-succinocarboxamidesynthase | **1.68** | 0.0002 |
| LO28_2395 | lmo1767 | *purM* | Phosphoribosylformylglycinamidine cyclo-ligase | **1.58** | 0.0001 |
| LO28_2396 | lmo1766 | *purN* | Phosphoribosylglycinamide formyltransferase | **1.69** | 0.0003 |
| LO28_2397 | lmo1765 | *purH* | IMP cyclohydrolase /Phosphoribosylaminoimidazolecarboxamide formyltransferase | **1.64** | 0.0000 |
| LO28_2564 | lmo1883 | | Chitinase | **2.40** | 0.0405 |
| LO28_2667 | lmo1984 | *ilvB* | Acetolactate synthase large subunit | **1.66** | 0.0089 |
| LO28_2669 | lmo1986 | *ilvC* | Ketol-acid reductoisomerase | **1.63** | 0.0405 |
| LO28_2670 | lmo1987 | *leuA* | 2-isopropylmalate synthase | **1.87** | 0.0212 |
| LO28_2672 | lmo1989 | *leuC* | 3-isopropylmalate dehydratase large subunit | **1.74** | 0.0152 |
| LO28_2844 | lmo2158 | | Hypothetical protein | **1.64** | 0.0041 |
| LO28_2878 | lmo2191 | *spxA* | Arsenate reductase family protein | **1.66** | 0.0000 |

Table S3.4: Expression of genes that were only upregulated in *L. monocytogenes* LO28 variant 15 compared to the wild type. Values in bold are considered significant

| LO28 | lmo | Gene | Product | variant 15 | |
|---|---|---|---|---|---|
| | | | | $log_2$ fold change | FDR |
| LO28_0309 | lmo1148 | | Cobalamin synthase | **4.03** | 0.0140 |
| LO28_1592 | lmo2369 | | General stress protein 13 | **1.83** | 0.0000 |
| LO28_0516 | lmo1292 | | Glycerophosphoryl diester phosphodiesterase | **1.68** | 0.0002 |
| LO28_1811 | lmo0791 | | Hypothetical protein | **2.19** | 0.0000 |
| LO28_0081 | lmo0904 | | Hypothetical protein | **1.66** | 0.0001 |
| LO28_0441 | | | Hypothetical protein | **1.66** | 0.0000 |
| LO28_0077 | lmo0900 | | Hypothetical protein | **1.63** | 0.0007 |
| LO28_0013 | lmo0839 | | Multidrug-efflux transporter, major facilitator superfamily (MFS) | **1.69** | 0.0152 |
| LO28_1591 | lmo2368 | | MutT/nudix family protein | **1.83** | 0.0000 |
| LO28_0848 | lmo1622 | | NAD(P)HX dehydratase | **1.63** | 0.0000 |
| LO28_0080 | lmo0903 | | OsmC/Ohr family protein | **1.75** | 0.0011 |
| LO28_1105 | lmo2772 | | PTS system, beta-glucoside-specific component | **1.61** | 0.0486 |
| LO28_2864 | lmo2178 | | Putative peptidoglycan bound protein (LPXTGmotif) Lmo2178 homolog | **1.64** | 0.0386 |
| LO28_2323 | lmo0292 | | Serine protease, DegP/HtrA, do-like | **1.80** | 0.0000 |
| LO28_2001 | lmo0606 | | Transcriptional regulator, MarR family | **1.64** | 0.0000 |
| LO28_2082 | lmo0526 | | Transcriptional regulator, MerR family | **1.66** | 0.0155 |
| LO28_2290 | lmo0325 | | Transcriptional regulator, MutR family | **1.70** | 0.0000 |
| LO28_0631 | lmo1408 | | Transcriptional regulator, PadR family | **1.72** | 0.0035 |
| LO28_0211 | lmo1032 | | Transketolase, N-terminal section | **1.99** | 0.0044 |
| LO28_1168 | lmo2836 | | Zinc-type alcohol dehydrogenase YcjQ | **1.80** | 0.0386 |

Table S3.5: Expression of genes that were only downregulated in variant 14 compared to the wild type. Values in bold are considered significant

| LO28 | lmo | Gene | Product | variant 14 | |
|---|---|---|---|---|---|
| | | | | $log_2$ fold change | FDR |
| LO28_0432 | | | DNA polymerase B region | **-2.06** | 0.0003 |
| LO28_0459 | | *lysA* | Endolysin, L-alanyl-D-glutamate peptidase [Bacteriophage A118] | **-1.73** | 0.0045 |
| LO28_1871 | | | Hypothetical protein | **-8.69** | 0.0000 |
| LO28_0351 | | | Hypothetical protein | **-4.27** | 0.0055 |
| LO28_1549 | lmo2568 | | Hypothetical protein | **-2.74** | 0.0085 |
| LO28_0462 | | | Hypothetical protein | **-2.12** | 0.0026 |
| LO28_0436 | | | Hypothetical protein | **-1.76** | 0.0048 |
| LO28_0409 | | | Hypothetical protein | **-1.68** | 0.0006 |
| LO28_0564 | lmo1341 | | Late competence protein ComGG, FIG007920 | **-3.71** | 0.0043 |
| LO28_0428 | | | Phage protein | **-1.65** | 0.0001 |
| LO28_1098 | lmo2765 | | PTS system, cellobiose-specific IIA component | **-2.10** | 0.0172 |
| LO28_1116 | lmo2783 | | PTS system, cellobiose-specific IIC component | **-1.87** | 0.0003 |
| LO28_0986 | lmo2665 | | PTS system, galactitol-specific IIC component | **-1.60** | 0.0007 |
| LO28_0009 | lmo0835 | | Putative peptidoglycan bound protein (LPXTGmotif) Lmo0835 homolog | **-1.96** | 0.0018 |
| LO28_2686 | lmo2003 | | Transcriptional regulator, GntR family | **-1.88** | 0.0353 |
| LO28_1787 | lmo0815 | | Transcriptional regulator, MarR family | **-1.96** | 0.0000 |

Table S3.6: Expression of genes that were only downregulated in variant 15 compared to the wild type. Values in bold are considered significant

| LO28 | lmo | Gene | Product | variant 15 | |
|---|---|---|---|---|---|
| | | | | $log_2$ fold change | FDR |
| LO28_1048 | lmo2717 | *cydB* | Cytochrome d ubiquinol oxidase subunit II | **-1.65** | 0.0002 |
| LO28_1231 | lmo0042 | *dedA* | DedA protein | **-1.64** | 0.0000 |
| LO28_2089 | lmo0519 | | Drug resistance transporter, EmrB/QacA family | **-1.60** | 0.0004 |
| LO28_0434 | | | Hypothetical protein | **-1.63** | 0.0008 |
| LO28_0420 | lmo2310 | | Hypothetical protein | **-1.88** | 0.0000 |
| LO28_0423 | | | Hypothetical protein | **-2.15** | 0.0000 |
| LO28_0954 | | | Hypothetical protein | **-2.25** | 0.0002 |
| LO28_2161 | lmo0450 | | Hypothetical protein | **-2.27** | 0.0000 |
| LO28_0653 | lmo1430 | | Hypothetical protein | **-2.59** | 0.0005 |
| LO28_2236 | | | Hypothetical protein | **-3.70** | 0.0222 |
| LO28_2332 | lmo0283 | | Methionine ABC transporter permease protein | **-1.61** | 0.0000 |
| LO28_1623 | lmo2362 | | Probable glutamate/gamma-aminobutyrateantiporter | **-2.09** | 0.0318 |
| LO28_1017 | lmo2685 | | PTS system, beta-glucoside-specific II A component | **-1.92** | 0.0005 |
| LO28_2186 | lmo0427 | | PTS system, fructose-specific IIB component | **-2.15** | 0.0012 |
| LO28_0971 | lmo2650 | | PTS system, lactose/cellobiose specific IIBsubunit | **-1.75** | 0.0156 |
| LO28_1286 | lmo0097 | | PTS system, mannose-specific IIC component | **-1.96** | 0.0000 |
| LO28_1287 | lmo0098 | | PTS system, mannose-specific IID component | **-1.89** | 0.0000 |
| LO28_1288 | lmo0099 | | Putative regulator of the mannose operon, ManO | **-2.12** | 0.0000 |
| LO28_0479 | lmo1254 | | Trehalose-6-phosphate hydrolase | **-1.92** | 0.0000 |
| LO28_2565 | lmo1884 | | Xanthine permease | **-1.64** | 0.0027 |

Table S3.7 (1 of 4): expression of genes that are part of the SigB operon as described by Mujahid et al., 2013, in both variant 14 and variant 15 compared to the wild type. Values in bold are considered significant

| LO28 | lmo | Gene | Product | variant 14 | | variant 15 | |
|---|---|---|---|---|---|---|---|
| | | | | $log_2$ fold change | FDR | $log_2$ fold change | FDR |
| LO28_1323 | lmo0134 | | Acetyltransferase, GNAT family | **4.10** | 0.0000 | **3.84** | 0.0000 |
| LO28_2069 | lmo0539 | | Tagatose 1,6-diphosphate aldolase | **4.07** | 0.0000 | **3.75** | 0.0000 |
| LO28_2054 | lmo0554 | | NADH-dependent butanol dehydrogenase A | **3.56** | 0.0000 | **3.10** | 0.0000 |
| LO28_1952 | lmo0654 | | Hypothetical protein | **2.26** | 0.0001 | **2.50** | 0.0000 |
| LO28_1881 | lmo0722 | | Pyruvate oxidase [ubiquinone, cytochrome] | **6.32** | 0.0000 | **6.31** | 0.0000 |
| LO28_1819 | lmo0783 | | PTS system, mannose-specific IIB component | **5.01** | 0.0000 | **4.37** | 0.0000 |
| LO28_1808 | lmo0794 | | Rrf2-linked NADH-flavin reductase | **3.58** | 0.0000 | **3.76** | 0.0000 |
| LO28_1806 | lmo0796 | | Ycel like family protein | **3.22** | 0.0000 | **3.40** | 0.0000 |
| LO28_0090 | lmo0913 | | Succinate-semialdehyde dehydrogenase [NAD(P)+] | **2.02** | 0.0242 | **1.86** | 0.0092 |
| LO28_0828 | lmo1602 | | General stress protein | **2.53** | 0.0000 | **3.02** | 0.0000 |
| LO28_2512 | lmo1830 | | Short chain dehydrogenase | **1.76** | 0.0033 | **1.81** | 0.0007 |
| LO28_2844 | lmo2158 | | Hypothetical protein | **1.64** | 0.0041 | 1.58 | 0.0012 |
| LO28_2900 | lmo2213 | | Uncharacterized protein, homolog of *B.subtilis yhgC* | **4.92** | 0.0000 | **4.87** | 0.0000 |
| LO28_1374 | lmo2398 | *ltrC* | Low temperature requirement C protein | **3.17** | 0.0000 | **2.93** | 0.0000 |
| LO28_1079 | lmo2748 | | General stress protein 26 | **5.39** | 0.0000 | **5.58** | 0.0000 |
| LO28_1738 | lmo0210 | *ldh* | L-lactate dehydrogenase | -0.44 | 0.1942 | -0.34 | 0.2524 |
| LO28_2273 | lmo0342 | | Transketolase | 0.84 | 0.1637 | -0.06 | 0.9711 |
| LO28_2272 | lmo0343 | | Transaldolase | 0.37 | 0.5284 | 0.66 | 0.1499 |
| LO28_2270 | lmo0345 | | Ribose 5-phosphate isomerase B | 0.15 | 1.0483 | 0.09 | 1.0372 |
| LO28_2269 | lmo0346 | | Triosephosphate isomerase | 0.03 | 0.8776 | -0.68 | 0.6495 |

Table S3.7 continued (2 of 4 ): expression of genes that are part of the SigB operon as described by Mujahid et al., 2013, in both variant 14 and variant 15 compared to the wild type. Values in bold are considered significant

| LO28 | lmo | Gene | Product | variant 14 | | variant 15 | |
|---|---|---|---|---|---|---|---|
| | | | | $log_2$ fold change | FDR | $log_2$ fold change | FDR |
| LO28_2268 | lmo0347 | | Phosphoenolpyruvate-dihydroxyacetonephosphotransferase, ADP-binding subunit DhaL | 1.10 | 0.0969 | 0.29 | 0.2029 |
| LO28_2267 | lmo0348 | | Phosphoenolpyruvate-dihydroxyacetonephosphotransferase, dihydroxyacetonebinding subunit DhaK | 0.21 | 0.7673 | 0.20 | 0.2838 |
| LO28_2206 | lmo0406 | | Possible glyoxylase family protein (Lactoylglutathione lyase) | 1.07 | 0.0054 | 1.24 | 0.0002 |
| LO28_2204 | lmo0408 | | Hypothetical protein | 1.07 | 0.0006 | 1.31 | 0.0000 |
| LO28_2084 | lmo0524 | | Sulfate permease | **1.84** | 0.0000 | **1.95** | 0.0000 |
| LO28_2028 | lmo0579 | | Bacterial seryl-tRNA synthetase related | **2.24** | 0.0000 | **2.31** | 0.0000 |
| LO28_2027 | lmo0580 | | Phospholipase/carboxylesterase family protein | **1.94** | 0.0000 | **2.02** | 0.0000 |
| LO28_2017 | lmo0590 | | DAK2 domain protein | **3.38** | 0.0000 | **2.89** | 0.0000 |
| LO28_1958 | lmo0648 | | Magnesium and cobalt transport protein CorA | **2.82** | 0.0000 | **2.60** | 0.0000 |
| LO28_0072 | lmo0896 | *rsbX* | Phosphoserine phosphatase RsbX | 1.54 | 0.0025 | 0.85 | 0.0206 |
| LO28_0133 | lmo0956 | | N-acetylglucosamine-6-phosphate deacetylase | **1.78** | 0.0000 | **1.89** | 0.0000 |
| LO28_0134 | lmo0957 | | Glucosamine-6-phosphate deaminase | 1.25 | 0.0000 | 1.19 | 0.0000 |
| LO28_0174 | lmo0995 | | Membrane protein | **2.80** | 0.0005 | **2.21** | 0.0004 |
| LO28_0486 | lmo1261 | | Membrane protein | **2.88** | 0.0000 | **2.31** | 0.0000 |
| LO28_0599 | lmo1376 | | 6-phosphogluconate dehydrogenase, decarboxylating | 0.10 | 0.7951 | 0.13 | 0.5666 |
| LO28_0610 | lmo1388 | *tcsA* | Unspecified monosaccharide ABC transportsystem, substrate-binding component / CD4+Tcell-stimulating antigen, lipoprotein | -0.05 | 0.8039 | -0.20 | 0.3716 |
| LO28_0655 | lmo1432 | | Hypothetical protein | **2.60** | 0.0000 | **2.43** | 0.0000 |
| LO28_0806 | lmo1580 | | Universal stress protein family | **2.22** | 0.0000 | **2.33** | 0.0000 |
| LO28_0831 | lmo1605 | *murC* | UDP-N-acetylmuramate--alanine ligase | 0.88 | 0.0034 | 0.72 | 0.0023 |
| LO28_0862 | lmo1636 | | ABC transporter, ATP-binding protein | 0.46 | 0.1937 | 0.29 | 0.3035 |
| LO28_0893 | lmo1666 | | Putative peptidoglycan bound protein (LPXTGmotif) Lmo1666 homolog | **2.49** | 0.0000 | **2.64** | 0.0000 |
| LO28_2610 | lmo1929 | *ndk* | Nucleoside diphosphate kinase | 0.25 | 0.5871 | 0.25 | 0.4768 |
| LO28_2611 | lmo1930 | | Heptaprenyl diphosphate synthase component II | 0.22 | 0.5759 | 0.10 | 0.6885 |
| LO28_2614 | lmo1933 | *folE* | GTP cyclohydrolase I | 0.00 | 1.0566 | -0.04 | 1.0323 |
| LO28_2725 | lmo2041 | *mraW* | rRNA small subunit methyltransferase H | 0.38 | 0.1735 | 0.44 | 0.0602 |
| LO28_2855 | lmo2169 | | Hypothetical protein | 1.03 | 0.0002 | 1.08 | 0.0000 |
| LO28_2878 | lmo2191 | *spxA* | Arsenate reductase family protein | **1.66** | 0.0000 | 1.32 | 0.0000 |
| LO28_1609 | lmo2386 | | membrane protein | 1.43 | 0.0037 | 1.13 | 0.0003 |
| LO28_1612 | lmo2389 | | NADH dehydrogenase | 0.97 | 0.0005 | 0.96 | 0.0002 |
| LO28_1519 | lmo2539 | *glyA* | Serine hydroxymethyltransferase | 0.87 | 0.1518 | 0.79 | 0.0224 |
| LO28_1311 | lmo0122 | | Phage tail fiber | 0.49 | 0.3229 | 0.36 | 0.3000 |
| LO28_1322 | lmo0133 | | Hypothetical protein | **2.41** | 0.0003 | **2.25** | 0.0001 |
| LO28_2341 | lmo0274 | | Hypothetical protein | **2.07** | 0.0000 | **2.36** | 0.0000 |
| LO28_2242 | lmo0372 | | Beta-glucosidase | 0.22 | 0.8304 | -0.81 | 0.0793 |
| LO28_2207 | lmo0405 | | Probable low-affinity inorganic phosphatetransporter | **2.38** | 0.0000 | **2.01** | 0.0000 |
| LO28_2179 | lmo0433 | *inlA* | Internalin A (LPXTG motif) | **3.64** | 0.0000 | **3.70** | 0.0000 |
| LO28_2178 | lmo0434 | *inlB* | Internalin B (GW modules) | **1.85** | 0.0029 | **2.15** | 0.0001 |
| LO28_2173 | lmo0439 | | Siderophore/Surfactin synthetase relatedprotein | **5.71** | 0.0000 | **5.41** | 0.0000 |
| LO28_0644 | lmo1421 | | Glycine betaine ABC transport system, ATP-binding protein OpuAA | **3.68** | 0.0000 | **3.96** | 0.0000 |
| LO28_2548 | lmo1866 | | ATP/GTP-binding protein, SA1392 homolog | -0.07 | 0.8389 | -0.19 | 0.4394 |
| LO28_2686 | lmo2003 | | Transcriptional regulator, GntR family | **-1.88** | 0.0353 | -1.43 | 0.0667 |
| LO28_1553 | lmo2572 | | Dihydrofolate reductase | **4.52** | 0.0000 | **4.15** | 0.0000 |
| LO28_1064 | lmo2733 | | PTS system, fructose-specific IIB component | 1.39 | 0.1769 | 0.56 | 0.3743 |
| LO28_2214 | lmo0398 | | PTS system, fructose-specific IIABC component | -1.17 | 0.0779 | -1.00 | 0.0916 |
| LO28_2213 | lmo0399 | | PTS system, fructose-specific IIBC component | -0.71 | 0.3698 | -0.81 | 0.1574 |
| LO28_0225 | lmo1046 | *moaC* | Molybdenum cofactor biosynthesis protein MoaC | 0.24 | 0.5287 | -0.04 | 0.8653 |
| LO28_0572 | lmo1349 | | Glycine dehydrogenase [decarboxylating](glycine cleavage system P1 protein) | 1.24 | 0.0005 | 1.18 | 0.0001 |
| LO28_0645 | lmo1422 | | Glycine betaine ABC transport system, permeaseprotein OpuAB / Glycine betaine ABC transport system | **3.60** | 0.0000 | **3.64** | 0.0000 |
| LO28_2730 | lmo2047 | *rpmF* | LSU ribosomal protein L32p | -0.61 | 0.0951 | -0.52 | 0.0945 |
| LO28_0765 | lmo1539 | | Glycerol uptake facilitator protein | **2.57** | 0.0001 | **1.95** | 0.0012 |
| LO28_1074 | lmo2743 | | Transaldolase | 0.23 | 0.5634 | -0.16 | 0.5461 |
| LO28_1029 | lmo2697 | | Phosphoenolpyruvate-dihydroxyacetonephosphotransferase, subunit DhaM; DHA-specific IIA component | **3.52** | 0.0001 | **3.21** | 0.0000 |
| LO28_1028 | lmo2696 | | Phosphoenolpyruvate-dihydroxyacetonephosphotransferase, ADP-binding subunit DhaL | **4.86** | 0.0000 | **4.81** | 0.0000 |

Table S3.7 continued (3 of 4 ): expression of genes that are part of the SigB operon as described by Mujahid et al., 2013, in both variant 14 and variant 15 compared to the wild type. Values in bold are considered significant

| LO28 | lmo | Gene | Product | variant 14 | | variant 15 | |
|---|---|---|---|---|---|---|---|
| | | | | $log_2$ fold change | FDR | $log_2$ fold change | FDR |
| LO28_1027 | lmo2695 | | Phosphoenolpyruvate-dihydroxyacetonephosphotransferase, dihydroxyacetonebinding subunit DhaK | **4.80** | 0.0000 | **4.58** | 0.0000 |
| LO28_0987 | lmo2666 | | PTS system, galactitol-specific IIB component (EC 2.7.1.69) | -0.80 | 0.0593 | -0.66 | 0.0774 |
| LO28_1299 | lmo0110 | | Esterase/lipase | -0.52 | 0.3411 | -0.39 | 0.4548 |
| LO28_2432 | lmo1730 | | N-Acetyl-D-glucosamine ABC transport system, sugar-binding protein | 0.55 | 0.5150 | 0.68 | 0.2635 |
| LO28_0827 | lmo1601 | | General stress protein | **2.48** | 0.0000 | **2.79** | 0.0000 |
| LO28_2892 | lmo2205 | | Phosphoglycerate mutase | **2.12** | 0.0000 | **2.34** | 0.0000 |
| LO28_0651 | lmo1428 | *opuCA* | Osmotically activated L-carnitine/choline ABCtransporter, ATP-binding protein OpuCA | **6.31** | 0.0000 | **6.04** | 0.0000 |
| LO28_0649 | lmo1426 | *opuCC* | Osmotically activated L-carnitine/choline ABCtransporter, substrate-binding protein OpuCC | **6.50** | 0.0000 | **6.28** | 0.0000 |
| LO28_1783 | lmo0819 | | Hypothetical protein | **1.85** | 0.0001 | 1.47 | 0.0001 |
| LO28_2350 | lmo0265 | | Acetylornithine deacetylase | **3.17** | 0.0037 | **3.03** | 0.0009 |
| LO28_1584 | lmo0169 | | Glucose uptake protein | **4.63** | 0.0000 | **4.32** | 0.0000 |
| LO28_1585 | lmo0170 | | Putative exported protein | **3.94** | 0.0000 | **3.71** | 0.0000 |
| LO28_2352 | lmo0263 | *inlH* | Internalin H (LPXTG motif) | **6.21** | 0.0000 | **6.18** | 0.0000 |
| LO28_2294 | lmo0321 | | Membrane protein | **4.07** | 0.0000 | **3.39** | 0.0000 |
| LO28_2167 | lmo0445 | | Hypothetical protein | **3.84** | 0.0000 | **3.88** | 0.0000 |
| LO28_2093 | lmo0515 | | Universal stress protein family | **3.10** | 0.0040 | **3.01** | 0.0009 |
| LO28_2053 | lmo0555 | | Di/tripeptide permease DtpT | **2.03** | 0.0000 | 1.55 | 0.0004 |
| LO28_2014 | lmo0593 | | Formate/nitrite transporter family protein | -0.75 | 0.1123 | -1.23 | 0.0034 |
| LO28_2011 | lmo0596 | | Hypothetical protein | **6.31** | 0.0000 | **5.86** | 0.0000 |
| LO28_2005 | lmo0602 | | Acetyltransferase, GNAT family | **5.58** | 0.0000 | **5.45** | 0.0000 |
| LO28_1997 | lmo0610 | | Internalin-like protein (LPXTG motif) Lmo0610 homolog | **4.84** | 0.0000 | **5.05** | 0.0000 |
| LO28_1979 | lmo0628 | | Hypothetical protein | **4.16** | 0.0001 | **3.93** | 0.0000 |
| LO28_1978 | lmo0629 | | Isochorismatase (EC 3.3.2.1) | **4.73** | 0.0001 | **4.65** | 0.0000 |
| LO28_1951 | lmo0655 | | Serine/threonine protein phosphatase | **2.84** | 0.0001 | **2.77** | 0.0000 |
| LO28_1935 | lmo0669 | | Oxidoreductase, short-chaindehydrogenase/reductase family | **5.74** | 0.0000 | **5.78** | 0.0000 |
| LO28_1934 | lmo0670 | | Hypothetical protein | **4.96** | 0.0000 | **4.95** | 0.0000 |
| LO28_1821 | lmo0781 | | PTS system, mannose-specific IID component | **4.55** | 0.0000 | **3.97** | 0.0000 |
| LO28_1820 | lmo0782 | | PTS system, mannose-specific IIC component | **4.85** | 0.0000 | **3.94** | 0.0000 |
| LO28_1818 | lmo0784 | | PTS system, mannose-specific IIA component / PTS system, mannose-specific IIB component | **4.94** | 0.0000 | **4.43** | 0.0000 |
| LO28_0056 | lmo0880 | | Putative peptidoglycan bound protein (LPXTGmotif) Lmo0880 homolog | **3.17** | 0.0024 | **3.40** | 0.0002 |
| LO28_0088 | lmo0911 | | Hypothetical protein | **1.62** | 0.0000 | 1.36 | 0.0000 |
| LO28_0114 | lmo0937 | | Hypothetical protein | **2.56** | 0.0001 | **2.75** | 0.0000 |
| LO28_0130 | lmo0953 | | Hypothetical protein | 0.46 | 0.3404 | 0.72 | 0.0516 |
| LO28_0173 | lmo0994 | | Hypothetical protein | **6.88** | 0.0000 | **6.11** | 0.0000 |
| LO28_0301 | lmo1140 | | Hypothetical protein | **3.68** | 0.0012 | **3.23** | 0.0004 |
| LO28_0464 | lmo1241 | | Putative exported protein | **2.63** | 0.0049 | **2.25** | 0.0029 |
| LO28_0519 | lmo1295 | | RNA-binding protein Hfq | 1.47 | 0.0000 | 1.34 | 0.0000 |
| LO28_0598 | lmo1375 | | Peptidase T | **2.08** | 0.0000 | **2.14** | 0.0000 |
| LO28_0648 | lmo1425 | *opuCD* | Osmotically activated L-carnitine/choline ABCtransporter, permease protein OpuCD | **6.49** | 0.0000 | **6.22** | 0.0000 |
| LO28_0656 | lmo1433 | | Glutathione reductase | **4.68** | 0.0000 | **4.67** | 0.0000 |
| LO28_0752 | lmo1526 | | Hypothetical protein | **2.97** | 0.0000 | **3.12** | 0.0000 |
| LO28_0832 | lmo1606 | | Cell division protein FtsK | 0.93 | 0.0008 | 0.93 | 0.0002 |
| LO28_2468 | lmo1694 | | Cell division inhibitor Slr1223 (YfcH in EC), contains epimerase/dehydratase | **5.08** | 0.0000 | **4.90** | 0.0000 |
| LO28_2464 | lmo1698 | | Ribosomal-protein-S5p-alanineacetyltransferase | 0.35 | 0.3974 | 0.56 | 0.0602 |
| LO28_2564 | lmo1883 | | Chitinase | **2.40** | 0.0405 | 1.44 | 0.0980 |
| LO28_2750 | lmo2067 | | Choloylglycine hydrolase | **4.47** | 0.0000 | **4.07** | 0.0000 |
| LO28_2770 | lmo2085 | | Putative peptidoglycan bound protein (LPXTGmotif) Lmo2085 homolog | **5.03** | 0.0000 | **4.48** | 0.0000 |
| LO28_2816 | lmo2130 | | Amino acid permease | -0.87 | 0.2052 | -1.45 | 0.0105 |
| LO28_2818 | lmo2132 | | Hypothetical protein | **2.34** | 0.0262 | **1.94** | 0.0200 |
| LO28_2843 | lmo2157 | *sepA* | Alkyl sulfatase (EC 3.1.6.-) | **3.52** | 0.0000 | **3.06** | 0.0000 |
| LO28_2917 | lmo2230 | | Arsenate reductase | **5.84** | 0.0000 | **6.04** | 0.0000 |
| LO28_2918 | lmo2231 | | Cobalt-zinc-cadmium resistance protein | **5.59** | 0.0000 | **5.31** | 0.0000 |
| LO28_2956 | lmo2269 | | Hypothetical protein | **4.76** | 0.0000 | **4.33** | 0.0000 |

Table S3.7 continued (4 of 4): expression of genes that are part of the SigB operon as described by Mujahid et al., 2013, in both variant 14 and variant 15 compared to the wild type. Values in bold are considered significant

| LO28 | lmo | Gene | Product | variant 14 | | variant 15 | |
|---|---|---|---|---|---|---|---|
| | | | | $log_2$ fold change | FDR | $log_2$ fold change | FDR |
| LO28_1610 | lmo2387 | | Hypothetical protein | **3.56** | 0.0000 | **3.39** | 0.0000 |
| LO28_1614 | lmo2391 | | Oxidoreductase ylbE | **3.36** | 0.0000 | **3.36** | 0.0000 |
| LO28_1622 | lmo2434 | | Glutamate decarboxylase | -1.51 | 0.1807 | -0.67 | 0.2576 |
| LO28_1431 | lmo2454 | | Lin2548 protein | 0.66 | 0.1342 | 0.57 | 0.1378 |
| LO28_1440 | lmo2463 | | Hypothetical protein | **3.96** | 0.0000 | **3.40** | 0.0000 |
| LO28_1462 | lmo2484 | | Membrane protein | **2.12** | 0.0016 | **1.60** | 0.0009 |
| LO28_1463 | lmo2485 | | PspC domain protein, truncated | **1.82** | 0.0015 | 1.50 | 0.0010 |
| LO28_1472 | lmo2494 | | Phosphate transport system regulatory proteinPhoU | **3.89** | 0.0001 | **4.15** | 0.0000 |
| LO28_1551 | lmo2570 | | Hypothetical protein | **4.41** | 0.0000 | **3.30** | 0.0000 |
| LO28_1552 | lmo2571 | | Nicotinamidase | **4.15** | 0.0000 | **3.92** | 0.0000 |
| LO28_1554 | lmo2573 | | Bifunctional protein: zinc-containing alcoholdehydrogenase; quinone oxidoreductase; similar to arginate lyase | **3.99** | 0.0000 | **3.84** | 0.0000 |
| LO28_0922 | lmo2602 | | Mg(2+) transport ATPase protein C | **3.39** | 0.0000 | **2.94** | 0.0000 |
| LO28_0923 | lmo2603 | | acetamidase/formamidase family protein | **2.64** | 0.0015 | **2.55** | 0.0003 |
| LO28_0991 | lmo2670 | | Hypothetical protein | 1.57 | 0.0088 | 1.26 | 0.0191 |
| LO28_0992 | lmo2671 | | Hypothetical protein | **1.96** | 0.0000 | **1.67** | 0.0000 |
| LO28_0993 | lmo2672 | | Transcriptional regulator, AraC family | **2.74** | 0.0000 | **2.48** | 0.0000 |
| LO28_0994 | lmo2673 | | Universal stress protein family | **7.06** | 0.0002 | **7.11** | 0.0000 |
| LO28_0995 | lmo2674 | | Ribose 5-phosphate isomerase B | **2.79** | 0.0000 | **2.46** | 0.0000 |
| LO28_1055 | lmo2724 | | PhnB protein; putative DNA binding3-demethylubiquinone-9 3-methyltransferase domain protein | 0.91 | 0.0642 | 0.79 | 0.0553 |
| LO28_1208 | lmo0019 | | Hypothetical protein | **5.29** | 0.0004 | **4.79** | 0.0001 |
| LO28_1232 | lmo0043 | | Arginine deiminase | **4.15** | 0.0000 | **3.93** | 0.0000 |

Table S3.8: Expression of genes associated with the ADI system in *L. monocytogenes* LO28 variant 14 and 15 over the wild type. Values in bold are considered significant

| LO28 | lmo | Gene | Product | variant 14 | | variant 15 | |
|---|---|---|---|---|---|---|---|
| | | | | $log_2$ fold change | FDR | $log_2$ fold change | FDR |
| LO28_1226 | lmo0037 | *arcD* | Agmatine/putrescine antiporter, associated with agmatine catabolism | **1.59** | 0.0060 | 0.84 | 0.1096 |
| LO28_1232 | lmo0043 | *arcA* | Arginine deiminase | **4.15** | 0.0000 | **3.93** | 0.0000 |
| LO28_1228 | lmo0039 | *arcC* | Carbamate kinase | **1.92** | 0.0022 | 1.57 | 0.0067 |
| LO28_1225 | lmo0036 | *arcB* | Putrescine carbamoyltransferase | **1.75** | 0.0037 | 0.89 | 0.1284 |

Table S3.9: Expression of genes associated with the GAD system in *L. monocytogenes* LO28 variant 14 and 15 over the wild type. Values in bold are considered significant

| LO28 | lmo | Gene | Product | variant 14 | | variant 15 | |
|---|---|---|---|---|---|---|---|
| | | | | $log_2$ fold change | FDR | $log_2$ fold change | FDR |
| LO28_1622 | lmo2363 | *gadD2* | Glutamate decarboxylase | -1.51 | 0.1807 | -0.67 | 0.2576 |
| LO28_1411 | lmo2434 | *gadD3* | Glutamate decarboxylase | **2.85** | 0.0000 | **2.41** | 0.0000 |
| LO28_2165 | lmo0447 | *gadD1* | Glutamate decarboxylase | -0.09 | 0.9550 | 0.58 | 0.2419 |
| LO28_2164 | lmo0448 | *gadT1* | Probable glutamate/gamma-aminobutyrateantiporter | **-1.71** | 0.5505 | -1.16 | 0.8712 |
| LO28_1623 | lmo2362 | *gadT2* | Probable glutamate/gamma-aminobutyrateantiporter | -0.91 | 0.8055 | **-2.09** | 0.0318 |

Table S3.10: Expression of genes associated with glycerol metabolism in *Listeria monocytogenes* LO28 variant 14 and 15 compared to the wild type. Values in bold are considered significant

| LO28 | lmo | Gene | Product | variant 14 | | variant 15 | |
|---|---|---|---|---|---|---|---|
| | | | | $log_2$ fold change | FDR | $log_2$ fold change | FDR |
| LO28_0765 | lmo1539 | *glpF1* | Glycerol uptake facilitator protein | **2.57** | 0.0001 | **1.95** | 0.0012 |
| LO28_0328 | lmo1167 | *glpF2* | Glycerol uptake facilitator protein | 0.72 | 0.3227 | 0.67 | 0.2381 |
| LO28_0764 | lmo1538 | *glpK1* | Glycerol kinase | **2.06** | 0.0003 | 1.34 | 0.0049 |
| LO28_0213 | lmo1034 | *glpK2* | Unknown pentose kinase TM0952 | -0.63 | 0.4643 | 0.62 | 0.9826 |
| LO28_1027 | lmo2695 | *dhaK* | Phosphoenolpyruvate-dihydroxyacetonephosphotransferase, dihydroxyacetonebinding subunit DhaK | **4.80** | 0.0000 | **4.58** | 0.0000 |
| LO28_1028 | lmo2696 | *dhaL* | Phosphoenolpyruvate-dihydroxyacetonephosphotransferase, ADP-binding subunit DhaL | **4.86** | 0.0000 | **4.81** | 0.0000 |
| LO28_0517 | lmo1293 | *glpD* | Aerobic glycerol-3-phosphate dehydrogenase | **2.38** | 0.0000 | **2.39** | 0.0000 |
| LO28_2271 | lmo0344 | *golD* | 3-oxoacyl-[acyl-carrier protein] reductase | 0.06 | 0.9325 | 0.67 | 0.3981 |
| LO28_1881 | lmo0722 | | Pyruvate oxidase [ubiquinone, cytochrome] | **6.32** | 0.0000 | **6.31** | 0.0000 |
| LO28_0603 | lmo1381 | | Predicted nucleoside phosphatase | 1.11 | 0.0004 | 1.25 | 0.0000 |

Table S3.11: Expression of genes of predicted flagella operon 1 in *Listeria monocytogenes* LO28 variant 14 and 15 compared to the wild type. Values in bold are considered significant

| LO28 | lmo | Gene | Product | variant 14 | | variant 15 | |
|---|---|---|---|---|---|---|---|
| | | | | $log_2$ fold change | FDR | $log_2$ fold change | FDR |
| LO28_1928 | lmo0675 | *fliN* | Flagellar motor switch protein FliN | **-2.53** | 0.0000 | **-2.29** | 0.0000 |
| LO28_1927 | lmo0676 | *fliP* | Flagellar biosynthesis protein FliP | **-2.91** | 0.0000 | **-2.93** | 0.0000 |
| LO28_1926 | lmo0677 | *fliQ* | Flagellar biosynthesis protein FliQ | **-2.99** | 0.0000 | **-3.04** | 0.0000 |
| LO28_1925 | lmo0678 | *fliR* | Flagellar biosynthesis protein FliR | **-3.12** | 0.0000 | **-2.85** | 0.0000 |
| LO28_1924 | lmo0679 | *flhB* | Flagellar biosynthesis protein FlhB | **-4.49** | 0.0000 | **-4.65** | 0.0000 |
| LO28_1923 | lmo0680 | *flhA* | Flagellar biosynthesis protein FlhA | **-5.31** | 0.0000 | **-4.83** | 0.0000 |
| LO28_1922 | lmo0681 | *flhF* | Flagellar biosynthesis protein FlhF | **-5.57** | 0.0000 | **-4.91** | 0.0000 |
| LO28_1921 | lmo0682 | *flgG* | Flagellar basal-body rod protein FlgG | **-6.03** | 0.0000 | **-6.37** | 0.0000 |
| LO28_1920 | lmo0683 | *cheR* | Chemotaxis protein methyltransferase CheR | **-5.16** | 0.0000 | **-4.97** | 0.0000 |
| LO28_1919 | lmo0684 | | Hypothetical protein | **-6.06** | 0.0000 | **-5.84** | 0.0000 |
| LO28_1918 | lmo0685 | *motA* | Flagellar motor rotation protein MotA | **-5.92** | 0.0000 | **-5.71** | 0.0000 |
| LO28_1917 | lmo0686 | *motB* | Flagellar motor rotation protein MotB | **-5.33** | 0.0000 | **-5.06** | 0.0000 |
| LO28_1916 | lmo0687 | | Hypothetical protein | **-4.93** | 0.0000 | **-4.75** | 0.0000 |
| LO28_1915 | lmo0688 | *gmaR* | Dolichol-phosphate mannosyltransferase in lipid-linked oligosaccharide synthesis cluster | **-4.89** | 0.0000 | **-4.24** | 0.0000 |
| LO28_1914 | lmo0689 | *cheV* | Chemotaxis protein CheV | **-5.55** | 0.0000 | **-5.26** | 0.0000 |

Table S3.12: Expression of genes of predicted flagella operon 2 in *Listeria monocytogenes* LO28 variant 14 and 15 compared to the wild type. Values in bold are considered significant

| LO28 | lmo | Gene | Product | variant 14 | | variant 15 | |
|---|---|---|---|---|---|---|---|
| | | | | $log_2$ fold change | FDR | $log_2$ fold change | FDR |
| LO28_1912 | lmo0691 | *cheY* | Chemotaxis regulator - transmits chemoreceptorsignals to flagelllar motor components CheY | **-6.12** | 0.0000 | **-5.53** | 0.0000 |
| LO28_1911 | lmo0692 | *cheA* | Signal transduction histidine kinase CheA | **-5.79** | 0.0000 | **-5.23** | 0.0000 |
| LO28_1910 | lmo0693 | *fliY* | Flagellar motor switch protein FliN | **-5.91** | 0.0000 | **-5.40** | 0.0000 |
| LO28_1909 | lmo0694 | | Hypothetical protein | **-4.49** | 0.0000 | **-4.04** | 0.0000 |
| LO28_1908 | lmo0695 | *fliK* | Hypothetical protein | **-4.08** | 0.0000 | **-3.98** | 0.0000 |
| LO28_1907 | lmo0696 | *flgD* | Flagellar basal-body rod modification protein FlgD | **-4.70** | 0.0000 | **-4.52** | 0.0000 |
| LO28_1906 | lmo0697 | *flgE* | Flagellar hook protein FlgE | **-5.44** | 0.0000 | **-5.20** | 0.0000 |
| LO28_1905 | lmo0698 | *fliN* | Flagellar motor switch protein FliN | **-5.64** | 0.0000 | **-5.35** | 0.0000 |
| LO28_1903 | lmo0700 | *cheC* | Flagellar motor switch protein FliN | **-5.66** | 0.0000 | **-5.29** | 0.0000 |
| LO28_1902 | lmo0701 | | Hypothetical protein | **-6.00** | 0.0000 | **-5.64** | 0.0000 |
| LO28_1901 | lmo0702 | | Hypothetical protein | **-5.43** | 0.0000 | **-5.02** | 0.0000 |

Table S3.13: Expression of selected motility regulatory genes in *Listeria monocytogenes* LO28 variant 14 and 15 compared to the wild type. Values in bold are considered significant

| LO28 | lmo | Gene | Product | variant 14 | | variant 15 | |
|---|---|---|---|---|---|---|---|
| | | | | $log_2$ fold change | FDR | $log_2$ fold change | FDR |
| LO28_1929 | lmo0674 | *mogR* | Motility gene repressor MogR | 0.93 | 0.0472 | 0.96 | 0.0184 |
| LO28_1913 | lmo0690 | *flaA* | Flagellin protein FlaA | **-6.70** | 0.0000 | **-6.27** | 0.0000 |
| LO28_1920 | lmo0683 | *cheR* | Chemotaxis protein methyltransferase CheR | **-5.16** | 0.0000 | **-4.97** | 0.0000 |
| LO28_0677 | lmo1454 | *rpoD* | RNA polymerase sigma factor RpoD | 0.35 | 0.2354 | 0.40 | 0.1392 |
| LO28_1494 | lmo2515 | *degU* | Transcriptional regulator DegU, LuxR family | 0.78 | 0.0012 | 0.92 | 0.0000 |

Table S3.14: Expression of genes regulated by PrfA in *Listeria monocytogenes* LO28 variant 14 and 15 compared to the wild type. Values in bold are considered significant

| LO28 | lmo | Gene | Product | variant 14 | | variant 15 | |
|---|---|---|---|---|---|---|---|
| | | | | $log_2$ fold change | FDR | $log_2$ fold change | FDR |
| LO28_1744 | lmo0204 | *actA* | Actin-assembly inducing protein ActA precursor | 0.05 | 0.9791 | 0.26 | 0.7970 |
| LO28_1743 | lmo0205 | *plcB* | Broad-substrate range phospholipase C (EC3.1.4.3) | -0.59 | 0.8742 | -1.45 | 0.2211 |
| LO28_2179 | lmo0433 | *inlA* | Internalin A (LPXTG motif) | **3.64** | 0.0000 | **3.70** | 0.0000 |
| LO28_2178 | lmo0434 | *inlB* | Internalin B (GW modules) | **1.85** | 0.0029 | **2.15** | 0.0001 |
| LO28_1358 | lmo1786 | *inlC* | Internalin C | 0.23 | 1.0391 | **-1.63** | 0.3974 |
| LO28_1747 | lmo0201 | *plcA* | Phosphatidylinositol-specific phospholipase C(EC 4.6.1.13) | -0.39 | 0.9871 | -0.22 | 0.7330 |
| LO28_0012 | lmo0837 | *hpt* | Sugar phosphate transporter | -0.98 | 0.6702 | 0.88 | 0.2103 |
| LO28_1746 | lmo0202 | *hly* | Thiol-activated cytolysin | -0.49 | 0.7944 | 0.12 | 0.6724 |
| LO28_1748 | lmo0200 | *prfA* | Virulence regulatory factor PrfA /Transcriptional regulator, CrP/Fnr family | **2.30** | 0.0000 | **2.45** | 0.0000 |
| LO28_1745 | lmo0203 | *mpl* | Zinc metalloproteinase precursor (EC3.4.24.29) | -0.12 | 0.8774 | 0.43 | 0.4801 |

Table S3.15: Expression of ribosomal genes in *Listeria monocytogenes* LO28 variant 14 and 15 compared to the wild type. Values in bold are considered significant

| LO28 | Gene | Protein | Product | variant 14 | | variant 15 | |
|---|---|---|---|---|---|---|---|
| | | | | $log_2$ fold change | FDR | $log_2$ fold change | FDR |
| LO28_2366 | *rplA* | L1 | LSU ribosomal protein L1p (L10Ae) | -0.31 | 0.5337 | -0.70 | 0.0244 |
| LO28_0949 | *rplB* | L2 | LSU ribosomal protein L2p (L8e) | 0.46 | 0.4249 | 0.18 | 0.5679 |
| LO28_0952 | *rplC* | L3 | LSU ribosomal protein L3p (L3e) | 0.52 | 0.3427 | 0.33 | 0.2843 |
| LO28_0951 | *rplD* | L4 | LSU ribosomal protein L4p (L1e) | 0.49 | 0.5712 | 0.39 | 0.2376 |
| LO28_0940 | *rplE* | L5 | LSU ribosomal protein L5p (L11e) | 0.07 | 0.9497 | -0.17 | 0.8789 |
| LO28_0937 | *rplF* | L6 | LSU ribosomal protein L6p (L9e) | 0.10 | 0.9386 | -0.09 | 1.0152 |
| LO28_1242 | *rplI* | L9 | LSU ribosomal protein L9p | 0.27 | 0.3371 | 0.18 | 0.4800 |
| LO28_2365 | *rplJ* | L10 | LSU ribosomal protein L10p (P0) | -0.37 | 0.7040 | -0.40 | 0.5256 |
| LO28_2367 | *rplK* | L11 | LSU ribosomal protein L11p (L12e) | -0.10 | 0.9071 | -0.45 | 0.0767 |
| LO28_2364 | *rplL* | L7/L12 | LSU ribosomal protein L7/L12 (P1/P2) | -0.66 | 0.1507 | -0.77 | 0.0304 |
| LO28_0917 | *rplM* | L13 | LSU ribosomal protein L13p (L13Ae) | -0.03 | 1.0214 | 0.14 | 0.5986 |
| LO28_0942 | *rplN* | L14 | LSU ribosomal protein L14p (L23e) | 0.09 | 1.0466 | -0.03 | 1.0488 |
| LO28_0933 | *rplO* | L15 | LSU ribosomal protein L15p (L27Ae) | 0.11 | 0.8750 | -0.13 | 0.8798 |
| LO28_0945 | *rplP* | L16 | LSU ribosomal protein L16p (L10e) | 0.36 | 0.4350 | -0.03 | 1.0095 |
| LO28_0925 | *rplQ* | L17 | LSU ribosomal protein L17p | -0.53 | 0.2495 | -0.77 | 0.0325 |
| LO28_0936 | *rplR* | L18 | LSU ribosomal protein L18p (L5e) | -0.07 | 1.0343 | -0.13 | 1.0176 |
| LO28_1359 | *rplS* | L19 | LSU ribosomal protein L19p | -0.14 | 0.6553 | 0.21 | 0.6003 |
| LO28_1354 | *rplT* | L20 | LSU ribosomal protein L20p | 0.33 | 0.2948 | 0.23 | 0.3477 |
| LO28_0768 | *rplU* | L21 | LSU ribosomal protein L21p | -0.03 | 1.0319 | 0.11 | 0.8626 |
| LO28_0947 | *rplV* | L22 | LSU ribosomal protein L22p (L17e) | 0.37 | 0.5493 | 0.05 | 0.8604 |
| LO28_0950 | *rplW* | L23 | LSU ribosomal protein L23p (L23Ae) | 0.60 | 0.2523 | 0.38 | 0.2589 |
| LO28_0941 | *rplX* | L24 | LSU ribosomal protein L24p (L26e) | 0.18 | 0.8382 | 0.01 | 0.9288 |
| LO28_1737 | *ctc* | L25 | LSU ribosomal protein L25p | **2.47** | 0.0000 | **1.84** | 0.0000 |
| LO28_0766 | *rpmA* | L27 | LSU ribosomal protein L27p | -0.21 | 0.7267 | -0.25 | 0.5329 |
| LO28_2498 | *rpmB* | L28 | LSU ribosomal protein L28p | 0.01 | 0.9614 | -0.30 | 0.4226 |
| LO28_0944 | *rpmC* | L29 | LSU ribosomal protein L29p (L35e) | 0.20 | 0.7945 | -0.17 | 0.8103 |
| LO28_0934 | *rpmD* | L30 | LSU ribosomal protein L30p (L7e) | 0.12 | 0.8760 | -0.05 | 1.0408 |
| LO28_1529 | *rpmE* | L31 | LSU ribosomal protein L31p | -0.26 | 0.2877 | 0.05 | 1.0322 |
| LO28_2122 | *rpmF* | L32 | LSU ribosomal protein L32p | 1.01 | 0.0141 | 0.77 | 0.0302 |
| LO28_1187 | *rpmH* | L34 | LSU ribosomal protein L34p | -0.09 | 0.9268 | 0.15 | 0.6130 |
| LO28_1355 | *rpmI* | L35 | LSU ribosomal protein L35p | 0.29 | 0.3122 | 0.79 | 0.0092 |
| LO28_0929 | *rpmJ* | L36 | LSU ribosomal protein L36p | 0.15 | 0.8194 | 0.13 | 0.7839 |
| LO28_2620 | *rpsA* | S1 | SSU ribosomal protein S1p | -1.43 | 0.0000 | -1.13 | 0.0000 |
| LO28_0885 | *rpsB* | S2 | SSU ribosomal protein S2p (SAe) | 0.41 | 0.1899 | 0.92 | 0.0025 |
| LO28_0946 | *rpsC* | S3 | SSU ribosomal protein S3p (S3e) | 0.20 | 0.7866 | 0.03 | 0.8843 |
| LO28_0822 | *rpsD* | S4 | SSU ribosomal protein S4p (S9e) | 0.10 | 0.8303 | 0.07 | 0.9749 |
| LO28_0935 | *rpsE* | S5 | SSU ribosomal protein S5p (S2e) | -0.06 | 0.9728 | -0.07 | 1.0043 |
| LO28_1233 | *rpsF* | S6 | SSU ribosomal protein S6p | 0.28 | 0.5503 | 0.36 | 0.5432 |
| LO28_0976 | *rpsG* | S7 | SSU ribosomal protein S7p (S5e) | 0.20 | 0.8589 | 0.21 | 0.7099 |
| LO28_0938 | *rpsH* | S8 | SSU ribosomal protein S8p (S15Ae) | 0.07 | 1.0146 | -0.07 | 0.9305 |
| LO28_0916 | *rpsI* | S9 | SSU ribosomal protein S9p (S16e) | -0.22 | 0.4486 | -0.38 | 0.0831 |
| LO28_0953 | *rpsJ* | S10 | SSU ribosomal protein S10p (S20e) | 0.52 | 0.2582 | 0.29 | 0.3533 |
| LO28_0927 | *rpsK* | S11 | SSU ribosomal protein S11p (S14e) | -0.31 | 0.6779 | -0.37 | 0.4710 |
| LO28_0977 | *rpsL* | S12 | SSU ribosomal protein S12p (S23e) | 0.14 | 0.8648 | 0.09 | 0.8041 |
| LO28_0928 | *rpsM* | S13 | SSU ribosomal protein S13p (S18e) | -0.02 | 1.0566 | -0.05 | 1.0450 |
| LO28_0939 | *rpsN* | S14 | SSU ribosomal protein S14p (S29e) | 0.12 | 0.9255 | -0.08 | 0.9136 |
| LO28_0554 | *rpsO* | S15 | SSU ribosomal protein S15p (S13e) | -0.02 | 0.9434 | -0.32 | 0.5679 |
| LO28_1369 | *rpsP* | S16 | SSU ribosomal protein S16p | -0.10 | 0.8401 | -0.41 | 0.1309 |
| LO28_0943 | *rpsQ* | S17 | SSU ribosomal protein S17p (S11e) | 0.12 | 0.9926 | -0.06 | 0.9753 |
| LO28_1235 | *rpsR* | S18 | SSU ribosomal protein S18p | -0.39 | 0.0825 | -0.19 | 0.3845 |
| LO28_0948 | *rpsS* | S19 | SSU ribosomal protein S19p (S15e) | 0.54 | 0.2667 | 0.11 | 0.7184 |
| LO28_0704 | *rpsT* | S20 | SSU ribosomal protein S20p | -0.21 | 0.6236 | -0.19 | 0.3512 |
| LO28_0693 | *rpsU* | S21 | SSU ribosomal protein S21p | **-7.37** | 0.0000 | **-2.15** | 0.0000 |

Figure S3.1: expression of motility associated genes in *Listeria monocytogenes* LO28 variants 14 and 15. Predicted flagellar transcription unit 1 and 2, based on *Listeria monocytogenes* 10403S (retrieved from Biocyc.org on 12/4/2017).

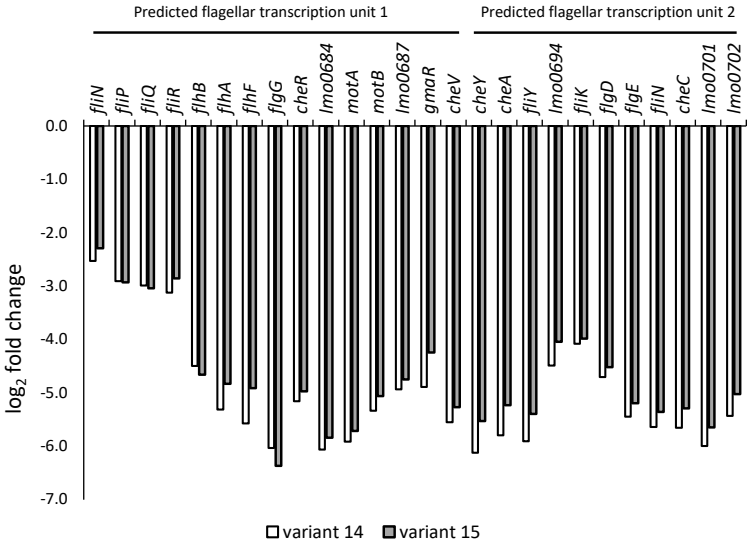

# 4

# Amino acid substitutions in ribosomal protein RpsU enable switching between high fitness and multiple-stress resistance in *Listeria monocytogenes*

Jeroen Koomen, Linda Huijboom, Xuchuan Ma, Marcel H. Tempelaars, Sjef Boeren, Marcel H. Zwietering, Heidy M.W. den Besten, and Tjakko Abee

**Published in:**

International Journal of Food Microbiology (2021) 351, 109269.

## Abstract

Microbial population heterogeneity contributes to differences in stress response between individual cells in a population, and can lead to the selection of genetically stable variants with increased stress resistance. We previously provided evidence that the multiple-stress resistant *Listeria monocytogenes* LO28 variant 15, carries a point mutation in the *rpsU* gene, resulting in an arginine-proline substitution in ribosomal protein RpsU ($RpsU^{17Arg\text{-}Pro}$). Here, we investigated the trade-off between general stress sigma factor SigB-mediated stress resistance and fitness in variant 15 using experimental evolution. By selecting for higher fitness in two parallel evolving cultures, we identified two evolved variants: 15EV1 and 15EV2. Whole genome sequencing and SNP analysis showed that both parallel lines mutated in the same codon in *rpsU* as the original mutation resulting in $RpsU^{17Pro\text{-}His}$ (15EV1) and $RpsU^{17Pro\text{-}Thr}$ (15EV2). Using a combined phenotyping and proteomics approach, we assessed the resistance of the evolved variants to both heat and acid stress, and found that in both lines reversion to WT-like fitness also resulted in WT-like stress sensitivity. Proteome analysis of *L. monocytogenes* LO28 WT, variant 15, 15EV1, and 15EV2 revealed high level expression of SigB regulon members only in variant 15, whereas protein profiles of both evolved variants were highly similar to that of the LO28 WT. Experiments with constructed $RpsU^{17Arg\text{-}Pro}$ mutants in *L. monocytogenes* LO28 and EGDe, and $RpsU^{17Arg\text{-}His}$ and $RpsU^{17Arg\text{-}Thr}$ in LO28, confirmed that single amino acid substitutions in RpsU enable switching between multiple-stress resistant and high fitness states in *L. monocytogenes*.

## Introduction

*Listeria monocytogenes* is a foodborne pathogen that is ubiquitously present in the environment, and can cause the rare but severe disease listeriosis (Radoshevich and Cossart, 2018; Lecuit, 2007; Vázquez-Boland et al., 2001). *L. monocytogenes* is considered a robust organism, since it can adapt to and survive a wide range of stress conditions such as low pH, low temperature and low water activity ($a_w$) (NicAogáin and O'Byrne, 2016). The inherent heterogeneity of microbial populations is one of the factors that contribute to the ubiquitous nature of *L. monocytogenes* supporting its capacity to cope with environmental stresses during its transmission from the environment to the human gastro-intestinal tract. Notably, differences in stress response between individual cells of a population can lead to survival of a small fraction of the population when the population is subjected to lethal stresses such as heat or low pH, leading to tailing of the inactivation curve. Tailing results in higher-than-expected numbers of cells surviving an inactivation treatment, either as transiently resistant subpopulations, or as genetically stable variants with increased stress resistance (Gollan et al., 2019; Karatzas et al., 2005; Metselaar et al., 2013; Van Boeijen et al., 2008).

Previously, Metselaar et al. (2015) combined phenotypic clustering of a collection of stable stress resistant *L. monocytogenes* variants, based on reduced growth rate and increased resistance against acid, heat, high hydrostatic pressure (HHP), and benzalkonium chloride, with a whole genome sequencing and Structural Variation (SV) analysis. This analysis showed that 11 of the 23 selected variants with a shared phenotype had a mutation in the ribosomal *rpsU* gene locus encoding S30 ribosomal protein RpsU (small ribosomal protein 21) (Metselaar et al., 2015). Subsequent work focused on two of the variants; variant 14, with a large deletion that spans the whole *rpsU* gene, as well as *yqeY* and half of *phoH*; and variant 15, with a single point mutation in *rpsU* that resulted in an amino acid substitution from arginine to proline in the RpsU protein, $RpsU^{17Arg\text{-}Pro}$ (Koomen et al., 2018). Comparative analysis of gene expression profiles and phenotypes of *L. monocytogenes* LO28 wildtype (WT) and multiple-stress resistant variants 14 and 15, revealed upregulation of 116 genes with a major contribution of genes controlled by the alternative stress sigma factor SigB (Koomen et al., 2018). Activation of SigB is controlled by the so-called stressosome, a cytoplasmic complex that relays a range of stress signals and activates the sigma B regulon providing multiple-stress resistance (Guldimann et al., 2016; NicAogáin and O'Byrne, 2016; Radoshevich and Cossart, 2018). Next to stress defence activation, the multiple-stress

resistant *L. monocytogenes* variants 14 and 15 had increased glycerol metabolic capacity and reduced expression of flagella (Koomen et al., 2018). Modelling and validation of the ecological behaviour of *L. monocytogenes* WT and stress resistant variants 14 and 15 led to the hypothesis that multiple stress resistance could contribute to performance and persistence in the food chain, which, in combination with the conceivable higher survival of acidic conditions in the stomach, could result in a higher exposure and risk of disease (Abee et al., 2016; Metselaar et al., 2016). An additional factor contributing to increased risk following the initial selection of multiple stress resistant variants (Abee et al., 2016) could be the subsequent selection of other variants that originate from the ancestor variant and have increased fitness and loss of the stress resistant phenotype.

In the current study, we addressed this issue and subjected *L. monocytogenes* LO28 variant 15, with its single point mutation in *rpsU*, resulting in RpsU$^{17Arg\text{-}Pro}$, to an experimental evolution regime where we selected for higher fitness, defined as an increased maximum specific growth rate ($\mu_{max}$), when compared to the ancestor variant 15. Subsequent genotyping and phenotyping of evolved variants has provided insights in *L. monocytogenes* switching between high fitness-low stress resistance, and low fitness-high stress resistance.

## Materials and methods

### Bacterial strains and culture conditions

For genotypic, proteomic and phenotypic analysis, *L. monocytogenes* LO28 wild type (WT) strain (Wageningen Food & Biobased Research, The Netherlands), stress resistant ancestor variant 15 (Koomen et al., 2018; Metselaar et al., 2013), and evolved variants (this study) were used. All bacterial cultures were grown as described elsewhere (Metselaar et al., 2013). Briefly, cells from -80°C stocks were grown at 30°C for 48 hours on brain heart infusion (BHI, Oxoid, Ltd., Basingstoke, England) agar (1.5 % [w/w], bacteriological agar no. 1 Oxoid) plates. A single colony was used to inoculate 20 ml of BHI broth in a 100 ml Erlenmeyer flask. After overnight (ON, 18-22 hours) culturing at 30°C under shaking at 160 rpm, (Innova 42, New Brunswick Scientific, Edison, NJ) 0.5% (v/v) inoculum was added to fresh BHI broth. Cells were grown under shaking at 160 rpm in BHI at 30°C until the late-exponential growth phase ($OD_{600}$ = 0.4-0.5).

## Experimental Evolution

Experimental evolution was performed by inoculating two parallel lines with 1% (v/v) of ON culture of *L. monocytogenes* LO28 variant 15, in 20 ml BHI in 100 ml Erlenmeyer flasks, resulting in approximately $1 \cdot 10^{7.5}$ cfu/ml. The cultures were incubated for 24 hours at 20°C under continuous shaking at 160 rpm (Innova 42). For each parallel line, 28 consecutive transfers were made using 24 hours-cultures and 1% (v/v) inoculum to inoculate fresh BHI. Each transfer allowed for a 2-log increase (~6.65 generations), and for 28 transfers this yields in total around 200 generations. From every second transfer, a 700 µL culture sample was taken, mixed with glycerol (Sigma-Aldrich, the Netherlands, 25% v/v final concentration), flash frozen in liquid nitrogen, and stored at -80°C, resulting in 14 stocks. These stocks were revived by streaking on BHI agar plates, and a single colony was used to inoculate 20 ml of BHI broth in a 100 ml Erlenmeyer flask. After ON culturing at 30°C under shaking at 160 rpm, (Innova 42) the culture was diluted 100,000 times in fresh BHI broth, and 200 µl of culture was inoculated in duplicate in wells of a honeycomb plate. The plate was incubated in a Bioscreen C (Oy Growth Curves AB Ltd, Helsinki, Finland) at 30°C and the respective growth curves were determined by measuring $OD_{600}$ over time, using biological triplicates. The starting stocks, and the first stocks where a clear shift to WT-like growth was observed, i.e., stock number 8 for 15EV1 (after 16 daily transfers) and number 9 for 15EV2 (after 18 daily transfers), were streaked on BHI agar, and respective single colonies were selected to prepare -80°C stocks of 15EV1 and 15EV2 and the ancestor variant 15. These stocks were used for whole genome sequencing and subsequent phenotyping experiments.

## Estimation of $\mu_{max}$

The maximum specific growth rate $\mu_{max}$ was determined for the two evolved strains (15EV1 and 15EV2), variant 15 and the LO28 WT strain. For that, ON cultures were diluted 1000 times in peptone physiological salt solution (PPS, Tritium Microbiologie B.V., the Netherlands), after which they were diluted another 100 times in BHI broth, resulting in a concentration of ~ $4 \cdot 10^4$ cfu/ml, which was confirmed by plating on BHI agar. The $\mu_{max}$ was estimated using the 2-fold dilution method, as described previously by (Biesta-Peters et al., 2010), which is based on the time-to-detection (TTD) of serially diluted cultures. Briefly, for each strain tested, a two-fold dilution series was made in duplicate from the first well to the fifth well, by mixing 200 µL of bacterial culture and 200 µL of fresh BHI in honeycomb plates. The plates were incubated in a Bioscreen C (Oy Growth Curves AB Ltd) at 30 °C with continuous shaking. The TTD was defined as the time at which a well reaches

an $OD_{600}$ value of 0.2. Data processing and estimation of the TTD was done in Microsoft Excel (Redmond, Washington, USA). The $\mu_{max}$ was calculated as the negative reciprocal slope of the linear regression between TTD and the natural logarithm of the initial bacterial concentration of the five wells for each culture, where $\mu_{max}$ equals ln(2)/generation time (i.e., $\mu_{max}$ = 1 represents a generation (doubling) time of approximately 0.7 h, or 42 minutes). Three biologically independent experiments were performed to estimate the mean and standard deviation of $\mu_{max}$.

### Inactivation kinetics at low pH

Acid inactivation experiments were performed as described previously (Metselaar et al., 2013). Briefly, 100 ml of late-exponential phase culture was pelleted for 5 minutes at 2,880 x *g* in a fixed-angle rotor (5804 R, Eppendorf). Pellets were washed in 10 ml BHI broth and pelleted again at 5 min at 2,880 x *g*. The pellet was resuspended in 1 ml PPS that was pre-warmed to 37°C and adjusted to pH 3.0 using 10 M of HCl, and placed in a 100 ml Erlenmeyer flask in a shaking water bath at 37°C. At different time intervals, samples were taken, decimally diluted in BHI broth and plated on BHI agar using an Eddy Jet spiral plater (Eddy Jet, IUL S.A.) Plates were incubated at 30°C for 4-6 days to allow for full recovery of damaged cells. Combined data of at least three biologically independent experiments were used for analysis

### Inactivation kinetics at high temperature

Heat inactivation experiments were performed as described before (Metselaar et al., 2015). Briefly, 400 µL of late-exponential phase culture was added to 40 ml of fresh BHI broth that was pre-heated to 55°C ± 0.3°C. A separate Erlenmeyer with BHI at room temperature was used to determine the initial microbial concentration. Samples were taken after various timepoints and decimally diluted in PPS. Appropriate dilutions were plated on BHI agar using an Eddy Jet spiral plater (Eddy Jet, IUL S.A.) in duplicate. Combined data of at least 3 biologically independent experiments were used for analysis.

### Proteomic analysis

Cultures of the LO28 WT, variant 15 and evolved 15EV1 and 15EV2 were grown as described in 2.1. For proteomic analysis, 2 ml of sample with $OD_{600}$ of 0.4-0.5 was flash frozen in liquid nitrogen and stored until further use. Samples were thawed on ice and pelleted at 17,000 x *g.* Pellets were washed twice with 100 mM Tris (pH 8) to remove traces of BHI. Pellets were

resuspended in 100 µL of 100 mM Tris (pH 8) and were sonicated three times for 30 seconds on ice to lyse the cells. Samples were prepared according to the filter assisted sample preparation protocol (FASP) (Wiśniewski et al., 2009) with the following steps: reduction with 15 mM dithiothreitol, alkylation with 20 mM acrylamide, and digestion with sequencing grade trypsin overnight. Each prepared peptide sample was analyzed by injecting (18 µL) into a nanoLC-MS/MS (Thermo nLC1000 connected to an LTQ-Orbitrap XL) as described previously (Lu et al., 2011; Wendrich et al., 2017). nLC-MSMS system quality was checked with PTXQC (Bielow et al., 2016) using the MaxQuant result files. LCMS data with all MS/MS spectra were analyzed with the MaxQuant quantitative proteomics software package (Cox et al., 2014) as described before (Smaczniak et al., 2012; Wendrich et al., 2017). A protein database with the protein sequences of *L. monocytogenes* LO28 (accession: PRJNA664298) was downloaded from NCBI (www.ncbi.nlm.nih.gov). Filtering and further bioinformatics and statistical analysis of the MaxQuant ProteinGroups file was performed with Perseus (Tyanova et al., 2016). Reverse hits and contaminants were filtered out. Protein groups were filtered to contain minimally two peptides for protein identification of which at least one is unique and at least one is unmodified. Also, each comparison (WT versus variants) required at least three valid values in either WT or variant. Data visualization was performed using the statistical programming language R (version 3.6.0). Significant up- or downregulation was defined as a change in abundance relative to the WT of at least 10 times (1 log), with a corrected P value ($-\log_{10}$ P value) above 2.

### Whole genome sequencing and SNP analysis

Genomic DNA of *L. monocytogenes* LO28 WT strain for PacBio sequencing was isolated using the DNeasy Blood and tissue kit (Qiagen, Hilden, Germany). Two times 2 ml of overnight culture was pelleted at 17,000 x *g*. The pellets were washed with 1 ml PPS and resuspended in 1 ml lysis buffer (20 mM Tris-HCl, 2 mM EDTA, 1.2% (w/v) Triton X-100, 20 mg/ml lysozyme, pH 8.0). The suspension was incubated at 37°C for one hour under gentle shaking in an Eppendorf Thermomixer 5436 (Eppendorf AG, Hamburg, Germany). Subsequently 10 µl of RNAse 20 mg/ml (Qiagen, Hilden, Germany) was added and incubated for 5 minutes at room temperature, after which 62.5 µl proteinase K and 500 µl AL buffer (provided by the manufacturer) were added. After incubation at 56°C for one hour under gentle shaking, 500 µL absolute ethanol was added. The suspension was transferred to a spin column provided by the kit and incubated for 10 minutes to allow for maximal binding of DNA. The columns were centrifuged for one minute at 6,000 x *g*. The filters were subsequently

washed two times with 500 μL of buffer AW1 (provided by the manufacturer) at 6,000 x *g*, and two times with 500 μL of buffer AW2 (provided by the manufacturer). To remove any trace of buffer the columns were centrifuged at 17,000 x *g* for 3 minutes. Subsequently, 53 μL of AE buffer was added to the centre of the column and incubated for 10 minutes before centrifugation at 6,000 x *g*. Samples were stored at 4°C until sequencing.

PacBio sequencing was performed by Eurofins GATC (Eurofins GATC Biotech GmbH. Germany) using a PacBio RS II system (Pacific Biosystems) resulting in 80,017 reads pre-filtering, with a N50 of 16970 bp. Read correction, trimming, and de-novo assembly were performed in Canu V1.8 (Koren et al., 2017) running on a 2018 MacBook Pro under MacOS Mojave Version 10.14.3. Overhangs were trimmed using Circlator (Hunt et al., 2015) resulting in a 2975254 bp linear genome with *dnaA* as the first gene. Error correction was done using Pilon version 1.123 with Illumina reads obtained previously (Metselaar et al., 2015). The resulting sequence and raw reads were submitted to GenBank and the sequence read archive respectively (at www.ncbi.nlm.nih.gov) with accession: PRJNA664298.

Strains used and Evolved variants 15EV1 and 15EV2 obtained in the evolution experiment were grown in 9 ml BHI tubes (Oxoid) for 18 ± 2 hours at 37°C. In total 1.8 ml of the culture was centrifuged for 5 minutes at 13,000 rpm to obtain a cell pellet. After removal of the supernatant the cell pellet was resuspended and stored in 450 μL DNA/RNA Shield (Zymo Research) at 4°C until DNA extraction. The DNA was extracted by BaseClear (Leiden, the Netherlands) and paired-end 2 × 150bp short-reads were generated using a Nextera XT library preparation (Illumina). The paired-end reads were sequenced on a NovaSeq 6000 system (Illumina). Raw reads were trimmed and de novo assembled using CLC Genomics Workbench v 10.0 (Qiagen, Hilden, Germany). SNP analysis of evolved variants against the LO28 WT reference was performed using SNIPPY 3.2 (Seemann, T 2015) and Pilon using the "--changes" argument (Walker et al., 2014)

## Mutant construction

Mutants (see Table 4.1) were constructed using the temperature sensitive suicide plasmid pAULA (Chakraborty et al., 1992). The *rpsU* gene from either variant 15, 15EV1, or 15EV2 was amplified from gDNA by KAPA HiFi Hotstart ReadyMix (KAPA Biosystems, USA), using the primers listed in Supplementary Table S4.1. The resulting fragments were ligated in frame to the pAULA multiple cloning site via EcoR1 and Sal1 restriction that were introduced to the fragments by the respective primers.

The resulting plasmid was electroporated (2.5 kV, 25 µF, 200 Ω), in a 0.2 cm cuvette using a BIO-RAD GenePulser, to the appropriate *L. monocytogenes* cells, and plated on BHI agar at 30°C with 5 µg/ml erythromycin to select for transformants.

Two erythromycin resistant colonies per construct were inoculated in separate tubes in BHI broth supplemented with 5 µg/ml erythromycin and grown overnight at 42°C to select for plasmid integration. Selected strains resulting from a single cross-over integration event were grown overnight in BHI at 30°C to induce double crossover events and were subsequently plated at 30°C. Resulting colonies were replica plated on BHI with and without 5 µg/ml erythromycin and incubated at 30°C. Colonies sensitive to erythromycin were selected. PCR using the primers listed in Supplementary Table S4.1 and DNA sequencing (BaseClear B.V. Leiden, The Netherlands) of erythromycin sensitive colonies confirmed the correct point mutation in the respective genes and the lack of additional mutations in the targeted region.

***Table 4.1:*** *Constructed* L. monocytogenes *mutants*

| Strain | Mutation introduced |
|---|---|
| LO28 WT | RpsU$^{Arg17Pro}$ |
| LO28 WT | RpsU$^{Arg17His}$ |
| LO28 WT | RpsU$^{Arg17The}$ |
| EGDe WT | RpsU$^{Arg17Pro}$ |

**Statistical testing**

Hypothesis testing was performed in the statistical programming language R (version 3.6.0) using the t.test() and var.test() functions.

## Results

### Growth kinetics of evolved variants

The experimental evolution regime resulted in the selection of two evolved variants, Evolved 1 and Evolved 2 (15EV1 and 15EV2, respectively). The growth kinetics of evolved variants 15EV1 and 15EV2 were assessed (Figure 4.1a) and showed that the experimental evolution regime had successfully selected for evolved variants after 16 and 18 daily transfers (~105 and ~120 generations), that showed increased $\mu_{max}$ when compared to variant 15 (Figure 4.1a). The $\mu_{max}$ of both evolved strains was significantly higher than that

of variant 15 whereas the $\mu_{max}$ of 15EV1 was even not significantly different from the $\mu_{max}$ of the LO28 WT strain, while strain 15EV2 had a slightly lower $\mu_{max}$ (Figure 4.1b).

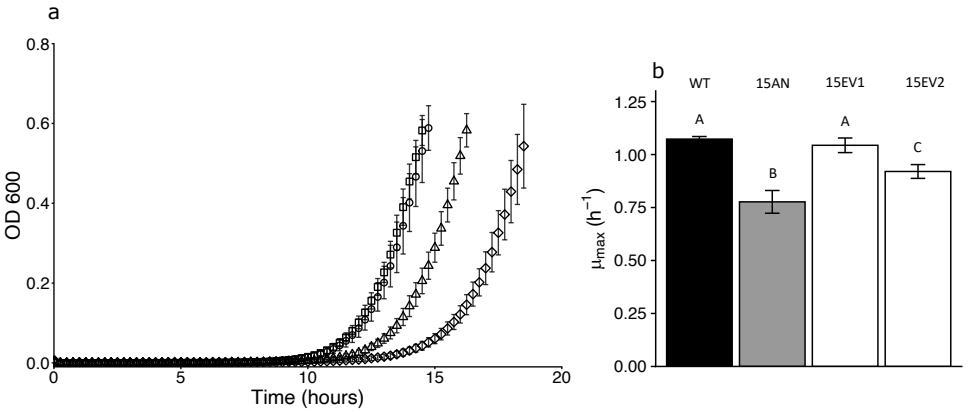


***Figure 4.1:*** *Growth performance of* L. monocytogenes *LO28 WT, variant 15, 15EV1, and 15EV2 (a) growth curves for LO28 WT (squares), variant 15 (diamonds), 15EV1 (circles), and 15EV2 (triangles), (b) Maximum specific growth rates ($\mu_{max}$) for L. monocytogenes LO28 WT, variant 15, 15EV1, and 15EV2. Different capital letters show statistically significant differences.*

### Multiple-stress resistance of evolved variants

Since the evolved variants 15EV1 and 15EV2 showed increased fitness, we compared their resistance to heat stress (55°C) and acid stress (pH 3.0) to that of variant 15 (Figure 4.2). In the heat stress experiments (Figure 4.2a), variant 15 started with approximately 6.8 log cfu/ml, and showed little inactivation after 20 minutes of exposure, with a concentration of around 6 log cfu/ml. In contrast, after 20 minutes of exposure the concentrations of both evolved variants 15EV1 and 15EV2 decreased and were not significantly different from the LO28 WT strain with concentrations of around 2.5 log cfu/ml ($p > 0.05$). For acid stress experiments (Figure 4.2b), variant 15 again only showed a small (< 1 log cfu/ml) decrease in cell counts after 20 minutes, while both evolved variants and also the LO28 WT strain showed over 5 log cfu/ml reduction after 20 minutes. These data indicate that both evolved variants 15EV1 and 15EV2 have lost their resistance to heat stress and acid stress when compared to variant 15.

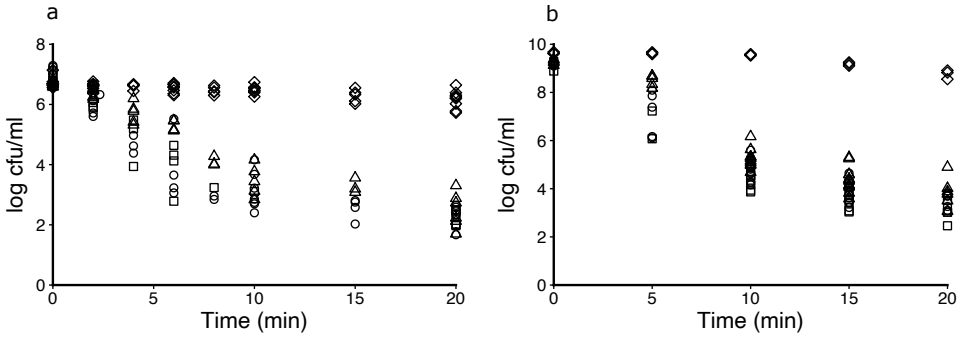


***Figure 4.2:*** *Survival of* L. monocytogenes *LO28 WT, variant 15, 15EV1, and 15EV2 after exposure to heat (55°C) (a) or acid stress (pH 3.0) (b). The wild type is represented by squares, variant 15 by diamonds, and variants 15EV1 and 15EV2, are represented by circles and triangles respectively.*

## Proteomic analysis of variant 15, 15EV1, and 15EV2

Comparative gene profiling analysis of *L. monocytogenes* LO28 WT and variant 15, previously showed upregulation of 116 genes with a major contribution of general stress sigma factor SigB dependent regulon members in late-exponential phase cells grown in non-stressed conditions in BHI (Koomen et al., 2018).

Here, we investigated the proteomes of late-exponential phase cells of *L. monocytogenes* LO28 WT, variant 15 and evolved variants 15EV1 and 15EV2 (Figure 4.3). Presenting the data compared to the WT, shows significant differences for variant 15 (Figure 4.3), in line with previously reported differences in gene expression profiles and phenotypes (Koomen et al., 2018). Notably, our proteomics analysis revealed that out of the 29 proteins annotated as belonging to the SigB regulon in this sample, 21 were higher expressed in variant 15 compared to LO28 WT, (Figure 4.3). These include stress resistance proteins such as OpuCA (lmo1428), OpuCC (lmo1426), and SepA (lmo2157) (Kazmierczak et al., 2003; Milohanic et al., 2003). For a full list, see supplementary Table S4.2. In accordance with gene expression data, and the non-motile phenotype of variant 15 (Koomen et al., 2018), proteomics data show a significant reduced expression of motility and chemotaxis associated proteins such as MotA (lmo0685), MotB (lmo0686), CheA (lmo0692), and chemotaxis response regulator CheY (lmo0691). As anticipated, the proteomic profiles for 15EV1 and 15EV2 were more similar to that of the WT, and we found seven and twenty proteins expressed above the

stringent threshold in 15EV1 and 15EV2, respectively (see supplementary Table S4.2 and S4.3). None of the genes that are upregulated in 15EV1 are part of the sigB regulon. Four of the upregulated proteins in 15EV2 were part of the SigB regulon, namely, succinate semialdehyde dehydrogenase (lmo0913), hypothetical protein lmo2748, opuCA (lmo1428), and the pyruvate oxidase lmo0722. The low relative abundance of SigB upregulated proteins matches the WT-like phenotypes of 15EV1 and 15EV2, including the higher fitness and loss of acid and heat stress resistance.

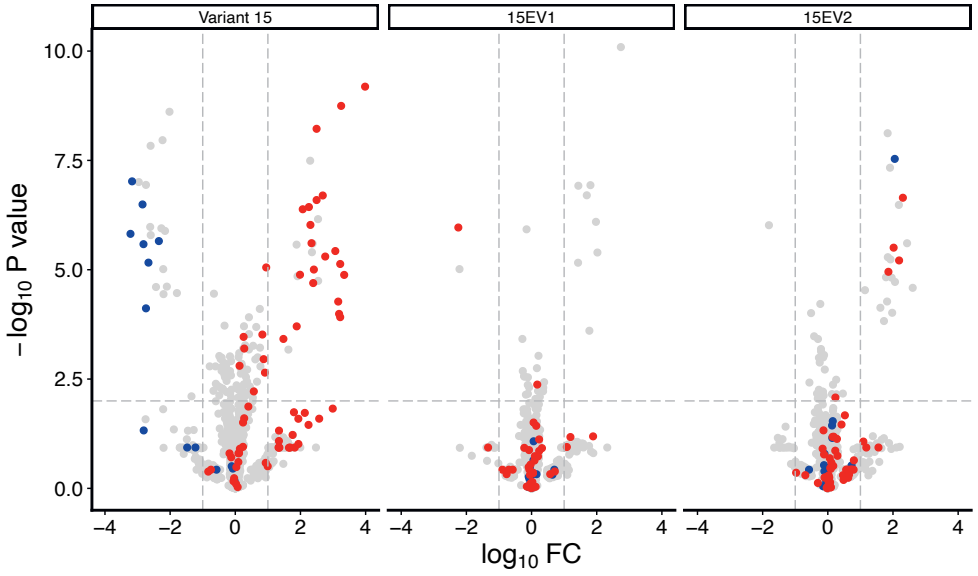


***Figure 4.3:*** *Volcano plot of significantly differentially abundant proteins of* L. monocytogenes *variant 15, 15EV1, and 15EV2 compared to the wild type. The* $-\log_{10}$ *(Benjamini–Hochberg corrected P value) is plotted against the* $\log_{10}$*(fold change (FC): variant over WT). Horizontal dotted line represents the cutoff for* $-\log_{10}$ *(P), vertical dotted lines represent* $\log_{10}$*(fold change) cutoff. Red dots represent genes regulated by sigB, blue dots represent genes involved in the formation and regulation of flagella. The expression of individual proteins is listed in supplementary Tables S4.2 – S4.4.*

## Whole genome sequencing of 15EV1 and 15EV2

Previous whole genome sequencing and Structural Variation (SV) analysis of *L. monocytogenes* LO28 WT and variant 15 revealed a Single Nucleotide Polymorphism (SNP) in the *rpsU* gene, coding for 30S ribosomal protein S21 (Metselaar et al., 2015). This SNP led to an arginine to proline substitution in the RpsU protein (denoted here as $RpsU^{17Arg\text{-}Pro}$). Strikingly, whole genome sequencing and Structural Variation (SV) analysis of *L. monocytogenes* evolved variants 15EV1 and 15EV2 revealed a single SNP in the same codon of the *rpsU* gene, while no other SNPs were identified. In the *rpsU* gene of 15EV1 the Cytosine in position 50 mutated to Adenine, while in 15EV2 the Cytosine in position 49 mutated into Adenine, (see Table 4.2) resulting in amino acid changes from Proline (codon, CCT) to Histidine (codon, CAT) in 15EV1 ($RpsU^{17Pro\text{-}His}$), and Threonine (codon, ACT) in 15EV2 ($RpsU^{17Pro\text{-}Thr}$) (Figure 4.4 a/b). Since amino acid substitutions can disrupt protein structure, potentially altering protein stability or function, we analysed the protein sequences of WT and variants using the online tool CFSSP (Ashok Kumar, 2013) Again, the protein structure of RpsU in WT and the evolved variants appeared similar, while an extra proline-associated turn was predicted in variant 15 (see Supplementary Figure S4.1). The putative proline-induced turn may disrupt the $RpsU^{17Arg\text{-}Pro}$ protein structure as proline has been described as a helix breaker (Chou and Fasman, 1974), which might result in loss of functionality and/or exclusion from the 30S ribosome in variant 15.

***Table 4.2:*** *Mutations in* L. monocytogenes *variants found by WGS and SNP analysis*

| Variant | Position | Strand | NT | AA | Locus tag | Product |
|---|---|---|---|---|---|---|
| 15 | 1521940 | - | 50G>C | 17R>P | IEJ01_07680 | 30S ribosomal protein S21 |
| 15EV1 | 1521940 | - | 50C>A | 17P>H | IEJ01_07680 | 30S ribosomal protein S21 |
| 15EV2 | 1521939 | - | 49C>A | 17P>T | IEJ01_07680 | 30S ribosomal protein S21 |

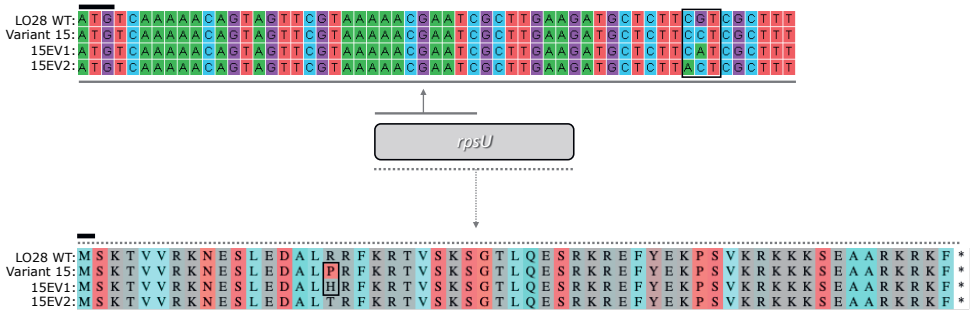


***Figure 4.4:*** *Sequence alignment of rpsU (top) and amino acid sequence of RpsU in* L. monocytogenes *LO28 WT and variant 15 and 15EV1 and 15EV2. The upper alignment represents the nucleotide sequence of the region where mutations were found. The black line indicates the start codon of the* rpsU *gene. The lower alignment represents the amino acid sequence of the complete RpsU protein and the effect of the mutations on the amino acid sequence. Amino acids predicted to cause turns in the tertiary protein structure are shaded red, and amino acids at position 17 are boxed, including the extra turn in variant 15 caused by proline (P).*

**Fitness and stress resistance of constructed mutants**

To confirm the arginine to proline substitution at position 17 in *rpsU* as the mutation underlying the multiple-stress resistant phenotype of variant 15, we introduced RpsU$^{17Arg\text{-}Pro}$ into a *L. monocytogenes* LO28 WT background. Additionally, we also introduced the two SNP's that were selected by experimental evolution in 15EV1 and 15EV2, namely, RpsU$^{17Arg\text{-}His}$ and RpsU$^{17Agr\text{-}Thr}$. Analysis of growth performance showed that the $\mu_{max}$ as proxy for fitness of the constructed RpsU$^{17Arg\text{-}Pro}$ mutant was similar to that of variant 15, and that of the constructed RpsU$^{17Arg\text{-}His}$ and RpsU$^{17Arg\text{-}Thr}$ mutants was similar to that of the corresponding evolved variants 15EV1 and 15EV2, respectively (Table S4). Subsequently, we tested the response of late exponential phase cells of the constructed mutants to heat (55°C) stress (Figure 4.5a) and acid (pH 3.0) stress (Figure 4.5b). As expected, the LO28 WT strain with the introduced RpsU$^{17Arg\text{-}Pro}$ substitution showed significant ($p < 0.05$) higher heat and acid resistance after 10 minutes of treatment than the LO28 WT strains with the introduced RpsU$^{17Arg\text{-}His}$ and RpsU$^{17Arg\text{-}Thr}$ substitutions. These results confirmed that only the RpsU$^{17Arg\text{-}Pro}$ substitution results in the multiple-stress resistant phenotype typical of variant

15, while RpsU amino acid substitutions mimicking variants 15EV1 and 15EV2 results in WT like fitness and stress sensitive phenotypes.

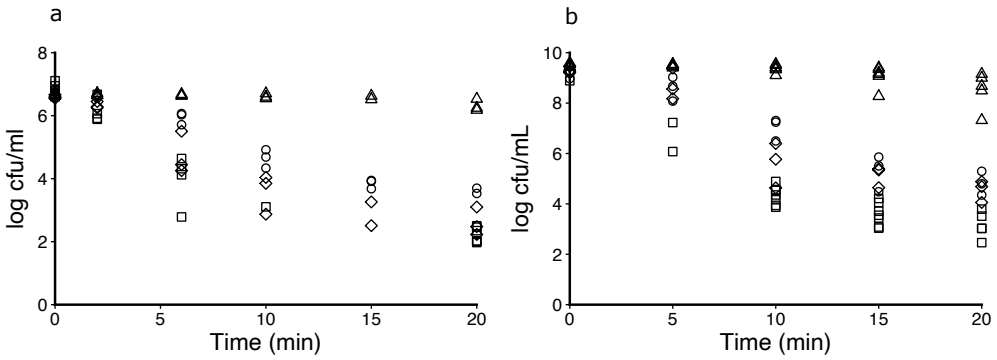


***Figure 4.5:*** *Survival of* L. monocytogenes *LO28 WT, and constructed mutants, during heat (55°C) (a) or acid (pH 3.0) (b) stress. LO28 WT is represented by squares, LO28 with RpsU$^{17Arg\text{-}Pro}$ is represented by triangles, LO28 with RpsU$^{17Arg\text{-}Thr}$, is represented by circles, and LO28 with RpsU$^{Arg17His}$ by diamonds.*

To test whether RpsU, with a proline at position 17, could induce phenotypic switching in other *L. monocytogenes* strains, we also introduced the RpsU$^{17Arg\text{-}Pro}$ mutation into *L. monocytogenes* EGDe, which is one of the best studied strains of *L. monocytogenes* including its stress survival capacity (Becavin et al., 2014). Analysis of the growth performance of EGDe WT and its RpsU$^{17Arg\text{-}Pro}$ mutant at 30 °C showed reduced fitness for the latter one, reflected in a lower $\mu_{max}$ (0.86 $h^{-1} \pm$ standard deviation 0.01 $h^{-1}$) compared to that of EGDe WT (1.10 $h^{-1} \pm$ standard deviation 0.02 $h^{-1}$) (Figure 4.6). A comparative analysis previously showed that EGDe has a higher resistance to heat stress than LO28 (Aryani et al., 2015), and this was also reflected in the inactivation data shown in Figure 4.7, where heat inactivation at 55°C resulted in a decrease of about 2.5 log cfu/ml in 20 minutes for the EGDe WT (Figure 4.7a). As expected, higher stress resistance was observed for the EGDe strain carrying the RpsU$^{17Arg\text{-}Pro}$ mutation, with stable cell counts maintained during the treatment time (Figure 4.7a). We observed a similar trend when both strains were exposed to acid stress, with enhanced acid stress survival for the RpsU$^{17Arg\text{-}Pro}$ EGDe mutant strain (Figure 4.7b). The combination of all results provides evidence that sequential mutations in *rpsU* resulting in RpsU$^{17Arg\text{-}Pro}$ and subsequently RpsU$^{17Pro\text{-}His}$ or RpsU$^{17Pro\text{-}Thr}$, enable a switch

between low fitness/high stress resistance and high fitness-low stress resistance phenotypes in *L. monocytogenes*.

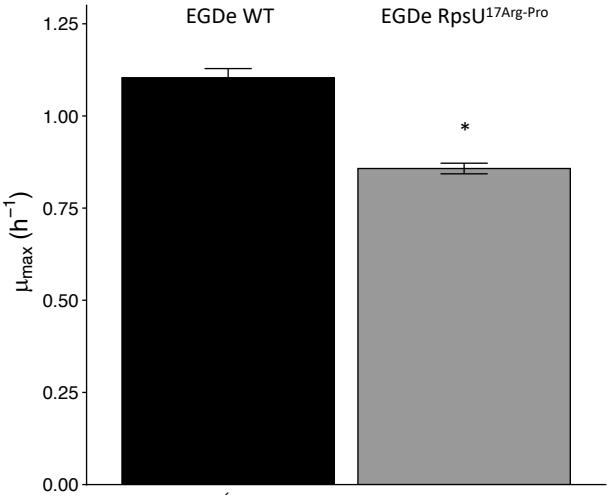


***Figure 4.6:*** *Maximum specific growth rates ($\mu_{max}$) for* L. monocytogenes *EGDe, and EGDe RpsU$^{17Arg\text{-}Pro}$. * indicates significant difference.*

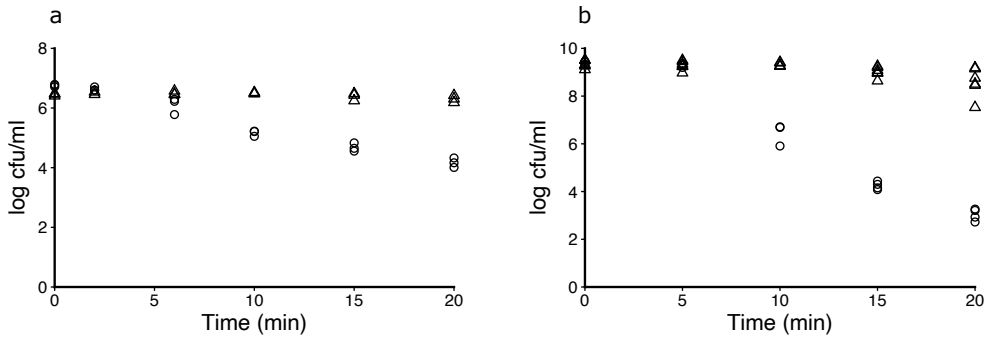


***Figure 4.7:*** *Survival of* L. monocytogenes *EGDe wild type, and EGDe RpsU$^{17Arg\text{-}Pro}$, after exposure to heat (55 °C) (a) or acid (pH 3.0) stress (b). The EGDe WT is represented by circles, EGDe RpsU$^{17Arg\text{-}Pro}$ by triangles.*

## Discussion

Previous genotyping and phenotyping studies showed that the multiple-stress resistance of *L. monocytogenes* LO28 variant 15 with RpsU$^{17Arg\text{-}Pro}$ was linked to induction of the SigB regulon, and was correlated with reduced fitness (Koomen et al. 2018). Here, we have used experimental evolution to select for mutations in variant 15 that increased fitness. The two evolved lines fixed two different mutations, leading to two different amino acid substitutions both at position 17 in RpsU, namely, RpsU$^{17Pro\text{-}His}$ (15EV1) and RpsU$^{17Pro\text{-}Thr}$ (15EV2) resulting in reversion to WT-like fitness (Figure 4.1) and stress resistance (Figure 4.2). The experimental evolution regime had successfully selected for evolved variants after 16 and 18 daily transfers (~105 and ~120 generations). We modelled the kinetics of the WT and variant 15 ancestor based on the $\mu_{max}$ reported by Metselaar et al. (2016) for the growing conditions that were used during experimental evolution. We used a 3-phase model based on Buchanan et al. 1997, with a $logN_{max}$ of 9.5 log cfu/ml, and took into account the Jameson effect (Jameson, 1962), that addresses growth suppression by the dominant strain in a multi strain population when the dominant strain reaches its stationary phase. We then estimated that after 6 rounds (~ 40 generations) one EV15 cell (with initial fraction $1{\cdot}10^{-7.5}$) could have reached the same population density as the variant 15 strain, which is in line with the successful outcome of the experimental evolution experiment.

Random insertion of a proline residue is known to disrupt protein structure, potentially altering the stability or function of the protein (Chou and Fasman, 1974). Combined with data obtained with the constructed RpsU$^{17Arg\text{-}Pro}$, RpsU$^{17Arg\text{-}His}$, and RpsU$^{17Arg\text{-}Thr}$ mutants, we provided evidence that replacing the putative disruptive proline at position 17 in *L. monocytogenes* variant 15 with amino acids that do not have such strong disruptive effects, i.e., threonine or histidine, can restore WT-like functioning of the RpsU protein with an arginine at position 17. Although both evolved lines fixed a compensatory mutation, they did not fix the same mutation, and we did not find a reversion to the original RpsU$^{17Arg}$. Based on the slight difference in $\mu_{max}$ and proteomic profile between 15EV1 and 15EV2, we hypothesize that the RpsU$^{17Arg\text{-}His}$ mutation is slightly more efficient in restoring the WT phenotype than RpsU$^{17Arg\text{-}Thr}$.

The previously described variant 14 with a complete deletion of *rpsU* and variant 15 have highly comparable phenotypical behaviour (Koomen et al., 2018; Metselaar et al., 2015), which indicates that RpsU is not essential for growth, and that RpsU$^{17Arg\text{-}Pro}$ in variant 15 either lost its functionality, or is not (efficiently) incorporated into the 30S ribosome that

together with the 50S ribosome constitutes the 70S ribosome. Notably, the additional introduction in the current study of the RpsU$^{17Arg\text{-}Pro}$ mutation in the well-studied *L. monocytogenes* EGDe strain, also resulted in a phenotypic switch from high fitness-low stress resistance to low fitness-high stress resistance (see Figure 4.6 and 4.7), providing evidence that the observed changes in behaviour are strain independent and caused by a single arginine-proline substitution at position 17 in RpsU. Moreover, studies in *Bacillus subtilis,* a closely related firmicute, have also shown that RpsU was not essential for growth, but that deletion of the protein leads to altered phenotypes including loss of motility and a reduced growth rate (Akanuma et al., 2012).

Induction of multiple-stress resistance in *L. monocytogenes* by SigB is tightly controlled by the so-called stressosome, a protein complex that acts as a signal relay hub integrating multiple environmental (stress) signals (Guariglia-Oropeza et al., 2014; Impens et al., 2017). Activation of a large fraction of the SigB regulon during non-stress growth conditions in LO28 variant 15 and in LO28 carrying the RpsU$^{17Arg\text{-}Pro}$ mutations points to an (in)direct interaction between the 70S ribosome and the stress signalling cascade. How the presumed loss of function of the 30S RpsU$^{17Arg\text{-}Pro}$ variant protein affects functioning of the 70S ribosome resulting in reduced fitness and activation of the SigB regulon remains to be elucidated.

Previous studies describing performance of multiple-stress resistant variants in a model food chain considered the trade-off between increased stress resistance and lower fitness (Abee et al., 2016; Metselaar et al., 2015). The information that selection of multiple-stress resistant variants following a single lethal stress exposure, could be followed by subsequent evolution of variants with increased fitness and loss of the stress resistant phenotype, may point to an additional layer of complexity that can be included in these scenario analyses. Notably, translation of these population dynamics that are based on the generation and performance of *L. monocytogenes* variants following single-nucleotide substitutions (SNPs) to ecology along the food chain and more specifically (over)representation in persistent strains, is currently not supported by analysis of WGS data. Recently, Harrand et al. (2020) studied the evolution of *L. monocytogenes* persistence in a food processing plant over multiple years and genotyping of isolates showed limited single-nucleotide substitutions (SNPs), and a more prominent role in strain diversification by gain and loss of prophages. Further studies are required to determine whether the observed lack of (over)representation of SNPs in RpsU, and specifically those resulting in RpsU$^{17Arg\text{-}Pro}$, in

sequenced *L. monocytogenes* isolates is caused by reduced fitness affecting performance of stress resistant variants in *L. monocytogenes* enrichments from food and food processing samples according to the ISO 11290-1:2017 method.

The experimental evolution setup used in the current study, combined with genotyping and phenotyping of the two evolved variants, and the construction of targeted mutants in *L. monocytogenes* LO28 and EGDe, provides evidence that single amino acid substitutions in RpsU enable *L. monocytogenes* to switch between high fitness-low stress resistance and low fitness-high stress resistance. The exact mechanism of SigB induction following RpsU$^{17Arg\text{-}Pro}$ substitution or RpsU deletion (Metselaar et al. 2015; Koomen et al. 2018) and the impact on 70S ribosome function and the stressosome-mediated signalling cascade is currently under investigation in our group. Ultimately, a better understanding of the processes involved will add to a further insight into factors contributing to strain diversity and population heterogeneity in *L. monocytogenes* stress sensing and survival capacity and its transmission in the food chain.

## Acknowledgments

The authors would like to thank Angela van Hoek of the Dutch National Institute for Public Health and the Environment (RIVM) for assistance with sequencing the evolved variants, and Birgitte H. Kallipolitis for discussing the optimal settings for electroporation of *L. monocytogenes*

## References

**Abee, T., Koomen, J., Metselaar, K.I., Zwietering, M.H., Den Besten, H.M.W.,** 2016. Impact of pathogen population heterogeneity and stress-resistant variants on food safety. Annu. Rev. Food Sci. Technol. 7, 439–456. doi:10.1146/annurev-food-041715-033128

**Akanuma, G., Nanamiya, H., Natori, Y., Yano, K., Suzuki, S., Omata, S., Ishizuka, M., Sekine, Y., Kawamura, F.,** 2012. Inactivation of ribosomal protein genes in *Bacillus subtilis* reveals importance of each ribosomal protein for cell proliferation and cell differentiation. J. Bacteriol. 194, 6282–6291. doi:10.1128/JB.01544-12

**Aryani, D.C., Den Besten, H.M.W., Hazeleger, W.C., Zwietering, M.H.,** 2015. Quantifying variability on thermal resistance of *Listeria monocytogenes*. Int. J. Food Microbiol. 193, 130–138. doi:10.1016/j.ijfoodmicro.2014.10.021

**Ashok Kumar, T.,** 2013, CFSSP: Chou and Fasman secondary structure prediction server. Wide Spectrum 1, 15-19.

**Becavin, C., Bouchier, C., Lechat, P., Archambaud, C., Creno, S., Gouin, E., Wu, Z., Kuhbacher, A., Brisse, S., Pucciarelli, M.G., Garcia-del Portillo, F., Hain, T., Portnoy, D.A., Chakraborty, T., Lecuit, M., Pizarro-Cerda, J., Moszer, I., Bierne, H., Cossart, P.,** 2014. Comparison of widely used *Listeria monocytogenes* strains EGD, 10403S, and EGD-e highlights genomic differences underlying variations in pathogenicity. mBio 5(2):e00969-14. doi:10.1128/mBio.00969-14.

**Bielow, C., Mastrobuoni, G., Kempa, S.,** 2016. Proteomics quality control: quality control software for MaxQuant results. J. Proteome Res. 15, 777–787. doi:10.1021/acs.jproteome.5b00780

**Biesta-Peters, E.G., Reij, M.W., Joosten, H., Gorris, L.G.M., Zwietering, M.H.,** 2010. Comparison of two optical-density-based methods and a plate count method for estimation of growth parameters of *Bacillus cereus*. Appl. Environ. Microbiol. 76, 1399–1405. doi:10.1128/AEM.02336-09

**Buchanan, R.L., Whiting, R.C., Damert, W.C.,** 1997. When is simple good enough: a comparison of the Gompertz, Baranyi, and three-phase linear models for fitting bacterial growth curves. Food Microbiol. 14, 313-326, doi:10.1006/fmic.1997.0125

**Chakraborty, T., Leimeister-Wächter, M., Domann, E., Hartl, M., Goebel, W., Nichterlein, T., Notermans, S.,** 1992. Coordinate regulation of virulence genes in *Listeria monocytogenes* requires the product of the *prfA* gene. J. Bacteriol. 174, 568–574. doi:10.1128/jb.174.2.568-574.1992

**Chou, P.Y., Fasman, G.D.,** 1974. Prediction of protein conformation. Biochemistry 13, 222–245. doi:10.1021/bi00699a002

**Cox, J., Hein, M.Y., Luber, C.A., Paron, I., Nagaraj, N., Mann, M.,** 2014. Accurate proteome-wide label-free quantification by delayed normalization and maximal peptide ratio extraction, termed MaxLFQ. Mol. Cell. Proteomics 13, 2513–2526. doi:10.1074/mcp.M113.031591

**Gollan, B., Grabe, G., Michaux, C., Helaine, S.,** 2019. Bacterial persisters and infection: past, present, and progressing. Annu. Rev. Microbiol. 73, 359–385. doi:10.1146/annurev-micro-020518-115650

**Guariglia-Oropeza, V., Orsi, R.H., Yu, H., Boor, K.J., Wiedmann, M., Guldimann, C**., 2014. Regulatory network features in *Listeria monocytogenes*-changing the way we talk. Front. Cell. Infect. Microbiol. 4, 14. doi:10.3389/fcimb.2014.00014

**Guldimann, C., Boor, K.J., Wiedmann, M., Guariglia-Oropeza, V.,** 2016. Resilience in the face of uncertainty: Sigma factor b fine-tunes gene expression to support homeostasis in Gram-positive bacteria. Appl. Environ. Microbiol. 82, 4456–4469. doi:10.1128/AEM.00714-16

**Hunt, M., Silva, N.D., Otto, T.D., Parkhill, J., Keane, J.A., Harris, S.R.,** 2015. Circlator: automated circularization of genome assemblies using long sequencing reads. Genome Biol. 16, 294. doi:10.1186/s13059-015-0849-0

**Impens, F., Rolhion, N., Radoshevich, L., Bécavin, C., Duval, M., Mellin, J., del Portillo, F.G., Pucciarelli, M.G., Williams, A.H., Cossart, P.,** 2017. N-terminomics identifies Prli42 as a membrane miniprotein conserved in Firmicutes and critical for stressosome activation in *Listeria monocytogenes.* Nat. Microbiol. 2, 1–13. doi:10.1038/nmicrobiol.2017.5

**Jameson, J.,** 1962 A discussion of the dynamics of *Salmonella* enrichment. J Hyg (Lond). 60, 193-207 doi: 10.1017/s0022172400039462

**Karatzas, K.A.G., Valdramidis, V.P., Wells-Bennik, M.H.J.,** 2005. Contingency locus in *ctsR* of *Listeria monocytogenes* Scott A: a strategy for occurrence of abundant piezotolerant isolates within clonal populations. Appl. Environ. Microbiol. 71, 8390–8396. doi:10.1128/AEM.71.12.8390-8396.2005

**Kazmierczak, M.J., Mithoe, S.C., Boor, K.J., Wiedmann, M.,** 2003. *Listeria monocytogenes* sigma B regulates stress response and virulence functions. J. Bacteriol. 185, 5722–5734. doi:10.1128/jb.185.19.5722-5734.2003

**Koomen, J., Den Besten, H.M.W., Metselaar, K.I., Tempelaars, M.H., Wijnands, L.M., Zwietering, M.H., Abee, T.,** 2018. Gene profiling-based phenotyping for identification of cellular parameters that contribute to fitness, stress-tolerance and virulence of *Listeria monocytogenes* variants. Int. J. Food Microbiol. 283, 14–21. doi:10.1016/j.ijfoodmicro.2018.06.003

**Koren, S., Walenz, B.P., Berlin, K., Miller, J.R., Bergman, N.H., Phillippy, A.M.,** 2017. Canu: scalable and accurate long-read assembly via adaptive k-mer weighting and repeat separation. Genome Res. 27, 722–736. doi:10.1101/gr.215087.116

**Lecuit, M.,** 2007. Human listeriosis and animal models. Microbes Infect. 9, 1216–1225. doi:10.1016/j.micinf.2007.05.009

**Lu, J., Boeren, S., de Vries, S.C., van Valenberg, H.J.F., Vervoort, J., Hettinga, K.,** 2011. Filter-aided sample preparation with dimethyl labeling to identify and quantify milk fat globule membrane proteins. J. Proteome 75, 34–43. doi:10.1016/j.jprot.2011.07.031

**Metselaar, K.I., Den Besten, H.M.W., Abee, T., Moezelaar, R., Zwietering, M.H.,** 2013. Isolation and quantification of highly acid resistant variants *of Listeria*

*monocytogenes*. Int. J. Food Microbiol. 166, 508–514. doi:10.1016/j.ijfoodmicro.2013.08.011

**Metselaar, K.I., Den Besten, H.M.W., Boekhorst, J., van Hijum, S.A.F.T., Zwietering, M.H., Abee, T.,** 2015. Diversity of acid stress resistant variants *of Listeria monocytogenes* and the potential role of ribosomal protein S21 encoded by *rpsU*. Front. Microbiol. 6, 422. doi:10.3389/fmicb.2015.00422

**Metselaar, K.I., Abee, T., Zwietering, M.H., Den Besten, H.M.W**., 2016. Modeling and validation of the ecological behavior of wild-type *Listeria monocytogenes* and stress-resistant variants. Appl. Environ. Microbiol. 82, 5389–5401. doi:10.1128/AEM.00442-16

**Milohanic, E., Glaser, P., Coppée, J.-Y., Frangeul, L., Vega, Y., Vázquez-Boland, J.A., Kunst, F., Cossart, P., Buchrieser, C.,** 2003. Transcriptome analysis of *Listeria monocytogenes* identifies three groups of genes differently regulated by PrfA. Mol. Microbiol. 47, 1613–1625. doi:10.1046/j.1365-2958.2003.03413.x

**NicAogáin, K., O'Byrne, C.P.,** 2016. The role of stress and stress adaptations in determining the fate of the bacterial pathogen *Listeria monocytogenes* in the food chain. Front. Microbiol. 7, 1865. doi:10.3389/fmicb.2016.01865

**Radoshevich, L., Cossart, P.,** 2018. *Listeria monocytogenes*: towards a complete picture of its physiology and pathogenesis. Nat. Rev. Microbiol. 16, 32–46. doi:10.1038/nrmicro.2017.126

**Seemann, T.,** 2015. Snippy: fast bacterial variant calling from NGS reads. https://github.com/tseemann/snippy

**Smaczniak, C., Immink, R.G.H., Muiño, J.M., Blanvillain, R., Busscher, M., Busscher-Lange, J., Dinh, Q.D.P., Liu, S., Westphal, A.H., Boeren, S., Parcy, F., Xu, L., Carles, C.C., Angenent, G.C., Kaufmann, K.,** 2012. Characterization of MADS-domain transcription factor complexes in *Arabidopsis* flower development. Proc. Natl. Acad. Sci. U.S.A. 109, 1560–1565. doi:10.1073/pnas.1112871109

**Tyanova, S., Temu, T., Sinitcyn, P., Carlson, A., Hein, M.Y., Geiger, T., Mann, M., Cox, J.,** 2016. The Perseus computational platform for comprehensive analysis of (prote)omics data. Nat. Methods 13, 731–740. doi:10.1038/nmeth.3901

**Van Boeijen, I.K.H., Moezelaar, R., Abee, T., Zwietering, M.H.,** 2008. Inactivation kinetics of three *Listeria monocytogenes* strains under high hydrostatic pressure. J. Food Prot. 71, 2007–2013. doi:10.4315/0362-028x-71.10.2007

**Vázquez-Boland, J.A., Kuhn, M., Berche, P., Chakraborty, T., Domínguez-Bernal, G., Goebel, W., González-Zorn, B., Wehland, J., Kreft, J.,** 2001. *Listeria* pathogenesis and molecular virulence determinants. Clin. Microbiol. Rev. 14, 584–640. doi:10.1128/CMR.14.3.584-640.2001

**Walker, B.J., Abeel, T., Shea, T., Priest, M., Abouelliel, A., Sakthikumar, S., Cuomo, C.A., Zeng, Q., Wortman, J., Young, S.K., Earl, A.M.,** 2014. Pilon: an integrated tool for comprehensive microbial variant detection and genome assembly improvement. PLoS One 9, e112963. doi:10.1371/journal.pone.0112963

**Wendrich, J.R., Boeren, S., Möller, B.K., Weijers, D., De Rybel, B.,** 2017. In Vivo identification of plant protein complexes using IP-MS/MS. Methods Mol. Biol. 1497, 147–158. doi:10.1007/978-1-4939-6469-7_14

**Wiśniewski, J.R., Zougman, A., Nagaraj, N., Mann, M.,** 2009. Universal sample preparation method for proteome analysis. Nat. Methods 6, 359–362. doi:10.1038/nmeth.1322

# Supplementary material

Table S4.1: Primers used in construction of *rpsU* mutants
EcoR1 and SalI sites are indicated in bold

| Direction | Gene | Sequence |
|---|---|---|
| Forward | rpsU | 5' -GAAG**GAATTC**CCAGAGAAGGCGAGGATAGTG- 3' |
| Reverse | rpsU | 5'- TGGT**GTCGAC**TCAGCTTTGCCCTTTACTTTAG- '3 |

Table S4.2: Proteins above or below the cutoff in *Listeria monocytogenes* LO28 variant 15 over wild type

| Protein IDs | Protein product | Gene | Locus tag | Regulon | Product | $-\log_{10}$ P value | log ratio |
|---|---|---|---|---|---|---|---|
| IEJ01_03515 | NP_464216.1 | - | lmo0689 | flagella_1 | chemotaxis protein CheV | 5.82 | -3.22 |
| IEJ01_03510 | NP_464215.1 | - | lmo0688 | flagella_1 | hypothetical protein lmo0688 | 7.02 | -3.17 |
| IEJ01_04515 | NP_464416.1 | *rsbS* | lmo0890 | - | negative regulation of sigma-B activity | 7.01 | -2.96 |
| IEJ01_03525 | NP_464218.1 | *cheY* | lmo0691 | flagella_2 | chemotaxis response regulator CheY | 6.49 | -2.85 |
| IEJ01_03530 | NP_464219.1 | *cheA* | lmo0692 | flagella_2 | two-component sensor histidine kinase CheA | 5.58 | -2.82 |
| IEJ01_03590 | NP_464231.1 | - | lmo0704 | - | hypothetical protein lmo0704 | 6.94 | -2.74 |
| IEJ01_03490 | NP_464211.1 | - | lmo0684 | flagella_1 | hypothetical protein lmo0684 | 4.12 | -2.74 |
| IEJ01_03495 | NP_464212.1 | *motA* | lmo0685 | flagella_1 | flagellar motor protein MotA | 5.16 | -2.66 |
| IEJ01_08960 | NP_465224.1 | - | lmo1699 | - | chemotaxis protein | 5.98 | -2.61 |
| IEJ01_01825 | NP_463884.1 | - | lmo0354 | - | fatty-acid--CoA ligase | 7.83 | -2.60 |
| IEJ01_11125 | NP_465650.1 | - | lmo2126 | - | maltogenic amylase | 5.79 | -2.60 |
| IEJ01_05170 | NP_464540.1 | *gbuB* | lmo1015 | - | glycine/betaine ABC transporter permease | 4.61 | -2.43 |
| IEJ01_03500 | NP_464213.1 | *motB* | lmo0686 | flagella_1 | flagellar motor rotation MotB | 5.66 | -2.35 |
| IEJ01_00255 | NP_463584.1 | - | lmo0051 | - | response regulator | 5.95 | -2.27 |
| IEJ01_03635 | NP_464240.1 | *fliF* | lmo0713 | - | flagellar MS-ring protein FliF | 7.96 | -2.23 |
| IEJ01_14350 | NP_466238.1 | *cydC* | lmo2716 | - | ABC transporter | 5.01 | -2.21 |
| IEJ01_04805 | NP_464468.1 | *fri* | lmo0943 | - | non-heme iron-binding ferritin | 4.44 | -2.20 |
| IEJ01_03565 | NP_464226.1 | *fliM* | lmo0699 | - | flagellar motor switch protein FliM | 5.89 | -2.16 |
| IEJ01_03645 | NP_464242.1 | *fliH* | lmo0715 | - | flagellar assembly protein H | 4.61 | -2.10 |
| IEJ01_07370 | NP_464932.1 | *pflC* | lmo1407 | - | pyruvate-formate lyase activating enzyme | 8.61 | -2.02 |
| IEJ01_10065 | NP_465440.1 | - | lmo1916 | - | peptidase | 4.47 | -1.79 |
| IEJ01_07680 | NP_464994.1 | *rpsU* | lmo1469 | - | 30S ribosomal protein S21 | 2.11 | -1.34 |
| IEJ01_04655 | NP_464439.1 | - | lmo0913 | SigB | succinate semialdehyde dehydrogenase | 9.19 | 3.98 |
| IEJ01_07475 | NP_464953.1 | *opuCA* | lmo1428 | SigB | glycine/betaine ABC transporter ATP-binding protein | 4.88 | 3.34 |
| IEJ01_03680 | NP_464249.1 | - | lmo0722 | SigB | pyruvate oxidase | 8.75 | 3.25 |
| IEJ01_09635 | NP_465355.1 | - | lmo1830 | SigB | short-chain dehydrogenase | 5.13 | 3.22 |
| IEJ01_14510 | NP_466270.1 | - | lmo2748 | SigB | hypothetical protein lmo2748 | 3.92 | 3.22 |
| IEJ01_11305 | NP_465681.1 | *sepA* | lmo2157 | SigB | hypothetical protein lmo2157 | 3.99 | 3.19 |
| IEJ01_11585 | NP_465737.1 | - | lmo2213 | SigB | hypothetical protein lmo2213 | 4.27 | 3.16 |
| IEJ01_07465 | NP_464951.1 | *opuCC* | lmo1426 | SigB | glycine/betaine ABC transporter substrate-binding protein | 5.43 | 3.07 |
| IEJ01_00670 | NP_463667.1 | - | lmo0134 | SigB | hypothetical protein lmo0134 | 5.30 | 2.76 |
| IEJ01_12965 | NP_465986.1 | - | lmo2463 | SigB | multidrug transporter | 6.70 | 2.68 |
| IEJ01_02335 | NP_463983.1 | - | lmo0454 | - | hypothetical protein lmo0454 | 4.74 | 2.54 |
| IEJ01_03105 | NP_464135.1 | - | lmo0608 | - | ABC transporter ATP-binding protein | 6.16 | 2.54 |
| IEJ01_07445 | NP_464947.1 | - | lmo1422 | SigB | glycine/betaine ABC transporter permease | 6.59 | 2.50 |
| IEJ01_04045 | NP_464323.1 | - | lmo0796 | SigB | hypothetical protein lmo0796 | 8.22 | 2.49 |
| IEJ01_01390 | NP_463796.1 | - | lmo0265 | SigB | succinyl-diaminopimelate desuccinylase | 5.00 | 2.41 |
| IEJ01_03985 | NP_464311.1 | - | lmo0784 | SigB | PTS mannose transporter subunit IIB | 4.70 | 2.39 |
| IEJ01_03395 | NP_464192.1 | - | lmo0665 | - | hypothetical protein lmo0665 | 5.60 | 2.37 |
| IEJ01_04155 | NP_464345.1 | - | lmo0818 | - | cation-transporting ATPase | 5.40 | 2.35 |
| IEJ01_08935 | NP_465219.1 | - | lmo1694 | SigB | CDP-abequose synthase | 5.61 | 2.34 |
| IEJ01_13525 | NP_466096.1 | - | lmo2573 | SigB | zinc-binding dehydrogenase | 6.02 | 2.31 |
| IEJ01_02115 | NP_463940.1 | - | lmo0411 | - | phosphoenolpyruvate synthase | 7.49 | 2.30 |
| IEJ01_02960 | NP_464107.1 | - | lmo0579 | SigB | hypothetical protein lmo0579 | 6.43 | 2.26 |
| IEJ01_01435 | NP_463805.1 | - | lmo0274 | SigB | hypothetical protein lmo0274 | 6.38 | 2.07 |
| IEJ01_02640 | NP_464043.1 | - | lmo0515 | SigB | hypothetical protein lmo0515 | 4.89 | 1.99 |
| IEJ01_08000 | NP_465057.1 | *ruvB* | lmo1532 | - | Holliday junction DNA helicase RuvB | 4.85 | 1.91 |
| IEJ01_03340 | NP_464181.1 | - | lmo0654 | SigB | hypothetical protein lmo0654 | 3.71 | 1.88 |
| IEJ01_12755 | NP_465944.1 | - | lmo2421 | - | two-component sensor histidine kinase | 5.57 | 1.88 |
| IEJ01_03865 | NP_464287.1 | - | lmo0760 | - | hypothetical protein lmo0760 | 3.17 | 1.63 |
| IEJ01_02760 | NP_464067.1 | - | lmo0539 | SigB | tagatose 1,6-diphosphate aldolase | 3.42 | 1.48 |

Table S4.3: Proteins above or below the cutoff in *Listeria monocytogenes* LO28 variant 15EV1 over wild type

| Protein IDs | Protein product | Gene | Locus tag | Regulon | Product | $-\log_{10}$ P value | log ratio |
|---|---|---|---|---|---|---|---|
| IEJ01_08375 | NP_465131.1 | - | lmo1606 | sigB | DNA translocase | 5.97 | -2.25 |
| IEJ01_14350 | NP_466238.1 | *cydC* | lmo2716 | - | ABC transporter | 5.01 | -2.21 |
| IEJ01_06615 | NP_464782.1 | - | lmo1257 | - | hypothetical protein lmo1257 | 10.09 | 2.74 |
| IEJ01_09215 | NP_465274.1 | - | lmo1749 | - | shikimate kinase | 5.39 | 2.02 |
| IEJ01_06660 | NP_464791.1 | - | lmo1266 | - | hypothetical protein lmo1266 | 6.10 | 1.98 |
| IEJ01_01400 | NP_463798.1 | - | lmo0267 | - | hypothetical protein lmo0267 | 6.93 | 1.81 |
| IEJ01_08250 | NP_465107.1 | - | lmo1582 | - | hypothetical protein lmo1582 | 3.61 | 1.77 |
| IEJ01_13180 | NP_466028.1 | *spl* | lmo2505 | - | peptidoglycan lytic protein P45 | 6.70 | 1.70 |
| IEJ01_14455 | NP_466259.1 | - | lmo2737 | - | LacI family transcriptional regulator | 6.92 | 1.44 |
| IEJ01_03915 | NP_464297.1 | - | lmo0770 | - | LacI family transcriptional regulator | 5.16 | 1.43 |

Table S4.4: Proteins above or below the cutoff in *Listeria monocytogenes* LO28 variant 15EV2 over wild type

| Protein IDs | Protein product | Gene | Locus tag | Regulon | Product | - log P-value | log ratio |
|---|---|---|---|---|---|---|---|
| IEJ01_04915 | NP_464490.1 | - | lmo0965 | - | hypothetical protein lmo0965 | 6.02 | -1.81 |
| IEJ01_06615 | NP_464782.1 | - | lmo1257 | - | hypothetical protein lmo1257 | 4.59 | 2.61 |
| IEJ01_02935 | NP_464102.1 | - | lmo0574 | - | beta-glucosidase | 5.61 | 2.43 |
| IEJ01_04655 | NP_464439.1 | - | lmo0913 | SigB | succinate semialdehyde dehydrogenase | 6.65 | 2.30 |
| IEJ01_14510 | NP_466270.1 | - | lmo2748 | SigB | hypothetical protein lmo2748 | 5.21 | 2.19 |
| IEJ01_04155 | NP_464345.1 | - | lmo0818 | - | cation-transporting ATPase | 6.48 | 2.18 |
| IEJ01_09625 | NP_465353.1 | - | lmo1828 | - | hypothetical protein lmo1828 | 4.72 | 2.06 |
| IEJ01_03445 | NP_464202.1 | - | lmo0675 | flagella_1 | hypothetical protein lmo0675 | 7.53 | 2.05 |
| IEJ01_07475 | NP_464953.1 | *opuCA* | lmo1428 | SigB | glycine/betaine ABC transporter ATP-binding protein | 5.50 | 2.02 |
| IEJ01_03615 | NP_464236.1 | - | lmo0709 | - | hypothetical protein lmo0709 | 4.02 | 1.98 |
| IEJ01_08250 | NP_465107.1 | - | lmo1582 | - | hypothetical protein lmo1582 | 4.82 | 1.96 |
| IEJ01_07170 | NP_464893.1 | *recN* | lmo1368 | - | DNA repair protein | 5.24 | 1.92 |
| IEJ01_09235 | NP_465278.1 | - | lmo1753 | - | lipid kinase | 7.33 | 1.91 |
| IEJ01_03680 | NP_464249.1 | - | lmo0722 | SigB | pyruvate oxidase | 4.95 | 1.86 |
| IEJ01_07825 | NP_465023.1 | - | lmo1498 | - | O-methyltransferase | 5.29 | 1.84 |
| IEJ01_06660 | NP_464791.1 | - | lmo1266 | - | hypothetical protein lmo1266 | 8.12 | 1.84 |
| IEJ01_12275 | NP_465867.1 | - | lmo2344 | - | hypothetical protein lmo2344 | 4.27 | 1.82 |
| IEJ01_08705 | NP_465197.1 | *menE* | lmo1672 | - | O-succinylbenzoic acid--CoA ligase | 4.83 | 1.79 |
| IEJ01_00260 | NP_463585.1 | - | lmo0052 | - | hypothetical protein lmo0052 | 3.83 | 1.72 |
| IEJ01_07925 | NP_465042.1 | - | lmo1517 | - | nitrogen regulatory PII protein | 4.13 | 1.61 |
| IEJ01_03865 | NP_464287.1 | - | lmo0760 | - | hypothetical protein lmo0760 | 4.53 | 1.14 |

Table S4.5: Maximum growth rates of *Listeria monocytogenes* LO28 WT, variants and constructed mutants.

| Strain | Maximum growth rate | SD |
|---|---|---|
| LO28 WT | 1.07 | 0.01 |
| LO28 Variant 15 | 0.78 | 0.05 |
| LO28 15EV1 | 1.04 | 0.03 |
| LO28 15EV2 | 0.92 | 0.03 |
| LO28 RpsUArg17Pro | 0.82 | 0.03 |
| LO28 RpsUArg17His | 1.03 | 0.03 |
| LO28 RpsUArg17Thr | 0.96 | 0.03 |
| EGDe WT | 1.1 | 0.02 |
| EGDe RpsUArg17Pro | 0.86 | 0.01 |


Figure S4.1: Predicted turn in *Listeria monocytogenes* LO28 RpsU. Secondary structure of the RpsU protein as predicted by the Chou and Fasman secondary structure prediction server (http://www.biogem.org/tool/chou-fasman/). The turn predicted by insertion of a proline residue at position 17 is shown in blue.

# 5

# Ribosomal mutations enable a switch between high fitness and high stress resistance in *Listeria monocytogenes*

Jeroen Koomen, Xuchuan Ma, Alberto Bombelli, Marcel H. Tempelaars, Sjef Boeren, Marcel H. Zwietering, Heidy M.W. den Besten, and Tjakko Abee

## Abstract

Multiple stress resistant variants of *Listeria monocytogenes* with mutations in *rpsU* encoding ribosomal protein RpsU have previously been isolated after a single exposure to acid stress. These variants, including *L. monocytogenes* LO28 variant 14 with a complete deletion of the *rpsU* gene, showed upregulation of the general stress sigma factor Sigma B-mediated stress resistance, and had a lower maximum specific growth rate than the LO28 WT, signifying a trade-off between stress resistance and fitness. In the current work we have subjected variant 14 to an experimental evolution regime, selecting for higher fitness in two parallel evolving cultures. This resulted in two evolved variants with WT-like fitness: 14EV1 and 14EV2. Comparative analysis of growth performance, acid and heat stress resistance, in combination with proteomics and RNA-sequencing, indicated that in both lines reversion to WT-like fitness also resulted in WT-like stress sensitivity, due to lack of Sigma B-activated stress defence. Notably, genotyping of 14EV1 and 14EV2 provided evidence for unique point-mutations in the ribosomal *rpsB* gene causing amino acid substitutions at the same position in RpsB, resulting in RpsB$^{22Arg\text{-}His}$ and RpsB$^{22Arg\text{-}Ser}$, respectively. Combined with data obtained with constructed RpsB$^{22Arg\text{-}His}$ and RpsB$^{22Arg\text{-}Ser}$ mutants in the variant 14 background, we provide evidence that loss of function of RpsU resulting in the multiple stress resistant and reduced fitness phenotype, can be reversed by single point mutations in *rpsB* leading to arginine substitutions in RpsB at position 22 into histidine or serine, resulting in WT-like high fitness and low stress resistance phenotype. This demonstrates the impact of genetic changes in *L. monocytogenes*' ribosomes on fitness and stress resistance.

## Introduction

*Listeria monocytogenes* is a foodborne pathogen that can cause the infrequent but deadly disease listeriosis (Toledo-Arana et al., 2009). *L. monocytogenes* is generally considered to be a robust microorganism, capable of growing in and surviving a wide range of adverse conditions such as low pH, low temperature and low $a_w$ (NicAogáin and O'Byrne, 2016). Microbial populations are innately heterogenous, which contributes to the spread of *L. monocytogenes* in different environmental niches, from soil to man (Abee et al., 2016; Maury et al., 2016). When a population of cells is exposed to stress, population heterogeneity can lead to the differential survival of a subset of cells, resulting in tailing of the inactivation curve. Previously, Metselaar et al. (2015) described stress resistant *L. monocytogenes* variants, acquired after a single exposure to acid stress, with a mutation in the ribosomal *rpsU* gene, encoding small ribosomal protein 21. Additional genotypic and phenotypic studies focussed on variant 14 with a deletion that covers the entire *rpsU* gene, as well as *yqeY* and half of *phoH*; and on variant 15 that harbours a point mutation in *rpsU* resulting in an amino acid substitution from arginine to proline in the RpsU protein, $RpsU^{17Arg\text{-}Pro}$ (Koomen et al., 2018). Gene expression data of *L. monocytogenes* LO28 wildtype (WT) and multiple-stress resistant variants 14 and 15 revealed an upregulation of 116 genes (Koomen et al., 2018), including a large fraction of genes controlled by the alternative stress sigma factor SigB, which are known to be involved in providing multiple-stress resistance (Liu et al., 2019).

In a follow-up study (Koomen et al., 2021), we subjected *L. monocytogenes* LO28 variant 15, with its single $RpsU^{17Arg\text{-}Pro}$ point mutation, to an experimental evolution protocol where we selected for increased fitness, defined as a higher maximum specific growth rate ($\mu_{max}$) compared to variant 15. Both evolved variants fixed mutations in *rpsU* (resulting in $RpsU^{17Pro\text{-}His}$ and $RpsU^{17Pro\text{-}Thr}$), and reverted back to WT-like high maximum specific growth rate and relative low stress resistance. The potentially disruptive effect of random insertion of a proline residue is known to alter the stability or function of proteins (Chou and Fasman, 1974). Consequently, we hypothesized that replacing the putative disruptive proline at position 17 in *L. monocytogenes* variant 15 with amino acids that do not have such strong disruptive effects, i.e., threonine or histidine, can restore WT-like functioning of the RpsU protein with originally an arginine at position 17. This was confirmed by targeted mutants in *L. monocytogenes* LO28 and type strain EGDe, showing that single amino acid substitutions in RpsU enabled *L. monocytogenes* to switch between high fitness-low stress

resistance and low fitness-high stress resistance.

This raised the follow-up question whether and how variant 14 could switch between low fitness-high stress resistance and high fitness-low stress resistance, since the whole *rpsU* gene is deleted and thus the known route to WT-like fitness and stress sensitivity via a single point mutation in *rpsU* is effectively blocked. Therefore, in the current study we subjected variant 14 to an experimental evolution regime and used a complementary genotypic, proteomic and phenotypic approach to evaluate how ribosomal mutations in *L. monocytogenes* enable a switch between fitness and stress resistance.

## Materials and methods

### Bacterial strains and culture conditions

*Listeria monocytogenes* LO28 wild type (WT) from the strain collection of Wageningen Food & Biobased Research, The Netherlands, and stress resistant ancestor variant 14 (Koomen et al., 2018; Metselaar et al., 2013), and evolved variants (this study) were used for all genotypic, proteomic and phenotypic analyses. All cultures were grown as described elsewhere (Metselaar et al., 2013). In brief, cells from -80°C stocks were incubated at 30°C for 48 hours on brain heart infusion (BHI, Oxoid, Hampshire), supplemented with agar (1.5 % [w/w], bacteriological agar no. 1 Oxoid, Hampshire). A single colony was used for inoculation of 20 ml of BHI broth in a 100 ml Erlenmeyer flask (Fisher, USA). After overnight (ON, 18-22 hours) growth at 30°C under shaking at 160 rpm, (Innova 42, New Brunswick Scientific, Edison, NJ) 0.5% (v/v) inoculum was added to fresh BHI broth. Cells were grown under constant shaking at 160 rpm in BHI at 30°C until the late-exponential growth phase ($OD_{600}$ = 0.4-0.5).

### Experimental evolution

Experimental evolution was performed as described in Koomen et al. (2021). Briefly, we inoculated two parallel lines with 1% (v/v) of ON culture of *L. monocytogenes* LO28 variant 14 in 20 ml BHI broth in 100 ml Erlenmeyer flasks. The cultures were then incubated for 24 hours at 20°C with continuous shaking at 160 rpm (Innova 42, New Brunswick Scientific, Edison, NJ). For each parallel line, 44 consecutive transfers were made from 24 hours-cultures, where 1% (v/v) inoculum was used to inoculate fresh BHI, resulting in about 290 generations for each of the two evolution lines. From every second transfer, a 700 µl culture sample was taken, mixed with glycerol (Sigma, 25% v/v final concentration), flash frozen in liquid nitrogen, and stored at -80°C, resulting in 22 stocks for both evolution lines. These

stocks were revived by streaking on BHI-agar plates, from which a single colony was used to inoculate 20 ml of BHI broth in a 100 ml Erlenmeyer flask. After ON culturing at 30°C with shaking at 160 rpm, the culture was diluted 100,000 times in fresh BHI broth, and 200 µl of culture was inoculated in duplicate in wells of a honeycomb plate. The plate was incubated in a Bioscreen C (Oy growth Curves AB Ltd, Helsinki, Finland) at 30°C and the respective growth curves were determined by measuring $OD_{600}$ over time. All growth experiments were performed with biologically independent triplicates. Stock number 14 of the first evolution line and stock number 22 of the second evolution line were streaked on BHI agar, and respective single colonies were selected to prepare -80°C stocks of 14EV1 and 14EV2.

### Estimation of $\mu_{max}$

The maximum specific growth rate $\mu_{max}$ ($h^{-1}$) was determined at 30°C for the two evolved strains (14EV1 and 14EV2), variant 14 and the *Listeria monocytogenes* LO28 WT, following the procedure as described previously by (Biesta-Peters et al., 2010), and Koomen et al. (2021). This method is based on the time-to-detection (TTD) of five serially diluted cultures of which the initial bacterial concentration is known. In this setup $\mu_{max}$ equals ln(2)/generation time (i.e., $\mu_{max}$ = 1 represents a generation (doubling) time of approximately 0.7 h, or 42 minutes). Three biologically independent experiments were performed to estimate the mean and standard deviation of $\mu_{max}$.

### Inactivation kinetics at low pH

Acid inactivation experiments were performed as described previously (Metselaar et al., 2013). Briefly, 100 ml of late-exponential phase culture was pelleted in a fixed-angle rotor (5804 R, Eppendorf) for 5 minutes at 2,880 x *g*. Pellets were washed using 10 ml BHI broth, and pelleted again at 5 min at 2,880 x *g*. The pellet was resuspended in 1 ml PPS that was pre-warmed to 37°C and adjusted to pH 3.0 using 10 M of HCl, and placed in a 100 ml Erlenmeyer flask in a shaking water bath at 37°C. At appropriate time intervals, samples were taken, decimally diluted in BHI broth and plated on BHI agar using an Eddy Jet spiral plater (Eddy Jet, IUL S.A.) Plates were incubated at 30°C for 4 to 6 days for full recovery of damaged cells. Data of at least three biologically independent experiments were used for analysis.

### Inactivation kinetics at high temperature

Heat inactivation experiments were performed as described before (Metselaar et al., 2015). Briefly, 400 µl of late-exponential phase culture was added to 40 ml of fresh BHI broth that was pre-heated to 55°C ± 0.3°C. For the determination of the initial microbial concentration, a separate Erlenmeyer with BHI at room temperature was used. Samples were taken after various timepoints, and were decimally diluted in Peptone Physiological Salt (PPS). Appropriate dilutions were plated on BHI agar using an Eddy Jet spiral plater and incubated at 30°C for 4-6 days. Combined data of at least three biologically independent experiments were used for analysis.

### Proteomic analysis

Proteomic analysis was performed on late-exponentially growing cells ($OD_{600}$ between 0.4-0.5) of variant 14 and evolved variants 14EV1 and 14EV2 as described before (Koomen et al., 2021). Briefly, 2 ml of late-exponentially growing cells ($OD_{600}$ of 0.4-0.5) cultures of the LO28 WT, variant 14 and evolved 14EV1 and 14EV2 were flash frozen in liquid nitrogen and stored. Samples were, thawed on ice, pelleted at 17,000 x *g*, and subsequently washed twice with 100 mM Tris (pH 8). Resuspended pellets were sonicated and samples were prepared according to the filter assisted sample preparation protocol (FASP) (Wiśniewski et al., 2009). Each prepared peptide sample was analysed by injecting (18 µl) into a nanoLC-MS/MS (Thermo nLC1000 connected to an LTQ-Orbitrap XL) as described previously (Lu et al., 2011; Wendrich et al., 2017). nLC-MSMS system quality was checked with PTXQC (Bielow et al., 2016) using the MaxQuant result files. LCMS data with all MS/MS spectra were analysed with the MaxQuant quantitative proteomics software package (Cox et al., 2014) as described before (Smaczniak et al., 2012; Wendrich et al., 2017). Filtering and further bioinformatics and statistical analysis of the MaxQuant ProteinGroups file was performed with Perseus. Proteins were considered Differentially Expressed (DE) if the $\log_{10}$ transformed ratio of variant over WT ($\log_{10}$ ratio) was below -1 or above 1, with a negative $\log_{10}$ transformed Benjamini–Hochberg corrected P value (-$\log_{10}$ P value) above 2. The mass spectrometry proteomics data have been deposited to the ProteomeXchange Consortium via the PRIDE (Vizcaíno et al., 2016) partner repository with the dataset identifier PXD022732.

### SNP analysis of evolved variants

Ancestor variant 14 and evolved variants 14EV1 and 14EV2 obtained in the evolution experiment were sequenced using Illumina chemistry as described before (Koomen et al., 2021). Briefly, cells were pelleted, and resuspended in 450 µl DNA/RNA Shield (Zymo Research) at 4°C until DNA extraction. The DNA was extracted by BaseClear (Leiden, the Netherlands) and paired-end 2 × 150bp short-reads were generated using a Nextera XT library preparation (Illumina). A NovaSeq 6000 system (Illumina) was used to generate paired-end reads. Raw reads were trimmed and de novo assembled using CLC Genomics Workbench v 10.0 (Qiagen, Hilden, Germany). SNIPPY 3.2 (Seemann, T 2015), and Pilon using the "--changes" argument (Walker et al., 2014) were used for SNP analysis of evolved variants against the LO28 WT as reference.

### Mutant construction

Mutant strains 14RpsB$^{22Arg\text{-}His}$ and 14RpsB$^{22Arg\text{-}Ser}$ were constructed in the variant 14 genetic background using the temperature sensitive suicide plasmid pAULA (Chakraborty et al., 1992). The *rpsB* gene from either variant 14EV1 or 14EV2 was amplified from genomic DNA by KAPA HiFi Hotstart ReadyMix (KAPA Biosystems, USA), using the primers listed in Supplementary Table S5.1. The resulting fragments were ligated in frame to the pAULA multiple cloning site via EcoR1 and Sal1 restriction that were introduced to the fragments by the respective primers. The resulting plasmid was electroporated (2.5 kV, 25 µF, 200 Ω), in a 0.2 cm cuvette using a BIO-RAD GenePulser, to the appropriate *L. monocytogenes* cells, and plated on BHI agar at 30°C with 5 µg/ml erythromycin to select for transformants.

Two erythromycin resistant colonies per construct were inoculated in separate tubes in BHI broth supplemented with 5 µg/ml erythromycin and grown overnight at 42°C to select for plasmid integration. Selected strains resulting from a single cross-over integration event were grown overnight in BHI at 30°C to induce double crossover events and were subsequently plated at 30°C. Resulting colonies were replica plated on BHI with and without 5 µg/ml erythromycin and incubated at 30°C. Colonies sensitive to erythromycin were selected. PCR using the primers listed in Supplementary Table S5.1 and subsequent DNA sequencing of the products (BaseClear B.V. Leiden, The Netherlands) of erythromycin sensitive colonies confirmed the correct point mutation in the respective genes and the lack of additional mutations in the targeted region.

**RNA-sequencing**

Total RNA was isolated from late-exponentially growing cells ($OD_{600}$ between 0.4-0.5) of variant 14 and evolved variants 14EV1 and 14EV2. Briefly, 100 ml of late-exponential phase culture was pelleted for 1 min at room temperature (RT) at 11,000 × *g* in a fixed-angle rotor (5804 R, Eppendorf). The pellet was resuspended in TRI-reagent (Ambion) in a beat-beater tube (lysing agent A) by vortexing and tubes were snap frozen in liquid nitrogen until use. Cells were disrupted using a beat-beater (MP Fast Prep-24, MP Biomedicals GmbH, Eschwege, Germany) set at 6 m/s for 4 times 20 seconds with two minutes of intermittent air cooling per cycle. Twenty percent of the starting volume of chloroform was added, mixed and incubated at RT for 10 min. Subsequently, samples were centrifuged at 17,000 x *g* and 4°C for 15 min. The upper aqueous phase (approximately 700 µl) was transferred to an RNase free Eppendorf tube, where 600 µl of isopropanol was added, mixed and incubated at RT for 10 min. Next, the samples were centrifuged at 17,000 x *g* and 4°C for 15 min. The pellet was washed with 700 µl of ice-cold 75% ethanol, after which the pellet was centrifuged again at 17,000 x *g* for 5 min at 4°C. The pellet was resuspended in 90 µl of nuclease-free water and incubated at 60°C for 2 minutes to finalize RNA isolation. RNA integrity was checked using gel electrophoresis, after which the RNA was stored by adding 0.1 volume of 3M sodium acetate at pH 5.2 with 2.5 volumes of ethanol absolute, and kept at −80°C. Before shipping the samples were centrifuges at 13,000 x *g* and 4°C for 10 minutes, and the supernatant was removed. The pellet was washed with 80% ethanol, and centrifuged again at 13,000 x *g* and 4°C for 10 minutes. After removal of the supernatant and air drying, the RNA was dissolved in 90 µl of nuclease-free water, and shipped on dry ice. Ribo-Zero rRNA depletion, and the generation of paired-end reads using a MiSeq system was done by BaseClear B.V. (Leiden, The Netherlands). QC and read mapping against the LO28 reference genome (NCBI accession: PRJNA664298) was performed via in-house methods, by BaseClear. Counting of reads was done by htseq-count (version 0.11.1) (Anders et al., 2015). Differential expression (DE) analysis was performed using the DEseq2 package (version 1.24.0) in the statistical programming language R (version 3.6.0). Genes were considered DE if $\log_2$ Fold Change ($\log_2$FC) was below -1.58 or above 1.58, with a Benjamini–Hochberg corrected P value below 0.01.

### Statistical testing

Hypothesis testing, comparing respective $\mu_{max}$ and log microbial counts, was performed in the statistical programming language R (version 3.6.0) using the t.test() and var.test() functions.

## Results

### Growth kinetics of evolved variants

The experimental evolution regime was set up using two parallel cultures of *L. monocytogenes* LO28 variant 14. After 28 and 44 daily transfers, implicating ~186 and ~292 generations, respectively, this regime resulted in the selection of two evolved variants, 14EV1 and 14EV2, that showed different growth kinetics compared to the ancestor variant 14 (Figure 5.1a). The $\mu_{max}$ of both evolved variants was significantly higher than that of variant 14, but just significantly lower than the $\mu_{max}$ of the original LO28 WT strain (Figure 5.1b). This indicated that the fitness of the evolved variants was increased compared to the ancestor variant 14 and almost similar to that of the WT strain.

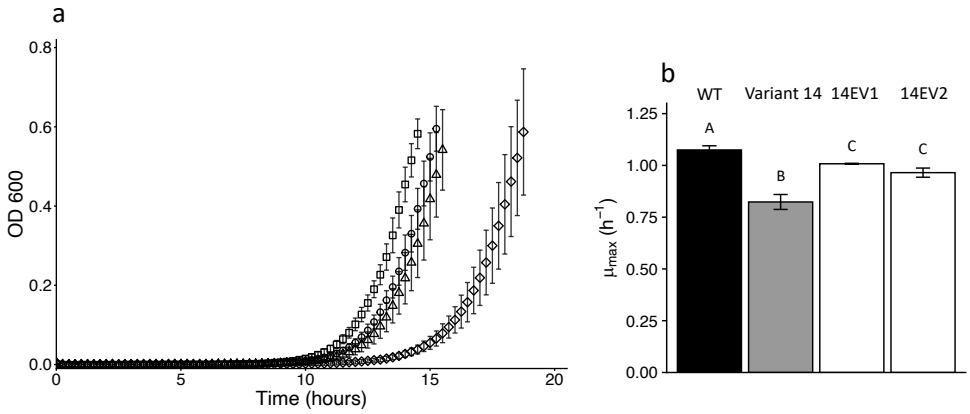


***Figure 5.1:*** *Growth performance of* L. monocytogenes *LO28 WT, variant 14, 14EV1, and 14EV2 (a) growth curves for LO28 WT (squares), variant 14 (diamonds), 14EV1 (circles), and 14EV2 (triangles), (b) Maximum specific growth rates* ($\mu_{max}$) *for* L. monocytogenes *LO28 WT, variant 14, 14EV1, and 14EV2. Different capital letters show statistically significant differences.*

**Multiple-stress resistance of evolved variants**

Since the evolved variants 14EV1 and 14EV2 showed increased fitness, we compared their heat and acid stress resistance to that of variant 14 (Figure 5.2). In the heat stress experiments (Figure 5.2a), variant 14 started with approximately 6.8 log cfu/ml, and showed little inactivation after 20 minutes of exposure, with a concentration of around 6 log cfu/ml. In contrast, after 20 minutes of exposure the concentrations of both evolved variants 14EV1 and 14EV2 decreased and were not significantly different from the LO28 WT strain with concentrations of around 2.5 log cfu/ml. For acid stress experiments (Figure 5.2b), variant 14 again only showed a small (< 1.0 log cfu/ml) decrease in cell counts after 20 minutes, while both evolved variants and also the LO28 WT strain showed more than 5 log cfu/ml reduction after 20 minutes. These data indicated that both evolved variants 14EV1 and 14EV2 lost their high resistance to heat stress and acid stress when compared to variant 14.

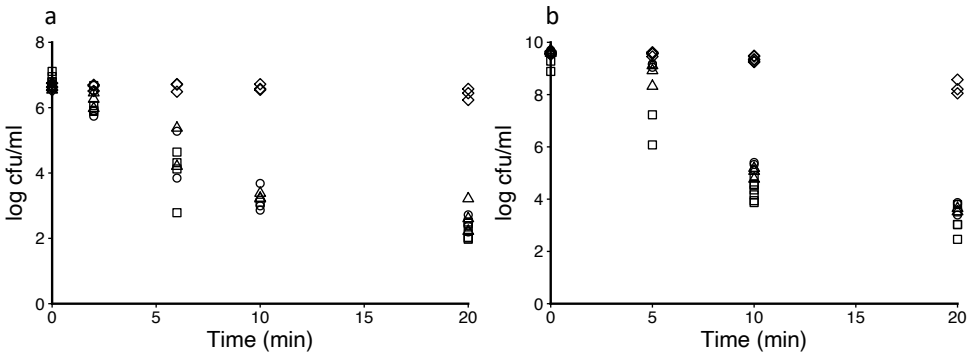


***Figure 5.2:*** *Survival of* L. monocytogenes *LO28 WT, variant 14, 14EV1, and 14EV2 after exposure to heat (55°C) (a) or acid stress (pH 3.0) (b). The wild type is represented by squares, variant 14 by diamonds, and variants 14EV1 and 14EV2, are represented by circles and triangles respectively.*

## Proteomic analysis of WT and variants 14, 14EV1, and 14EV2

Comparative analysis of proteomes of late-exponential phase cells of *L. monocytogenes* LO28 WT, variant 14 and evolved variants 14EV1 and 14EV2 showed significant differences for variant 14 compared to WT, and evolved (Figure 5.3). The proteomics analysis revealed that 28 proteins were significantly higher expressed in variant 14 compared to LO28 WT, of which 27 proteins belonged to the SigB regulon (Figure 5.3). Upregulated proteins included the general stress marker Ctc (lmo0211) (Ferreira et al., 2004; Kazmierczak et al., 2003;

Oliver et al., 2010; Raengpradub et al., 2008), and subunits of the known OpuC glycine betaine osmolyte transporter, OpuCA (lmo1428) and OpuCC (lmo1426). SigB (lmo0895) itself was upregulated, but did not pass the stringent cut-off values applied to the proteomics data (>1 or <-1 $\log_{10}$ FC, with adjusted $-\log_{10}(P) < 2$). See supplementary Table S5.2-S5.4 for a full overview.

Comparative proteome analysis identified in total 16 proteins that were downregulated in variant 14 compared to the WT. In line with previously obtained gene expression data and the non-motile phenotype of variant 14 (Koomen et al., 2018), 7 of these 16 downregulated proteins are involved in motility and chemotaxis, such as MotA (lmo0685), MotB (lmo0686), CheA (lmo0692), and chemotaxis response regulators CheY (lmo0691), and CheV (lmo0689). Notably, RsbS (lmo0890), one of the main components of the stressosome "signal integration hub" (Guerreiro et al., 2020) was approximately 67-fold downregulated ($\log_{10}$ FC -1.83, adjusted -log(P) > 2) in variant 14 compared to the WT, 14EV1 and 14EV2 (see supplementary Table S5.7).

These results indicated that in line with the return to WT-like growth kinetics of 14EV1 and 14EV2, the proteomic profiles of the two evolved variants were highly similar to that of the WT. Only four and five proteins were differentially expressed in 14EV1 and 14EV2 compared to the WT, respectively, including one protein that is part of the SigB regulon, lmo0110; lipase) (see Figure 5.3, and supplementary Tables S5.3-S5.4).

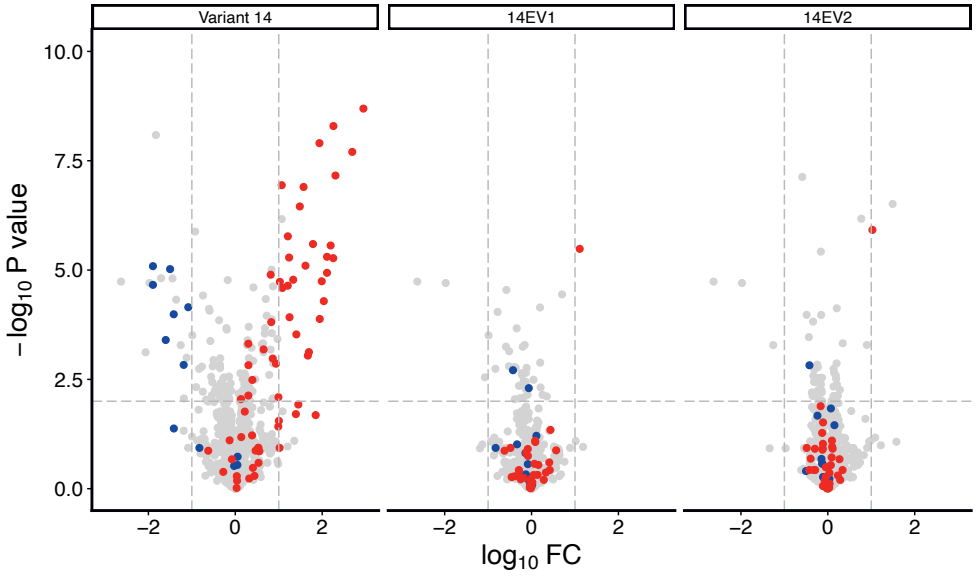


***Figure 5.3:*** *Volcano plot of significantly differentially abundant proteins of* L. monocytogenes *variant 14, 14EV1, and 14EV2 compared to the wild type. The* $-log_{10}$ *(Benjamini–Hochberg corrected P value) is plotted against the* $log_{10}$ *FC (fold change: Variant over WT). Horizontal dotted line represents the cutoff for* $-log_{10}$ *(P), vertical dotted lines represent* $log_{10}$*(fold change) cutoff. Red dots indicate proteins regulated by SigB; blue dots indicate proteins involved in motility. The expression of individual proteins is listed in Tables S1 - S3.*

RNAseq data were line with the observed differences in proteomes of ancestor variant 14 compared to that of the WT, 14EV1 and 14EV2. Due to the higher sensitivity of our RNA-seq approach, we found 106 genes belonging to the SigB regulon as significantly upregulated in variant 14 when compared to the WT (supplementary Table S5.5-S5.7). This is in line with the 70% upregulation of the SigB regulon we reported previously based on DNA-micro array data (Koomen et al., 2018). The upregulated genes included of all *opuCABCD* genes, (lmo1425-1428), glutamate decarboxylase (lmo2434), and *spxA* (ArsC family transcriptional regulator (lmo2191). Other genes considered upregulated in the RNA-seq analyses included the virulence regulator *prfA* (lmo0200), and *inlA* (lmo0433) and *inlB* (lmo0434) that encode internalin A and B involved in human epithelial cell adhesion. Genes *sigB* and *rsbX*, (serine

phosphatase; indirect negative regulation of sigma B dependent gene expression) were upregulated in variant 14, but not in WT and in 14EV1 and 14EV2 (see supplementary Table S5.8 for an overview of differentially expressed genes in the stressosome). In addition, for variant 14, both RNA-seq and proteome analysis indicate (slight) upregulation of anti-anti sigma factor *rsbV* (lmo0893) and *rsbX* (lmo0896) (see Supplementary Tables S7 and S8). Notably, the RNAseq analyses did not show a significant difference in expression of *rsbS* between the four strains. This suggests that the observed low RsbS level in variant 14 is due to posttranslational regulation (supplementary Table S5.8).

### Whole genome sequencing of 14EV1 and 14EV2

Since variant 14 lacks the *rpsU* gene, single or multiple compensatory mutations could be expected in 14EV1 and 14EV2. Strikingly, whole genome sequencing of 14EV1 and 14EV2 revealed that both evolved lines only fixed a single nonsynonymous mutation. Both evolved variants fixed this mutation in another ribosomal protein, ribosomal protein S2 (RpsB). In the *rpsB* gene of line 14EV1, the Guanine on position 65 mutated to Adenine (codon CGT to CAT), leading to an amino acid change from Arginine to Histidine on position 22 of RpsB ($RpsB^{22Arg\text{-}His}$), while in 14EV2, the Cytosine on position 64 (codon CGT to AGT) mutated into Adenine, resulting in a substitution from Arginine to Serine in codon 22 resulting in $RpsB^{22Arg\text{-}Ser}$. Proteomic analysis revealed no significant shifts in the levels of RpsB in variant 14 compared to WT, and also no significant shifts were observed in the levels of $RpsB^{22Arg\text{-}His}$ and $RpsB^{22Arg\text{-}Ser}$ in the evolved variants compared to the WT. Combining these results suggests that short term evolution experiments selecting for enhanced fitness, resulted in the isolation of 14EVs with mutations in *rpsB* to compensate for reduced fitness resulting from the loss of *rpsU*.

### Fitness and stress resistance of constructed mutants

To assess the effect of the substitutions that were selected during experimental evolution, we introduced $RpsB^{22Arg\text{-}His}$ and $RpsB^{22Arg\text{-}Ser}$ into the variant 14 genetic background. We measured $\mu_{max}$ as a proxy for fitness, and found that both constructed mutants of variant 14 had indeed a maximum specific growth rate that was significantly higher than that of variant 14. With that of variant 14 carrying the $RpsB^{22Arg\text{-}His}$ mutation significantly lower than that of LO28 WT ($P < 0.001$), while that of variant 14 carrying $RpsB^{22Arg\text{-}Ser}$ was not significantly different from the LO28 WT (Figure 5.4). Subsequently, we tested the stress response of these constructed mutants, by exposure to heat (55°C, Figure 5.5a), and acid

stress (pH 3, Figure 5.5b). As expected, both constructed mutants were significantly less resistant to heat and acid stress after 20 minutes of exposure compared to variant 14 ($P < 0.05$), although their resistance was still higher than LO28 WT at this timepoint.

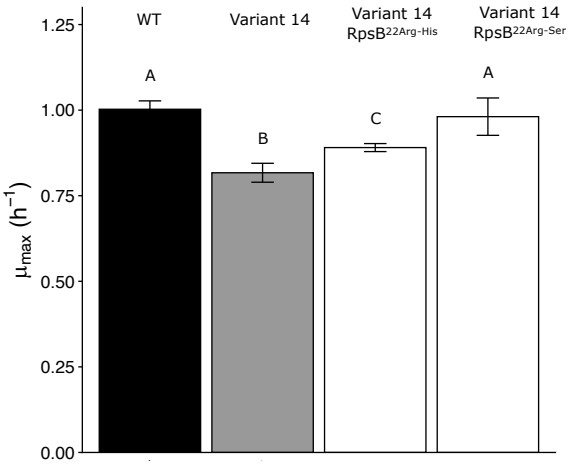


***Figure 5.4:*** *Maximum specific growth rates ($\mu_{max}$) for* L. monocytogenes *LO28 WT, variant 14, and constructed mutants. Different capital letters show statistically significant differences.*

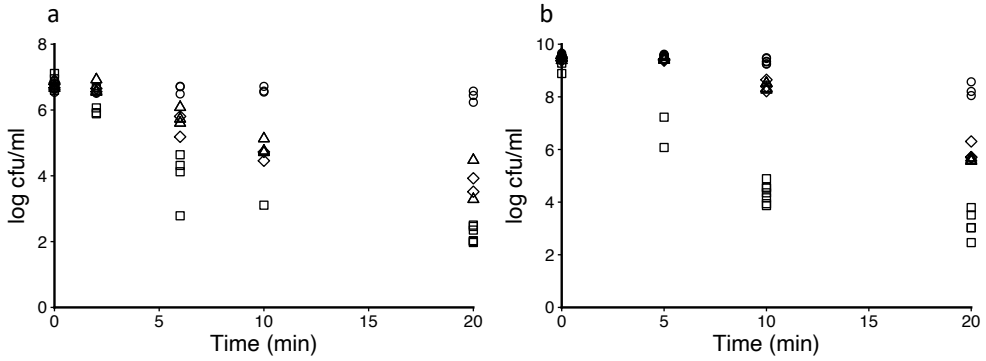


***Figure 5.5:*** *Survival of* L. monocytogenes *LO28 WT, and constructed mutants, during heat (55°C) (a) or acid (pH 3.0) (b) stress. LO28 WT is represented by squares, variant 14 is represented by circles, mutant of variant 14 with RpsB*$^{22Arg\text{-}His}$ *is represented by triangles, mutant of variant 14 with RpsB*$^{22Arg\text{-}Ser}$ *is represented by diamonds.*

## Discussion

Previously, we described multiple stress resistance in *L. monocytogenes* LO28 variants 14 and 15 after a single exposure to acid stress (Koomen et al., 2018). We linked stress resistance in variants 14 and 15 with a complete gene deletion, or point mutation in *rpsU* respectively, to induction of the SigB regulon, and showed the correlation between increased stress resistance and reduced fitness. By using experimental evolution to select for increased fitness in variant 15 in two parallel lines, we were previously able to show that this trade-off was reversible (although not fully) via point mutations in RpsU at the same location of the initial mutation: RpsU$^{17Pro\text{-}His}$ and RpsU$^{17Pro\text{-}Thr}$, respectively (Koomen et al., 2021). Here, we applied a similar experimental evolution approach using *L. monocytogenes* LO28 variant 14, that has a complete deletion of *RpsU*, and by selecting for higher fitness in two parallel lines, we were able to select two evolved variants of variant 14 (14EV1, and 14EV2). Both evolved variants had higher fitness, lower stress resistance, severely reduced induction of SigB regulon members compared to variant 14, and fixed a single non-synonymous mutation in the ribosomal S2 gene (*rpsB*, lmo1658). Our RNA analysis indicated that both *sigB,* and *rsbX* were actively transcribed in variant 14. RsbX is a SigB regulated feedback phosphatase (Xia et al., 2016) and is thought to reset the stressosome after

induction, to prevent a positive feedback loop in the absence of a stress signal. In the current stressosome model (Williams et al., 2019), the phosphatase activator RsbT is released from the stressosome after phosphorylation of RsbS, and acts on the signaling cascade of RsbU, RsbV, RsbW, ending in the activation of SigB. The strong downregulation of RsbS in variant 14 suggests activation of the stressosome via the absence of RsbS. Moreover, in our whole genome sequencing of the evolved strains, we did not find (additional) mutations that resulted in premature stop codons within the genes of the *sigB* operon that positively regulate SigB activity, as previously described (Guerreiro et al., 2020a). These authors showed that such mutations leading to the loss of SigB function confer a competitive advantage manifested in an increased growth rate under conditions of sublethal heat stress, at 42˚C, but not in non-stressed conditions.
The fact that in our study *L. monocytogenes* evolved variants with higher fitness originate from slow growing, multiple stress resistant variant 14 under non-stressed conditions, while no mutation(s) were found within genes of the SigB operon, suggests that the apparent activation of SigB regulon in variant 14 and loss of SigB regulon activation in EV1 and EV2, originates from alterations in ribosome functioning.

One of the stresses that can induce SigB and its operon, is nutrient stress. In addition, nutritional stress can indirectly effect ribosome functioning through uncharged tRNA's, leading to the stringent response via RelA (Taylor et al., 2002). Notably, we find significant upregulation of genes involved in metabolism of branched chain amino acids (BCAA) in variant 14. Although *relA* (lmo1523) is not differentially expressed in our RNA-seq or proteomics, activation of the indicated pathway may point to an interplay between the mutations in the *rpsU* and *rpsB* genes affecting ribosome functioning, linked to apparent stringency, and a stress signal leading to *sigB* activation. Nutrient stress-induced activation has been described for *L. monocytogenes*, but how the *L. monocytogenes* stressosome responds to metabolic stress is currently unknown (Guerreiro et al., 2020; Williams et al., 2019).

When assessing fitness and stress resistance of the constructed mutants (variant 14 $RpsB^{Arg22His}$ and variant 14 $RpsB^{Arg22Ser}$), we found that WT stress sensitivity was not fully restored in the constructed mutants. Although no additional mutations were found in the sequenced genome, we cannot exclude the possibility of factors that are not detectable via Illumina DNA-sequencing to play a role, such as for example DNA methylation, that was

previously shown to affect translation initiation and elongation in *L. monocytogenes* (Wang et al. 2020), and modulation of protein functionality by (de)phosphorylation reactions including Rsb proteins constituting the stressosome, that orchestrates signal input for the activation of SigB (Guerreiro et al., 2020; Williams et al., 2019).

The role of individual small (S30) and large (S50) subunit ribosomal proteins in *L. monocytogenes* has not been studied, but due to high conservation of S70 ribosome functioning, possible effects of *rpsU* and *rpsB* mutations can be discussed based on structural and functional data in well studied bacteria, including *Escherichia coli*. In *E. coli*, ribosomal protein S21 (RpsU) is part of the so-called ribosomal platform, together with S6, S11, S15, and S18 (Held et al. 1970), that functions in the initial steps of the translation process. Ribosomal protein S2 (RpsB) and the adjacent S1 (RpsA) are connected to the platform region of the 30S ribosome, and are crucial in translation initiation (Duval et al., 2013; Marzi et al., 2007) and translation efficiency, which can vary over two orders of magnitude. (Espah Borujeni et al., 2014). The correct binding of RpsB to the 30S subunit is critical for the association of RpsA to the platform region and a fully competent 30S ribosome. This could indicate that partial reversion of the trade-off between growth and stress resistance in V14EV1 and V14EV2, carrying a compensatory mutation in RpsB, has a positive effect on binding of RpsA to the pre-initiation complex. Thereby enhancing translation efficiency, this presumably results in increased fitness and reduced triggering of the Sigma B stress response reflected in the WT-like phenotype of evolved variants. Whether the significant downregulation of the RsbS level in variant 14 versus WT and evolved variants is coupled with altered functioning of the S70 ribosome and stressosome-mediated SigB activation remains to be elucidated.

Here, we show that the apparent trade-off between increased stress resistance and lower fitness that has been described before in *L. monocytogenes* LO28 RpsU deletion mutant variant 14 and $Rpsu^{17Arg\text{-}Pro}$ mutant variant 15 (Abee et al., 2016; Koomen et al., 2018; Metselaar et al., 2015) can be reversed by compensatory mutations in *rpsB* and *rpsU*, respectively (Figure 5.6). Studies in yeast and higher eukaryotes have indicated that ribosomes may provide an additional layer of finetuning in protein expression in response to environmental factors (Gerst, 2018) However, the possibility of a dynamic ribosome, with shifts in ribosome composition and/or functionality of ribosomal proteins, via phosphorylation as a function of the environment, has mainly received attention in

eukaryotes (Genuth and Barna, 2018). The results presented the current study suggest that the 70S ribosome is involved in a signaling cascade to the stressosome. Alternatively, stressosome independent means of signal transduction cannot be excluded, as previous publications showed that even in the absence of RsbV, some SigB activation can occur under some growth conditions (Brigulla et al., 2003; Utratna et al., 2014). Further work is required to elucidate in more detail the underlying mechanisms of this signaling cascade and the components involved in S70 ribosome-induced modulation of *L. monocytogenes* fitness and stress resistance.

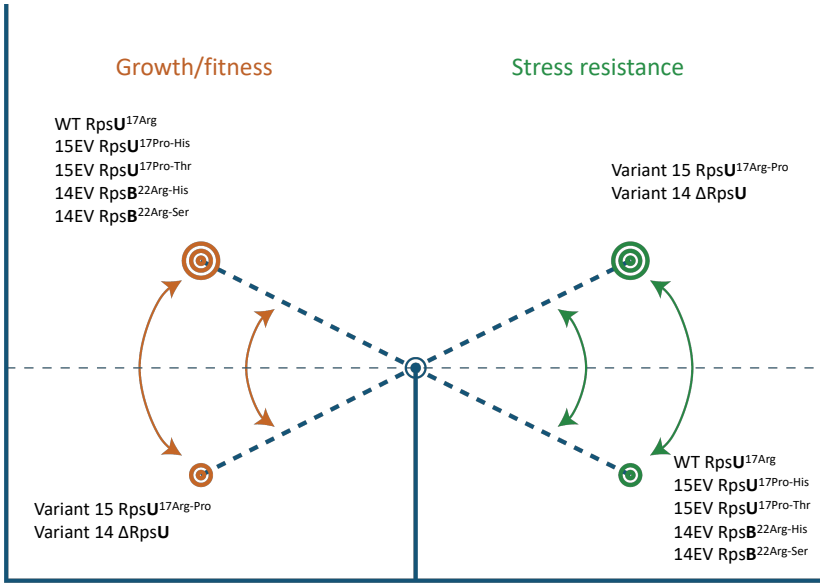


***Figure 5.6:*** *Ribosomal mutations enable a switch between high fitness and multiple-stress resistance.*

## References

**Abee, T., Koomen, J., Metselaar, K.I., Zwietering, M.H., Den Besten, H.M.W.,** 2016. Impact of pathogen population heterogeneity and stress-resistant variants on food safety. Annu. Rev. Food Sci. Technol. 7, 439–456. doi:10.1146/annurev-food-041715-033128

**Anders, S., Pyl, P., Huber, W.,** 2015 HTSeq — A Python framework to work with high-throughput sequencing data. Bioinformatics,;31(2):166-169. doi: 10.1093/bioinformatics/btu638

**Bielow, C., Mastrobuoni, G., Kempa, S.,** 2016. Proteomics quality control: quality control software for MaxQuant results. J. Proteome Res. 15, 777–787. doi:10.1021/acs.jproteome.5b00780

**Biesta-Peters, E.G., Reij, M.W., Joosten, H., Gorris, L.G.M., Zwietering, M.H.,** 2010. Comparison of two optical-density-based methods and a plate count method for estimation of growth parameters of *Bacillus cereus*. Appl. Environ. Microbiol. 76, 1399–1405. doi:10.1128/AEM.02336-09

**Brigulla, M., Hoffmann, T., Krisp, A., Völker, A., Bremer, E., Völker, U.,** 2003. Chill induction of the SigB-dependent general stress response in *Bacillus subtilis* and its contribution to low-temperature adaptation. J. Bacteriol. 185, 4305–4314. doi:10.1128/jb.185.15.4305-4314.2003

**Chakraborty, T., Leimeister-Wächter, M., Domann, E., Hartl, M., Goebel, W., Nichterlein, T., Notermans, S.,** 1992. Coordinate regulation of virulence genes in *Listeria monocytogenes* requires the product of the prfA gene. J. Bacteriol. 174, 568–574. doi:10.1128/jb.174.2.568-574.1992

**Chou, P.Y., Fasman, G.D.,** 1974. Prediction of protein conformation. Biochemistry 13, 222–245. doi:10.1021/bi00699a002

**Cox, J., Hein, M.Y., Luber, C.A., Paron, I., Nagaraj, N., Mann, M.,** 2014. Accurate proteome-wide label-free quantification by delayed normalization and maximal peptide ratio extraction, termed MaxLFQ. Mol. Cell. Proteomics 13, 2513–2526. doi:10.1074/mcp.M113.031591

**Duval, M., Korepanov, A., Fuchsbauer, O., Fechter, P., Haller, A., Fabbretti, A., Choulier, L., Micura, R., Klaholz, B.P., Romby, P., Springer, M., Marzi, S.,** 2013. *Escherichia coli* ribosomal protein S1 unfolds structured mRNAs onto the ribosome for active translation initiation. PLoS. Biol. 11, e1001731. doi:10.1371/journal.pbio.1001731

**Espah Borujeni, A., Channarasappa, A.S., Salis, H.M.,** 2014. Translation rate is controlled by coupled trade-offs between site accessibility, selective RNA unfolding and sliding at upstream standby sites. Nucleic Acids Res. 42, 2646–2659. doi:10.1093/nar/gkt1139

**Ferreira, A., Gray, M., Wiedmann, M., Boor, K.J.,** 2004. Comparative genomic analysis of the sigB operon in *Listeria monocytogenes* and in other Gram-positive bacteria. Curr. Microbiol. 48, 39–46. doi:10.1007/s00284-003-4020-x

**Genuth, N.R., Barna, M.,** 2018. The discovery of ribosome heterogeneity and its implications for gene regulation and organismal life. Mol. Cell 71, 364–374. doi:10.1016/j.molcel.2018.07.018

**Gerst, J.E.,** 2018. Pimp my ribosome: Ribosomal protein paralogs specify translational control. Trends Genet. 34, 832–845. doi:10.1016/j.tig.2018.08.004

**Guerreiro, D.N., Arcari, T., O'Byrne, C.P.,** 2020. The σB-mediated general stress response of *Listeria monocytogenes*: life and death decision making in a pathogen. Front. Microbiol. 11, 1505. doi:10.3389/fmicb.2020.01505

**Kazmierczak, M.J., Mithoe, S.C., Boor, K.J., Wiedmann, M.,** 2003. *Listeria monocytogenes* sigma B regulates stress response and virulence functions. J. Bacteriol. 185, 5722–5734. doi:10.1128/jb.185.19.5722-5734.2003

**Koomen, J., Den Besten, H.M.W., Metselaar, K.I., Tempelaars, M.H., Wijnands, L.M., Zwietering, M.H., Abee, T.,** 2018. Gene profiling-based phenotyping for identification of cellular parameters that contribute to fitness, stress-tolerance and virulence of *Listeria monocytogenes* variants. Int. J. Food Microbiol. 283, 14–21. doi:10.1016/j.ijfoodmicro.2018.06.003

**Koomen, J., Huijboom, L., Ma, X., Tempelaars, M.H., Boeren, S., Zwietering, M.H., Den Besten, H.M.W., Abee, T.,** 2021. Amino acid substitutions in ribosomal protein RpsU enable switching between high fitness and multiple-stress resistance in *Listeria monocytogenes*. Int. J. Food Microbiol. 351, 109269. doi:10.1016/j.ijfoodmicro.2021.109269

**Liu, Y., Orsi, R.H., Gaballa, A., Wiedmann, M., Boor, K.J., Guariglia-Oropeza, V.,** 2019. Systematic review of the *Listeria monocytogenes* σB regulon supports a role in stress response, virulence and metabolism. Future Microbiol. 14, 801–828. doi:10.2217/fmb-2019-0072

**Lu, J., Boeren, S., de Vries, S.C., van Valenberg, H.J.F., Vervoort, J., Hettinga, K.,** 2011. Filter-aided sample preparation with dimethyl labeling to identify and quantify milk fat globule membrane proteins. J. Proteomics 75, 34–43. doi:10.1016/j.jprot.2011.07.031

**Marzi, S., Myasnikov, A.G., Serganov, A., Ehresmann, C., Romby, P., Yusupov, M., Klaholz, B.P.,** 2007. Structured mRNAs regulate translation initiation by binding to the platform of the ribosome. Cell 130, 1019–1031. doi:10.1016/j.cell.2007.07.008

**Maury, M.M., Tsai, Y.-H., Charlier, C., Touchon, M., Chenal-Francisque, V., Leclercq, A., Criscuolo, A., Gaultier, C., Roussel, S., Brisabois, A., Disson, O., Rocha, E.P.C., Brisse, S., Lecuit, M.,** 2016. Uncovering *Listeria monocytogenes* hypervirulence by harnessing its biodiversity. Nature Genet. 2016 48:3 48, 308–313. doi:10.1038/ng.3501

**Metselaar, K.I., Den Besten, H.M.W., Abee, T., Moezelaar, R., Zwietering, M.H.,** 2013. Isolation and quantification of highly acid resistant variants of *Listeria monocytogenes.* Int. J. Food Microbiol. 166, 508–514. doi:10.1016/j.ijfoodmicro.2013.08.011

**Metselaar, K.I., Den Besten, H.M.W., Boekhorst, J., van Hijum, S.A.F.T., Zwietering, M.H., Abee, T.,** 2015. Diversity of acid stress resistant variants of *Listeria monocytogenes*

and the potential role of ribosomal protein S21 encoded by *rpsU*. Front. Microbiol. 6, 422. doi:10.3389/fmicb.2015.00422

**NicAogáin, K., O'Byrne, C.P.,** 2016. The role of stress and stress adaptations in determining the fate of the bacterial pathogen *Listeria monocytogenes* in the food chain. Front. Microbiol. 7, 1865. doi:10.3389/fmicb.2016.01865

**Oliver, H.F., Orsi, R.H., Wiedmann, M., Boor, K.J.,** 2010. *Listeria monocytogenes* sigB has a small core regulon and a conserved role in virulence but makes differential contributions to stress tolerance across a diverse collection of strains. Appl. Environ. Microbiol. 76, 4216–4232. doi:10.1128/AEM.00031-10

**Raengpradub, S., Wiedmann, M., Boor, K.J.,** 2008. Comparative analysis of the σB-dependent stress responses in *Listeria monocytogenes* and *Listeria innocua* strains exposed to selected stress conditions. Appl. Environ. Microbiol. 74, 158–171. doi:10.1128/AEM.00951-07

**Smaczniak, C., Immink, R.G.H., Muiño, J.M., Blanvillain, R., Busscher, M., Busscher-Lange, J., Dinh, Q.D.P., Liu, S., Westphal, A.H., Boeren, S., Parcy, F., Xu, L., Carles, C.C., Angenent, G.C., Kaufmann, K.,** 2012. Characterization of MADS-domain transcription factor complexes in *Arabidopsis* flower development. Proc. Natl. Acad. Sci. U.S.A. 109, 1560–1565. doi:10.1073/pnas.1112871109

**Taylor, C.M., Beresford, M., Epton, H.A.S., Sigee, D.C., Shama, G., Andrew, P.W., Roberts, I.S., 2002.** *Listeria monocytogenes relA* and *hpt* mutants are impaired in surface-attached growth and virulence. J. Bacteriol. 184, 621–628. doi:10.1128/JB.184.3.621-628.2002

**Toledo-Arana, A., Dussurget, O., Nikitas, G., Sesto, N., Guet-Revillet, H., Balestrino, D., Loh, E., Gripenland, J., Tiensuu, T., Vaitkevicius, K., Barthelemy, M., Vergassola, M., Nahori, M.-A., Soubigou, G., Régnault, B., Coppée, J.-Y., Lecuit, M., Johansson, J., Cossart, P.,** 2009. The *Listeria* transcriptional landscape from saprophytism to virulence. Nature 459, 950–956. doi:10.1038/nature08080

**Utratna, M., Cosgrave, E., Baustian, C., Ceredig, R.H., O'Byrne, C.P.,** 2014. Effects of growth phase and temperature on σB activity within a *Listeria monocytogenes* population: evidence for RsbV-independent activation of σB at refrigeration temperatures. Biomed Res. Int. 2014, 1–11. doi:10.1155/2014/641647

**Vizcaíno, J.A., Csordas, A., Del-Toro, N., Dianes, J.A., Griss, J., Lavidas, I., Mayer, G., Perez-Riverol, Y., Reisinger, F., Ternent, T., Xu, Q.-W., Wang, R., Hermjakob, H.,** 2016. 2016 update of the PRIDE database and its related tools. Nucleic Acids Res. 44, 11033. doi:10.1093/nar/gkw880

**Walker, B.J., Abeel, T., Shea, T., Priest, M., Abouelliel, A., Sakthikumar, S., Cuomo, C.A., Zeng, Q., Wortman, J., Young, S.K., Earl, A.M.,** 2014. Pilon: an integrated tool for comprehensive microbial variant detection and genome assembly improvement. PLoS One 9, e112963. doi:10.1371/journal.pone.0112963

**Wendrich, J.R., Boeren, S., Möller, B.K., Weijers, D., De Rybel, B.,** 2017. In vivo identification of plant protein complexes using IP-MS/MS. Methods Mol. Biol. 1497, 147–158. doi:10.1007/978-1-4939-6469-7_14

**Williams, A.H., Redzej, A., Rolhion, N., Costa, T.R.D., Rifflet, A., Waksman, G., Cossart, P.,** 2019. The cryo-electron microscopy supramolecular structure of the bacterial stressosome unveils its mechanism of activation. Nat. Commun. 10, 1–10. doi:10.1038/s41467-019-10782-0

**Wiśniewski, J.R., Zougman, A., Nagaraj, N., Mann, M.,** 2009. Universal sample preparation method for proteome analysis. Nat. Methods 6, 359–362. doi:10.1038/nmeth.1322

**Xia, Y., Xin, Y., Li, X., Fang, W., Björkroth, J.,** 2016. To modulate survival under secondary stress conditions, *Listeria monocytogenes* 10403S employs RsbX to downregulate σB activity in the poststress recovery stage or stationary phase. Appl. Environ. Microbiol. 82, 1126–1135. doi:10.1128/AEM.03218-15

# Supplementary material

Table S5.1: Primers used in construction of *rpsB* mutants
EcoR1 and SalI sites are indicated in bold

| Direction | Gene | Sequence |
|---|---|---|
| Forward | rpsB | 5'- TTAT**GAATTC**TTATGACAAGAGCGAGAGCACCAA- 3' |
| Reverse | rpsB | 5'- ACTT**GTCGAC**TAGCGTCAGCCATTTTAGCAGTTA- '3 |

Table S5.2: Proteins above or below the cutoff in *Listeria monocytogenes LO28* variant 14 over wild type

| LO28 ID | Protein product | Locus tag EGDe | Locus | Product | -$\log_{10}$ P value | $\log_{10}$ ratio |
|---|---|---|---|---|---|---|
| IEJ01_07680 | NP_464994.1 | lmo1469 | *rpsU* | 30S ribosomal protein S21 | 4.74 | -2.63 |
| IEJ01_03685 | NP_464250.1 | lmo0723 | - | metyl-accepting chemotaxis protein | 3.12 | -2.06 |
| IEJ01_07675 | NP_464993.1 | lmo1468 | - | hypothetical protein lmo1468 | 4.70 | -1.98 |
| IEJ01_03515 | NP_464216.1 | lmo0689 | *CheV* | chemotaxis protein CheV | 4.66 | -1.90 |
| IEJ01_03520 | NP_464217.1 | lmo0690 | *flaA* | flagellin | 5.09 | -1.90 |
| IEJ01_04515 | NP_464416.1 | lmo0890 | *rsbS* | negative regulation of sigma-B activity | 8.09 | -1.83 |
| IEJ01_04895 | NP_464486.1 | lmo0961 | - | protease | 4.81 | -1.71 |
| IEJ01_03490 | NP_464211.1 | lmo0684 | - | hypothetical protein lmo0684 | 3.40 | -1.60 |
| IEJ01_03525 | NP_464218.1 | lmo0691 | *cheY* | chemotaxis response regulator CheY | 5.02 | -1.50 |
| IEJ01_04890 | NP_464485.1 | lmo0960 | - | protease | 4.81 | -1.45 |
| IEJ01_03495 | NP_464212.1 | lmo0685 | *MotA* | flagellar motor protein MotA | 3.99 | -1.42 |
| IEJ01_13505 | NP_466092.1 | lmo2569 | - | peptide ABC transporter substrate-binding protein | 4.32 | -1.36 |
| IEJ01_11125 | NP_465650.1 | lmo2126 | - | maltogenic amylase | 3.28 | -1.26 |
| IEJ01_03530 | NP_464219.1 | lmo0692 | *cheA* | two-component sensor histidine kinase CheA | 2.83 | -1.19 |
| IEJ01_03640 | NP_464241.1 | lmo0714 | *fliG* | flagellar motor switch protein FliG | 3.00 | -1.12 |
| IEJ01_03500 | NP_464213.1 | lmo0686 | *motB* | flagellar motor rotation MotB | 4.15 | -1.08 |
| IEJ01_04655 | NP_464439.1 | lmo0913 | - | succinate semialdehyde dehydrogenase | 8.69 | 2.95 |
| IEJ01_03415 | NP_464196.1 | lmo0669 | - | oxidoreductase | 7.70 | 2.69 |
| IEJ01_11305 | NP_465681.1 | lmo2157 | *sepA* | hypothetical protein lmo2157 | 7.16 | 2.31 |
| IEJ01_03680 | NP_464249.1 | lmo0722 | - | pyruvate oxidase | 8.29 | 2.26 |
| IEJ01_07475 | NP_464953.1 | lmo1428 | *opuCA* | glycine/betaine ABC transporter ATP-binding protein | 5.27 | 2.26 |
| IEJ01_14510 | NP_466270.1 | lmo2748 | - | hypothetical protein lmo2748 | 5.56 | 2.20 |
| IEJ01_11585 | NP_465737.1 | lmo2213 | - | hypothetical protein lmo2213 | 5.30 | 2.11 |
| IEJ01_09635 | NP_465355.1 | lmo1830 | - | short-chain dehydrogenase | 4.94 | 2.11 |
| IEJ01_03340 | NP_464181.1 | lmo0654 | - | hypothetical protein lmo0654 | 4.29 | 2.04 |
| IEJ01_07970 | NP_465051.1 | lmo1526 | - | hypothetical protein lmo1526 | 4.74 | 1.99 |
| IEJ01_11545 | NP_465729.1 | lmo2205 | - | phosphoglyceromutase | 3.88 | 1.94 |
| IEJ01_07465 | NP_464951.1 | lmo1426 | *opuCC* | glycine/betaine ABC transporter substrate-binding protein | 7.90 | 1.94 |
| IEJ01_12965 | NP_465986.1 | lmo2463 | - | multidrug transporter | 5.60 | 1.79 |
| IEJ01_12600 | NP_465914.1 | lmo2391 | - | hypothetical protein lmo2391 | 3.12 | 1.69 |
| IEJ01_02760 | NP_464067.1 | lmo0539 | - | tagatose 1,6-diphosphate aldolase | 3.04 | 1.67 |
| IEJ01_08935 | NP_465219.1 | lmo1694 | - | CDP-abequose synthase | 5.10 | 1.62 |
| IEJ01_00670 | NP_463667.1 | lmo0134 | - | hypothetical protein lmo0134 | 6.90 | 1.57 |
| IEJ01_01390 | NP_463796.1 | lmo0265 | - | succinyl-diaminopimelate desuccinylase | 6.45 | 1.48 |
| IEJ01_02960 | NP_464107.1 | lmo0579 | - | hypothetical protein lmo0579 | 3.53 | 1.41 |
| IEJ01_00550 | NP_463643.1 | lmo0110 | - | lipase | 4.78 | 1.33 |
| IEJ01_13525 | NP_466096.1 | lmo2573 | - | zinc-binding dehydrogenase | 3.92 | 1.25 |
| IEJ01_07445 | NP_464947.1 | lmo1422 | - | glycine/betaine ABC transporter permease | 5.29 | 1.24 |
| IEJ01_03985 | NP_464311.1 | lmo0784 | - | PTS mannose transporter subunit IIB | 5.77 | 1.21 |
| IEJ01_00215 | NP_463576.1 | lmo0043 | - | arginine deiminase | 4.64 | 1.21 |
| IEJ01_02640 | NP_464043.1 | lmo0515 | - | hypothetical protein lmo0515 | 4.59 | 1.08 |
| IEJ01_08600 | NP_465176.1 | lmo1651 | - | ABC transporter ATP-binding protein | 6.16 | 1.07 |
| IEJ01_01435 | NP_463805.1 | lmo0274 | - | hypothetical protein lmo0274 | 6.94 | 1.07 |
| IEJ01_01045 | NP_463742.1 | lmo0211 | *ctc* | 50S ribosomal protein L25 | 4.73 | 1.03 |

Table S5.3: Proteins above or below the cutoff in *Listeria monocytogenes* LO28 14EV1 over wild type

| LO28 ID | Protein product | Locus tag | Locus | Product | -$\log_{10}$ P value | $\log_{10}$ ratio |
|---|---|---|---|---|---|---|
| IEJ01_00550 | NP_463643.1 | lmo0110 | - | lipase | 5.48 | 1.11 |
| IEJ01_07680 | NP_464994.1 | lmo1469 | *rpsU* | 30S ribosomal protein S21 | 4.74 | -2.63 |
| IEJ01_07675 | NP_464993.1 | lmo1468 | - | hypothetical protein lmo1468 | 4.70 | -1.98 |
| IEJ01_12355 | NP_465883.1 | lmo2360 | - | transmembrane protein | 2.55 | -1.07 |

Table S5.4: Proteins above or below the cutoff in *Listeria monocytogenes* LO28 14EV1 over wild type

| LO28 ID | Protein product | Locus tag | Locus | Product | -$\log_{10}$ P value | $\log_{10}$ ratio |
|---|---|---|---|---|---|---|
| IEJ01_06620 | NP_464783.1 | lmo1258 | - | hypothetical protein lmo1258 | 6.51 | 1.49 |
| IEJ01_00550 | NP_463643.1 | lmo0110 | - | lipase | 5.92 | 1.03 |
| IEJ01_07680 | NP_464994.1 | lmo1469 | *rpsU* | 30S ribosomal protein S21 | 4.74 | -2.63 |
| IEJ01_07675 | NP_464993.1 | lmo1468 | - | hypothetical protein lmo1468 | 4.70 | -1.98 |
| IEJ01_11125 | NP_465650.1 | lmo2126 | - | maltogenic amylase | 3.28 | -1.26 |

Table S5.5 (1 of 6): Differentially expressed genes in variant 14 when compared to *Listeria monocytogenes* LO28 WT

| | | | | | Variant 14 | |
|---|---|---|---|---|---|---|
| LO28 ID | Protein product | Locus tag | Locus | Product | Padj | $\log_2$ fold change |
| IEJ01_04465 | NP_464406.1 | lmo0880 | - | wall associated protein precursor | 0.000 | 9.70 |
| IEJ01_05065 | NP_464519.1 | lmo0994 | - | hypothetical protein lmo0994 | 0.000 | 8.59 |
| IEJ01_04655 | NP_464439.1 | lmo0913 | - | succinate semialdehyde dehydrogenase | 0.000 | 8.58 |
| IEJ01_01380 | NP_463794.1 | lmo0263 | *inlH* | internalin H | 0.000 | 7.58 |
| IEJ01_03045 | NP_464124.1 | lmo0596 | - | hypothetical protein lmo0596 | 0.000 | 7.54 |
| IEJ01_05070 | NP_464520.1 | lmo0995 | - | hypothetical protein lmo0995 | 0.000 | 7.50 |
| IEJ01_03420 | NP_464197.1 | lmo0670 | - | hypothetical protein lmo0670 | 0.000 | 7.44 |
| IEJ01_11865 | NP_465793.2 | lmo2269 | - | hypothetical protein lmo2269 | 0.000 | 7.41 |
| IEJ01_01390 | NP_463796.1 | lmo0265 | - | succinyl-diaminopimelate desuccinylase | 0.000 | 7.37 |
| IEJ01_00665 | NP_463666.1 | lmo0133 | - | hypothetical protein lmo0133 | 0.000 | 7.24 |
| IEJ01_03415 | NP_464196.1 | lmo0669 | - | oxidoreductase | 0.000 | 7.23 |
| IEJ01_14510 | NP_466270.1 | lmo2748 | - | hypothetical protein lmo2748 | 0.000 | 7.20 |
| IEJ01_07460 | NP_464950.1 | lmo1425 | *opuCD* | glycine/betaine ABC transporter permease | 0.000 | 7.16 |
| IEJ01_07465 | NP_464951.1 | lmo1426 | *opuCC* | glycine/betaine ABC transporter substrate-binding protein | 0.000 | 7.04 |
| IEJ01_11670 | NP_465754.1 | lmo2230 | - | arsenate reductase | 0.000 | 6.95 |
| IEJ01_11585 | NP_465737.1 | lmo2213 | - | hypothetical protein lmo2213 | 0.000 | 6.92 |
| IEJ01_03075 | NP_464129.1 | lmo0602 | - | transcripitonal regulator | 0.000 | 6.86 |
| IEJ01_09635 | NP_465355.1 | lmo1830 | - | short-chain dehydrogenase | 0.000 | 6.77 |
| IEJ01_11305 | NP_465681.1 | lmo2157 | *sepA* | hypothetical protein lmo2157 | 0.000 | 6.67 |
| IEJ01_08935 | NP_465219.1 | lmo1694 | - | CDP-abequose synthase | 0.000 | 6.67 |
| IEJ01_07475 | NP_464953.1 | lmo1428 | *opuCA* | glycine/betaine ABC transporter ATP-binding protein | 0.000 | 6.57 |
| IEJ01_07470 | NP_464952.1 | lmo1427 | *opuCB* | glycine/betaine ABC transporter permease | 0.000 | 6.52 |
| IEJ01_00095 | NP_463552.1 | lmo0019 | - | hypothetical protein lmo0019 | 0.000 | 6.49 |
| IEJ01_14255 | NP_466219.1 | lmo2697 | - | PTS mannose transporter subunit IIA | 0.000 | 6.43 |
| IEJ01_11310 | NP_465682.1 | lmo2158 | - | hypothetical protein lmo2158 | 0.000 | 6.36 |
| IEJ01_14065 | NP_466195.1 | lmo2673 | - | hypothetical protein lmo2673 | 0.000 | 6.28 |
| IEJ01_04775 | NP_464462.1 | lmo0937 | - | hypothetical protein lmo0937 | 0.000 | 6.19 |
| IEJ01_03205 | NP_464155.1 | lmo0628 | - | hypothetical protein lmo0628 | 0.000 | 6.18 |
| IEJ01_00670 | NP_463667.1 | lmo0134 | - | hypothetical protein lmo0134 | 0.000 | 6.01 |
| IEJ01_10915 | NP_465609.1 | lmo2085 | - | peptidoglycan binding protein | 0.000 | 5.90 |
| IEJ01_14250 | NP_466218.1 | lmo2696 | - | dihydroxyacetone kinase | 0.000 | 5.86 |
| IEJ01_06525 | NP_464766.1 | lmo1241 | - | hypothetical protein lmo1241 | 0.000 | 5.81 |
| IEJ01_03680 | NP_464249.1 | lmo0722 | - | pyruvate oxidase | 0.000 | 5.71 |
| IEJ01_04855 | NP_464478.1 | lmo0953 | - | hypothetical protein lmo0953 | 0.000 | 5.66 |
| IEJ01_01670 | NP_463851.1 | lmo0321 | - | hypothetical protein lmo0321 | 0.000 | 5.57 |
| IEJ01_02255 | NP_463968.1 | lmo0439 | - | hypothetical protein lmo0439 | 0.000 | 5.48 |
| IEJ01_02640 | NP_464043.1 | lmo0515 | - | hypothetical protein lmo0515 | 0.000 | 5.45 |
| IEJ01_13525 | NP_466096.1 | lmo2573 | - | zinc-binding dehydrogenase | 0.000 | 5.31 |

Table S5.5 continued (2 of 6): Differentially expressed genes in variant 14 when compared to *Listeria monocytogenes* LO28 WT

| LO28 ID | Protein product | Locus tag | Locus | Product | Variant 14 | |
|---|---|---|---|---|---|---|
| | | | | | Padj | $log_2$ fold change |
| IEJ01_10820 | NP_465591.1 | lmo2067 | - | bile acid hydrolase | 0.000 | 5.30 |
| IEJ01_03975 | NP_464309.1 | lmo0782 | - | PTS mannose transporter subunit IIC | 0.000 | 5.20 |
| IEJ01_02250 | NP_463967.1 | lmo0438 | - | hypothetical protein lmo0438 | 0.000 | 5.20 |
| IEJ01_12600 | NP_465914.1 | lmo2391 | - | hypothetical protein lmo2391 | 0.000 | 5.18 |
| IEJ01_05700 | NP_464665.1 | lmo1140 | - | hypothetical protein lmo1140 | 0.000 | 5.16 |
| IEJ01_03970 | NP_464308.1 | lmo0781 | - | PTS mannose transporter subunit IID | 0.000 | 5.08 |
| IEJ01_14245 | NP_466217.1 | lmo2695 | - | dihydroxyacetone kinase subunit DhaK | 0.000 | 4.97 |
| IEJ01_13515 | NP_466094.1 | lmo2571 | - | nicotinamidase | 0.000 | 4.91 |
| IEJ01_13510 | NP_466093.1 | lmo2570 | - | hypothetical protein lmo2570 | 0.000 | 4.86 |
| IEJ01_04035 | NP_464321.1 | lmo0794 | - | hypothetical protein lmo0794 | 0.000 | 4.83 |
| IEJ01_03115 | NP_464137.1 | lmo0610 | - | internalin | 0.000 | 4.68 |
| IEJ01_12820 | NP_465957.1 | lmo2434 | - | glutamate decarboxylase | 0.000 | 4.67 |
| IEJ01_13520 | NP_466095.1 | lmo2572 | - | dihydrofolate reductase subunit A | 0.000 | 4.66 |
| IEJ01_02285 | NP_463974.1 | lmo0445 | - | transcripitonal regulator | 0.000 | 4.63 |
| IEJ01_13710 | NP_466125.1 | lmo2602 | - | hypothetical protein lmo2602 | 0.000 | 4.62 |
| IEJ01_03980 | NP_464310.1 | lmo0783 | - | PTS mannose transporter subunit IIB | 0.000 | 4.60 |
| IEJ01_02760 | NP_464067.1 | lmo0539 | - | tagatose 1,6-diphosphate aldolase | 0.000 | 4.58 |
| IEJ01_11180 | NP_465656.1 | lmo2132 | - | hypothetical protein lmo2132 | 0.000 | 4.52 |
| IEJ01_07970 | NP_465051.1 | lmo1526 | - | hypothetical protein lmo1526 | 0.000 | 4.43 |
| IEJ01_12580 | NP_465910.1 | lmo2387 | - | hypothetical protein lmo2387 | 0.000 | 4.38 |
| IEJ01_00845 | NP_463702.1 | lmo0169 | - | glucose transporter | 0.000 | 4.36 |
| IEJ01_03985 | NP_464311.1 | lmo0784 | - | PTS mannose transporter subunit IIB | 0.000 | 4.34 |
| IEJ01_00215 | NP_463576.1 | lmo0043 | - | arginine deiminase | 0.000 | 4.22 |
| IEJ01_07440 | NP_464946.1 | lmo1421 | - | glycine/betaine ABC transporter ATP-binding protein | 0.000 | 4.12 |
| IEJ01_02225 | NP_463962.1 | lmo0433 | *inlA* | internalin A | 0.000 | 4.01 |
| IEJ01_11675 | NP_465755.1 | lmo2231 | - | hypothetical protein lmo2231 | 0.000 | 3.88 |
| IEJ01_03010 | NP_464117.1 | lmo0589 | - | hypothetical protein lmo0589 | 0.000 | 3.87 |
| IEJ01_13130 | NP_466018.1 | lmo2495 | - | phosphate ABC transporter ATP-binding protein | 0.000 | 3.86 |
| IEJ01_07445 | NP_464947.1 | lmo1422 | - | glycine/betaine ABC transporter permease | 0.000 | 3.85 |
| IEJ01_00125 | NP_463558.1 | lmo0025 | - | phosphoheptose isomerase | 0.000 | 3.78 |
| IEJ01_12640 | NP_465921.1 | lmo2398 | *ltrC* | hypothetical protein lmo2398 | 0.000 | 3.77 |
| IEJ01_07500 | NP_464958.1 | lmo1433 | - | glutathione reductase | 0.000 | 3.77 |
| IEJ01_04645 | NP_464437.1 | lmo0911 | - | hypothetical protein lmo0911 | 0.000 | 3.75 |
| IEJ01_12965 | NP_465986.1 | lmo2463 | - | multidrug transporter | 0.000 | 3.72 |
| IEJ01_13080 | NP_466008.1 | lmo2485 | - | hypothetical protein lmo2485 | 0.000 | 3.70 |
| IEJ01_11870 | NP_465794.1 | lmo2270 | *comK'* | competence protein ComK | 0.000 | 3.67 |
| IEJ01_03340 | NP_464181.1 | lmo0654 | - | hypothetical protein lmo0654 | 0.000 | 3.67 |
| IEJ01_04045 | NP_464323.1 | lmo0796 | - | hypothetical protein lmo0796 | 0.000 | 3.66 |
| IEJ01_03345 | NP_464182.1 | lmo0655 | - | phosphoprotein phosphatase | 0.000 | 3.63 |
| IEJ01_14390 | NP_466246.1 | lmo2724 | - | hypothetical protein lmo2724 | 0.000 | 3.63 |
| IEJ01_02835 | NP_464082.1 | lmo0554 | - | NADH-dependent butanol dehydrogenase | 0.000 | 3.59 |
| IEJ01_02090 | NP_463935.1 | lmo0405 | - | phosphate transporter | 0.000 | 3.58 |
| IEJ01_12925 | NP_465977.1 | lmo2454 | - | hypothetical protein lmo2454 | 0.000 | 3.53 |
| IEJ01_03310 | NP_464175.1 | lmo0648 | - | hypothetical protein lmo0648 | 0.000 | 3.49 |
| IEJ01_13715 | NP_466126.1 | lmo2603 | - | hypothetical protein lmo2603 | 0.000 | 3.47 |
| IEJ01_06635 | NP_464786.1 | lmo1261 | - | hypothetical protein lmo1261 | 0.000 | 3.28 |
| IEJ01_03015 | NP_464118.1 | lmo0590 | - | hypothetical protein lmo0590 | 0.000 | 3.27 |
| IEJ01_03020 | NP_464119.1 | lmo0591 | - | hypothetical protein lmo0591 | 0.000 | 3.18 |
| IEJ01_12335 | NP_465879.1 | lmo2356 | - | hypothetical protein lmo2356 | 0.000 | 3.15 |
| IEJ01_13125 | NP_466017.1 | lmo2494 | - | PhoU family transcriptional regulator | 0.000 | 3.15 |
| IEJ01_08035 | NP_465064.1 | lmo1539 | - | glycerol transporter | 0.000 | 3.09 |
| IEJ01_01675 | NP_463852.1 | lmo0322 | - | hypothetical protein lmo0322 | 0.000 | 3.07 |
| IEJ01_09895 | NP_465407.1 | lmo1883 | - | chitinase | 0.000 | 3.06 |
| IEJ01_03305 | NP_464174.1 | lmo0647 | - | hypothetical protein lmo0647 | 0.000 | 3.04 |
| IEJ01_11545 | NP_465729.1 | lmo2205 | - | phosphoglyceromutase | 0.000 | 3.01 |
| IEJ01_14060 | NP_466194.1 | lmo2672 | - | AraC family transcriptional regulator | 0.000 | 2.92 |
| IEJ01_00850 | NP_463703.1 | lmo0170 | - | hypothetical protein lmo0170 | 0.000 | 2.79 |
| IEJ01_01045 | NP_463742.1 | lmo0211 | *ctc* | 50S ribosomal protein L25 | 0.000 | 2.74 |
| IEJ01_13150 | NP_466022.1 | lmo2499 | - | phosphate ABC transporter substrate-binding protein | 0.000 | 2.71 |
| IEJ01_12355 | NP_465883.1 | lmo2360 | - | transmembrane protein | 0.000 | 2.70 |

Table S5.5 continued (3 of 6): Differentially expressed genes in variant 14 when compared to *Listeria monocytogenes* LO28 WT

| LO28 ID | Protein product | Locus tag | Locus | Product | Variant 14 | |
|---|---|---|---|---|---|---|
| | | | | | Padj | $log_2$ fold change |
| IEJ01_08350 | NP_465126.1 | lmo1601 | - | general stress protein | 0.000 | 2.69 |
| IEJ01_09480 | NP_465324.1 | lmo1799 | - | peptidoglycan binding protein | 0.000 | 2.69 |
| IEJ01_10430 | NP_465513.1 | lmo1989 | *leuC* | isopropylmalate isomerase large subunit | 0.000 | 2.68 |
| IEJ01_10440 | NP_465515.1 | lmo1991 | *ilvA* | threonine dehydratase | 0.000 | 2.66 |
| IEJ01_12360 | NP_465884.1 | lmo2361 | - | hypothetical protein lmo2361 | 0.000 | 2.64 |
| IEJ01_03210 | NP_464156.1 | lmo0629 | - | hypothetical protein lmo0629 | 0.000 | 2.63 |
| IEJ01_10435 | NP_465514.1 | lmo1990 | *leuD* | isopropylmalate isomerase small subunit | 0.000 | 2.62 |
| IEJ01_08355 | NP_465127.1 | lmo1602 | - | hypothetical protein lmo1602 | 0.000 | 2.59 |
| IEJ01_08240 | NP_465105.1 | lmo1580 | - | hypothetical protein lmo1580 | 0.000 | 2.56 |
| IEJ01_11175 | NP_465655.1 | lmo2131 | - | hypothetical protein lmo2131 | 0.000 | 2.53 |
| IEJ01_06805 | NP_464820.1 | lmo1295 | - | host factor-1 protein | 0.000 | 2.51 |
| IEJ01_10425 | NP_465512.1 | lmo1988 | *leuB* | 3-isopropylmalate dehydrogenase | 0.000 | 2.48 |
| IEJ01_01435 | NP_463805.1 | lmo0274 | - | hypothetical protein lmo0274 | 0.000 | 2.44 |
| IEJ01_12575 | NP_465909.1 | lmo2386 | - | hypothetical protein lmo2386 | 0.000 | 2.43 |
| IEJ01_11390 | NP_465698.1 | lmo2174 | - | hypothetical protein lmo2174 | 0.000 | 2.41 |
| IEJ01_10420 | NP_465511.1 | lmo1987 | *leuA* | 2-isopropylmalate synthase | 0.000 | 2.40 |
| IEJ01_01695 | NP_463856.1 | lmo0326 | - | transcriptional regulator | 0.003 | 2.38 |
| IEJ01_00725 | WP_015084540.1 | NA | NA | NA | 0.002 | 2.38 |
| IEJ01_13075 | NP_466007.1 | lmo2484 | - | hypothetical protein lmo2484 | 0.000 | 2.36 |
| IEJ01_08030 | NP_465063.1 | lmo1538 | *glpK* | glycerol kinase | 0.000 | 2.34 |
| IEJ01_04805 | NP_464468.1 | lmo0943 | *fri* | non-heme iron-binding ferritin | 0.000 | 2.32 |
| IEJ01_07210 | NP_464900.1 | lmo1375 | - | aminotripeptidase | 0.000 | 2.32 |
| IEJ01_12835 | NP_465960.1 | lmo2437 | - | hypothetical protein lmo2437 | 0.000 | 2.31 |
| IEJ01_09435 | NP_465315.1 | lmo1790 | - | hypothetical protein lmo1790 | 0.000 | 2.30 |
| IEJ01_02840 | NP_464083.1 | lmo0555 | - | di-tripeptide transporter | 0.000 | 2.29 |
| IEJ01_02685 | NP_464052.1 | lmo0524 | - | sulfate transporter | 0.000 | 2.27 |
| IEJ01_08600 | NP_465176.1 | lmo1651 | - | ABC transporter ATP-binding protein | 0.000 | 2.26 |
| IEJ01_03315 | NP_464176.1 | lmo0649 | - | transcriptional regulator | 0.000 | 2.15 |
| IEJ01_09425 | NP_465313.1 | lmo1788 | - | transcriptional regulator | 0.000 | 2.15 |
| IEJ01_02230 | NP_463963.1 | lmo0434 | *inlB* | internalin B | 0.000 | 2.12 |
| IEJ01_08675 | NP_465191.1 | lmo1666 | - | peptidoglycan-linked protein | 0.000 | 2.12 |
| IEJ01_02960 | NP_464107.1 | lmo0579 | - | hypothetical protein lmo0579 | 0.000 | 2.10 |
| IEJ01_02965 | NP_464108.1 | lmo0580 | - | hypothetical protein lmo0580 | 0.000 | 2.07 |
| IEJ01_10400 | NP_465507.1 | lmo1983 | *ilvD* | dihydroxy-acid dehydratase | 0.000 | 2.06 |
| IEJ01_10415 | NP_465510.1 | lmo1986 | *ilvC* | ketol-acid reductoisomerase | 0.000 | 2.05 |
| IEJ01_14050 | NP_466192.1 | lmo2670 | - | hypothetical protein lmo2670 | 0.000 | 2.05 |
| IEJ01_10410 | NP_465509.1 | lmo1985 | *ilvH* | acetolactate synthase small subunit | 0.000 | 2.05 |
| IEJ01_11475 | NP_465715.1 | lmo2191 | *spxA* | ArsC family transcriptional regulator | 0.000 | 2.02 |
| IEJ01_13145 | NP_466021.1 | lmo2498 | - | phosphate ABC transporter permease | 0.000 | 2.01 |
| IEJ01_04725 | NP_464453.1 | lmo0928 | - | 3-methyladenine DNA glycosylase | 0.000 | 1.97 |
| IEJ01_10405 | NP_465508.1 | lmo1984 | *ilvB* | acetolactate synthase | 0.000 | 1.95 |
| IEJ01_13135 | NP_466019.1 | lmo2496 | - | phosphate ABC transporter ATP-binding protein | 0.000 | 1.95 |
| IEJ01_13210 | NP_466034.1 | lmo2511 | - | hypothetical protein lmo2511 | 0.000 | 1.94 |
| IEJ01_03105 | NP_464135.1 | lmo0608 | - | ABC transporter ATP-binding protein | 0.000 | 1.94 |
| IEJ01_04545 | NP_464422.1 | lmo0896 | *rsbX* | indirect negative regulation of sigma B dependant gene expression | 0.000 | 1.93 |
| IEJ01_03280 | NP_464169.1 | lmo0642 | - | hypothetical protein lmo0642 | 0.000 | 1.93 |
| IEJ01_09030 | NP_465238.1 | lmo1713 | - | rod shape-determining protein MreB | 0.000 | 1.92 |
| IEJ01_09430 | NP_465314.1 | lmo1789 | - | hypothetical protein lmo1789 | 0.000 | 1.90 |
| IEJ01_07030 | NP_464865.1 | lmo1340 | - | hypothetical protein lmo1340 | 0.000 | 1.89 |
| IEJ01_13140 | NP_466020.1 | lmo2497 | - | phosphate ABC transporter permease | 0.000 | 1.89 |
| IEJ01_00195 | NP_463572.1 | lmo0039 | - | carbamate kinase | 0.000 | 1.88 |
| IEJ01_01810 | NP_463881.1 | lmo0351 | - | phosphotransferase mannnose-specific family component IIA | 0.000 | 1.88 |
| IEJ01_09475 | NP_465323.1 | lmo1798 | - | hypothetical protein lmo1798 | 0.000 | 1.87 |
| IEJ01_01690 | NP_463855.1 | lmo0325 | - | transcriptional regulator | 0.000 | 1.86 |
| IEJ01_06795 | NP_464818.1 | lmo1293 | *glpD* | glycerol-3-phosphate dehydrogenase | 0.000 | 1.86 |
| IEJ01_01525 | NP_463823.1 | lmo0292 | - | heat-shock protein htrA serine protease | 0.000 | 1.85 |
| IEJ01_08595 | NP_465175.1 | lmo1650 | - | hypothetical protein lmo1650 | 0.000 | 1.83 |
| IEJ01_03320 | NP_464177.1 | lmo0650 | - | hypothetical protein lmo0650 | 0.000 | 1.81 |
| IEJ01_03090 | NP_464132.1 | lmo0605 | - | hypothetical protein lmo0605 | 0.000 | 1.81 |
| IEJ01_01520 | NP_463822.1 | lmo0291 | - | hypothetical protein lmo0291 | 0.000 | 1.81 |

Table S5.5 continued (4 of 6): Differentially expressed genes in variant 14 when compared to *Listeria monocytogenes* LO28 WT

| LO28 ID | Protein product | Locus tag | Locus | Product | Variant 14 | |
|---|---|---|---|---|---|---|
| | | | | | Padj | $log_2$ fold change |
| IEJ01_08585 | NP_465173.1 | lmo1648 | - | hypothetical protein lmo1648 | 0.000 | 1.79 |
| IEJ01_12645 | NP_465922.1 | lmo2399 | - | hypothetical protein lmo2399 | 0.000 | 1.76 |
| IEJ01_04610 | NP_464430.1 | lmo0904 | - | hypothetical protein lmo0904 | 0.000 | 1.74 |
| IEJ01_00990 | NP_463731.1 | lmo0200 | *prfA* | listeriolysin positive regulatory protein | 0.000 | 1.73 |
| IEJ01_04540 | NP_464421.1 | lmo0895 | *sigB* | RNA polymerase sigma factor SigB | 0.000 | 1.68 |
| IEJ01_03865 | NP_464287.1 | lmo0760 | - | hypothetical protein lmo0760 | 0.000 | 1.68 |
| IEJ01_14055 | NP_466193.1 | lmo2671 | - | hypothetical protein lmo2671 | 0.000 | 1.67 |
| IEJ01_00190 | NP_463571.1 | lmo0038 | - | agmatine deiminase | 0.000 | 1.67 |
| IEJ01_13600 | NP_466110.1 | lmo2587 | - | hypothetical protein lmo2587 | 0.000 | 1.67 |
| IEJ01_13265 | NP_466045.1 | lmo2522 | - | cell wall-binding protein | 0.000 | 1.65 |
| IEJ01_14475 | NP_466263.1 | lmo2741 | - | multidrug transporter | 0.000 | 1.64 |
| IEJ01_02115 | NP_463940.1 | lmo0411 | - | phosphoenolpyruvate synthase | 0.000 | 1.63 |
| IEJ01_08605 | NP_465177.1 | lmo1652 | - | ABC transporter ATP-binding protein | 0.000 | 1.63 |
| IEJ01_03100 | NP_464134.1 | lmo0607 | - | ABC transporter ATP-binding protein | 0.000 | 1.62 |
| IEJ01_09320 | NP_465295.1 | lmo1770 | *purL* | phosphoribosylformylglycinamidine synthase I | 0.000 | 1.61 |
| IEJ01_02985 | NP_464112.1 | lmo0584 | - | hypothetical protein lmo0584 | 0.000 | 1.61 |
| IEJ01_02590 | NP_464033.1 | lmo0505 | - | ribulose-5-phosphate 3-epimerase | 0.000 | 1.60 |
| IEJ01_09825 | NP_465393.1 | lmo1868 | - | hypothetical protein lmo1868 | 0.000 | 1.59 |
| IEJ01_07495 | NP_464957.1 | lmo1432 | - | hypothetical protein lmo1432 | 0.000 | 1.58 |
| IEJ01_14465 | NP_466261.1 | lmo2739 | - | NAD-dependent deacetylase | 0.000 | 1.58 |
| IEJ01_11330 | NP_465686.1 | lmo2162 | - | hypothetical protein lmo2162 | 0.000 | -1.58 |
| IEJ01_01550 | NP_463828.1 | lmo0297 | - | transcriptional antiterminator BglG | 0.000 | -1.58 |
| IEJ01_08360 | NP_465128.1 | lmo1603 | - | aminopeptidase | 0.000 | -1.61 |
| IEJ01_06405 | WP_009917708.1 | NA | NA | terminase large subunit | 0.000 | -1.63 |
| IEJ01_11020 | YP_008475638.1 | lmo2104a | - | hypothetical protein lmo2104a | 0.000 | -1.63 |
| IEJ01_02190 | NP_463955.1 | lmo0426 | - | PTS fructose transporter subunit IIA | 0.000 | -1.64 |
| IEJ01_14180 | NP_466205.1 | lmo2683 | - | PTS cellbiose transporter subunit IIB | 0.000 | -1.65 |
| IEJ01_10985 | NP_465623.1 | lmo2099 | - | transcriptional antiterminator | 0.000 | -1.67 |
| IEJ01_11325 | NP_465685.1 | lmo2161 | - | hypothetical protein lmo2161 | 0.000 | -1.67 |
| IEJ01_06335 | NP_463822.1 | lmo0291 | - | hypothetical protein lmo0291 | 0.000 | -1.67 |
| IEJ01_00485 | NP_463630.1 | lmo0097 | - | PTS mannose transporter subunit IIC | 0.000 | -1.71 |
| IEJ01_14040 | NP_466190.1 | lmo2668 | - | transcriptional antiterminator BglG | 0.000 | -1.74 |
| IEJ01_11125 | NP_465650.1 | lmo2126 | - | maltogenic amylase | 0.000 | -1.78 |
| IEJ01_13505 | NP_466092.1 | lmo2569 | - | peptide ABC transporter substrate-binding protein | 0.000 | -1.78 |
| IEJ01_01985 | NP_463914.1 | lmo0384 | - | lolB protein | 0.006 | -1.85 |
| IEJ01_04890 | NP_464485.1 | lmo0960 | - | protease | 0.000 | -1.85 |
| IEJ01_04550 | NP_464423.1 | lmo0897 | - | transporter | 0.000 | -1.89 |
| IEJ01_14310 | NP_466230.1 | lmo2708 | - | PTS cellbiose transporter subunit IIC | 0.000 | -1.92 |
| IEJ01_02060 | NP_463929.1 | lmo0399 | - | PTS fructose transporter subunit IIB | 0.000 | -1.96 |
| IEJ01_01570 | NP_463832.1 | lmo0301 | - | PTS beta-glucoside transporter subunit IIA | 0.000 | -1.96 |
| IEJ01_14780 | NP_466322.1 | lmo2800 | - | dehydrogenase | 0.000 | -1.99 |
| IEJ01_04355 | NP_464385.1 | lmo0859 | - | sugar ABC transporter substrate-binding protein | 0.000 | -2.02 |
| IEJ01_04235 | NP_464362.1 | lmo0835 | - | peptidoglycan binding protein | 0.000 | -2.03 |
| IEJ01_02245 | NP_463966.1 | lmo0437 | - | hypothetical protein lmo0437 | 0.000 | -2.07 |
| IEJ01_04895 | NP_464486.1 | lmo0961 | - | protease | 0.000 | -2.10 |
| IEJ01_06450 | WP_003731642.1 | NA | NA | DUF3168 domain-containing protein | 0.000 | -2.10 |
| IEJ01_14185 | NP_466206.1 | lmo2684 | - | PTS cellbiose transporter subunit IIC | 0.000 | -2.12 |
| IEJ01_06455 | WP_012581455.1 | NA | NA | phage tail protein | 0.000 | -2.13 |
| IEJ01_06470 | WP_012951553.1 | NA | NA | phage tail tape measure protein | 0.000 | -2.16 |
| IEJ01_06480 | WP_012951555.1 | NA | NA | phage tail protein | 0.000 | -2.16 |
| IEJ01_11335 | NP_465687.1 | lmo2163 | - | oxidoreductase | 0.000 | -2.17 |
| IEJ01_00765 | NP_463686.1 | lmo0153 | - | zinc ABC transporter substrate-binding protein | 0.000 | -2.21 |
| IEJ01_11780 | NP_465776.1 | lmo2252 | - | aspartate aminotransferase | 0.000 | -2.21 |
| IEJ01_06465 | WP_009931626.1 | NA | NA | hypothetical protein | 0.000 | -2.23 |
| IEJ01_08295 | NP_465116.1 | lmo1591 | *argC* | N-acetyl-gamma-glutamyl-phosphate reductase | 0.000 | -2.26 |
| IEJ01_11105 | NP_465646.1 | lmo2122 | - | maltodextrose utilization protein MalA | 0.000 | -2.28 |
| IEJ01_06430 | WP_015987290.1 | NA | NA | hypothetical protein | 0.000 | -2.29 |
| IEJ01_08290 | NP_465115.1 | lmo1590 | *argJ* | bifunctional ornithine acetyltransferase/N-acetylglutamate synthase | 0.002 | -2.30 |
| IEJ01_07670 | NP_464992.1 | lmo1467 | - | phosphate starvation-induced protein PhoH | 0.000 | -2.34 |
| IEJ01_06390 | WP_014930130.1 | NA | NA | hypothetical protein | 0.000 | -2.36 |

Table S5.5 continued (5 of 6): Differentially expressed genes in variant 14 when compared to *Listeria monocytogenes* LO28 WT

| LO28 ID | Protein product | Locus tag | Locus | Product | Variant 14 | |
|---|---|---|---|---|---|---|
| | | | | | Padj | $log_2$ fold change |
| IEJ01_11120 | NP_465649.1 | lmo2125 | - | sugar ABC transporter substrate-binding protein | 0.000 | -2.39 |
| IEJ01_14785 | NP_466323.1 | lmo2801 | - | N-acetylmannosamine-6-phosphate 2-epimerase | 0.000 | -2.41 |
| IEJ01_06460 | WP_014930131.1 | NA | NA | hypothetical protein | 0.000 | -2.41 |
| IEJ01_11100 | NP_465645.1 | lmo2121 | - | maltose phosphorylase | 0.000 | -2.42 |
| IEJ01_06475 | WP_014601422.1 | NA | NA | phage tail family protein | 0.000 | -2.49 |
| IEJ01_03690 | NP_464251.1 | lmo0724 | - | hypothetical protein lmo0724 | 0.000 | -2.52 |
| IEJ01_06400 | WP_014929542.1 | NA | NA | P27 family phage terminase small subunit | 0.000 | -2.53 |
| IEJ01_06385 | WP_010991275.1 | NA | NA | DUF559 domain-containing protein | 0.000 | -2.54 |
| IEJ01_06395 | WP_000988331.1 | NA | NA | HNH endonuclease | 0.000 | -2.58 |
| IEJ01_06420 | NP_465991.1 | lmo2468 | *clpP* | ATP-dependent Clp protease proteolytic subunit | 0.000 | -2.58 |
| IEJ01_03685 | NP_464250.1 | lmo0723 | - | metyl-accepting chemotaxis protein | 0.000 | -2.58 |
| IEJ01_06415 | WP_014929544.1 | NA | NA | phage portal protein | 0.000 | -2.59 |
| IEJ01_06440 | WP_014929549.1 | NA | NA | phage head-tail adapter protein | 0.000 | -2.66 |
| IEJ01_11115 | NP_465648.1 | lmo2124 | - | sugar ABC transporter permease | 0.000 | -2.69 |
| IEJ01_06425 | WP_012581458.1 | NA | NA | phage major capsid protein | 0.000 | -2.75 |
| IEJ01_06445 | WP_009917701.1 | NA | NA | hypothetical protein | 0.000 | -2.81 |
| IEJ01_11110 | NP_465647.1 | lmo2123 | - | sugar ABC transporter permease | 0.000 | -2.87 |
| IEJ01_10940 | NP_465614.1 | lmo2090 | *argG* | argininosuccinate synthase | 0.000 | -3.05 |
| IEJ01_11770 | NP_465774.1 | lmo2250 | *arpJ* | amino acid ABC transporter permease | 0.000 | -3.07 |
| IEJ01_06435 | WP_012951549.1 | NA | NA | phage gp6-like head-tail connector protein | 0.000 | -3.07 |
| IEJ01_10945 | NP_465615.1 | lmo2091 | *argH* | argininosuccinate lyase | 0.000 | -3.17 |
| IEJ01_11775 | NP_465775.1 | lmo2251 | - | amino acid ABC transporter ATP-binding protein | 0.000 | -3.28 |
| IEJ01_03660 | NP_464245.1 | lmo0718 | - | hypothetical protein lmo0718 | 0.000 | -4.46 |
| IEJ01_03650 | NP_464243.1 | lmo0716 | *fliI* | flagellum-specific ATP synthase | 0.000 | -4.57 |
| IEJ01_03655 | NP_464244.1 | lmo0717 | - | transglycosylase | 0.000 | -4.64 |
| IEJ01_03645 | NP_464242.1 | lmo0715 | *fliH* | flagellar assembly protein H | 0.000 | -4.70 |
| IEJ01_03640 | NP_464241.1 | lmo0714 | *fliG* | flagellar motor switch protein FliG | 0.000 | -4.70 |
| IEJ01_03635 | NP_464240.1 | lmo0713 | *fliF* | flagellar MS-ring protein FliF | 0.000 | -4.86 |
| IEJ01_03490 | NP_464211.1 | lmo0684 | - | hypothetical protein lmo0684 | 0.000 | -5.19 |
| IEJ01_03630 | NP_464239.1 | lmo0712 | *fliE* | flagellar hook-basal body protein FliE | 0.000 | -5.30 |
| IEJ01_03510 | NP_464215.1 | lmo0688 | - | hypothetical protein lmo0688 | 0.000 | -5.30 |
| IEJ01_03495 | NP_464212.1 | lmo0685 | - | flagellar motor protein MotA | 0.000 | -5.43 |
| IEJ01_03595 | NP_464232.1 | lmo0705 | *flgK* | flagellar hook-associated protein FlgK | 0.000 | -5.44 |
| IEJ01_03470 | NP_464207.1 | lmo0680 | *flhA* | flagellar biosynthesis protein FlhA | 0.000 | -5.48 |
| IEJ01_03605 | NP_464234.1 | lmo0707 | *fliD* | flagellar capping protein FliD | 0.000 | -5.50 |
| IEJ01_03515 | NP_464216.1 | lmo0689 | - | chemotaxis protein CheV | 0.000 | -5.51 |
| IEJ01_03600 | NP_464233.1 | lmo0706 | *flgL* | flagellar hook-associated protein FlgL | 0.000 | -5.55 |
| IEJ01_03610 | NP_464235.1 | lmo0708 | - | flagellar protein | 0.000 | -5.58 |
| IEJ01_03505 | NP_464214.1 | lmo0687 | - | hypothetical protein lmo0687 | 0.000 | -5.58 |
| IEJ01_03485 | NP_464210.1 | lmo0683 | - | chemotaxis protein CheR | 0.000 | -5.60 |
| IEJ01_03585 | NP_464230.1 | lmo0703 | - | hypothetical protein lmo0703 | 0.000 | -5.60 |
| IEJ01_03550 | NP_464223.1 | lmo0696 | *flgD* | flagellar basal body rod modification protein | 0.000 | -5.61 |
| IEJ01_03475 | NP_464208.1 | lmo0681 | - | flagellar biosynthesis regulator FlhF | 0.000 | -5.61 |
| IEJ01_03615 | NP_464236.1 | lmo0709 | - | hypothetical protein lmo0709 | 0.000 | -5.64 |
| IEJ01_03535 | NP_464220.1 | lmo0693 | - | flagellar motor switch protein FliY | 0.000 | -5.64 |
| IEJ01_03540 | NP_464221.1 | lmo0694 | - | hypothetical protein lmo0694 | 0.000 | -5.65 |
| IEJ01_03625 | NP_464238.1 | lmo0711 | *flgC* | flagellar basal body rod protein FlgC | 0.000 | -5.65 |
| IEJ01_03590 | NP_464231.1 | lmo0704 | - | hypothetical protein lmo0704 | 0.000 | -5.66 |
| IEJ01_03620 | NP_464237.1 | lmo0710 | *flgB* | flagellar basal-body rod protein FlgB | 0.000 | -5.67 |
| IEJ01_03465 | NP_464206.1 | lmo0679 | *flhB* | flagellar biosynthesis protein FlhB | 0.000 | -5.70 |
| IEJ01_03545 | NP_464222.1 | lmo0695 | - | hypothetical protein lmo0695 | 0.000 | -5.86 |
| IEJ01_03480 | NP_464209.1 | lmo0682 | *flgG* | flagellar basal body rod protein FlgG | 0.000 | -5.87 |
| IEJ01_08960 | NP_465224.1 | lmo1699 | - | chemotaxis protein | 0.000 | -5.89 |
| IEJ01_03575 | NP_464228.1 | lmo0701 | - | hypothetical protein lmo0701 | 0.000 | -5.91 |
| IEJ01_03565 | NP_464226.1 | lmo0699 | *fliM* | flagellar motor switch protein FliM | 0.000 | -5.91 |
| IEJ01_03570 | NP_464227.1 | lmo0700 | - | flagellar motor switch protein FliY | 0.000 | -5.91 |
| IEJ01_03580 | NP_464229.1 | lmo0702 | - | hypothetical protein lmo0702 | 0.000 | -5.92 |
| IEJ01_03500 | NP_464213.1 | lmo0686 | *motB* | flagellar motor rotation MotB | 0.000 | -5.92 |
| IEJ01_03555 | NP_464224.1 | lmo0697 | *flgE* | flagellar hook protein FlgE | 0.000 | -5.92 |
| IEJ01_03530 | NP_464219.1 | lmo0692 | *cheA* | two-component sensor histidine kinase CheA | 0.000 | -5.95 |

Table S5.5 continued (6 of 6): Differentially expressed genes in variant 14 when compared to *Listeria monocytogenes* LO28 WT

| LO28 ID | Protein product | Locus tag | Locus | Product | Variant 14 | |
|---|---|---|---|---|---|---|
| | | | | | Padj | $log_2$ fold change |
| IEJ01_03525 | NP_464218.1 | lmo0691 | *cheY* | chemotaxis response regulator CheY | 0.000 | -5.99 |
| IEJ01_03460 | NP_464205.1 | lmo0678 | *fliR* | flagellar biosynthesis protein FliR | 0.000 | -6.03 |
| IEJ01_08965 | NP_465225.1 | lmo1700 | - | hypothetical protein lmo1700 | 0.000 | -6.12 |
| IEJ01_03560 | NP_464225.1 | lmo0698 | - | flagellar motor switch protein | 0.000 | -6.16 |
| IEJ01_03520 | NP_464217.1 | lmo0690 | *flaA* | flagellin | 0.000 | -7.43 |
| IEJ01_07680 | NP_464994.1 | lmo1469 | *rpsU* | 30S ribosomal protein S21 | 0.000 | -19.80 |
| IEJ01_07675 | NP_464993.1 | lmo1468 | - | hypothetical protein lmo1468 | 0.000 | -20.08 |

Table S5.6: Differentially expressed genes in variant 14EV1 when compared to *Listeria monocytogenes* LO28 WT

| LO28 ID | Protein product | Locus tag | Locus | Protein name | 14EV1 | |
|---|---|---|---|---|---|---|
| | | | | | Padj | $log_2$ fold change |
| IEJ01_13955 | NP_466173.1 | lmo2651 | - | PTS mannitol transporter subunit IIA | 0.000 | 3.58 |
| IEJ01_13950 | NP_466172.1 | lmo2650 | - | MFS transporter | 0.000 | 3.55 |
| IEJ01_13940 | NP_466170.1 | lmo2648 | - | phosphotriesterase | 0.000 | 3.29 |
| IEJ01_13935 | NP_466169.1 | lmo2647 | - | creatinine amidohydrolase | 0.001 | 3.15 |
| IEJ01_13945 | NP_466171.1 | lmo2649 | *ulaA* | PTS system ascorbate transporter subunit IIC | 0.000 | 2.64 |
| IEJ01_04465 | NP_464406.1 | lmo0880 | - | wall associated protein precursor | 0.000 | 2.31 |
| IEJ01_05065 | NP_464519.1 | lmo0994 | - | hypothetical protein lmo0994 | 0.000 | 2.25 |
| IEJ01_13925 | YP_008475644.1 | lmo2644a | - | hypothetical protein lmo2644a | 0.000 | 1.94 |
| IEJ01_11585 | NP_465737.1 | lmo2213 | - | hypothetical protein lmo2213 | 0.000 | 1.73 |
| IEJ01_13930 | NP_466168.1 | lmo2646 | - | hypothetical protein lmo2646 | 0.002 | 1.73 |
| IEJ01_01380 | NP_463794.1 | lmo0263 | *inlH* | internalin H | 0.000 | 1.61 |
| IEJ01_04655 | NP_464439.1 | lmo0913 | - | succinate semialdehyde dehydrogenase | 0.000 | 1.60 |
| IEJ01_07670 | NP_464992.1 | lmo1467 | - | phosphate starvation-induced protein PhoH | 0.000 | -1.86 |
| IEJ01_07680 | NP_464994.1 | lmo1469 | *rpsU* | 30S ribosomal protein S21 | 0.000 | -19.62 |
| IEJ01_07675 | NP_464993.1 | lmo1468 | - | hypothetical protein lmo1468 | 0.000 | -19.89 |

Table S5.7: Differentially expressed genes in variant 14EV2 when compared to *Listeria monocytogenes* LO28 WT

| LO28 ID | Protein product | Locus tag | Locus | Protein name | 14EV2 | |
|---|---|---|---|---|---|---|
| | | | | | Padj | $log_2$ fold change |
| IEJ01_13940 | NP_466170.1 | lmo2648 | - | phosphotriesterase | 0.000 | 3.33 |
| IEJ01_13935 | NP_466169.1 | lmo2647 | - | creatinine amidohydrolase | 0.001 | 2.85 |
| IEJ01_13950 | NP_466172.1 | lmo2650 | - | MFS transporter | 0.000 | 2.17 |
| IEJ01_13955 | NP_466173.1 | lmo2651 | - | PTS mannitol transporter subunit IIA | 0.000 | 2.16 |
| IEJ01_13930 | NP_466168.1 | lmo2646 | - | hypothetical protein lmo2646 | 0.000 | 2.09 |
| IEJ01_13925 | YP_008475644.1 | lmo2644a | - | hypothetical protein lmo2644a | 0.000 | 2.05 |
| IEJ01_11560 | NP_465732.1 | lmo2208 | - | hypothetical protein lmo2208 | 0.000 | 1.81 |
| IEJ01_13945 | NP_466171.1 | lmo2649 | *ulaA* | PTS system ascorbate transporter subunit IIC | 0.000 | 1.72 |
| IEJ01_02250 | NP_463967.1 | lmo0438 | - | hypothetical protein lmo0438 | 0.008 | 1.69 |
| IEJ01_11955 | NP_465814.1 | lmo2290 | - | protein gp13 | 0.000 | -1.58 |
| IEJ01_12000 | NP_465823.1 | lmo2299 | - | portal protein | 0.000 | -1.58 |
| IEJ01_11970 | NP_465817.1 | lmo2293 | - | protein gp10 | 0.000 | -1.59 |
| IEJ01_11985 | NP_465820.1 | lmo2296 | - | phage coat protein | 0.000 | -1.66 |
| IEJ01_14310 | NP_466230.1 | lmo2708 | - | PTS cellbiose transporter subunit IIC | 0.000 | -1.67 |
| IEJ01_12015 | WP_012582399.1 | NA | NA | NA | 0.000 | -1.76 |
| IEJ01_11995 | NP_465822.1 | lmo2298 | - | protein gp4 | 0.000 | -1.81 |
| IEJ01_11975 | NP_465818.1 | lmo2294 | - | protein gp9 | 0.000 | -1.86 |
| IEJ01_11980 | NP_465819.1 | lmo2295 | - | protein gp8 | 0.000 | -1.90 |
| IEJ01_07670 | NP_464992.1 | lmo1467 | - | phosphate starvation-induced protein PhoH | 0.000 | -1.92 |
| IEJ01_11965 | NP_465816.1 | lmo2292 | - | protein gp11 | 0.000 | -1.93 |
| IEJ01_11950 | NP_465813.1 | lmo2289 | - | protein gp14 | 0.000 | -1.94 |
| IEJ01_00525 | NP_463638.1 | lmo0105 | - | chitinase B | 0.000 | -1.94 |
| IEJ01_11960 | NP_465815.1 | lmo2291 | - | major tail shaft protein | 0.000 | -2.13 |
| IEJ01_11570 | NP_465734.1 | lmo2210 | - | hypothetical protein lmo2210 | 0.000 | -2.43 |
| IEJ01_07680 | NP_464994.1 | lmo1469 | *rpsU* | 30S ribosomal protein S21 | 0.000 | -19.96 |
| IEJ01_07675 | NP_464993.1 | lmo1468 | - | hypothetical protein lmo1468 | 0.000 | -20.24 |

Table S5.8: Expression of genes involved in the stressosome in variants 14, 14EV1, 14EV2 when compared to *Listeria monocytogenes* LO28 WT

| | | | | | Variant 14 | | 14EV1 | | 14EV2 | |
|---|---|---|---|---|---|---|---|---|---|---|
| **LO28 ID** | **Protein product** | **Locus tag** | **Locus** | **Protein name** | **Padj** | **$log_2$ fold change** | **Padj** | **$log_2$ fold change** | **Padj** | **$log_2$ fold change** |
| IEJ01_04510 | NP_464415.1 | lmo0889 | *rsbR1* | positive regulator of sigma-B activity | 0.847 | 0.02 | 0.836 | 0.03 | 0.904 | -0.01 |
| IEJ01_00805 | NP_463694.1 | lmo0161 | *rsbR2* | hypothetical protein lmo0161 | 0.000 | -0.83 | 0.748 | 0.04 | 0.040 | 0.23 |
| IEJ01_08555 | NP_465167.1 | lmo1642 | *rsbR3* | sigma factor regulator | 0.000 | 0.93 | 0.227 | 0.13 | 0.625 | 0.05 |
| IEJ01_09695 | NP_465367.1 | lmo1842 | *rsbR4* | hypothetical protein lmo1842 | 0.719 | 0.04 | 0.983 | -0.01 | 0.295 | -0.11 |
| IEJ01_04060 | NP_464326.1 | lmo0799 | *rsbL* | hypothetical protein lmo0799 | 0.565 | 0.07 | 0.990 | 0.00 | 0.500 | 0.09 |
| IEJ01_04515 | NP_464416.1 | lmo0890 | *rsbS* | negative regulation of sigma-B activity | 0.028 | -0.26 | 0.370 | -0.12 | 0.204 | -0.15 |
| IEJ01_04525 | NP_464418.1 | lmo0892 | *rsbU* | serine phosphatase | 0.365 | -0.08 | 0.989 | 0.00 | 0.256 | 0.11 |
| IEJ01_04530 | NP_464419.1 | lmo0893 | *rsbV* | anti-anti-sigma factor (antagonist of RsbW) | 0.000 | 1.39 | 0.648 | -0.06 | 0.091 | 0.17 |
| IEJ01_04535 | NP_464420.1 | lmo0894 | *rsbW* | serine-protein kinase RsbW | 0.000 | 1.26 | 0.794 | 0.04 | 0.058 | 0.17 |
| IEJ01_04540 | NP_464421.1 | lmo0895 | *sigB* | RNA polymerase sigma factor SigB | 0.000 | **1.68** | 0.113 | 0.14 | 0.001 | 0.27 |
| IEJ01_04545 | NP_464422.1 | lmo0896 | *rsbX* | indirect negative regulation of sigma B dependant gene expression (serine phosphatase) | 0.000 | **1.93** | 0.000 | 0.27 | 0.000 | 0.35 |

# 6

# General discussion

## Introduction

*Listeria monocytogenes* is generally considered to be a robust microorganism, capable of growing and surviving in a wide range of adverse conditions such as low pH, low temperature and low $a_w$ (NicAogáin and O'Byrne, 2016), and can adapt efficiently to changing environments including conditions inside the human body. These features allow *L. monocytogenes* to persist in the food chain, and establish life-threatening listeriosis in the very young, elderly, immunocompromised, and in pregnant women (NicAogáin and O'Byrne, 2016; Toledo-Arana et al., 2009).

There is an inherent heterogeneity in microbial populations that further contributes to the ubiquitous nature of *L. monocytogenes* by enhancing its capacity to cope with environmental stresses during transmission from the environment to the human host. This heterogeneity leads to stochastic differences in stress response between individual cells of a population, and to differential survival of a small fraction of the population after exposure to lethal stresses such as heat or low pH, resulting in tailing of the inactivation curve. *L. monocytogenes* has served as a model species in a large number of studies on the impact of strain diversity and the role of population heterogeneity in adaptive stress response and subsequent survival capacity (Karatzas et al., 2005; Metselaar et al., 2013; Van Boeijen et al., 2010; Van der Veen and Abee, 2011; Vanlint et al., 2012).

### Mutation rate and isolation of a mutator strain

Most authors have investigated the diversity and heterogeneity of *L. monocytogenes* by working on standing genetic variation. I.e., they have investigated the diversity and heterogeneity that was already present in populations. In contrast, in chapter 2, we have investigated the rate at which new mutations are generated. Mutations in bacteria are either produced stochastically during replication of DNA, or after environmental insults that lead to DNA damage, and require repair by genes involved in the SOS response (Van der Veen et al., 2010).

The trade-off between the positive (adaptive) effect of beneficial mutations, and the negative effects of deleterious mutations that increase genetic load, is believed to be the cause of the low mutation rates that are typically observed in populations (Desai and Fisher, 2011; Lynch, 2011; Sniegowski and Raynes, 2013; Wielgoss et al., 2013). We investigated the mutation rate of 20 strains of *L. monocytogenes*, and found one mutator strain (FBR16) with a 100-1000-fold increase in mutation rate, and identified an insertion in the DNA mismatch repair gene *mutS* (lmo1403) that was responsible for the observed phenotype. In addition, we found another strain (H7767) that had a high sequence diversity in the *mutS* but this did not result in a mutator phenotype for this strain. One explanation would be the presence of additional repair systems in H7767, which could be elucidated by measuring the mutation rate of a Δ*mutS* mutation in strain H7767.

The fluctuation analysis that is used in chapter 2 is a powerful tool to estimate mutation rates. However, there are practical limitations to this technique. It derives a mutation rate from a single gene under specific conditions, and the fitness of the phenotype that is under study (rifampicin resistance) has a strong influence on the number of mutants that can be found. This can lead to bias in the estimation of mutation rates in conditions such as low temperature, where the *rpoB* mutants are known to be less fit (data not shown). However, when these limitations are taken into account, mutation rates can be quickly compared between strains in the same conditions. Although mutation rate has received little attention in *L. monocytogenes*, recent studies have investigated the mutation rate in persister strains found in food processing facilities (Harrand et al., 2020). The authors have found very little differences in SNPs, and suggested that the main factor driving strain diversification in processing facilities are prophages.

Although an organism's mutation rate is generally considered to be almost constant (Lynch, 2010; Drake, 1991), the optimal mutation rate depends on the specific environment that the cells are in (Elena and Lenski, 2003; Eyre-Walker and Keightley, 2007; Kimura, 1967; Perfeito et al., 2007). Under optimal (e.g., laboratory) conditions, mutator strains only occur sporadically (Boe et al., 2000; de Visser, 2002; Marinus, 2010), and very high mutation rates have been shown to be potentially detrimental to fitness (Sprouffske et al., 2018). However, in natural environments, where (mild) stress is the default (Hallsworth, 2018), a much higher prevalence of mutator strains has been observed (Hall and Henderson-Begg, 2006). Examples are mutator strains amongst clinical isolates of pathogenic *E. coli* (Denamur et al., 2002) *Pseudomonas aeruginosa* (Oliver, 2015), and food pathogens such as *Salmonella* spp. and *Staphylococcus aureus* (Sheng et al., 2020; Wang et al., 2018; Wang et al., 2013). This raises questions about the absence of suspected mutator genotypes of *L. monocytogenes* in databases such as RefSeq (see chapter 2). As the optimal mutation rate is a function of genotype and environment, it is possible that mutator strains are less adaptive in a species such as *L. monocytogenes* that is able to thrive in diverse conditions (Freitag et al., 2009). Did we happen to find a very rare mutator in *L. monocytogenes*, caused by an insertion in *mutS*? Or is there selection against mutator strains, caused by the genetic load of a high mutation rate, explaining their absence from the databases? Competition experiments between mutator and WT strains of *L. monocytogenes* EGD have suggested that competitive fitness and virulence of the mutator strain were lower in a mouse model (Mérino et al., 2002), while homologous recombination was increased 15-fold, pointing to a transient mutator phenotype. In addition, very high mutation rates have been shown to limit adaptation in *E. coli* (Sprouffske et al., 2018). Whether the lower fitness that was observed for the mutator strain of EGD (Mérino et al., 2002) translates to FBR16 remains to be elucidated, by direct competition experiments in FBR16 and FBR16_mutS_repaired.

### Variants can be found in multiple strains after exposure to a variety of stresses

Population heterogeneity, generated for instance by mutations, has been studied by inactivation of multiple strains of *L. monocytogenes* by high hydrostatic pressure (HHP) (Van Boeijen et al., 2010), heat, and acid (Metselaar et al., 2013) and revealed considerable tailing of inactivation curves, allowing for isolation of stable resistant variants from the tail. Previous work used phenotyping and genomic analysis to investigate *L. monocytogenes* LO28 variants that were exposed to HHP, revealed significant population diversity, including

a subset with mutations and deletions in the *ctsR* gene. The *ctsR* variants had a multiple-stress resistant phenotype, which was linked to the increased expression of genes encoding Clp proteases resulting from a defect in the repressor function of CtsR (Van Boeijen et al., 2010). However, these *ctsR* variants were shown to have a reduced maximum specific growth rate and also a reduced virulence potential in a mouse model (Van Boeijen et al., 2010). Interestingly, these HHP selected variants showed cross resistance to other stresses including heat and acid stress. Further work by Metselaar et al. (2013) resulted in isolation of additional variants that were isolated after a single exposure to acid stress. Chapter 3 focusses on two of these latter variants; variant 14, with a large deletion that spans the whole *rpsU* gene, as well as *yqeY* and half of *phoH*; and variant 15, with a single point mutation in *rpsU* that resulted in an amino acid substitution from arginine to proline in the RpsU protein, $RpsU^{17Arg\text{-}Pro}$. For these variants, enhanced stress-resistance was correlated with increased activity of the glutamate decarboxylase (GAD) system (Metselaar et al., 2015), previously reported to contribute to *L. monocytogenes* acid resistance (Cotter et al., 2001; Feehily and Karatzas, 2013; Karatzas et al., 2012). In chapter 3, we investigated additional mechanisms contributing to the observed multiple stress-resistant phenotype of the variants. In variants 14 and 15, about 70% of the 145 genes of the SigB regulon included in the analysis, were upregulated, although no mutations in the *sigB* gene or its regulatory genes were found (Metselaar et al., 2015). The activation of SigB-mediated stress defence offers an explanation for the multiple-stress resistant phenotype observed in *rpsU* variants 14 and 15. Moreover, our variants 14 and 15, when grown in BHI, display a pattern of gene expression that suggests mitigation of catabolite repression, and elevated glycerol consumption, with the associated high activity of the virulence regulator gene *prfA*. Notably, the upregulation of the PrfA/SigB-regulated attachment and invasion genes *inlA* and *inlB* in these variants and the observed higher adhesion/invasion to Caco-2 cells of the variants compared to the WT (Koomen et al., 2018) suggests that virulence potential of these variants is higher than that of the *L. monocytogenes* LO28 WT, but additional studies are required to confirm this.

Modelling and validation of the ecological behaviour of *L. monocytogenes* WT and stress resistant variants 14 and 15 indicated that multiple stress resistance could contribute to increased performance along the food chain, which, in combination with the conceivable higher survival of acidic conditions in the stomach, could result in a higher exposure and probability of disease (Abee et al., 2016; Metselaar et al., 2016). It cannot be excluded that

following the initial selection of multiple stress resistant variants (Abee et al., 2016), other variants with additional mutations can originate from the ancestor variant. In chapters 4 and 5 we tested this idea by subjecting two parallel cultures for variant 15, and two parallel cultures for variant 14, to an experimental evolution regime (see Figure 6.1) where we selected for increased fitness, measured as maximum specific growth rate ($\mu_{max}$). Both for variant 15, with a point mutation in *rpsU*, and for variant 14 with a whole deletion of *rpsU*, the selection for increased fitness resulted in fixing additional mutations that lead to shifting the trade-off between fitness and stress resistance, as summarized in Figure 6.4. Although variant 15EV1 and variant 15EV2 both fixed a compensatory mutation in the 17$^{th}$ codon of *rpsU* (codons CAT and ACT respectively), they did not fix the same mutation, and we did not find a reversion to the CGT codon that results in RpsU$^{17Arg}$ that is present in the LO28 WT. Within a single mutational step, one of 9 different codon changes can occur at position 17, of which 6 lead to a codon that does not code for proline on position 17 in RpsU (see Table 6.1) and only one of the nine mutations results in an arginine, conceivably offering an explanation for why we did not select a variant with the WT RpsU$^{17Arg}$ codon. In addition, based on the slight difference in $\mu_{max}$ and proteomic profile between 15EV1 and 15EV2, we hypothesize that the RpsU$^{17Arg\text{-}His}$ of 15EV1 is slightly more efficient in restoring the WT phenotype than RpsU$^{17Arg\text{-}Thr}$ of 15EV2.

***Table 6.1:*** *Possible mutations in one mutational step from variant 15*

| Isolate | Codon | Amino acid | AA change |
|---|---|---|---|
| Variant 15 | C C T | Proline | - |
| | C C G | Proline | No |
| | C C A | Proline | No |
| | C C C | Proline | No |
| | G C T | Alanine | Yes |
| 15EV2 | A C T | Threonine | Yes |
| | T C T | Phenylalanine | Yes |
| LO28 WT | C G T | Arginine | Yes |
| 15EV1 | C A T | Histidine | Yes |
| | C T T | Leucine | Yes |

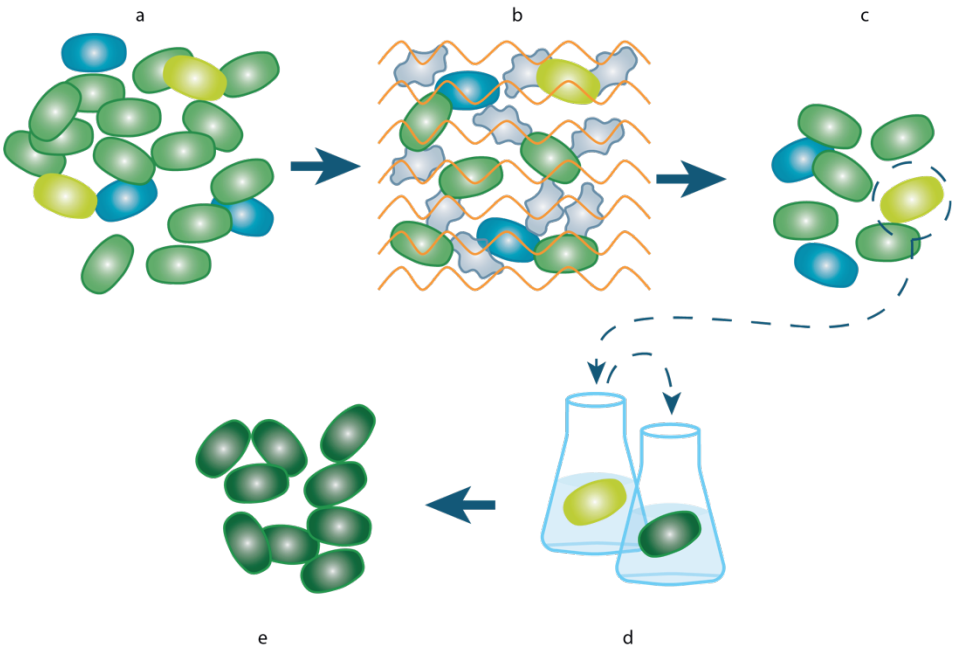


***Figure 6.1:*** *Summary of the experimental procedure used in this thesis.*
*A heterogeneous population of cells including WT and stress resistant variants (a) was exposed to acid stress (b), leading to differential survival. From the surviving population (c), single cells with a constitutively higher stress resistance but reduced fitness were selected and exposed to consecutive rounds of experimental evolution (d), ultimately selecting for evolved variants with increased growth rate and reduced, WT-like, stress resistance (e).*

**Lower fitness in variants is only indirectly linked to SigB activation**

In chapter 4 and 5, we described evolved variants with higher fitness, that originated from variants with lower fitness and multiple stress resistance under non-stressed conditions (see Figure 6.1). If the major negative effect on fitness would come from energy-consuming SigB activation, we would expect the experimental evolution to select for mutations that inactivate either *sigB* or its regulating sequences. However, no mutation(s) were found in *sigB*, or genes of the SigB operon, which suggests that the apparent induction, and subsequent relaxation of SigB may be linked to the observed differences in the ribosomes. From an evolutionary perspective, we expect most mutations to be deleterious (Elena and Lenski, 2003; Eyre-Walker and Keightley, 2007; Kimura, 1967; Perfeito et al., 2007), and we expect the number of mutations that disrupt SigB activation to be much higher than the

number of mutations that restore ribosome functioning. As we did not find any mutations that disrupt the function of SigB, we suggest that the fitness gain is the primary trait under selection, and that the SigB activation is a response to it, not its cause. However, the interaction between mutations in RpsU and activation of SigB is still unknown.

In addition, in *L. monocytogenes*, stress induces the dimerization of 70S ribosomes into translationally silent 100S ribosomes that are associated with dormancy and robustness (Kline et al., 2015). Cells with a larger fraction of 100S ribosomes are more robust to stress, however, at the expense of fitness, as the 100S ribosomes need to be split into 70S ribosomes before they become active again. Preliminary results of sucrose density centrifugation showed that in variants 14 and 15 a larger fraction of 100S ribosomes exist, with relatively more unassembled ribosomes in variant 14 (see Figure 6.2). The existence of 100S ribosomes in both variants suggests an additional level of interaction between the ribosomes and the stress response that may add to the lower fitness phenotype.

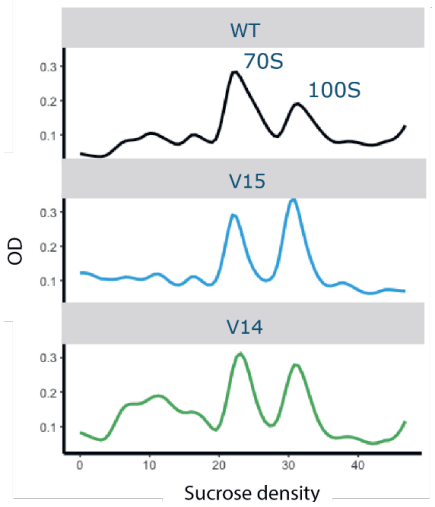


***Figure 6.2:*** *Ribosome profiles of* L. monocytogenes *LO28 wild type, and variants 14 and 15.*

### Possible interaction between RpsU and SigB

The RpsU$^{17Arg\text{-}Pro}$ mutation in variant 15, in combination with the downregulation of *rpsU* in this variant (Metselaar et al., 2015; Koomen et al., 2018) is presumably responsible for a loss of RpsU function that has phenotypic effects that are highly similar to the complete deletion of *rpsU* in variant 14. This is supported by the observation that the RpsB$^{22Arg\text{-}Ser}$

substitution in the ribosomal S2 gene (*rpsB*, lmo1658) that was found in variant 14EV2, when introduced to variant 15, also decreased stress resistance and increased the maximum specific growth rate (data not shown). Activation of SigB is controlled by the stressosome, that integrates and relays a range of stress signals and activates the SigB regulon (Guldimann et al., 2016; NicAogáin and O'Byrne, 2016; Radoshevich and Cossart, 2018, Dessaux et al., 2020). The exact mechanism by which the stressosome responds to signals from, or induced by, the ribosome remains largely unknown. In the widely accepted (in vitro) stressosome model proposed by Williams et al. (2019) a signaling cascade of RsbU, RsbV and RsbW and ending in the activation of SigB, is triggered by the stressosome after phosphorylation of RsbR and RsbS (see Figure 6.3). In both variant 14 and variant 15, proteomics shows a strong downregulation of RsbS. The expression of the *rsbS* gene is not significantly downregulated in the DNA-microarray data of variants 14 and 15, nor in the RNA-seq analysis of variant 14, suggesting that the low level of RsbS protein in variants 14 and 15 is the result of post-translational regulation. Conceivably, this downregulation of RsbS leads to the release of RsbT, as proposed in the model of Williams et al. (2019) (see Figure 6.3), that can then associate with RsbU to generate a downstream signal, ultimately leading to the release of SigB. Our RNA analysis indicated that both *sigB* and *rsbX* were transcribed in variant 14. RsbX is a feedback phosphatase (Xia et al., 2016) under direct control of SigB, and thought to reset the stressosome to its inactive position after induction. The upregulation of this negative feedback system without a reversion of the SigB levels to default, suggests that the stress signal coming from the ribosome is continuous during exponential growth. In addition, the revised stressosome model presented by Dessaux and co-authors (2020a) suggests an additional role for the paralogues of RsbR in modulating the generation of active stressosome complexes upon the sensing of stress. The only receptor for which a clear trigger is described is the blue-light sensor RsbL (Dorey et al., 2019). Additional studies with RpsU$^{17Arg\text{-}Pro}$ – Δ*rsbR*, and Δ*rsbR* paralogue double mutants are needed to identify the exact stress that triggers stressosome activation in the *rpsU* variants. Moreover, as the RsbR paralogues are hypothesized to negatively regulate the stressosome, they might provide an explanation for the decrease of the multiple-stress resistance of variants 14 and 15 that has been found for stationary cells at 20°C (Metselaar et al., 2015b).

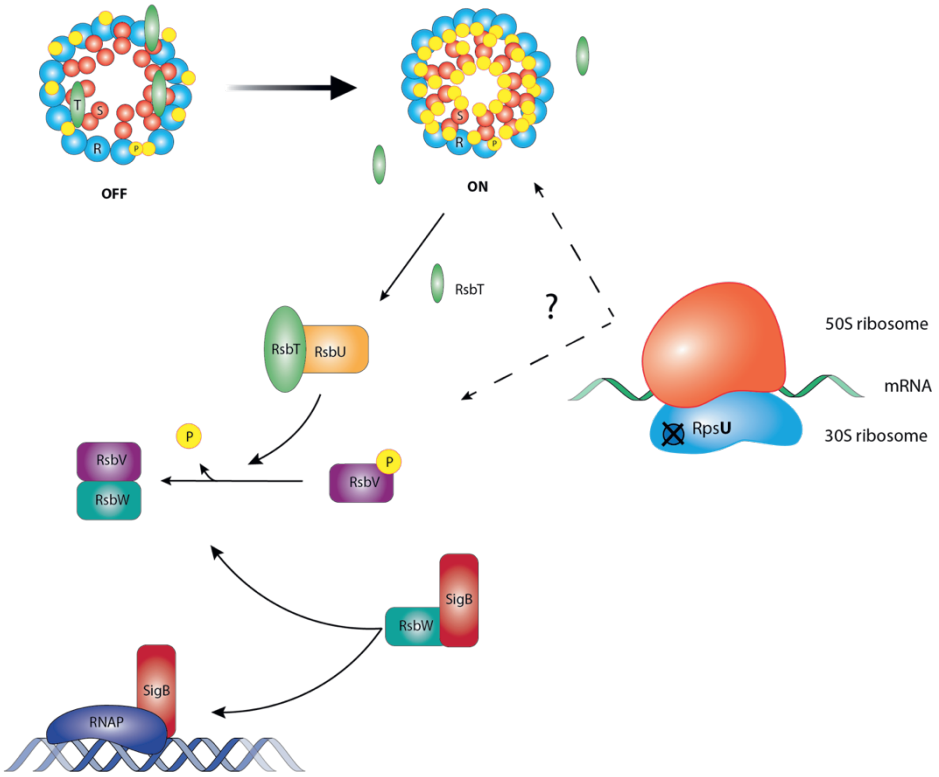


***Figure 6.3:*** *Schematic overview of the stressosome and SigB activation.*
*From the top left, following perception of a stress signal, RsbT dissociates from RsbR and RsbS (indicated by T, R and S in the stressosome), after activation of its kinase activity. After release from the stressosome RpsT binds to RsbU. The phosphatase activity of RbsU is activated and removes a phosphate (P) group from RbsV. The anti-sigma factor RsbW has a higher affinity for the now dephosphorylated RsbV than for SigB, resulting in release of SigB allowing it to bind to RNA polymerase and initiate transcription of SigB regulon members. RpsU function, and/or attachment to the 30S ribosome is disrupted similarly by a point mutation resulting in* $RpsU^{Arg\text{-}Pro}$*, or a full deletion of* rpsU *in variants 15 and 14 respectively, relaying a signal to either the stressosome, or directly to RsbV (see main text for details). Adapted from Dessaux et al., 2020a, Williams 2019, and Cabeen et al., 2017.*

One of the stresses that might trigger SigB activation is nutrient stress. Nutrient stress-induced activation has been described for *L. monocytogenes*, but how the *L. monocytogenes* stressosome responds to metabolic stress is currently unknown (Guerreiro et al., 2020; Williams et al., 2019). Nutritional stress can be perceived indirectly through uncharged tRNA's associated to ribosomes, leading to the stringent response via RelA (Taylor et al., 2002). Alternatively, an indirect link between ribosomes and (nutritional) stress via translation efficiency, is discussed in chapter 5. The compensatory mutations in *rpsB* that were fixed by the two evolving lines of variant 14 suggested an effect on the correct binding of RpsB to the 30S subunit of the ribosome. This binding is critical for the association of RpsA to the ribosomal platform region, and leads to a fully competent 30S ribosome. This could indicate that partial reversion of the trade-off between growth and stress resistance in V14EV1 and V14EV2, carrying a compensatory mutation in RpsB, has a positive effect on binding of RpsA to the pre-initiation complex. This mode of activation suggests an effect of the *rpsB* mutations on restoring translation efficiency in evolved variants V14EV1 and V14EV2. Impaired binding of RpsA to the pre-initiation complex and a lowered translation efficiency would be more pronounced at lower temperatures (Marzi et al., 2007 and references therein), and offer a possible explanation for the lower fitness of the variants at low temperatures. Although challenging in prokaryotes, recent approaches combining ribosome profiling with RNA-sequencing have been used to study translation efficiency (Mohammad et al., 2019), and could be used to investigate the conceived differences in translation efficiency of the variants compared to the LO28 WT.

The results presented in chapters 4 and 5 suggest that the 70S ribosome is involved in a signaling cascade to the stressosome. In addition, stressosome-independent means of signal transduction cannot be excluded, as previous publications showed that even in the absence of RsbV, some SigB activation can occur under some growth conditions (Brigulla et al., 2003; Utratna et al., 2014).

**Impact of population heterogeneity on food safety**

The effects of the introduction of the RpsU$^{17Arg\text{-}Pro}$ mutation in *rpsU* were not limited to strain LO28. The same phenotypic switch from high fitness-low stress resistance to low fitness-high stress resistance was observed after the introduction of the RpsU$^{17Arg\text{-}Pro}$ mutation into the background of *L. monocytogenes* EGDe, proving that the single arginine-proline substitution at position 17 in RpsU can explain the observed changes in phenotype. The

possibility of selecting resistant variants from non-model strains has been raised before, and can now be experimentally explored in strains that are much more resistant already, without a reduction on fitness, such as L6 (Aryani et al., 2015). In our current model, stress resistance comes from activation of SigB. It is yet unclear whether activation of SigB in strains that are already very stress resistant will lead to even higher stress resistance, or that the relative effect is lower in these strains. By studying the effect of *rpsU* mutations in these strains, we can quantify if already stress resistant strains pose an additional risk when mutated, and whether there is a trade-off between fitness and stress resistance, as summarized in Figure 6.4. Previous work has described variants 14 and 15 as much more stress resistant than the LO28 WT (Metselaar et al., 2015). However, the *D*-value and $\mu_{max}$ of the variants stay within the limits of those currently found in literature (den Besten et al., 2017), and these limits provide valuable input to include *L. monocytogenes* variability in growth and inactivation for quantitative microbial risk assessment (QMRA).

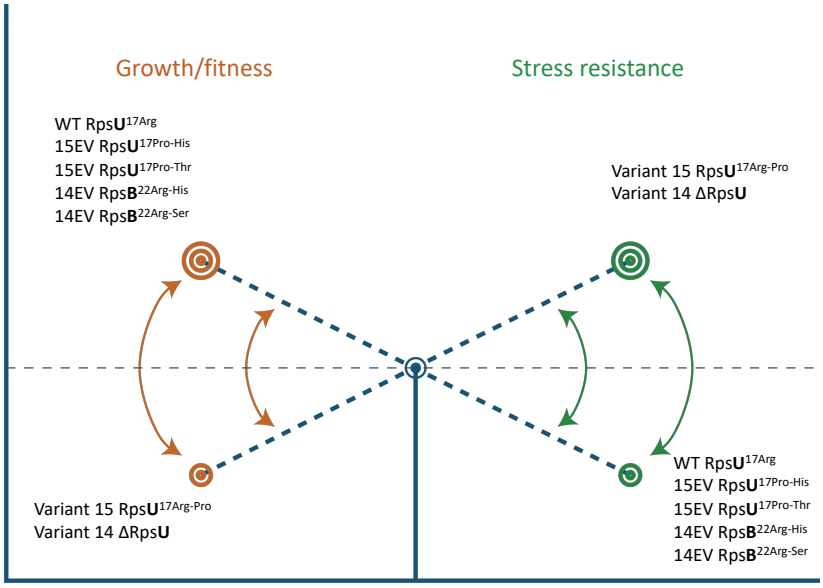


***Figure 6.4:*** *The trade-off between fitness and stress resistance, as in Figure 5.6. WT LO28 and evolved variants have a high growth rate, coupled to a low stress resistance (diagonal from upper left corner to lower right corner). The variants have high stress resistance, coupled to low fitness (diagonal from upper right corner to lower left corner). Selection for the inverse phenotype flips the balance.*

One of the remaining questions is whether this trade-off is inevitable; would it be possible to push the population to an evolutionary solution that will increase both fitness and stress resistance? The (in)evitability of a trade-off is relevant information for QMRA, where the hypothetical combination of the most stress resistant and the fastest grower can be used as an "extreme worst-case scenario", using the highest growth rate and stress resistance observed among a group of strains. But if these strains could not exist this would be an unrealistic scenario to include, and a biological trade-off would translate in a correlation between input parameters within QMRA. Interestingly, a recent study that incorporated strain variability in the design of heat treatments showed that strains with the highest resistance are determinant for the overall achieved inactivation, even if the probability of cells having such extreme heat resistance is very low (Zwietering et al. 2021), and it remains to be quantified whether the strain differences in fitness have a similar impact.

Notably, although multiple-stress resistant variants of *L. monocytogenes* have been found after a single exposure to lethal stress (Karatzas and Bennik, 2002; Metselaar et al., 2015; 2013; Rajkovic et al., 2009; Van Boeijen et al., 2011; 2008), we were thus far unable to identify these variants in the various online sequence databases (e.g., the GenBank database hosted at www.ncbi.nlm.nih.gov). Not finding *rpsU* variants in the databases can be a reflection of the biased content of the databases, which are focussed on strains used in research, as well as the strict rules that the databases have for genome quality and layout before admission. On the other hand, the testing methods used to detect *L. monocytogenes* in food, might also contribute to the fact that *rpsU* variants have not been reported as foodborne isolates. One factor might be that the assessment of stress resistance is done in laboratory conditions, while in a real-life scenario, stress parameters might change, as environmental conditions such as temperature have been described as potent modulators of stress response (Chen et al., 2020). In addition, growth of *L. monocytogenes* in biofilms has been shown to influence the stress response (Van der Veen and Abee, 2010), and might disrupt the trade-off between stress resistance and fitness in the LO28 variants. Moreover, testing foods for the presence of *L. monocytogenes* is routinely done by the food industry and the food inspection authorities and the test methods are based on standardized enrichments. Enrichments are needed to resuscitate damaged cells and selectively amplify the initial low concentrations of cells, and are followed by detection procedures. The growth kinetics during enrichment can be strongly influenced by the history of the cells (Abee et al. 2016; Bannenberg et al., 2021), with yet unknown effects on the probability of isolating a

variant cell. Therefore, it remains to be elucidated whether the difference in fitness between variants and WT strains might also result in a lower probability to detect variants when enrichment-based detection procedures are used.

**Conclusions and perspectives**

This thesis provided insight into the rate with which diversity in *L. monocytogenes* is generated by mutations. It was shown for the first time, that a strain isolated from food was a mutator strain, and an insertion in the DNA mismatch repair gene *mutS*, was identified as the cause of the mutator phenotype. Additional studies included two previously isolated multiple-stress resistant variants with low fitness and a very similar phenotype, that was linked to the upregulation of SigB, even though one carried a point mutation in the ribosomal *rpsU* gene, while the other had a full deletion of *rpsU*. Recurring selection on increased fitness by experimental evolution revealed a tradeoff between a low-fitness, stress-resistant state, and a high-fitness, low stress-resistant state. We identified additional mutations in the ribosomes of the evolved variants, which revealed a link between the ribosomes and the activation of stress resistance by SigB.

Future research will focus on the current model of reversion of fitness effects via increased translation efficiency. This model suggests a limited extra fitness burden on the variants from the global upregulation of SigB. This can be experimentally verified by generating RpsU$^{17Arg\text{-}Pro}$–Δ*sigB* double mutants, that are expected to have WT stress resistance, combined with low fitness, as they lack the constitutive expression of *sigB*, while still being faced with the fitness effects of the mutation in *rpsU*. Moreover, generation of RpsU$^{17Arg\text{-}Pro}$ mutants in genetic backgrounds missing one or multiple stressosome components can shed light on the interaction between the ribosome and the stressosome. In addition, as suggested by Dessaux et al. (2020b) phosphoproteomics are needed to investigate the phosphorylation state of the individual stressosome and ribosome components, in order to gain more insight into the signalling cascade leading to SigB activation.

A better understanding of the factors that influence mutation rate, and thereby the adaptive potential of populations is valuable to increase control of this pathogen. A mechanistic understanding of the observed trade-off between stress resistance and fitness will impact fundamental research, and ultimately, incorporation of these trade-offs into predictive models and risk assessments will add to producing minimally processed foods that are microbiologically safe.

## References

**Abee, T., Koomen, J., Metselaar, K.I., Zwietering, M.H., Den Besten, H.M.W.**, 2016. Impact of pathogen population heterogeneity and stress-resistant variants on food safety. Annu. Rev. Food Sci. Technol. 7, 439–456. doi:10.1146/annurev-food-041715-033128

**Aryani, D.C., Den Besten, H.M.W., Hazeleger, W.C., Zwietering, M.H**., 2015. Quantifying variability on thermal resistance of *Listeria monocytogenes.* Int. J. Food Microbiol. 193, 130–138. doi:10.1016/j.ijfoodmicro.2014.10.021

**Bannenberg, J.W., Abee, T., Zwietering, M.H., Den Besten, H.M.W.,** 2021. Variability in lag duration of *Listeria monocytogenes* strains in half Fraser enrichment broth after stress affects the detection efficacy using the ISO 11290-1 method. Int. J. Food Microbiol. 337, 108914. doi:10.1016/j.ijfoodmicro.2020.108914

**Den Besten, H.M.W., Aryani, D.C., Metselaar, K.I., Zwietering, M.H.,** 2017. Microbial variability in growth and heat resistance of a pathogen and a spoiler: All variabilities are equal but some are more equal than others. Int. J. Food Microbiol. 240, 24–31. doi:10.1016/j.ijfoodmicro.2016.04.025

**Boe, L., Danielsen, M., Knudsen, S., Petersen, J.B., Maymann, J., Jensen, P.R.,** 2000. The frequency of mutators in populations of *Escherichia coli.* Mutat. Res.-Fundam. Mol. Mech. Mutagen. 448, 47–55. doi:10.1016/S0027-5107(99)00239-0

**Brigulla, M., Hoffmann, T., Krisp, A., Völker, A., Bremer, E., Völker, U**., 2003. Chill induction of the SigB-dependent general stress response in *Bacillus subtilis* and its contribution to low-temperature adaptation. J. Bacteriol. 185, 4305–4314. doi:10.1128/jb.185.15.4305-4314.2003

**Cabeen, M.T., Russell, J.R., Paulsson, J., Losick, R.,** 2017. Use of a microfluidic platform to uncover basic features of energy and environmental stress responses in individual cells of *Bacillus subtilis*. PLOS Genet. 13, e1006901. doi:10.1371/journal.pgen.1006901

**Chen, R., Skeens, J., Orsi, R.H., Wiedmann, M., Guariglia-Oropeza, V.,** 2020. Pre-growth conditions and strain diversity affect nisin treatment efficacy against *Listeria monocytogenes* on cold-smoked salmon. Int. J. Food Microbiol. 333, 108793. doi:10.1016/j.ijfoodmicro.2020.108793

**Cotter, P.D., O'REILLY, K., Hill, C.,** 2001. Role of the glutamate decarboxylase acid resistance system in the survival of *Listeria monocytogenes* LO28 in low pH foods. J. Food Prot. 64, 1362–1368. doi:10.4315/0362-028x-64.9.1362

**De Visser, J.A.G.M.,** 2002. The fate of microbial mutators. Microbiology 148, 1247–1252. doi:10.1099/00221287-148-5-1247

**Denamur, E., Bonacorsi, S., Giraud, A., Duriez, P., Hilali, F., Amorin, C., Bingen, E., Andremont, A., Picard, B., Taddei, F., Matic, I.,** 2002. High frequency of mutator strains among human uropathogenic *Escherichia coli* Isolates. J. Bacteriol. 184, 605–609. doi:10.1128/JB.184.2.605-609.2002

**Desai, M.M., Fisher, D.S.,** 2011. The balance between mutators and nonmutators in asexual populations. Genetics 188, 997–1014. doi:10.1534/genetics.111.128116

**Dessaux, C., Guerreiro, D.N., Pucciarelli, M.G., O'Byrne, C.P., García-Del Portillo, F.,** 2020a. Impact of osmotic stress on the phosphorylation and subcellular location of *Listeria monocytogenes* stressosome proteins. Sci. Rep. 10, 20837–15. doi:10.1038/s41598-020-77738-z

**Dorey, A.L., Lee, B.-H., Rotter, B., O'Byrne, C.P.,** 2019. Blue light sensing in *Listeria monocytogenes* is temperature-dependent and the transcriptional response to it is predominantly SigB-dependent. Front. Microbiol. 10, 2497. doi:10.3389/fmicb.2019.02497

**Elena, S.F., Lenski, R.E.,** 2003. Evolution experiments with microorganisms: the dynamics and genetic bases of adaptation. Nat. Rev. Genet. 4, 457–469. doi:10.1038/nrg1088

**Eyre-Walker, A., Keightley, P.D.,** 2007. The distribution of fitness effects of new mutations. Nat. Rev. Genet. 8, 610–618. doi:10.1038/nrg2146

**Feehily, C., Karatzas, K.A.G.,** 2013. Role of glutamate metabolism in bacterial responses towards acid and other stresses. J. Appl. Microbiol. 114, 11–24. doi:10.1111/j.1365-2672.2012.05434.x

**Freitag, N.E., Port, G.C., Miner, M.D.,** 2009. *Listeria monocytogenes* - from saprophyte to intracellular pathogen. Nat. Rev. Microbiol. 7, 623–628. doi:10.1038/nrmicro2171

**Genuth, N.R., Barna, M.,** 2018. The discovery of ribosome heterogeneity and its implications for gene regulation and organismal Life. Mol. Cell 71, 364–374. doi:10.1016/j.molcel.2018.07.018

**Gerst, J.E.,** 2018. Pimp my ribosome: Ribosomal protein paralogs specify translational control. Trends Genet. 34, 832–845. doi:10.1016/j.tig.2018.08.004

**Guerreiro, D.N., Arcari, T., O'Byrne, C.P.,** 2020. The σB-mediated general stress response of *Listeria monocytogenes*: Life and death decision making in a pathogen. Front. Microbiol. 11, 1505. doi:10.3389/fmicb.2020.01505

**Guldimann, C., Boor, K.J., Wiedmann, M., Guariglia-Oropeza, V.,** 2016. Resilience in the face of uncertainty: Sigma factor B fine-tunes gene expression to support homeostasis in Gram-positive bacteria. Appl. Environ. Microbiol. 82, 4456–4469. doi:10.1128/AEM.00714-16

**Hall, L.M.C., Henderson-Begg, S.K.,** 2006. Hypermutable bacteria isolated from humans – a critical analysis. Microbiology 152, 2505–2514. doi:10.1099/mic.0.29079-0

**Hallsworth, J.E.,** 2018. Stress-free microbes lack vitality. Fungal Biol. 122, 379–385. doi:10.1016/j.funbio.2018.04.003

**Harrand, A.S., Jagadeesan, B., Baert, L., Wiedmann, M., Orsi, R.H., Dudley, E.G.,** 2020. Evolution of *Listeria monocytogenes* in a food processing plant involves limited single-nucleotide substitutions but considerable diversification by gain and loss of prophages. Appl. Environ. Microbiol. 86, 38. doi:10.1128/AEM.02493-19

**Karatzas, K.A.G., Suur, L., O'Byrne, C.P.,** 2012. Characterization of the intracellular glutamate decarboxylase system: analysis of its function, transcription, and role in the acid resistance of various strains of *Listeria monocytogenes*. Appl. Environ. Microbiol. 78, 3571–3579. doi:10.1128/AEM.00227-12

**Karatzas, K.A.G., Bennik, M.H.J.,** 2002. Characterization of a *Listeria monocytogenes* Scott A isolate with high tolerance towards high hydrostatic pressure. Appl. Environ. Microbiol. 68, 3183–3189. doi:10.1128/AEM.68.7.3183-3189.2002

**Karatzas, K.A.G., Valdramidis, V.P., Wells-Bennik, M.H.J.,** 2005. Contingency locus in ctsR of *Listeria monocytogenes* Scott A: a strategy for occurrence of abundant piezotolerant isolates within clonal populations. Appl. Environ. Microbiol. 71, 8390–8396. doi:10.1128/AEM.71.12.8390-8396.2005

**Katju, V., Bergthorsson, U.,** 2019. Old trade, new tricks: Insights into the spontaneous mutation process from the partnering of classical mutation accumulation experiments with high-throughput genomic approaches. Genome Biol. Evol. 11, 136–165. doi:10.1093/gbe/evy252

**Kimura, M.,** 1967. On the evolutionary adjustment of spontaneous mutation rates. Genet. Res. 9, 23–34. doi:10.1017/S0016672300010284

**Kline, B.C., McKay, S.L., Tang, W.W., Portnoy, D.A.,** 2015. The *Listeria monocytogenes* hibernation-promoting factor is required for the formation of 100S ribosomes, optimal fitness, and pathogenesis. J. Bacteriol. 197, 581–591. doi:10.1128/JB.02223-14

**Koomen, J., Den Besten, H.M.W., Metselaar, K.I., Tempelaars, M.H., Wijnands, L.M., Zwietering, M.H., Abee, T.,** 2018. Gene profiling-based phenotyping for identification of cellular parameters that contribute to fitness, stress-tolerance and virulence of *Listeria monocytogenes* variants. Int. J. Food Microbiol. 283, 14–21. doi:10.1016/j.ijfoodmicro.2018.06.003

**Lynch, M.,** 2011. The lower bound to the evolution of mutation rates. Genome Biol. Evol. 3, 1107–1118. doi:10.1093/gbe/evr066

**Marinus, M.G.,** 2010. DNA methylation and mutator genes in *Escherichia coli* K-12. Mutat. Res. Fundam. Mol. Mech. Mutagen. 705, 71–76. doi:10.1016/j.mrrev.2010.05.001

**Marzi, S., Myasnikov, A.G., Serganov, A., Ehresmann, C., Romby, P., Yusupov, M., Klaholz, B.P.,** 2007. Structured mRNAs regulate translation initiation by binding to the platform of the ribosome. Cell 130, 1019–1031. doi:10.1016/j.cell.2007.07.008

**Metselaar, K.I., Abee, T., Zwietering, M.H., Den Besten, H.M.W.,** 2016. Modeling and validation of the ecological behavior of wild-type *Listeria monocytogenes* and stress-resistant variants. Appl. Environ. Microbiol. 82, 5389–5401. doi:10.1128/AEM.00442-16

**Metselaar, K.I., Den Besten, H.M.W., Abee, T., Moezelaar, R., Zwietering, M.H.,** 2013. Isolation and quantification of highly acid resistant variants of *Listeria monocytogenes.* Int. J. Food Microbiol. 166, 508–514. doi:10.1016/j.ijfoodmicro.2013.08.011

**Metselaar, K.I., Den Besten, H.M.W., Boekhorst, J., van Hijum, S.A.F.T., Zwietering, M.H., Abee, T.,** 2015. Diversity of acid stress resistant variants of *Listeria monocytogenes* and the potential role of ribosomal protein S21 encoded by *rpsU.* Front. Microbiol. 6, 422. doi:10.3389/fmicb.2015.00422

**Metselaar, K.I., Ibusquiza, P.S., Camargo, A.R.O., Krieg, M., Zwietering, M.H., Den Besten, H.M.W., Abee, T.,** 2015b. Performance of stress resistant variants of *Listeria*

*monocytogenes* in mixed species biofilms with *Lactobacillus plantarum*. Int. J. Food Microbiol. 213, 1–7. doi:10.1016/j.ijfoodmicro.2015.04.021

**Mérino, D., Poupet, H.R., Berche, P., Charbit, A.,** 2002. A hypermutator phenotype attenuates the virulence of *Listeria monocytogenes* in a mouse model. Mol. Microbiol. 44, 877–887. doi:10.1046/j.1365-2958.2002.02929.x

**Mohammad, F., Green, R., Buskirk, A.R.,** 2019. A systematically-revised ribosome profiling method for bacteria reveals pauses at single-codon resolution. Elife 8, 8324. doi:10.7554/eLife.42591

**NicAogáin, K., O'Byrne, C.P.,** 2016. The role of stress and stress adaptations in determining the fate of the bacterial pathogen *Listeria monocytogenes* in the food chain. Front. Microbiol. 7, 1865. doi:10.3389/fmicb.2016.01865

**Olier, M., Pierre, F., Rousseaux, S., Lemaitre, J.P., Rousset, A., Piveteau, P., Guzzo, J.,** 2003. Expression of truncated internalin A is involved in impaired internalization of some *Listeria monocytogenes* isolates carried asymptomatically by humans. Infect. Immun. 71, 1217–1224. doi:10.1128/IAI.71.3.1217-1224.2003

**Oliver, A.,** 2015. Clinical relevance of *Pseudomonas aeruginosa* hypermutation in cystic fibrosis chronic respiratory infection. J. Cyst. Fibros 14, e1–e2. doi:10.1016/j.jcf.2014.12.009

**Perfeito, L., Fernandes, L., Mota, C., Gordo, I.,** 2007. Adaptive mutations in bacteria: high rate and small effects. Science 317, 813–815. doi:10.1126/science.1142284

**Radoshevich, L., Cossart, P.,** 2018. *Listeria monocytogenes*: towards a complete picture of its physiology and pathogenesis. Nat. Rev. Microbiol. 16, 32–46. doi:10.1038/nrmicro.2017.126

**Rajkovic, A., Smigic, N., Uyttendaele, M., Medic, H., de Zutter, L., Devlieghere, F.,** 2009. Resistance of *Listeria monocytogenes*, *Escherichia coli* O157:H7 and *Campylobacter jejuni* after exposure to repetitive cycles of mild bactericidal treatments. Food Microbiol. 26, 889–895. doi:10.1016/j.fm.2009.06.006

**Sheng, H., Huang, J., Han, Z., Liu, M., Lü, Z., Zhang, Q., Zhang, J., Yang, J., Cui, S., Yang, B.,** 2020. Genes and proteomes associated with increased mutation frequency and multidrug resistance of naturally occurring mismatch repair-deficient *Salmonella* Hypermutators. Front. Microbiol. 11, 770. doi:10.3389/fmicb.2020.00770

**Sniegowski, P., Raynes, Y.,** 2013. Mutation rates: how low can you go? Curr. Biol. 23, R147–R149. doi:10.1016/j.cub.2013.01.018

**Sprouffske, K., Aguílar-Rodríguez, J., Sniegowski, P., Wagner, A.,** 2018. High mutation rates limit evolutionary adaptation in *Escherichia coli*. PLOS Genet. 14, e1007324. doi:10.1371/journal.pgen.1007324

**Taylor, C.M., Beresford, M., Epton, H.A.S., Sigee, D.C., Shama, G., Andrew, P.W., Roberts, I.S.,** 2002. *Listeria monocytogenes relA* and *hpt* mutants are impaired in surface-attached growth and virulence. J. Bacteriol. 184, 621–628. doi:10.1128/JB.184.3.621-628.2002

**Toledo-Arana, A., Dussurget, O., Nikitas, G., Sesto, N., Guet-Revillet, H., Balestrino, D., Loh, E., Gripenland, J., Tiensuu, T., Vaitkevicius, K., Barthelemy, M., Vergassola, M., Nahori, M.-A., Soubigou, G., Régnault, B., Coppée, J.-Y., Lecuit, M.,**

**Johansson, J., Cossart, P.,** 2009. The *Listeria* transcriptional landscape from saprophytism to virulence. Nature 459, 950–956. doi:10.1038/nature08080

**Utratna, M., Cosgrave, E., Baustian, C., Ceredig, R.H., O'Byrne, C.P**., 2014. Effects of growth phase and temperature on activity within a *Listeria monocytogenes* Population: evidence for RsbV-independent activation of σB at refrigeration temperatures. Biomed Res. Int. 2014, 1–11. doi:10.1155/2014/641647

**Van Boeijen, I.K.H., Chavaroche, A.A.E., Valderrama, W.B., Moezelaar, R., Zwietering, M.H., Abee, T.,** 2010. Population diversity of *Listeria monocytogenes* LO28: phenotypic and genotypic characterization of variants resistant to high hydrostatic pressure. Appl. Environ. Microbiol. 76, 2225–2233. doi:10.1128/AEM.02434-09

**Van Boeijen, I.K.H., Francke, C., Moezelaar, R., Abee, T., Zwietering, M.H**., 2011. Isolation of highly heat-resistant *Listeria monocytogenes* variants by use of a kinetic modeling-based sampling scheme. Appl. Environ. Microbiol. 77, 2617–2624. doi:10.1128/AEM.02617-10

**Van Boeijen, I.K.H., Moezelaar, R., Abee, T., Zwietering, M.H**., 2008. Inactivation kinetics of three *Listeria monocytogenes* strains under high hydrostatic pressure. J. Food Prot. 71, 2007–2013. doi:10.4315/0362-028x-71.10.2007

**Van der Veen, S., Abee, T.,** 2011. Generation of variants in *Listeria monocytogenes* continuous-flow biofilms is dependent on radical-induced DNA damage and RecA-mediated repair. PLoS One 6, e28590–8. doi:10.1371/journal.pone.0028590

**Van der Veen, S., Abee, T.,** 2010. Importance of SigB for *Listeria monocytogenes* static and continuous-flow biofilm formation and disinfectant resistance. Appl. Environ. Microbiol. 76, 7854–7860. doi:10.1128/AEM.01519-10

**Van der Veen, S., van Schalkwijk, S., Molenaar, D., de Vos, W.M., Abee, T., Wells-Bennik, M.H.J.,** 2010. The SOS response of *Listeria monocytogenes* is involved in stress resistance and mutagenesis. Microbiology (Reading, Engl.) 156, 374–384. doi:10.1099/mic.0.035196-0

**Vanlint, D., Rutten, N., Michiels, C.W., Aertsen, A.,** 2012. Emergence and stability of high-pressure resistance in different food-borne pathogens. Appl. Environ. Microbiol. 78, 3234–3241. doi:10.1128/AEM.00030-12

**Wang, H., Xing, X., Wang, J., Pang, B., Liu, M., Larios-Valencia, J., Liu, T., Liu, G., Xie, S., Hao, G., Liu, Z., Kan, B., Zhu, J.,** 2018. Hypermutation-induced in vivo oxidative stress resistance enhances *Vibrio cholerae* host adaptation. PLoS Pathog. 14, e1007413. doi:10.1371/journal.ppat.1007413

**Wang, S., Wu, C., Shen, J., Wu, Y., Wang, Y.,** 2013. Hypermutable *Staphylococcus aureus* strains present at high frequency in subclinical bovine mastitis isolates are associated with the development of antibiotic resistance. Vet. Microbiol. 165, 410–415. doi:10.1016/j.vetmic.2013.04.009

**Wielgoss, S., Barrick, J.E., Tenaillon, O., Wiser, M.J., Dittmar, W.J., Cruveiller, S., Chane-Woon-Ming, B., Médigue, C., Lenski, R.E., Schneider, D.,** 2013. Mutation rate dynamics in a bacterial population reflect tension between adaptation and genetic load. Proc. Natl. Acad. Sci. U.S.A. 110, 222–227. doi:10.1073/pnas.1219574110

**Williams, A.H., Redzej, A., Rolhion, N., Costa, T.R.D., Rifflet, A., Waksman, G., Cossart, P.,** 2019. The cryo-electron microscopy supramolecular structure of the bacterial stressosome unveils its mechanism of activation. Nat. Commun. 10, 3005–3010. doi:10.1038/s41467-019-10782-0

**Xia, Y., Xin, Y., Li, X., Fang, W., Björkroth, J.,** 2016. To modulate survival under secondary stress conditions, *Listeria monocytogenes* 10403S employs RsbX to downregulate σB activity in the poststress recovery stage or stationary phase. Appl. Environ. Microbiol. 82, 1126–1135. doi:10.1128/AEM.03218-15

**Zwietering, M.H., Garre, A., Den Besten, H.M.W.,** 2021. Incorporating strain variability in the design of heat treatments: A stochastic approach and a kinetic approach. Food Res. Int. 139, 109973. doi:10.1016/j.foodres.2020.109973

# S

## Summary

## Summary

The production of healthy, nutritious, tasty, and safe foods requires efficient strategies to control foodborne pathogens along the food chain. One of these pathogens is the notorious foodborne *Listeria monocytogenes. L. monocytogenes* is a robust, ubiquitously present human pathogen, and the cause of life-threatening listeriosis in the very young, elderly, pregnant, and immunocompromised persons, the so-called YOPI population. The incidence of *L. monocytogenes* infections is low, but the severity of listeriosis and the high mortality rate rank it among the top three causes of death by foodborne disease.

There is an inherent heterogeneity in microbial populations, and this heterogeneity gives *L. monocytogenes* the capacity to cope with stresses during transmission from the environment to the human host. Stochastic differences in stress response between individual cells of a population, lead to the differential survival of cells after lethal stresses such as heat or low pH, and ultimately result in tailing of the inactivation curve. The heterogeneity in a population can be either transient, where certain cells temporarily have different properties, or stable, where individual cells have undergone genetic changes that make them better able to resist (lethal) stress. Cells with genetic changes are called stable variants, and can be isolated from the tail of the inactivation curve.

Almost all research that has been done with *L. monocytogenes* has focussed on the diversity that is already present in a population. Therefore, in chapter 2, we investigated the rate at which new diversity is generated by mutations. Using a high-throughput protocol, we have experimentally determined the mutation rate of 20 *L. monocytogenes* strains, and found a mutator strain with an insertion in the DNA mismatch repair gene *mutS*, that resulted in a 100-1000-fold increase in mutation rate. To our knowledge, this is the first mutator strain of *L. monocytogenes* isolated from food.

In chapter 3 we focussed on two previously isolated multiple-stress resistant variants, both with a mutation in the ribosomal *rspU* gene, one with a point mutation in the *rpsU* gene, and one with a deletion of the whole *rpsU* gene. We described the overlap in the stress response of these two variants, and found that even though the mutation in *rpsU* was very different, the phenotypic responses were remarkably similar. Both variants were multiple-stress resistant due to massive upregulation of genes under the control of the stress-response regulator SigB. Moreover, both variants showed increased attachment to Caco-2 cells, so potentially more infective, and a significantly lower maximum specific growth rate, i.e., lower fitness.

Strains are known to persist in the food processing environment for many years, where they are exposed to continuous selection pressures. In chapters 4 and 5 we used experimental

evolution to explore what can happen when these stress-resistant variants with lower fitness are exposed to continuous selection for increased fitness. We focused on the same two variants as in Chapter 3, with a point mutation in and with a complete deletion of *rpsU*. We were able to select for additional mutations that reversed the phenotype from low-fitness and stress-resistant, to high-fitness with low stress-resistance, thereby revealing a tradeoff between these two states. Complementary whole genome sequencing and SNP analysis showed that in the point mutation variant, the additional compensating mutation occurred in *rpsU*, while in the deletion mutant, the additional mutation occurred in the ribosomal *rpsB* gene. Thereby we have revealed a link between the ribosomes and the activation of stress resistance by SigB.

In conclusion, the work presented in this thesis highlights various microbial adaptive and evolutionary mechanisms that contribute to the heterogeneous behavior of *L. monocytogenes*. This thesis revealed a trade-off between stress resistance and fitness in stress-isolated variants and it heightened our understanding of how this notorious pathogen is able to grow and survive in changing environments. A mechanistic understanding of the observed trade-off between stress resistance and fitness will impact fundamental research, and ultimately, incorporation of these trade-offs into risk assessments will add to producing minimally processed foods that are microbiologically safe.

## Acknowledgements

Graag wil ik hier van de gelegenheid gebruik maken om iedereen te bedanken die heeft bijgedragen aan het tot stand komen van dit proefschrift. Allereerst wil ik mijn promotoren en co-promotor heel erg bedanken. Tjakko, bedankt voor je continue enthousiasme, en voor het feit dat je deur altijd openstond voor overleg. We hebben vele uren hebben gediscussieerd over nieuwe experimenten en richtingen voor de papers, en ook al vond ik het soms lastig te navigeren door de explosie van ideeën die we konden hebben, het heeft zeker geleid tot innovatieve experimenten. Dank ook voor je optimisme gedurende de tijden dat het lastig ging, en voor de samenwerking in het *Salmonella* project. Heidy, van jouw kritische blik, en zeer scherpe oog voor detail, heb ik veel geleerd. Het was een waardevolle aanvulling, en je scherpe blik heeft enorm bijgedragen aan de kwaliteit van de manuscripten. Marcel, bedankt voor je input, je enthousiasme, het feit dat ik altijd kon binnenlopen voor de meest uiteenlopende vragen, het faciliteren van de jaarlijkse barbecue en uitjes, en natuurlijk alle hardlooprondjes in binnen- en buitenland.

Oscar, we hebben bijna 5 jaar een kantoor gedeeld voordat we thuis moesten gaan werken. Ik heb genoten van onze discussies over de meest uiteenlopende onderwerpen, en van het feit dat je altijd klaar stond om mee te denken en mee te rekenen aan selectie- en groeivragen. Frank, ook al woonde je bijna op het lab, het was gezellig om een kantoor te delen, en om samen te werken aan de bio-informatica analyse achter je eerste paper. Alex, je was een goede aanvulling op ons kantoor, en belangrijk voor de leuke balans tussen *Listeria* en fermentatie mensen.

A big thanks to all former and current collegues of the Food Microbiology lab. I will miss the discussions about everything from science to music and movies, the running on Thursday, the hotpot evenings, dinners, VrijMiBo's, cakes, and all other moments that we shared. I would like to thank you all for contributing to the atmosphere in the group. This has been essential in keeping me grounded in the difficult times that arose during the PhD process. It has been a great experience to work with so many smart and talented people!

Gerda, bedankt voor alles wat je doet om de sfeer in de groep goed te houden, en voor het doen van alle administratie. Ingrid, bedankt voor het op orde houden van de keuken, en voor alle bestellingen die je de afgelopen jaren voor me hebt gedaan.

I am very glad to have had the chance to work with so many different and great MSc students during this project. Dear Luiza, Xi, Jian, Maria, Peter, Ginevra, Sandra, Aaron, Linda, Xuchuan, Yongge, Alberto B., Lubeibei, and Klara, thank you all for showing interest in one of my projects. Linda, Alberto B. and Xuchuan, it was very nice to have you as colleagues at FHM after your MSc projects and I wish you all the best in your own journey as a researcher.

Zonder de technische support op het lab zouden veel experimenten niet zo goed gegaan zijn. Marcel T., bedankt voor alle groeicurven, cloneringen, en RNA-isolaties die we samen hebben gedaan. Ook wil ik je bedanken voor alle discussies over wetenschap en de technische details van het labwerk. Jouw ervaring is van onschatbare waarde voor de afdeling. Luc, bedankt voor je hulp bij de experimenten met caco cellen die ik met jou en Maren bij het RIVM mocht doen. Het is goed om te zien dat er postdocs zijn met zoveel labervaring! Sjef, bedankt voor je hulp met het opzetten van de proteomics experimenten, en met de analyse van de data. Deze experimenten in Helix zijn een belangrijke pijler onder de hoofdstukken van deze thesis gebleken. Dear Leoni and Bing, even though our experiments with the ribosome gradients only made a subtle entry into the chapters of this thesis, I am very grateful for the help that I received in Radix, and for the promising results that we obtained. Alberto Garre, I have learned a lot from seeing an R expert at work. Your project at our lab has lifted the standard for cooperation, and I am very thankful for all our discussions on R, on how to deal with reviewer comments, and on working in science in general.

I am also very grateful to Prof. Michiel Kleerebezem, Dr. Indra Bergval, Prof. Conor O'Byrne, and Dr. Masja Nierop Groot for accepting the invitation to be part of my thesis committee, and taking the time to critically review this thesis.

A special thanks to my paranymphs. Linda, your cheerful, yet structured and very ambitious approach to labwork during your thesis has really lifted my spirit. Our cooperation was pivotal in the direction of this thesis, and it is great to see that you now work with the same enthusiasm and dedication on your own project. Xuchuan, thank you for continuing the project in a more molecular direction. I am sure that your hard work and determination in mutant construction will lead to novel insights for your own thesis.

Ik wil hier ook mijn (voormalige) huisgenoten bedanken. We hebben een interessante mix van mensen in een huis en ik ben heel blij dat we altijd bij elkaar konden binnenlopen als het tegenzat met werk, studie, of de zoektocht naar werk. Floris, bedankt voor je bijdrage aan de figuren van hoofdstuk 6.

Als laatste wil ik mijn vrienden, familie en natuurlijk mijn ouders bedanken. Jullie hebben me altijd gesteund tijdens mijn lange weg. Bedankt voor het al vertrouwen wat jullie in mij hadden, en voor de vele discussies over de beste aanpak.

## Publications

Tendolkar, U., Van Diepeningen, A., Joshi, A., **Koomen, J.**, Bradoo, R., Baveja, S., and Agrawal, S. 2015. Rhinosinusitis caused by Saksenaea erythrospora in an immunocompetent patient in India: a first report. JMM Case Reports. 2. 10.1099/jmmcr.0.000044

Abee, T., **Koomen, J**., Metselaar, K. I., Zwietering, M. H., & Besten, den, H. M. W. 2016. Impact of Pathogen Population Heterogeneity and Stress-Resistant Variants on Food Safety. Annual Review of Food Science and Technology, 7(1), 439–456. http://doi.org/10.1146/annurev-food-041715-033128

Salverda, M. L. M., **Koomen, J**., Koopmanschap, B., Zwart, M. P., & de Visser, J. A. G. M. 2017. Adaptive benefits from small mutation supplies in an antibiotic resistance enzyme. Proceedings of the National Academy of Sciences of the United States of America, 114(48), 12773–12778. http://doi.org/10.1073/pnas.1712999114

**Koomen, J**., Besten, den, H. M. W., Metselaar, K. I., Tempelaars, M. H., Wijnands, L. M., Zwietering, M. H., & Abee, T. 2018. Gene profiling-based phenotyping for identification of cellular parameters that contribute to fitness, stress-tolerance and virulence of *Listeria monocytogenes* variants. Int. J. Food Microbiol. 283, 14–21. http://doi.org/10.1016/j.ijfoodmicro.2018.06.003

**Koomen, J**., Huijboom, L., Ma, X., Tempelaars, M.H., Boeren, S., Zwietering, M.H., Den Besten, H.M.W., Abee, T. 2021. Amino acid substitutions in ribosomal protein RpsU enable switching between high fitness and multiple-stress resistance in *Listeria monocytogenes*. Int. J. Food Microbiol. 351, 109269. https://doi.org/10.1016/j.ijfoodmicro.2021.109269

Lake, F.B., van Overbeek, L.S., Baars, J.J.P., **Koomen, J**., Abee, T., Den Besten, H.M.W. 2021. Genomic characteristics of *Listeria monocytogenes* isolated during mushroom (*Agaricus bisporus*) production and processing, Int. J. Food Microbiol. 360, 109438. https://doi.org/10.1016/j.ijfoodmicro.2021.109438.

Garre, A., **Koomen, J**., Den Besten, H.M.W., Zwietering, M.H. Modelling population growth in R with the biogrowth package. *Submitted for publication.*

## Overview of completed training activities

**Discipline specific activities**

*Courses*

| | |
|---|---|
| Genetics and physiology of food-associated microorganisms VLAG, Wageningen, NL) | 2016 |
| Reaction kinetics in Food Science (VLAG, Wageningen, NL) | 2016 |
| Management of Microbiological Hazards in Foods (VLAG, Wageningen, NL) | 2017 |
| Data Scientist with R (DataCamp, online) | 2018 |

*Conferences*

| | |
|---|---|
| FEMS (Valencia, ES) | 2017 |
| FEMS Microbial stress meeting (Kinsale, IE) | 2018 |
| KNVM Symposium (Bilthoven, NL) | 2018 |
| NLSEB (Ede, NL) | 2018 |
| ISOPOL (Toronto, CA) | 2019 |

**General courses**

| | |
|---|---|
| Teaching and supervising thesis students (ESD) | 2015 |
| VLAG PhD week (VLAG) | 2015 |
| Transmission Electron Microscopy (WEMC) | 2017 |
| Career orientation (WGS) | 2018 |
| Data visualization with R (DataCamp) | 2018 |
| Data analyst with R | 2019 |

**Optional courses and activities**

| | |
|---|---|
| Preparation of research proposal | 2015 |
| FHM weekly meetings | 2015-2020 |
| Seminars Microbial Population Genetics | 2016-2019 |
| FHM PhD study tour Italy | 2017 |
| Organization FHM PhD study tour Italy | 2017 |

The research in this thesis was financially supported by Food Microbiology (Wageningen University, Wageningen, The Netherlands).

**Cover design by** Vera van Beek
**Printed by** Digiforce | ProefschriftMaken